AFML-TR-70-101

IMPROVED FABRICATION METHODS OF JET ENGINE ROTORS

G. Korton
K. W. Stalker
Material and Process Technology Laboratories
Aircraft Engine Group
General Electric Company

TECHNICAL REPORT AFML-TR-70-101
May 1970

Manufacturing Technology Division
Air Force Materials Laboratory
Air Force Systems Command
Wright-Patterson Air Force Base, Ohio

NOTICES

When Government drawings, specifications, or other data are used for any purpose other than in connection with a definitely related Government procurement operation, the United States Government thereby incurs no responsibility nor any obligation whatsoever; and the fact that the government may have formulated, furnished, or in any way supplied the said drawings, specifications, or other data, is not to be regarded by implication or otherwise as in any manner licensing the holder or any other person or corporation, or conveying any rights or permission to manufacture, use, or sell any patented invention that may in any way be related thereto.

This document is subject to special export controls and each transmittal to foreign governments or foreign nationals may be made only with prior approval of the Manufacturing Technology Division, MAT, Air Force Materials Laboratory, Wright-Patterson AFB, Ohio 45433.

The distribution of this report is limited because it contains technology identifiable with items on the strategic embargo lists excluded from export or re-export under U. S. Export Control Act of 1949 (63 STAT. 7), as amended (50 U. S. C. Appn. 2020-2031), as implemented by AFR 400-10, AFR 310-2, and AFSCR 80-20.

Copies of this report should not be returned unless return is required by security considerations, contractual obligations, or notice on a specific document.

IMPROVED FABRICATION METHODS OF JET ENGINE ROTORS

G. Korton
K. W. Stalker

FOREWORD

This final technical report covers all work performed under Contract F33615-67-C-1884 from 1 July 1967 to 31 March 1970. The manuscript was released by the authors in April 1970 for publication.

This contract with General Electric Company, Cincinnati, Ohio, was initiated under Manufacturing Methods Project 874-7, "Improved Fabrication Methods of Jet Engine Rotors". It was administered under the technical direction of Mr. John O. Snyder, Fabrication Branch (MATF), Manufacturing Technology Division, Air Force Materials Laboratory, Wright-Patterson Air Force Base, Ohio.

This contract was conducted under Messrs. K. W. Stalker, Manager, Process Development, and G. Korton, Project Engineer. Others who contributed to the program were, Russell Smashey and James Barker, Metallurgical Engineers.

This project has been accomplished as a part of the Air Force Manufacturing Methods Program, the primary objective of which is to develop on a timely basis, manufacturing processes, techniques and equipment for use in economical production of USAF materials and components.

Your comments are solicited on the potential utilization of the information contained herein as applied to your present and/or future production programs. Suggestions concerning additional manufacturing methods development required on this or other subjects will be appreciated.

This technical report has been reviewed and is approved.

JACK R. MARSH
Chief, Fabrication Branch
Manufacturing Technology Division

ABSTRACT

A program to provide an improved method of jet engine compressor rotor manufacture and fabricate a TF39 Stages 14-16 compressor rotor spool is described. The inertia welding parameters, energy and pressure, were determined for three jet engine alloys; 20 K to 26 K ft-lbs/in.^{2} and 35 K to 40 ksi for Inconel 718, 60 K to 80 K ft-lbs/in.^{2} and 50 K to 60 ksi for Udimet 700 and 8 K to 15 K ft-lbs/in.^{2} and 4 K to 8 ksi for Ti-6Al-4V. Inertia welded joint properties were generally equivalent to parent metal properties except for ductility, stress-rupture and low cycle fatigue life. Inconel 718 cross rolled plate properties were better than forging properties. Cold working Inconel 718 had no significant effect on mechanical properties but heat-treating above 1900F lowered notch ductility. Cold rim forming process parameters were established for fabricating rotor disks from cross rolled plate. Machine deflections and improperly heat-treated plates were major problem areas. Scale-up inertia welding of 4, 12 and 24 inch diameter Inconel 718 specimens showed total upset could be empirically related to joint area, weld energy and thrust load. Ductility, rupture and low cycle fatigue life of Inconel 718 weld joints were lowered by liquated grain boundary phases formed in welding above 700 SFM. The results of welding five rotor spools showed concentricity and parallelism tolerances of 0.010 inch FIR could be held. Post-weld cracking in the HAZ was found related to the method of flash machining. One TF39 Stages 14-16 compressor rotor was finish machined successfully. The fabricated rotor process was found applicable to the manufacture of a broad range of jet engine compressor rotors. Larger inertia welders and redesigned forming machines are required to introduce the process into manufacturing on a wider scale.

TABLE OF CONTENTS

Section		Page
I	INTRODUCTION	1
II	INERTIA WELDING PROCESS	2
III	INERTIA WELDING STUDIES	3
	A. Parametric Studies	3
	B. Mechanical Properties of Inertia Welds	4
	C. Inconel 718 Diameter and Wall Thickness Study	19
	D. Metallographic Studies	29
IV	COLD FORMING INCONEL 718 CROSS ROLLED PLATE	38
	A. Heat-Treating Studies	38
	B. Mechanical Property Studies	41
	C. Cold Rim Forming Development	47
V	COMPRESSOR ROTOR FABRICATION	69
	A. Fabrication From Cross Rolled Plate	69
	B. Fabrication From Forged Stock	100
VI	OVERALL PROGRAM ANALYSIS AND EVALUATION	118
	A. Summary Analysis of Results	118
	B. Applicability of the Fabricated Rotor Process	124
	C. Cost Comparison of Forged and Machined vs. Fabricated Rotors	126
	D. Required Inertia Welding Machine Sizes	127
	E. Impact on Design Flexibility	132

Appendix		Page
I	Tables	135
II	Statistical Analysis of Parametric Welding Studies	183
III	T58 Type Rotor Test	214
IV	F100/F400 Type Rotor Test	217

LIST OF ILLUSTRATIONS

Figure		Page
1	Inertia Welded Inconel 718 Test Cylinders	6
2	Inertia Welded Udimet 700 Test Cylinders	7
3	Quench Crack Failure resulting from 2100° F/4 Hr/Oil Quench Post Weld Heat Treatment	8
4	Tensile Properties - Inertia Welded Inconel 718 - Room Temperature.	9
5	Tensile Properties - Inertia Welded Udimet 700	10
6	Tensile Properties - Inertia Welded Ti-6Al-4V	12
7	Stress Rupture Properties - Inertia Welded Inconel 718	13
8	Stress Rupture Properties - Inertia Welded Udimet 700	14
9	Stress Rupture Properties - Inertia Welded Ti 6Al-4V	15
10	Rotating Beam Fatigue Properties - Inertia Welded Inconel 718 - Room Temperature	16
11	Rotating Beam Fatigue Properties - Inertia Welded Ti-6Al-4V- Room Temperature	17
12	Rotating Beam Fatigue Properties - Inertia Welded Udimet 700 - Room Temperature	18
13	Inertia Welded Inconel 718 Four Inch OD Test Specimens	20
14	Inertia Welded Inconel 718 Test Cylinders - 12 Inch OD by 0.100 Inch Wall	21
15	Inertia Welded 24 Inch Diameter Inconel 718 Test Rings	22
16	Total Upset vs Energy - Four Inch Diameter Inconel 718 Test Rings	23
17	Total Upset vs Energy - 12 Inch Dia. Inconel 718 Test Rings	24
18	Total Upset vs Energy - 24 Inch Diameter Inconel 718 Test Rings.	25
19	Total Upset vs Energy - 24 Inch Dia. Inconel 718 Test Rings with 0.180 Inch Walls	26
20	Load X Energy versus Total Upset for Various Diameters and Wall Thicknesses of Inconel 718	27
21	Load X Energy for Zero Upset versus Weld Joint Area - Inconel 718	28
22	Microstructure of Inertia Weld Zone in 0.250 Inch Wall 4 Inch OD Inco 718 Test Specimen 8-28 (0.155 Inch Upset) Showing Duplex Parent Metal Structure, Sublayer Flow and Fine Grained Structure in Weld Interface (Hcl, H_2O, H_2O_2 Etch)	31
23	Photomicrograph of Inertia Weld Microstructure in Center of Weld Showing Equiaxed Recrystallized Grains in Weld Interface. Inconel 718 Test Rings 14-35, 12 Inch OD x 0.100 Inch Wall, Run No. 400-8-15, 0.189 Inch Total Upset	32
24	Photomicrograph of Heat Affected Zone Microstructure of 0.375 Inch Wall 4 Inch OD Inconel 718 Test Specimen 19-39 (0.134 Inch Upset) Showing Liquated Phases at the Grain Boundaries	33
25	Inertia Welded Joints - Effect of Etching and Surface Lighting	35
26	Electron Photomicrograph of Inertia Weld Interface in Inconel 718	37
27	Inco 718 Cold Formed by Impactor	39

LIST OF ILLUSTRATIONS (Cont.)

Figure		Page
28	Effort of Annealing on Microstructure of Cols Worked Inconel 718	40
29	Effect of Various Annealing Treatments on Microstructure of Cold Worked Inconel 718	43
30	Tensile Properties of Cold Worked Inconel 718 Cross Rolled Plate	44
31	Tensile Properties of Cold Worked and Heat-Treated Inconel 718 Cross Rolled Plate	45
32	Tensile Properties of Heat-Treated Inconel 718 Cross Rolled Plate	46
33	Tensile Properties of Cold Rim Formed (Rim Section) Inconel 718 Cross Rolled Plate	48
34	Tensile Properties of Cold Rim Formed (Web Section) Inconel 718 Cross Rolled Plate	49
35	Stress Rupture Properties of Cold Rim Formed Inconel 718 Cross Rolled Plate	50
36	Interrupted Low Cycle Fatigue Properties of Cold Rim Formed Inconel 718 Cross Rolled Plate	51
37	Rotating Beam Fatigue Properties of Cold Rim Formed Inconel 718 Cross Rolled Plate	52
38	Compressor Disc Blank Prior to Cold Forming	53
39	Mild Steel - Compressor Disc after Cold Forming	55
40	Sequence of Cold Rim Forming Operation	56
41	Configuration of Multi-Stage Compressor Rotor Inertia Welded from Cross Rolled Plate	57
42	Machine Layout - 42" x 50" Hydrospin	58
43	Tool Rings for Cold Forming Compressor Disc Rims	59
44	Cross Section of Work Area Before and After "Finish" Pass	60
45	Spread Configuration	64
46	Finish Configuration	64
47	Stage 15 Component During the "Angle" Operation	65
48	Stage 16 Component During "Angle" Operation	66
49	Stage 14 Disc After Rim Forming	66
50	Stage 15 Disc After Rim Forming	67
51	Stage 16 Disc After Rim Forming	68
52	Duplex microstructures of as-received Inconel 718 cross rolled plate	70
53	Recrystallized Structure of Plates after 1950+0-50°F/90 Min/AC Prior to Cold Rim Forming Step	71
54	Stage 14 Attachment Ring TF39	73
55	Finish Machined Cold Rim Formed Inco 718 Compressor Rotor Disc Stage 15	74
56	Stage 14 or 16 Disk TF39	75
57	Preweld Configuration of Attach. Ring - Stage 14	76
58	Preweld Configuration - Stage 14	77
59	Preweld Configuration - Stage 15	78
60	Preweld Configuration - Stage 16	79
61	Assembly Layout for Rotor Weld No. 1	81
62	Assembly Layout for Rotor Weld No. 2	82
63	Assembly Layout for Rotor Weld No. 3	83

LIST OF ILLUSTRATIONS (Cont.)

Figure		Page
64	Upset vs. Unit Energy in Inertia Welding Cold Rim Formed Inconel 718 Cross Rolled Plate	84
65	Photograph of Rotor 1 after Weld No. 2 Ready for Dimensional Inspection	85
66	Close-up View of Weld Flash of Rotor 1 after Weld No. 2	86
67	Close-up View of Weld Flash of Rotor 2 after Weld No. 3	87
68	Close-up View of Weld Flash of Rotor 3 after Weld No. 3	88
69	Photographs of Rotors, 1, 2, and 3 after Weld No. 3	89
70	Photograph of Rotor 4 after Weld No. 3	90
71	Close-up View Flash at Rotor 4 after Weld No. 3	91
72	Maximum Radial Displacements of Welded Rotor Stages	93
73	Close-up View of Rotor 1 after Machining Weld Flash	94
74	Forward View of Partially Machined Rotor No. 4	95
75	Aft View of Partially Machined Rotor No 4	96
76	Forward View of Finish Machined Rotor No. 4	98
77	Aft View of Finish Machined Rotor No. 4	99
78	Macrophotograph of Fracture Specimen from Rotor No. 3 Showing Spacer Wall Crack Originating at Outer Diameter	101
79	Macrophotograph of Fracture Specimen from Rotor No. 3 Showing Spacer Wall Crack Originating at Inner Diameter	102
80	Macrophotograph of Fracture Specimen from Rotor No. 3 Showing Complete Crack Penetration Through Spacer Wall	103
81	Photomicrograph of Intergranular Spacer Wall Crack in Rotor No. 3	104
82	Photomicrograph of Weld Flash of Test Weld No. 400-9-105 Showing Porosity and Cracks in Flash Curls	105
83	Forward View of Inertia Welded Rotor No. 5	108
84	Aft View of Inertia Welded Rotor No. 5	109
85	Close-up View of Weld Joints in Rotor No. 5	110
86	Forward View of Finish Machined Rotor No. 5	111
87	Aft View of Finish Machined Rotor No. 5	112
88	Close-up View of OD of Finish Machined Rotor No. 5	113
89	Stress Rupture Properties of 4 and 24 inch Diameter Inconel 718 Test Welds	115
90	Comparison of Low Cycle Fatigue Test Results of Inertia Welded Inconel 718 with TG39 Cyclic Test Requirements	116
91	Room Temperature Tensile Properties of Inconel 718 Forgings, As Rolled Plates and Rim Formed Plates	119
92	1200° F Tensile Properties of Inconel 718 Forgings, As Rolled Plates and Rim Formed Plates	120
93	1200° F - KSI Stress Rupture Properties of Forgings, As Rolled Plates and Rim Formed Plates	121
94	Labor Hour Reduction as a Function of the Learning Curve Phenomenon	128
95	Load and Flywheel Requirements for Welding Inconel 718 Rotors - 0.200 Inch Wall	129
96	Load and Flywheel Requirements for Welding Udimet 700 Rotors - 0.200 Inch Wall	130

Figure		Page
97	Load and Flywheel Requirements for Welding Ti-6Al-4V Rotors - 0.200 Inch Wall	131
98	Half Normal Probability Plot for Upset of Inconel 718 0.100 Inch Wall	198
99	Half Normal Probability Plot for Upset of Inconel 718 0.200 Inch Wall	199
100	Half Normal Probability Plot for Quality of Inconel 718 0.100 Inch Wall	200
101	Half Normal Probability Plot for Quality of Inconel 718 0.200 Inch Wall	201
102	Observed and Calculated Upset Values - Inconel 718 0.100 Inch Wall	202
103	Observed and Calculated Upset Values - Inconel 718 0.200 Inch Wall	203
104	Observed and Calculated Quality Rankings - Inconel 718 0.100 Inch Wall	204
105	Observed and Calculated Quality Rankings - Inconel 718 0.200 Inch Wall	205
106	Half Normal Probability Plot for Upset of Udimet 700	206
107	Half Normal Probability Plot for Quality Ranking of Udimet 700	207
108	Observed and Calculated Upset for Udimet 700	208
109	Observed and Calculated Quality Rankings for Udimet 700	209
110	Half Normal Probability Plot for Upset of Titanium 6Al-4V	210
111	Half Normal Probability Plot for Quality Ranking of Titanium 4V	211
112	Observed and Calculated Upset for Titanium 6Al-4V	212
113	Observed and Calculated Quality Ranking of Titanium 6Al-4V	213
114	Inertia Welded T58 Compressor Rotor - Inco 718	215
115	Inertia Welded F100 Rotor - Rene' 95	216

LIST OF TABLES

Table	Title	Page
I	Inconel 718 Test Specimen Weld Parameters	136
II	Udimet-700 Test Speciment Weld Parameters	137
III	Titanium 6A1-4V Test Specimen Weld Parameters	138
IV	Tensile Properties of Inertia Welded Inconel 718	139
V	Tensile Properties of Inertia Welded Udimet-700	140
VI	Tensile Properties of Inertia Welded Ti 6A1-4V	141
VII	Stress-Rupture Properties of Inertia Welded Inconel 718	142
VIII	Stress-Rupture Properties of Inertia Welded U-700	143
IX	Stress-Rupture Properties of Inertia Welded Ti 6A1-4V	144
X	Cyclic Rupture Properties of Inertia Welded Inconel 718, Udimet-700 and Ti 6A1-4V	145
XI	Room Temperature Rotating Beam Fatigue Properties of Inertia Welded Inconel 718, Udimet-700 and Ti 6A1-4V	146
XII	Parameters of Inertia Welding Study of 4-Inch Diameter Samples of Inco 718	147
XIII	Welding Parameters and Results for 12 and 24 Inch OD Inconel 718 Test Rings[1]	148
XIV	Welding Parameters and Results for 12 and 24 Inch OD Inconel 718 Test Disks[1]	149
XV	Tensile Properties of Inconel 718 Cross Rolled Plate	150
XVI	Tensile Properties of Inconel 718 Cross Rolled Plate Aged at 1250°F for 64 Hours	151
XVII	Tensile Properties of Cold Worked Inconel 718 Cross Rolled Plate	152
XVIII	Stress-Rupture Properties of Cold Worked Inconel 718 Cross Rolled Plate	153
XIX	Cyclic Rupture Properties - Cold Worked Inconel 718 Cross Rolled Plate	154
XX	Rotating Beam Fatigue Properties - Cold Worked Inconel 718 Cross Rolled Plate	155
XXI	Comparison of Tensile Properties of Double and Single Aged Inconel 718	156
XXII	Comparison of Single and Double Aged Inconel 718 Stress-Rupture Properties	157
XXIII	Comparison of Cyclic Rupture Properties of Double and Single Aged Inconel 718	158
XXIV	Mild Steel Component Process Development	159
XXV	Inconel 718 Process Development Results	160
XXVI	Cold Form Parameters -- 42 Inch X 50 Inch Cincinnati Hydrospin	162

LIST OF TABLES (Cont.)

Table	Title	Page
XXVII	Certificate of Chemical Analysis Inconel 718 Cross Rolled Plate	163
XXVIII	Certificate of Test Mechanical Properties[1] Inconel 718 Cross Rolled Plate	164
XXIX	Inconel 718 Cold Form Parameters - 42 Inch X 50 Inch Cincinnati Hydrospin	165
XXX	Inconel 718 Cold Forming Results	166
XXXI	Selection of Rotor Stages for Spool Assemblies	167
XXXII	Welding Parameters and Results for TF39 Stages 14-16 Rotor Spools[1]	168
XXXIII	Summary of Zyglo Inspection Results	169
XXXIV	Stock Removal at Weld Joints Prior to Aging Heat Treatment	170
XXXV	Summary of Weld Parameters and Results for Rotor No. 5	171
XXXVI	Tensile and Stress Rupture Properties of Parent Metal[1] and Weld Specimens[2] - Forged Stock	172
XXXVII	Effect of Post-Weld Treatments on 1200F Tensile and Stress Rupture	173
XXXVIII	Tensile Properties of TF39 Stg. 14-16 Forgings[1]	174
XXXIX	1200F Stress Rupture Properties of TF39 Forgings	175
XL	Tensile Properties of Cross Rolled Plate	176
XLI	1200F-100 Ksi Stress Rupture Properties of Cross Rolled Plate	177
XLII	Labor Summary Fabricated Vs. Forged Rotors on a Percentage Basis	178
XLIII	Labor Breakdown by Operation for Fabricated Rotors on Percentage Basis	179
XLIV	Comparison of Material Inputs-Fabricated Rotors vs. Forged Rotors on a Percentage Basis	180
XLV	Comparison of Material Costs-Fabricated Rotors vs. Forged Rotors on a Percentage Basis	181
XLVI	Inertia Welding Machine Parameters	182
XLVII	Inertia Welding Machine Capabilities	182
XLVIII	Inconel 718 Inertia Welding Parametric Studies	186
XLIX	Inconel 718 Inertia Welding Parametric Studies	187
L	Inconel 718 - 1.0 Inch O.D. X 0.1 Inch Wall Upset Measurements	188
LI	Inconel 718 - 1.0 Inch O.D. X 0.2 Inch Wall Upset Measurements	189
LII	Inconel 718 - 1.0 Inch O.D. X 0.2 Inch Wall Quality Ranking	190
LIII	Inconel 718 - 1.0 Inch O.D. X 0.2 Inch Wall Quality Rating	191
LIV	Udimet-700 Inertia Welding Parametric Studies	192
LV	Udimet-700 1.0 Inch O.D. X 0.1 Inch Wall Upset Measurements	193
LVI	Udimet-700 1.0 Inch O.D. X 0.1 Inch Wall Quality Ranking	194
LVII	Titanium 6AL-4V Inertia Welding Parametric Studies	195
LVIII	Titanium 6AL-4V 1.0 Inch O.D. X 0.3 Inch Wall Upset Measurements	196

LIST OF TABLES (Cont.)

Table	Title	Page
LIX	Titanium 6AL-4V 1.0 Inch O.D. X 0.3 Inch Wall Quality Ranking	197
LX	Stress in Rene' 95 Spool Inertia Welds Under Design and Test Loadings	219

SECTION I

INTRODUCTION

Significant savings in weight and improvement in reliability of advanced jet engine compressor rotors are realized from integral multistage rotors as compared to assemblies of individual stages bolted together. Present methods of manufacturing integral rotors by necessity start with a bulky forging and machine away the excess metal to obtain the desired configuration. This practice is extremely wasteful of material for as much as 90 weight percent of the forging can be converted to chips and turnings, depending on the rotor design.

The principal objective of this program was to provide an improved fabrication method based on inertia welding individual discs together to form an integral multistage rotor. The primary benefits anticipated from this approach were:

1. Maximum utilization of expensive material produced at minimum cost by using cross rolled plate for disc fabrication.

2. Solid state bonded joints with mechanical properties equal to or better than parent metal.

3. More uniform properties throughout the rotor by using heavily worked cross rolled plate in place of bulky forgings.

The specific objectives established by contract were:

1. Determine the inertia welding process parameters for the jet engine disc alloys Inconel 718, Ti-6Al-4V, and Udimet 700, and obtain mechanical properties of welds made by optimum parameters.

2. Determine the processing parameters for Inconel 718 cross rolled plate that has been cold formed from 5 to 40%. The purpose of the cold forming is to add configuration to a plate to make a disc geometry.

3. Fabricate a TF39 Stage 14-15 compressor rotor from cold formed cross rolled Inconel 718 plate by inertia welding.

4. Evaluate the applicability of the fabricated rotor process developed to engine designs and the effect on plant and suppliers' facilities.

The overall program was broken down into three phases: Phase I was the development of inertia welding parameters and the processing of cold worked Inconel 718 cross rolled plate. Phase II was the manufacturing of engine parts. Phase III was the evaluation of the applicability of the overall system.

SECTION II.

INERTIA WELDING PROCESS

Inertia welding is a solid state welding process which produces bonding from frictional heating obtained from rubbing two mating surfaces held together under pressure. The process is based on rotating one part at relatively high controlled speeds against a stationary member to which it is to be joined.

Inertia welding uses a stored and predetermined amount of rotational kinetic energy applied to one workpiece, plus axial pressure to weld onto a stationary second workpiece. The main part of the energy is converted to heat by frictional rubbing of the workpieces at the interface; the balance is converted to mechanical energy in forging an upset weld. Any liquification that may occur is expelled along with surface oxides, contaminates and the most plastic solid metal into a flash formed by the upset.

In application a flywheel with a known moment of inertia and the rotating workpiece are accelerated to a predetermined angular velocity, disconnected from the drive mechanism and pressed against the stationary workpiece under a heavy and constant axial thrust. The kinetic energy stored in the rotating mass is rapidly converted to frictional heat at the interface. Initial bonding occurs as soon as the critical peripheral speed for the material being welded is attained. Torque buildup begins and rises to a peak as the flywheel slows down and coalescence occurs across the weld interface. During this final stage the material in the weld interface is worked mechanically to a very high degree and practically all the upsetting occurs during this instant of vigorous forging action.

There are three welding parameters that are interrelated. They are: initial sliding velocity at the faying surface which relates to the flywheel - spindle RPM and the weld diameter; the moment of inertia of the flywheel - spindle system; and the axial thrust force in psi at the weld interface. If RPM and inertia mass are considered weld parameters, then the weld energy is defined by the equation

$$E_K = \frac{WK^2 (RPM)^2}{5873}$$

where E_K is the input energy in foot-pounds, W is the weight of the flywheel system in pounds, K is the radius of gyration in feet, and the constant accounts for the conversion of mass to weight through g and from revolutions per second to RPM. The work done by applying axial pressure in upsetting is small by comparison and is usually neglected.

With an established flywheel size there are only two parameters to control, thrust and speed, which leads to good process reproducibility. Once correct weld conditions have been established based on mechanical property tests, microexamination, visual examination of the size and nature of the flash and nondestructive inspections, the amount of weld upset by length reduction of the weldment is the basic quality control technique for welds. Any large differences in upset will usually indicate a machine malfunction or some change in the workpieces.

SECTION III.

INERTIA WELDING STUDIES

A. PARAMETRIC STUDIES

A statistical testing plan designed to analyze the interactions of the process variables with a minimum of testing was used in parametric studies of inertia welding Inconel 718, Udimet 700 and Ti-6A1-4V. The plan was based on a 3 x 2 x 3 factorial experiment with the factors tested at unequally spaced levels. The variables selected were three levels of flywheel moment of inertia, two levels of surface speed and three levels of pressure.

Weld quality rankings were assigned numerical sequence ratings from 1-18 with number 1 ranking being best and number 18 being the worst. Weld quality was based on the following criteria:

- Visual Examination
  - Flash appearance - cracked or smooth
  - Uniform or irregular flash
  - Temperature appearance of the flash
- Upset Measurements
- Metallographic Examination
  - Continuous bond or discontinuous bonding
  - Uniformity of heat affected zone.

The analytical method used was a variation of Yates algorithm for two level experiments. Since this method is strictly applicable only to equally spaced factor levels, the significant coefficients were adjusted for the unequal spacing. Since the design is completely orthogonal regardless of spacing, the method was statistically valid. The Yates algorithm also includes an inverse calculation which, when applied to the significant coefficient and the mean value, yielded a best fit equation for the test conditions.

The procedure used to analyze the data and a complete summary of the results are contained in Appendix II. The significant results for each alloy studied are presented below.

1. Inconel 718 - The parametric study of Inconel 718 was done on one inch O.D. x 0.100 and 0.200 inch wall cylinders using the following parametric ranges:

Moment of inertia	4.4 to 19.5 lb-ft^2
Angular velocity	1600 to 7200 RPM
Surface velocity	420 to 1900 SFM
Upset pressure	32 to 48 ksi
Actual energy input	23,300 to 38,900 ft-lbs/in^2

Statistical analysis of the test data showed that flywheel moment of inertia had little influence on the amount of upset or weld quality. The best welds were made with angular velocity and ram pressure at the low end of their ranges, i.e. actual energy inputs of 23,300 to 24,400 ft-lbs/in^2 and upset pressures of 32 and 38 ksi.

2. Udimet 700 - One inch O.D. x 0.100 inch wall cylinders of Udimet 700 were inertia welded using the following parametric ranges:

Moment of inertia	3.9 to 19.0 lb-ft^2
Angular velocity	1600 to 5200 RPM
Surface velocity	420 to 1400 SFM
Upset pressure	32 to 48 ksi
Actual energy input	25,100 to 38,800 ft-lb/in^2

Similar to the Inconel 718 results, statistical analysis of the data showed moment of inertia was not very significant and the best welds were made with the low energy inputs and upset pressure, 25,000 ft-lbs/in^2 and 32 to 38 ksi respectively.

3. Ti-6A1-4V - One inch O.D. x 0.300 inch wall cylinders were inertia welded using the following parametric ranges:

Moment of inertia	1.8 to 3.9 lb-ft^2
Angular velocity	5000 to 8000 RPM
Surface velocity	1310 to 2100 SFM
Upset pressure	4.5 to 9.0 ksi
Actual energy input	4,800 to 30,400 ft-lbs/in^2

The statistical analysis indicated upset pressure was least significant while moment of inertia and angular velocity were significant. Best welds were made at low energy levels, 6700 to 12,800 ft-lbs/in^2.

B. MECHANICAL PROPERTIES OF INERTIA WELDS

1. Test Specimen Preparation

(a) Inconel 718 - Test specimens for tensile, stress rupture and low cycle fatigue testing were machined from two of the inertia welded four inch O.D. by 0.290 inch wall cylinders shown in Figure 1. Weld parameters are listed in Table I.

Prior to welding the cylinders were solution treated and aged: 1775°F/1 hr/AC + 1325°F/8 hr/FC to 1150°F @ 100°F per hr + 1150°F/8 hr/AC. After welding and flash removal the cylinders were re-aged at 1325° and 1150°F and then given an additional 64 hours at 1250°F to conform to the heat treatment developed at that time for cross rolled plate.

Test specimens for rotating beam fatigue testing were machined from inertia welded 0.800 inch O.D. solid bars since the walls of the four inch O.D. cylinders were too thin to obtain rotating beam specimens. The weld parameters used were:

Flywheel WK^2, lb-ft^2	19.0
RPM	3000.0

SFM	314
Max input energy ft-lbs/in^2	48,200.0
Upset pressure, psi	40,000.0
Total upset, inch	0.093

The same heat-treat cycles were used as for the four inch O.D. cylinders both before and after welding.

(b) Udimet 700 - All test specimens were machined from inertia welded 0.875 inch diameter solid cylinders, Figure 2. Weld parameters are listed in Table II. As shown in Table II, two different post weld heat treatments were used. After finding parent metal quench cracks in oil quenched specimens, Figure 3, a salt quench was used effectively to prevent cracking.

(c) Titanium 6Al-4V - All test specimens were machined from inertia welded one inch diameter solid cylinders. The weld parameters are listed in Table III. Test specimens were given one of two heat treatments:

- 1300° F/2 hr/AC + weld + test
- 1300° F/2 hr/AC + weld + 1750° F/1 hr/WQ + 1300° F/2 hr/AC + test

2. Test Results

(a) Tensile Properties

(1) Inconel 718 - Smooth, notched and radius tensile results for parent metal and inertia welded specimens are listed in Table IV and plotted in Figure 4 with General Electric average design book curves for comparison purposes. As shown in Figure 4, smooth bar weld properties correspond well with the average design book curves. Except for yield strength they also equal parent metal values. The strength and ductility of the 0.083 inch upset weld was markedly lower than that of the 0.220 inch upset weld. Specimens from both welds failed mainly in the heat affected zone or at the weld line. This generally indicates welds with some defect in structure. Metallographic examination of both weld joints showed evidence of localized grain boundary melting in the heat affected zones. The high temperature notch strength appeared to be affected significantly. Room temperature radius bar results where the weld is in the area of maximum stress do not indicate these particular welds were significantly stronger than parent metal.

(2) Udimet 700 - Smooth bar results are plotted in Figure 5 with GE average design book curves for comparison. Table V lists smooth, notched and radius bar results. As shown in Figure 5 the smooth bar weld tensile properties are equivalent to design book values except for the 1500° F results. The incidence of quench crack failures limited the amount of valid test data. Notched bar results appear to be somewhat low. Radius bar values are slightly higher than smooth bar values.

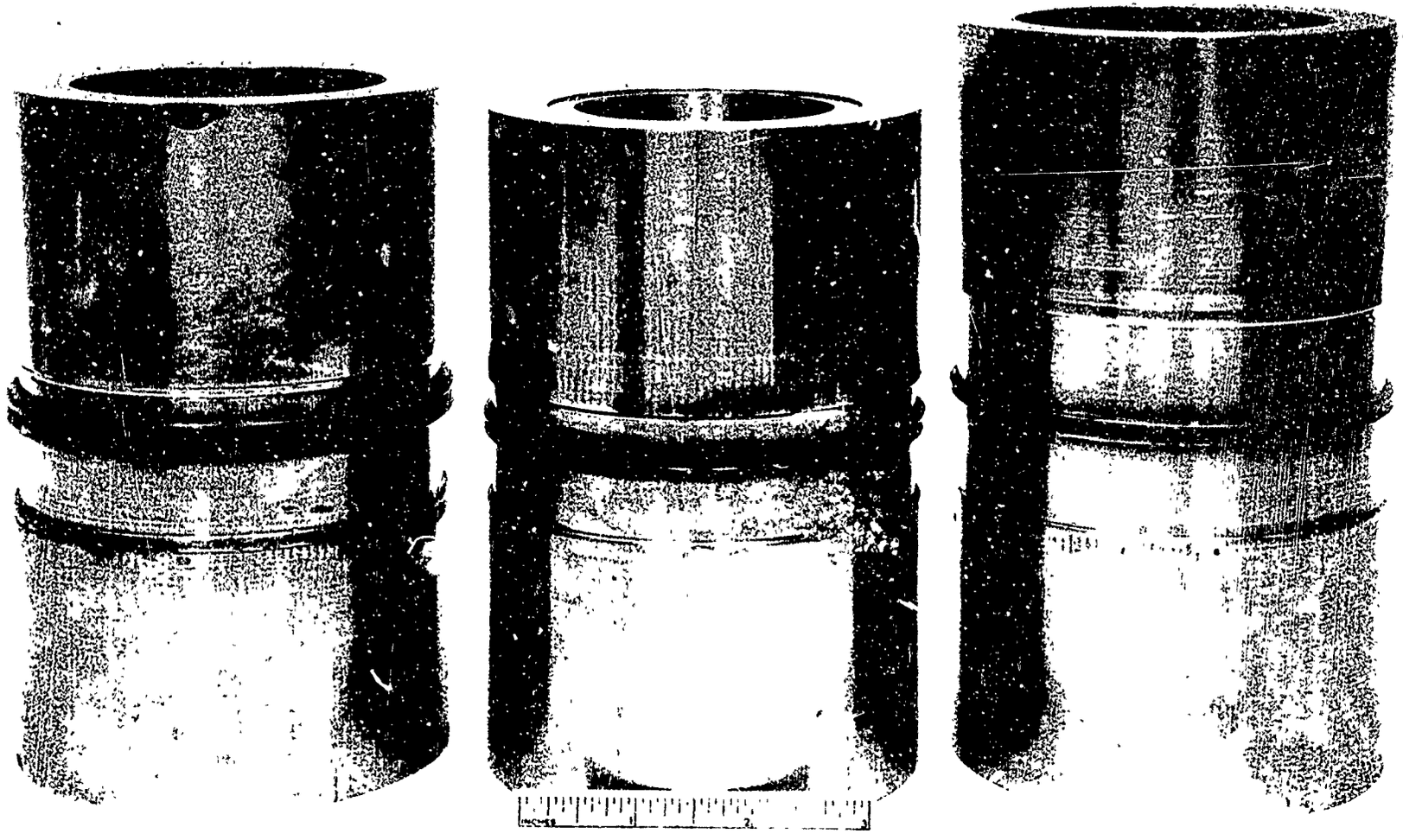

Figure 1. Inertia Welded Inconel 718 Test Cylinders

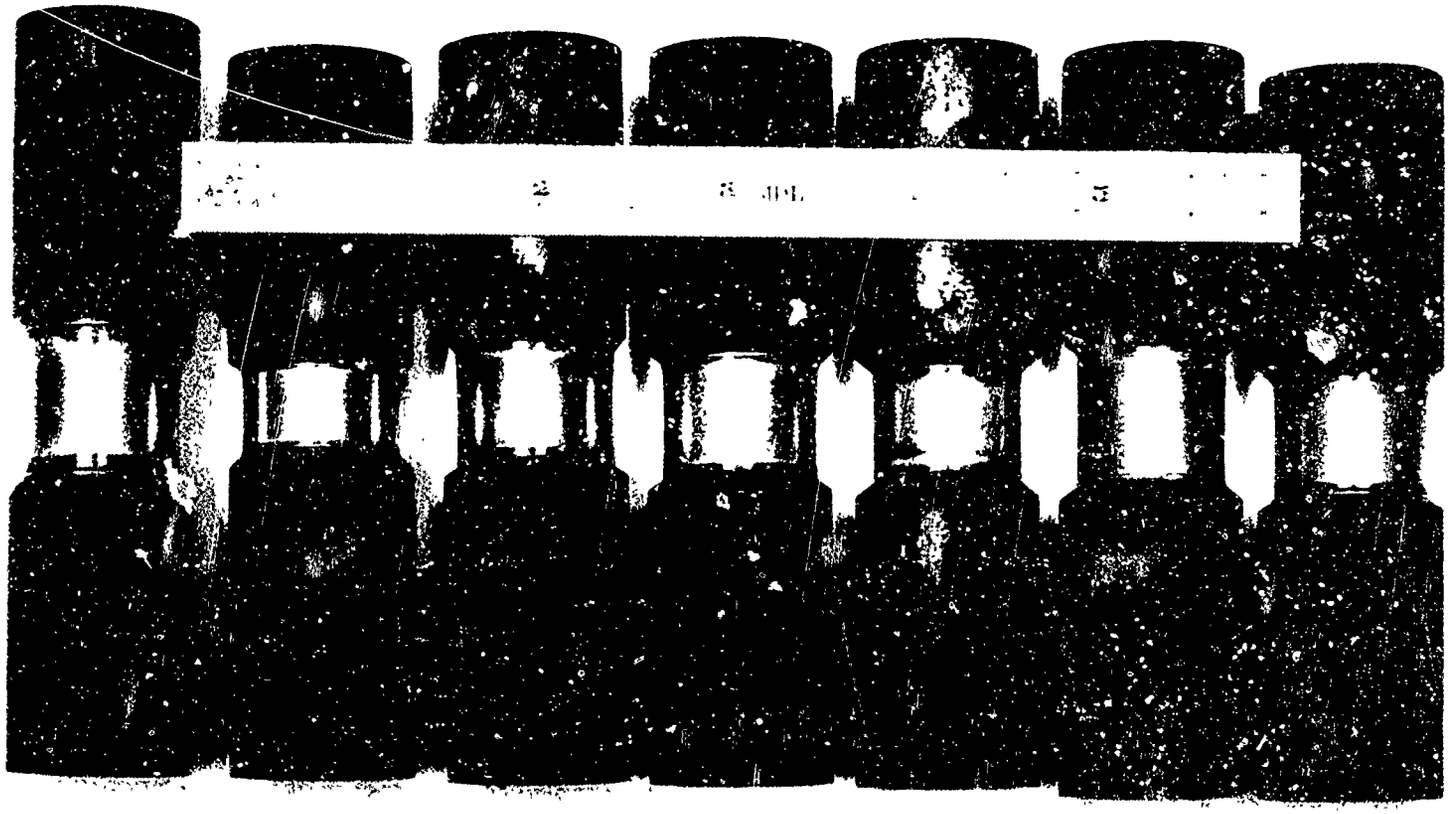

8-54 8-56 8-57 8-58 8-59 8-53 8-64

Figure 2 Inertia Welded Udimet 700 Test Cylinders

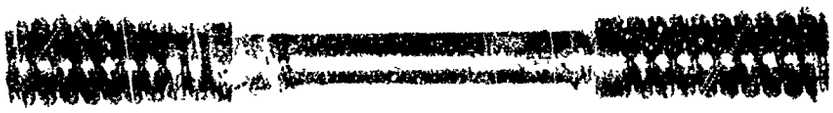

Neg. C68091709 Mag. 2X

Weld No. 8-57-2. 1200°F Smooth Tensile Test. Failure occurred away from weld with weld located in the center of the gage section.

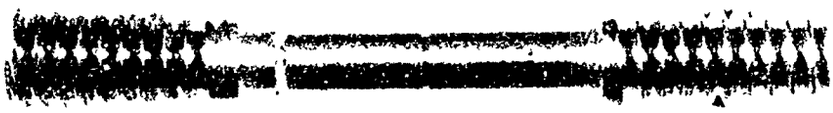

Neg. C68091710 Mag. 2X

Weld No. 8-58-C. R.T. notched tensile test. Weld is located at the notch in the gage section. Failure occurred at a quench crack in the bar away from weld.

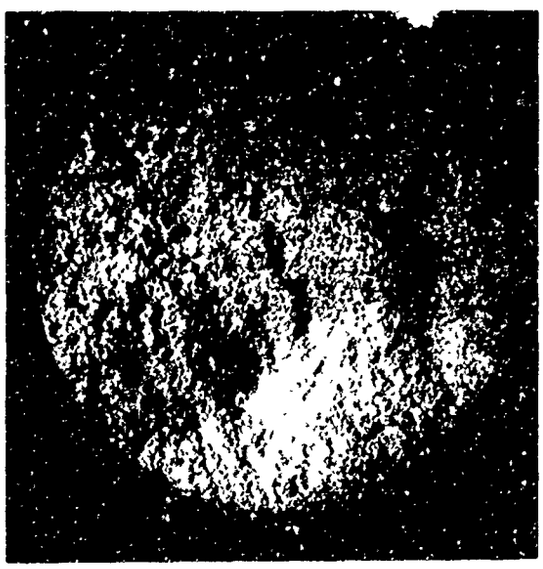

Fracture face of specimen which broke during machining. Dark area represents quench crack. Light area represents fracture.

Figure 3 Quench Crack Failure resulting from 2100°F/4 Hr/Oil Quench Post Weld Heat Treatment

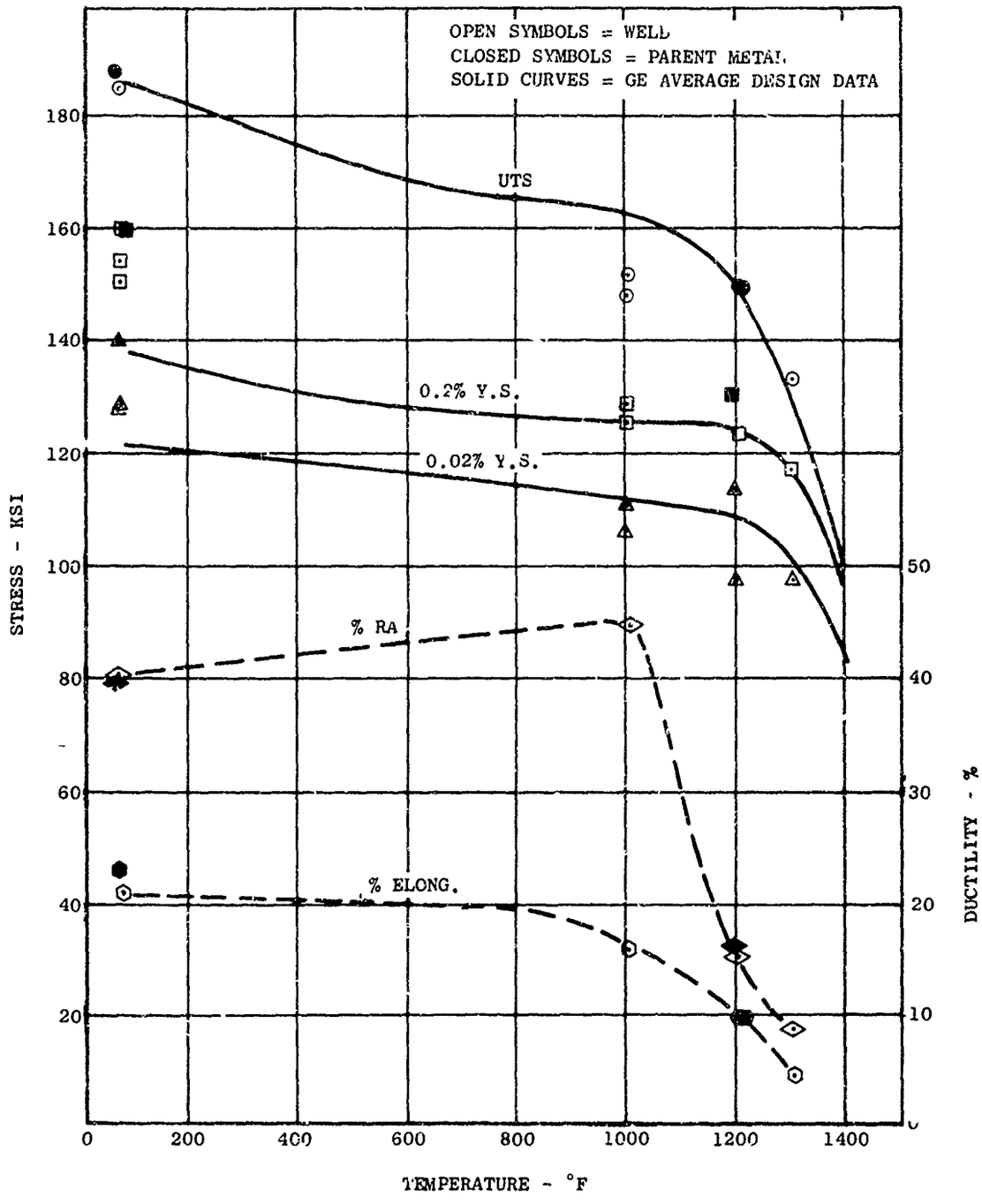

Figure 4 Tensile Properties - Inertia Welded Inconel 718 - Room Temperature

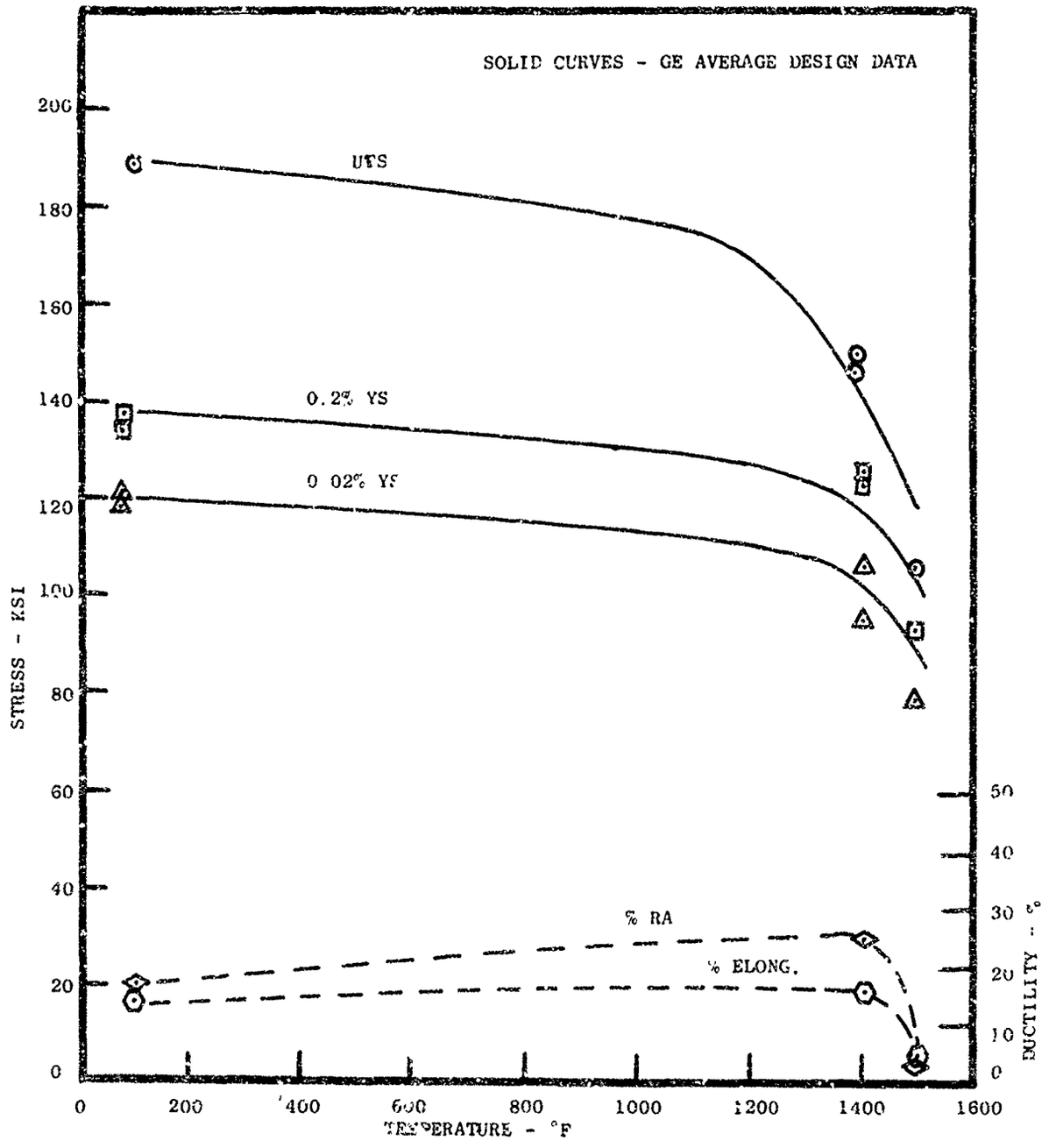

Figure 5 Tensile Properties - Inertia Welded Udimet 700

(3) Titanium 6Al-4V - Smooth bar results are plotted in Figure 6 with GE average design book curves for comparison. Table VI lists all the tensile properties. The smooth bar properties are equivalent to the design book curves except for being lower in 0.2% yield strength. Notched bar results appear very good. The radius bar results show the weld itself to be significantly stronger than the parent metal.

(b) Stress Rupture Properties

(1) Inconel 718 - Table VII and Figure 7 summarize the results obtained for Inconel 718. Although no test samples met the GE specification of 25 hour minimum life at 1200°F and 100 ksi stress, the time temperature parameter plot, Figure 7, indicates the majority (5 out of 7) of the data points fall within three deviation units of the average design book curve.

(2) Udimet 700 - Table VIII and Figure 8 summarize the results obtained for Udimet 700. As in the case of Inconel 718 no test sample met the GE specification of 30 hour minimum life at 1400°F and 85 ksi stress. However, the time temperature parameter plot, Figure 8, shows half the data points within 3 deviation units of the average design book curve. Three of the four data points falling below the lower 3 sigma curve were parent metal failures.

(3) Ti-6Al-4V - Initially, two test specimens were tested to the GE C50TF12 stress rupture specification of 170 ksi at room temperature. Both of these specimens failed on loading. The next two specimens were then step loaded beginning at 155 ksi, increasing 5 ksi every 5 hours. Both specimens failed at 160 ksi. Table IX and Figure 9 summarize the test results. The time temperature parameter plot shows the elevated temperature test results are above the average design book curve.

(c) Cyclic Rupture Properties - Table X summarizes cyclic rupture test results for all three alloys. None of the Inconel 718 weld specimens approached the cyclic life performance of the parent metal test specimens. The presence of liquated grain boundaries in the heat affected zones is believed responsible for this significant reduction in low cycle fatigue strength.

Since no parent metal Udimet 700 and Ti-6Al-4V test specimens were tested and no other comparable data is available the Udimet 700 and Ti-6Al-4V test results are simply presented for record purposes.

(d) Rotating Beam Fatigue Properties - Room temperature rotating beam fatigue test results for the three alloys are presented in Table XI and Figures 10, 11 and 12. All three alloy weld specimens showed better results than existing data for the parent metals. The Inconel 718 weld specimens also showed better fatigue properties than the parent metal specimen tested.

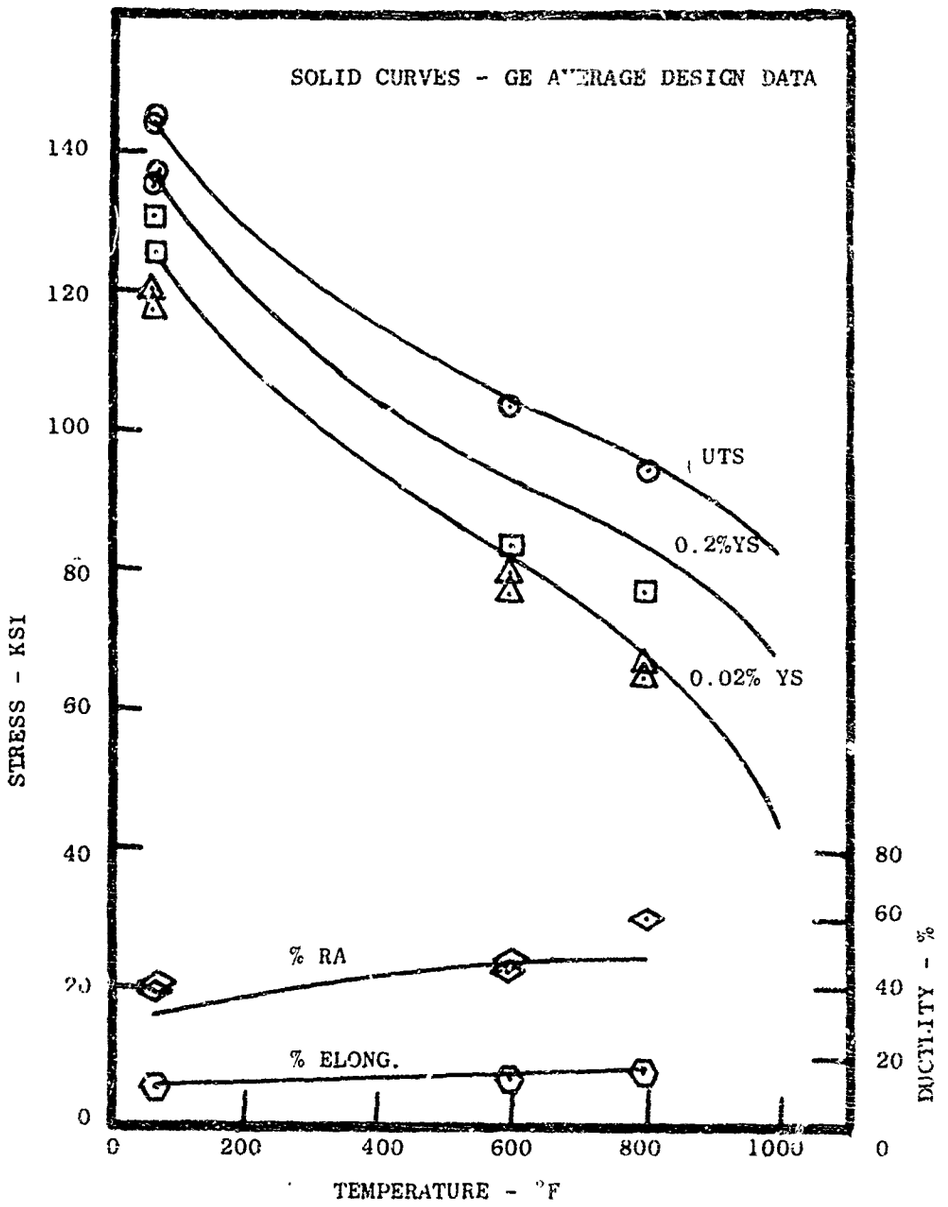

Figure 6 Tensile Properties - Inertia Welded Ti-6Al-4V

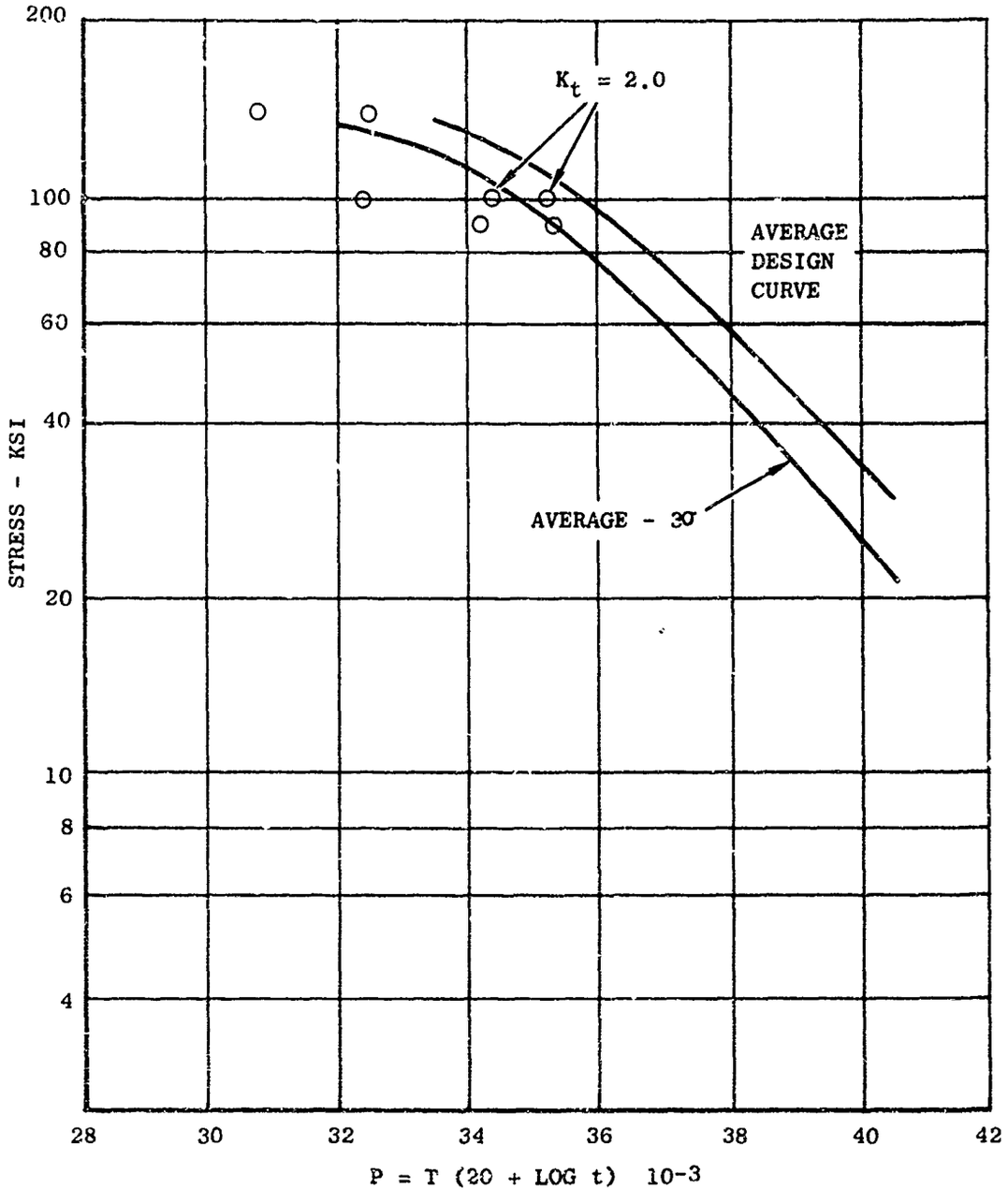

Figure 7 Stress Rupture Properties - Inertia Welded Inconel 718

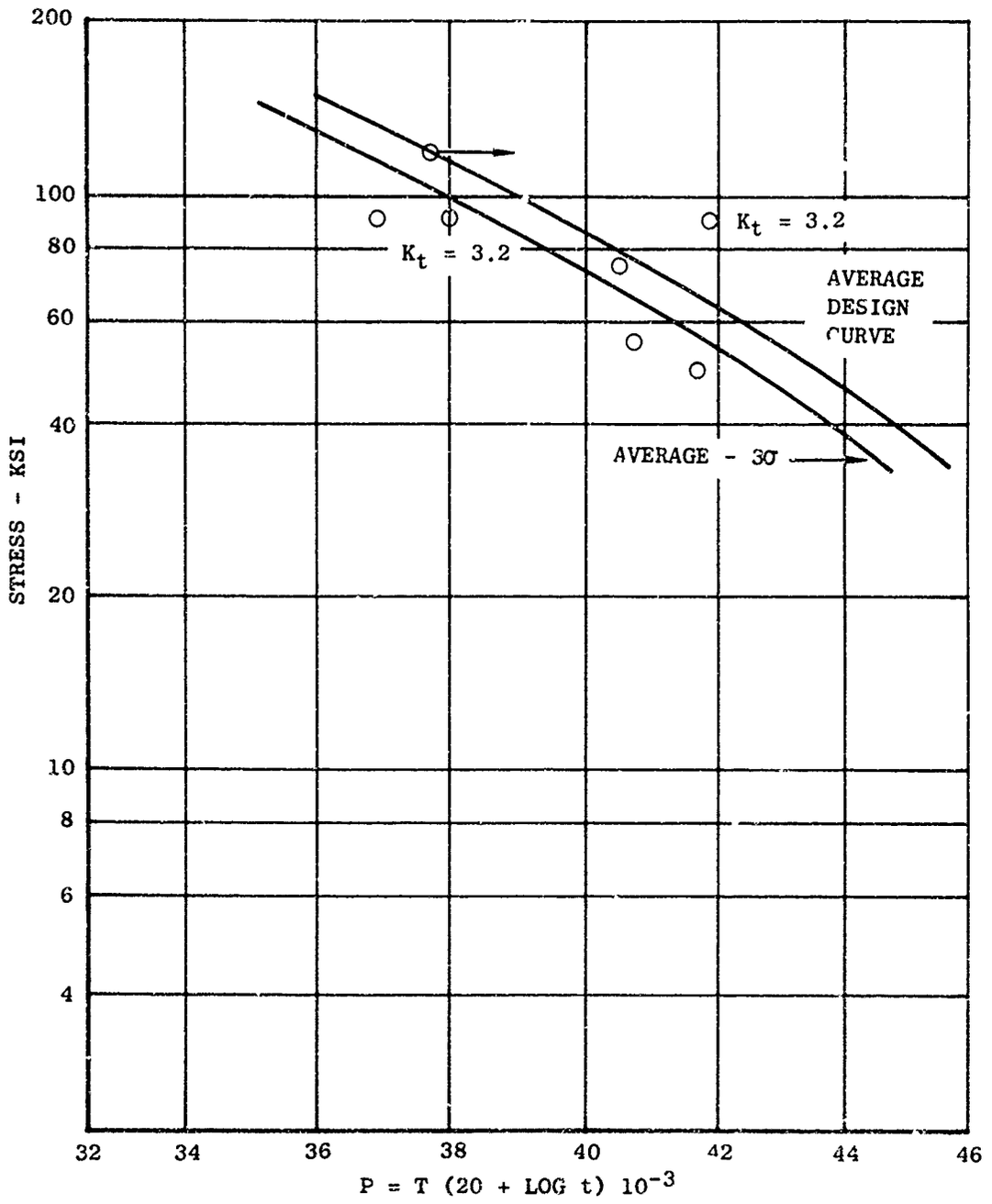

Figure 8 Stress Rupture Properties - Inertia Welded Udimet 700

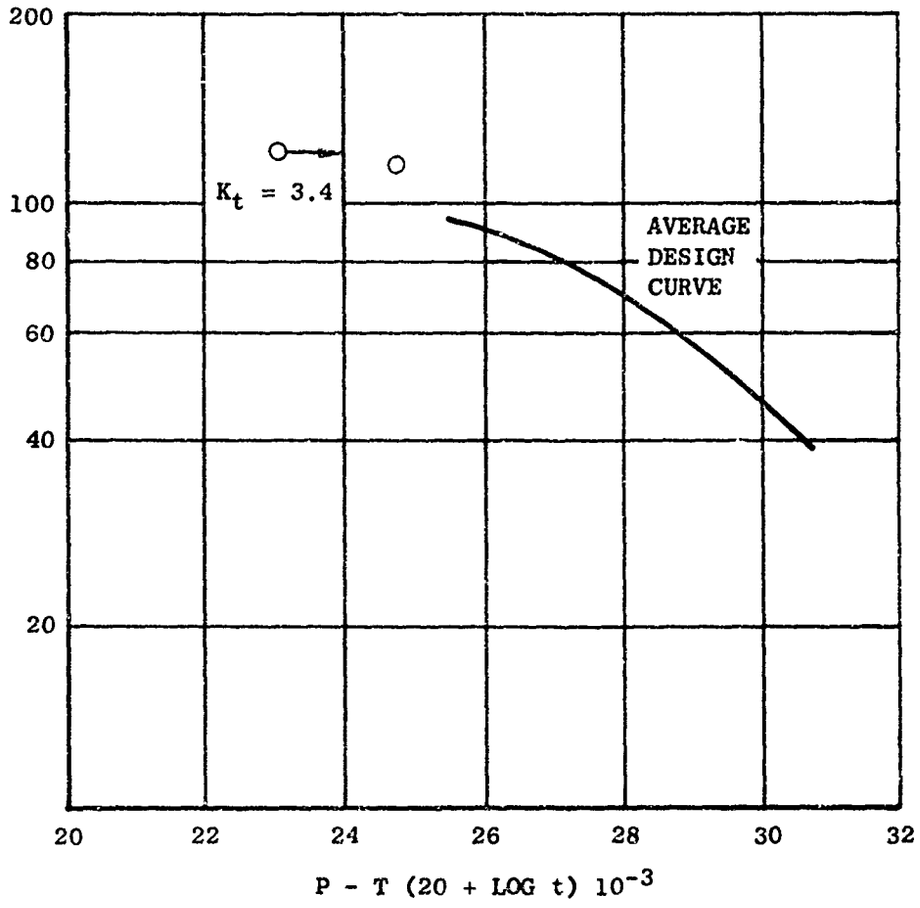

Figure 9 Stress Rupture Properties - Inertia Welded Ti 6Al-4V

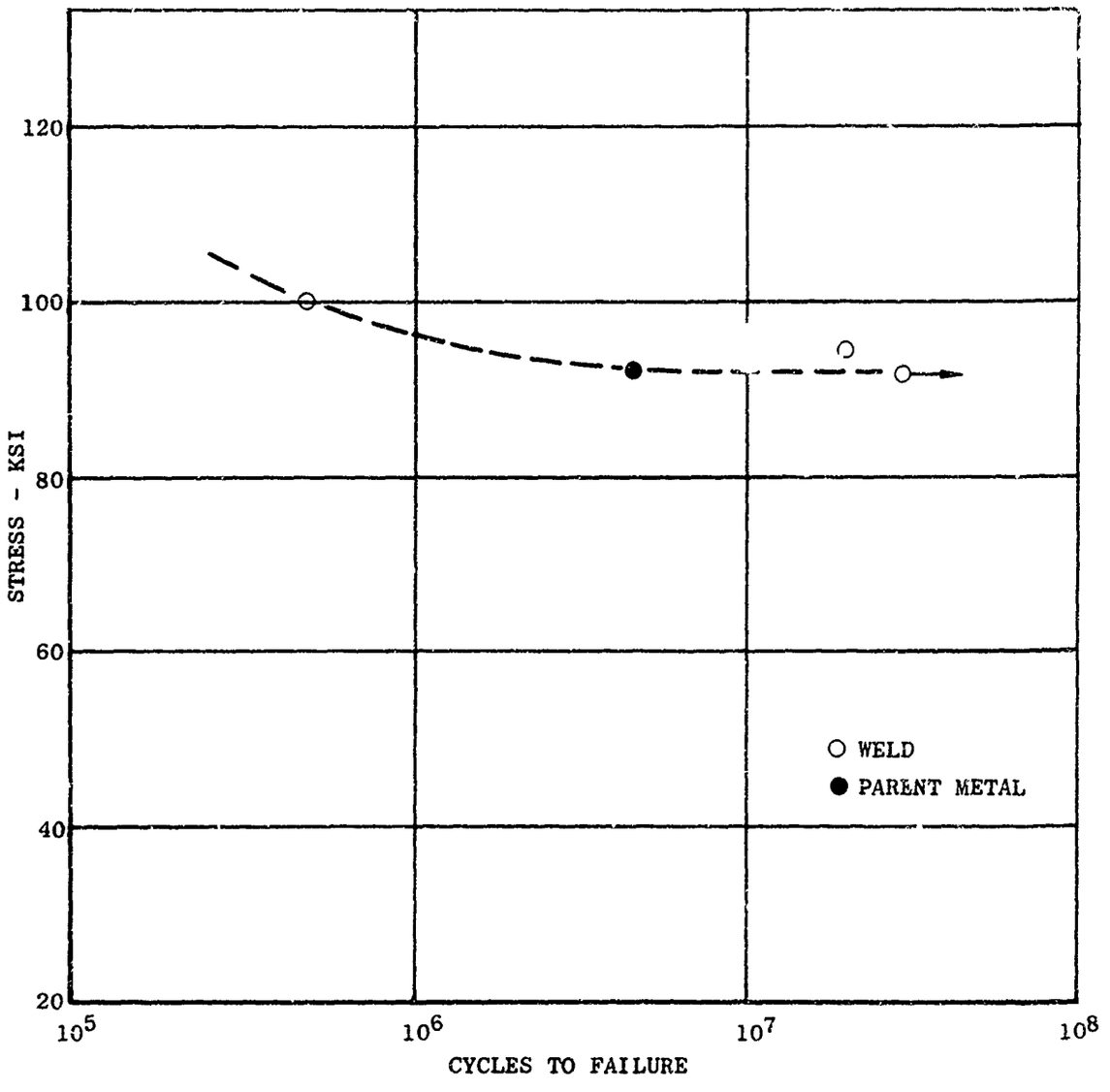

Figure 10 Rotating Beam Fatigue Properties - Inertia Welded Inconel 718 - Room Temperature

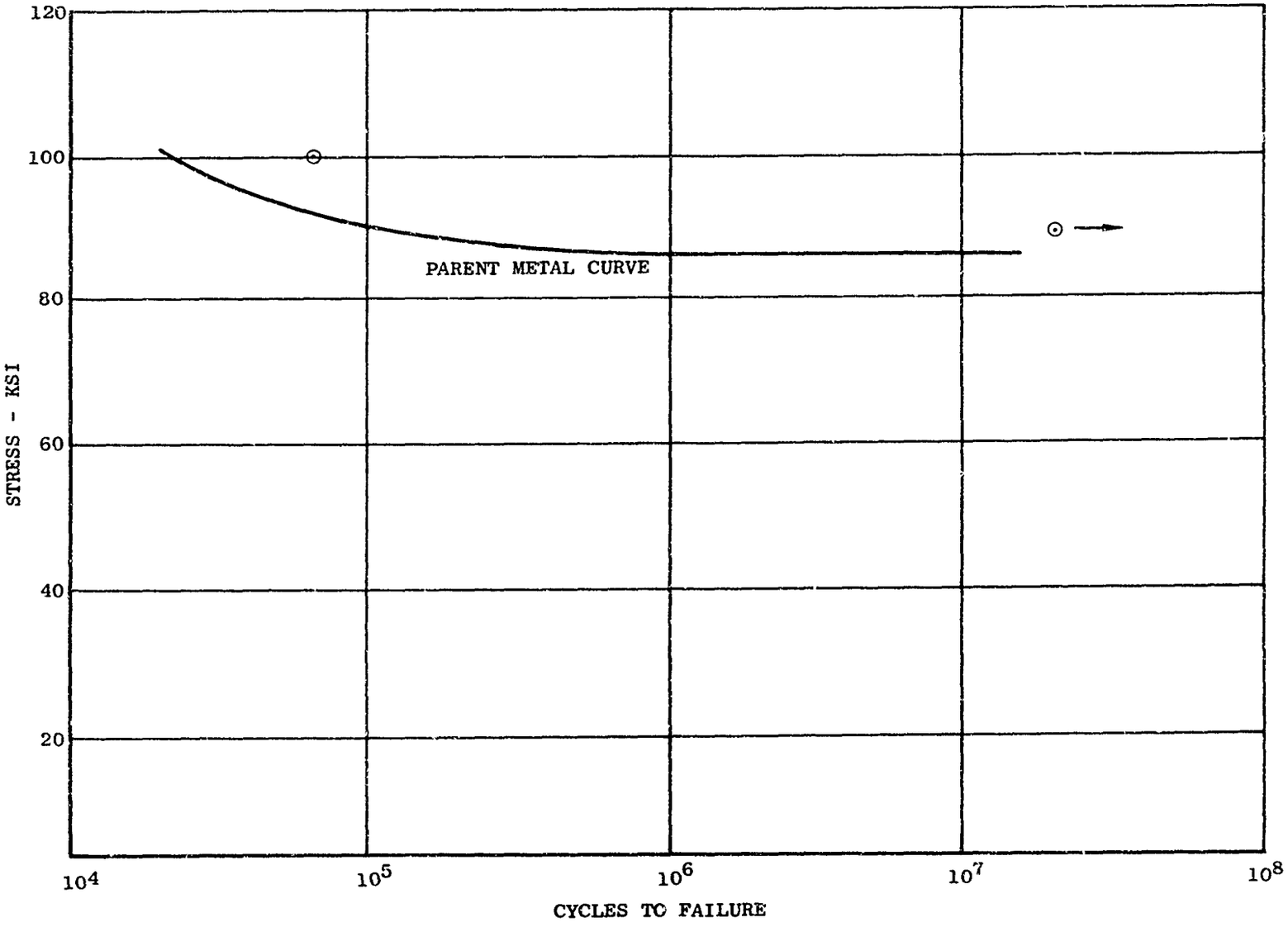

Figure 11 Rotating Beam Fatigue Properties - Inertia Welded Ti-6Al-4V-Room Temperature

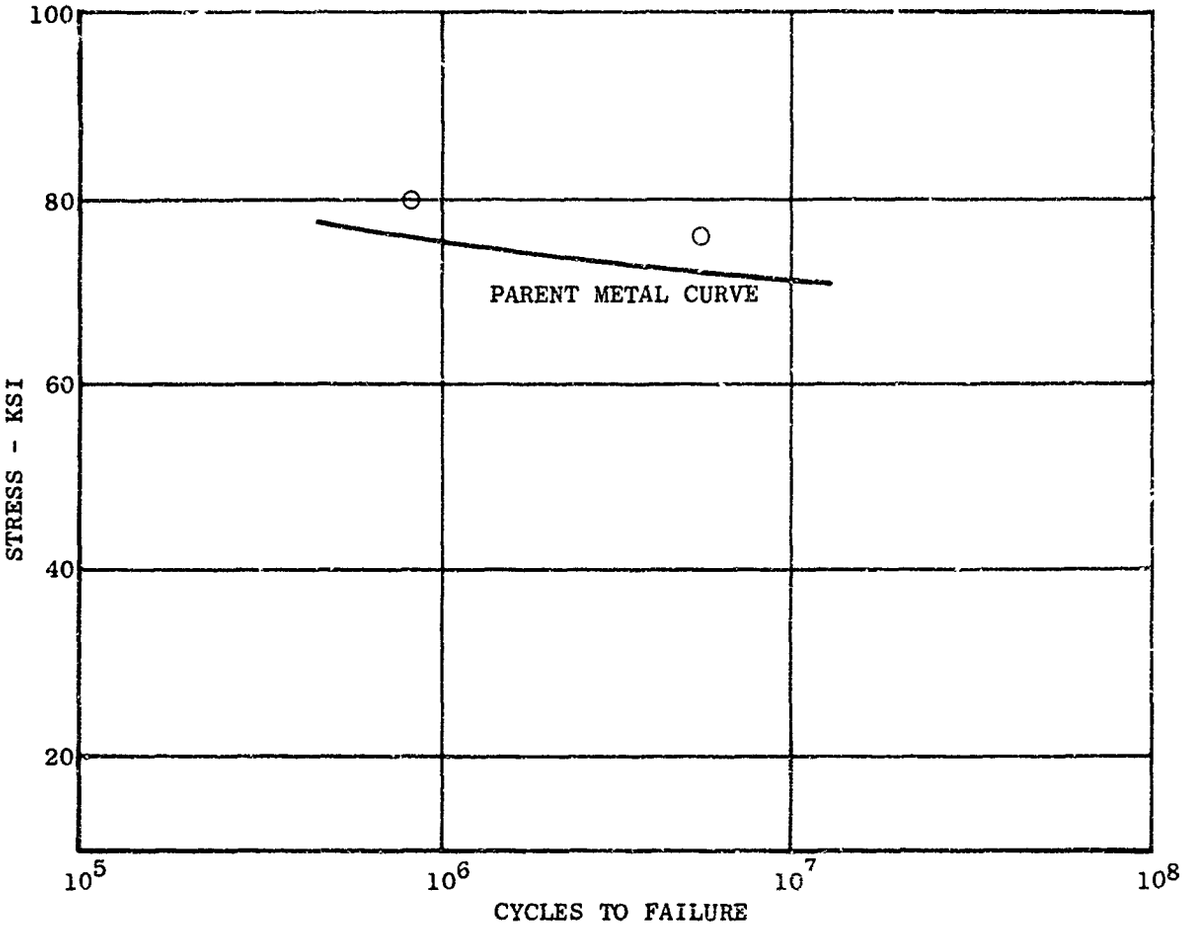

Figure 12 Rotating Beam Fatigue Properties - Inertia Welded Udimet 700 - Room Temperature

C. INCONEL 718 DIAMETER AND WALL THICKNESS STUDY

To determine the effect of diameter and wall thickness on the amount of upsetting obtained under various energy inputs and contact pressures, 4, 12, and 24 inch diameter cylinders of various wall thicknesses were prepared. Inertia welding parameters were varied by changing ram loads, flywheel moments of inertia and contact welding speeds. Wall thicknesses ranged from 0.070 to 0.375 inch. All cylinders were solution treated and aged before welding. In addition to determining the amount of upset, selected weldments were zyglo and ultrasonically inspected and sectioned for metallographic analysis.

All four inch diameter specimens were welded on a Caterpillar Model 250 machine while the 12 and 24 inch diameter cylinders were welded on a Caterpillar Model 400 inertia welder. A square hub configuration was used to drive and hold the four inch diameter samples. Splines machined on the periphery of 24 inch diameter steel back-up discs were used for driving and holding the 12 and 24 inch diameter cylinders. Steel pilots and bronze bushings were used to assist in maintaining alignment during welding. The weld preps of all specimens were geometrically similar, i.e., the weld preps were nominally 0.150 inch in length and the wall thicknesses of mating weld preps differed by 0.015 to 0.020 inch. Typical welded specimens are shown in Figures 13, 14 and 15.

1. Welding Parameter Study Results - Upsets obtained for the various diameters and wall thicknesses with different welding parameters are listed in Tables XII, XIII and XIV. Initial attempts to correlate upset, diameter and wall thickness with energy input and contact pressure led to the plots shown in Figures 16, 17, 18 and 19 of upset as a function of unit energy input.

These plots showed: (1) for a given diameter, wall thickness and contact pressure, the total upset appeared to be a straight line function of the unit energy input; (2) the slopes of the straight lines appeared to be nearly the same and (3) upset pressure and unit energy input varied inversely for a given upset. Pre-selection of process parameters based on such data would require multiple sets of parametric curves to cover the ranges of diameter, wall thickness, unit energy input and upset pressure. Since energy and pressure appeared to vary inversely with total upset the product of total load and total energy input (corrected for efficiency) was plotted for each diameter and wall thickness as a function of total upset on semi-logarithimic coordinate paper. As shown in Figure 20 most of the data points for a given diameter and wall thickness (weld joint area) fall on straight lines of the same slope having the general equation:

$$y = C \cdot 10^{mx} \qquad (1)$$

where y = load total energy = $L \cdot E_t$
x = total upset = U
C = value of y at $x = 0$
m = slope + scale value of the paper = $.126/.09 = 1.4$

Values of C for each diameter and wall thickness were then plotted on logarithmic coordinate paper as a function of weld joint area, Figure 21. The equation of the straight line was determined to be:

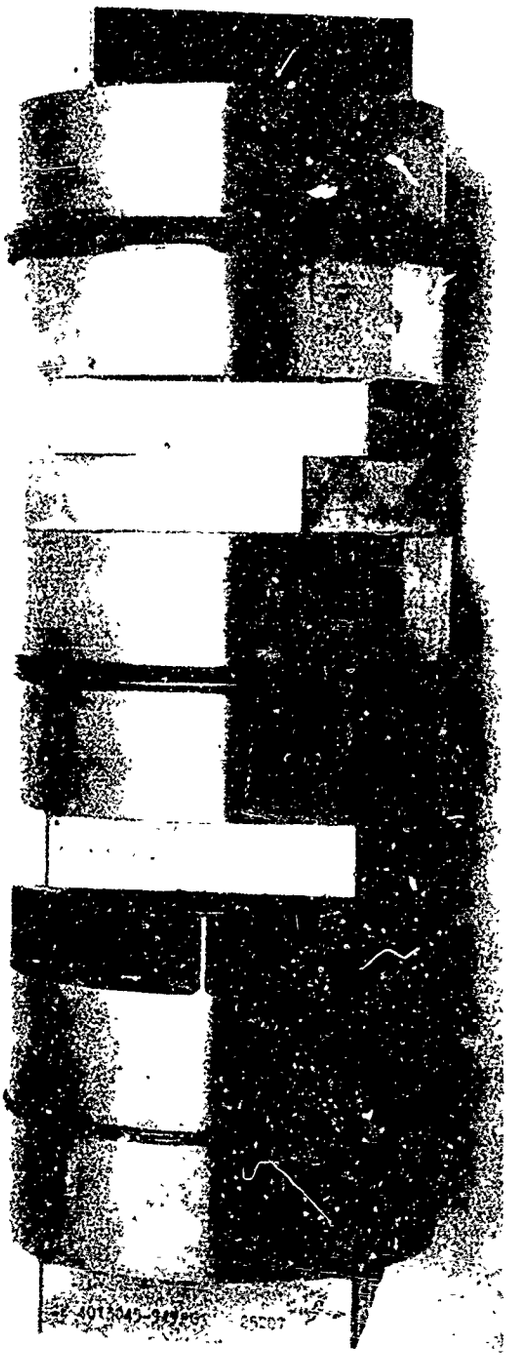

Figure 13 Inertia Welded Inconel 718 Four Inch OD Test Specimens

Figure 14. Inertia Welded Inconel 718 Test Cylinders - 12 Inch OD by 0.100 Inch Wall

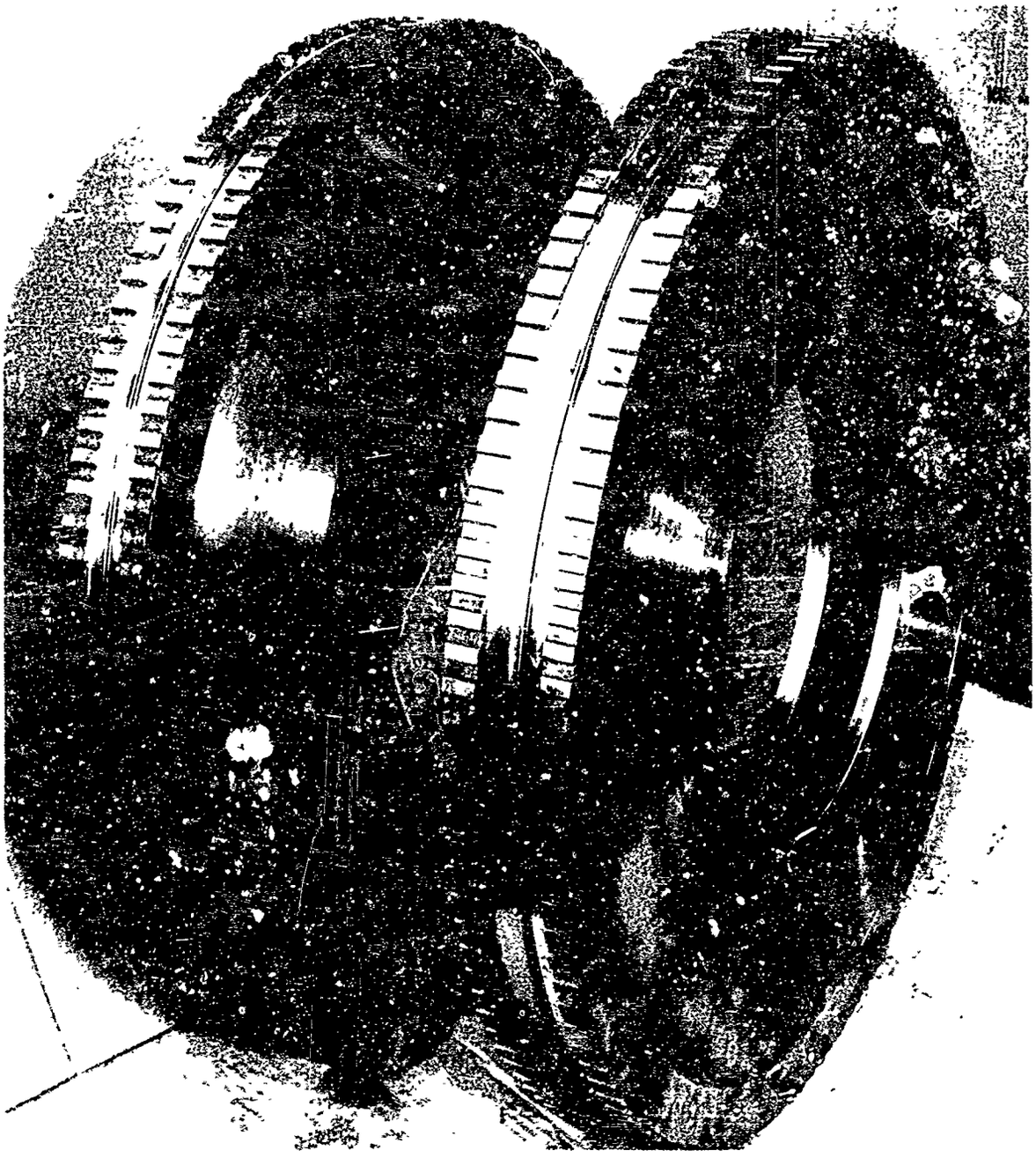

Figure 15. Inertia Welded 24 Inch Diameter Inconel 718 Test Rings

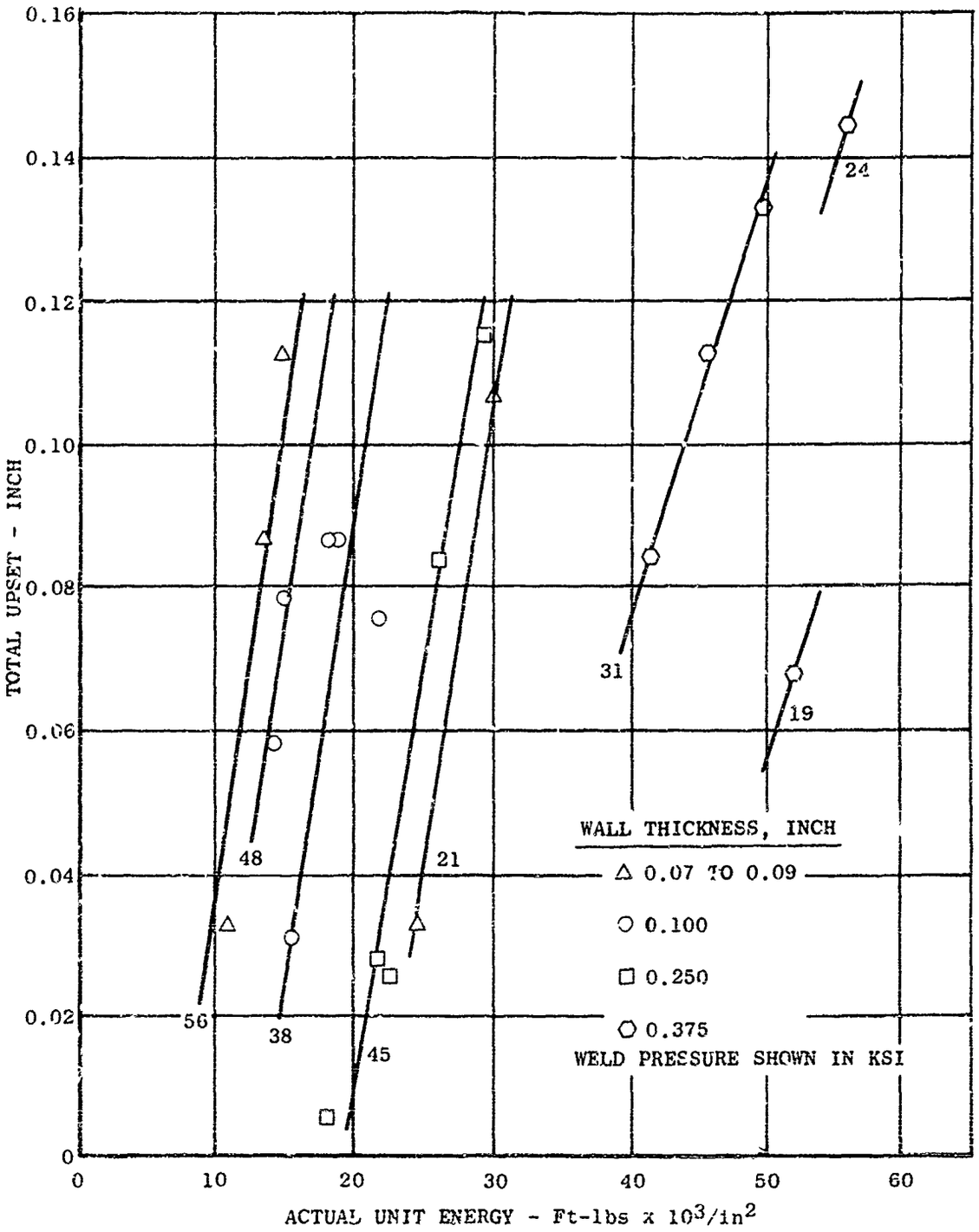

Figure 16 Total Upset vs Energy - Four Inch Diameter Inconel 718 Test Rings

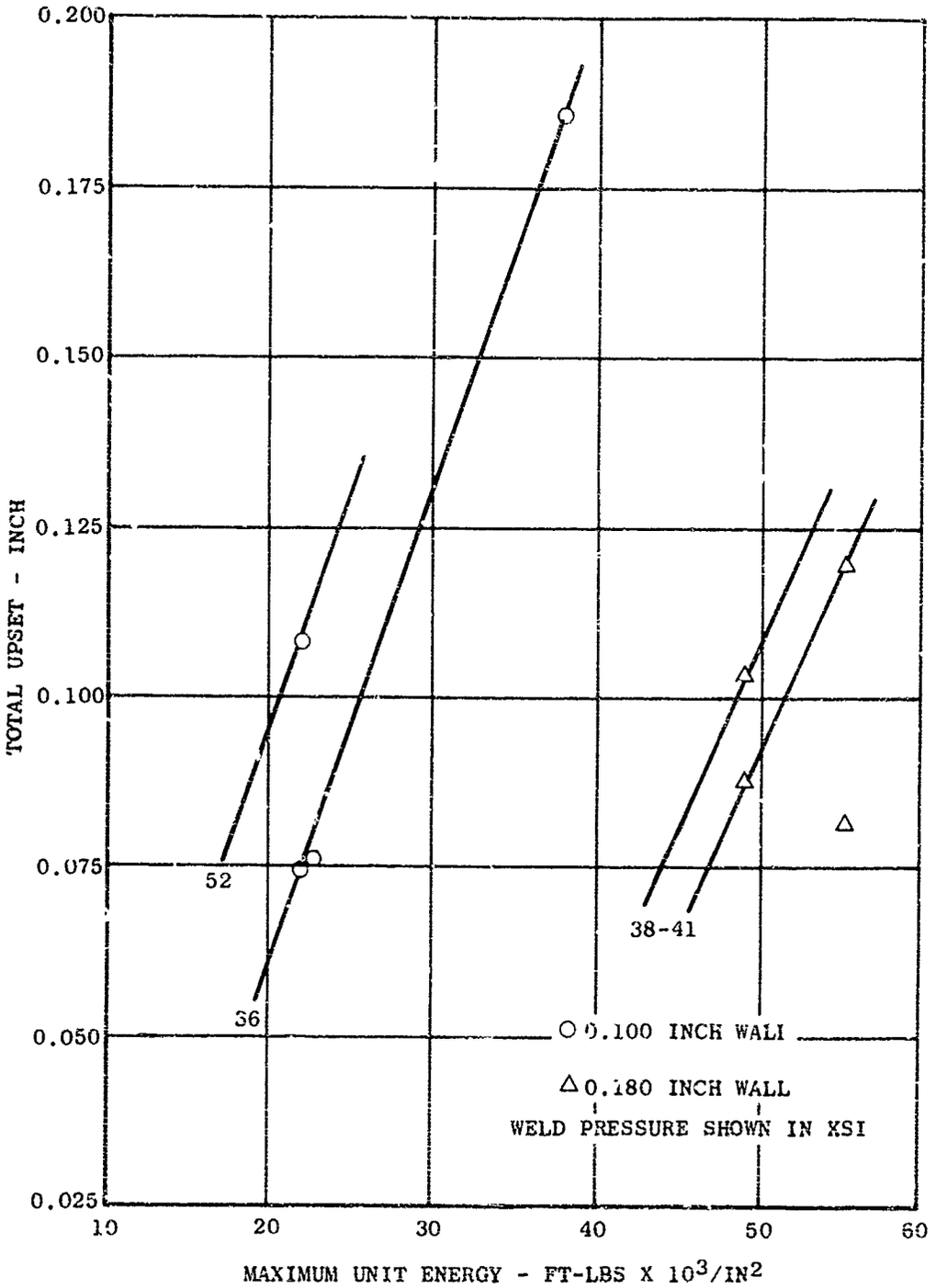

Figure 17 Total Upset vs Energy - 12 Inch Diameter Inconel 718 Test Rings.

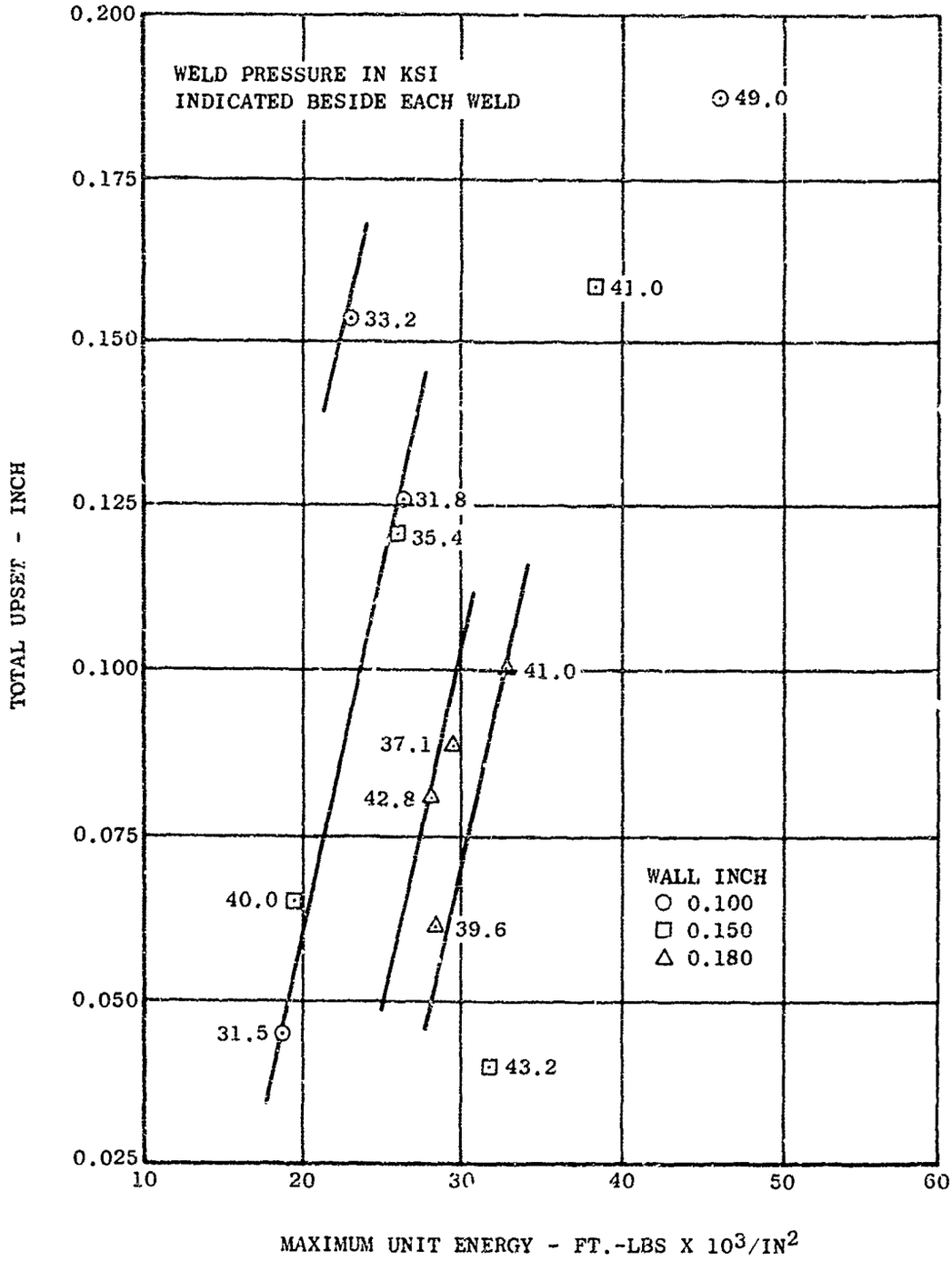

Figure 18 Total Upset vs. Energy - 24 Inch Diameter Inconel 718 Test Rings

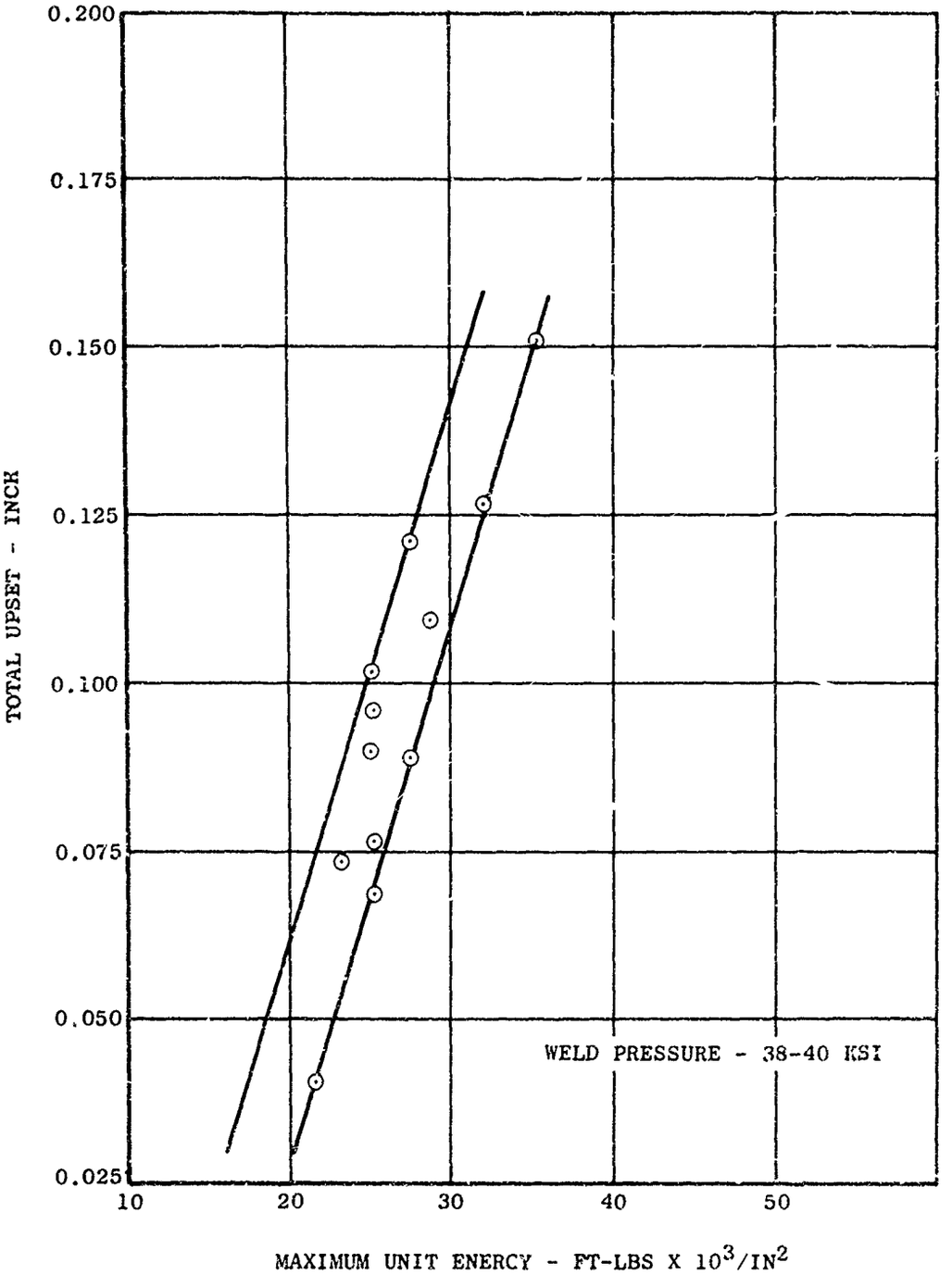

Figure 19 Total Upset vs Energy - 24 Inch Diameter Inconel 718 Test Rings with 0.180 Inch Walls.

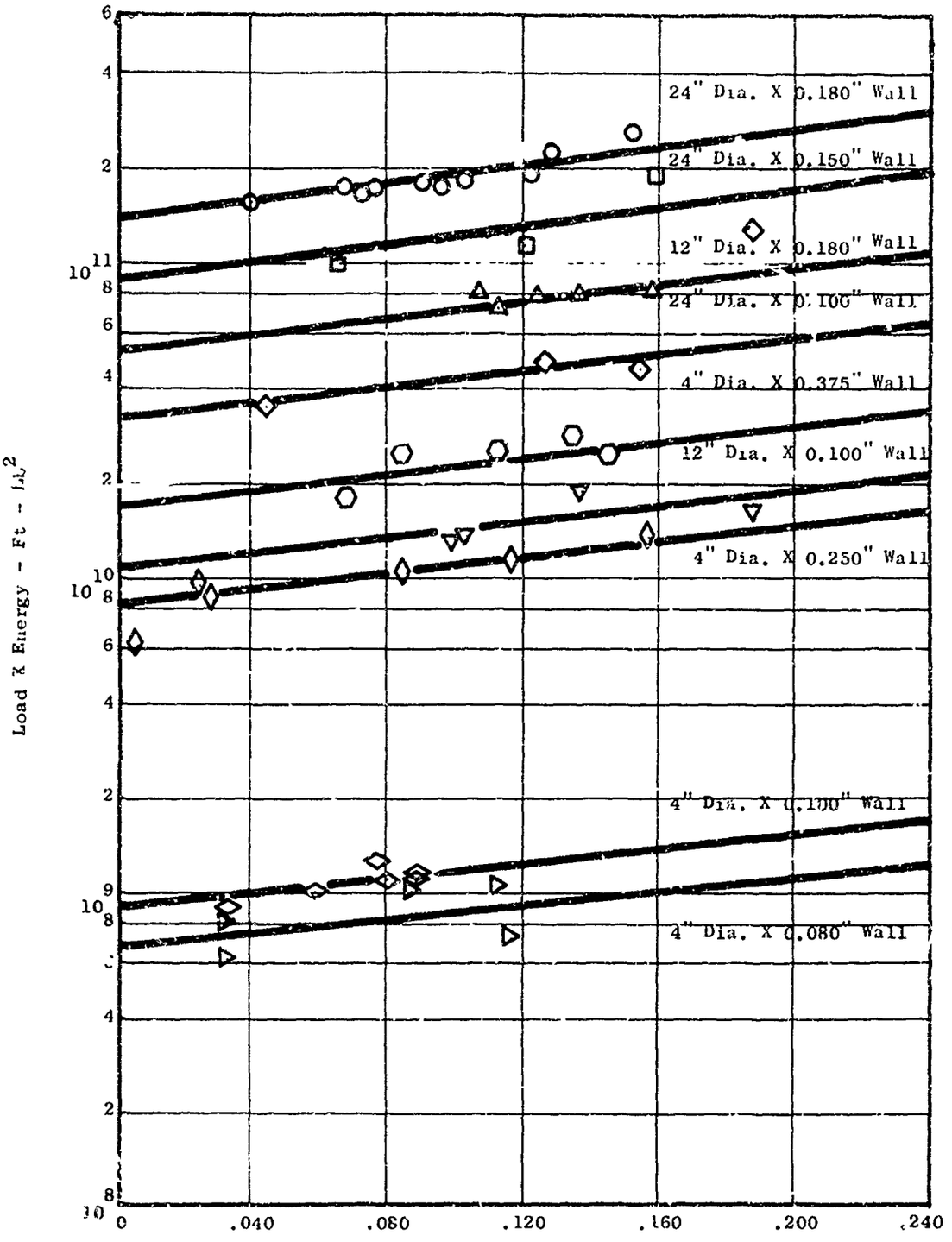

Figure 20 Load X Energy versus Total Upset for Various Diameters and Wall Thicknesses of Inconel 718

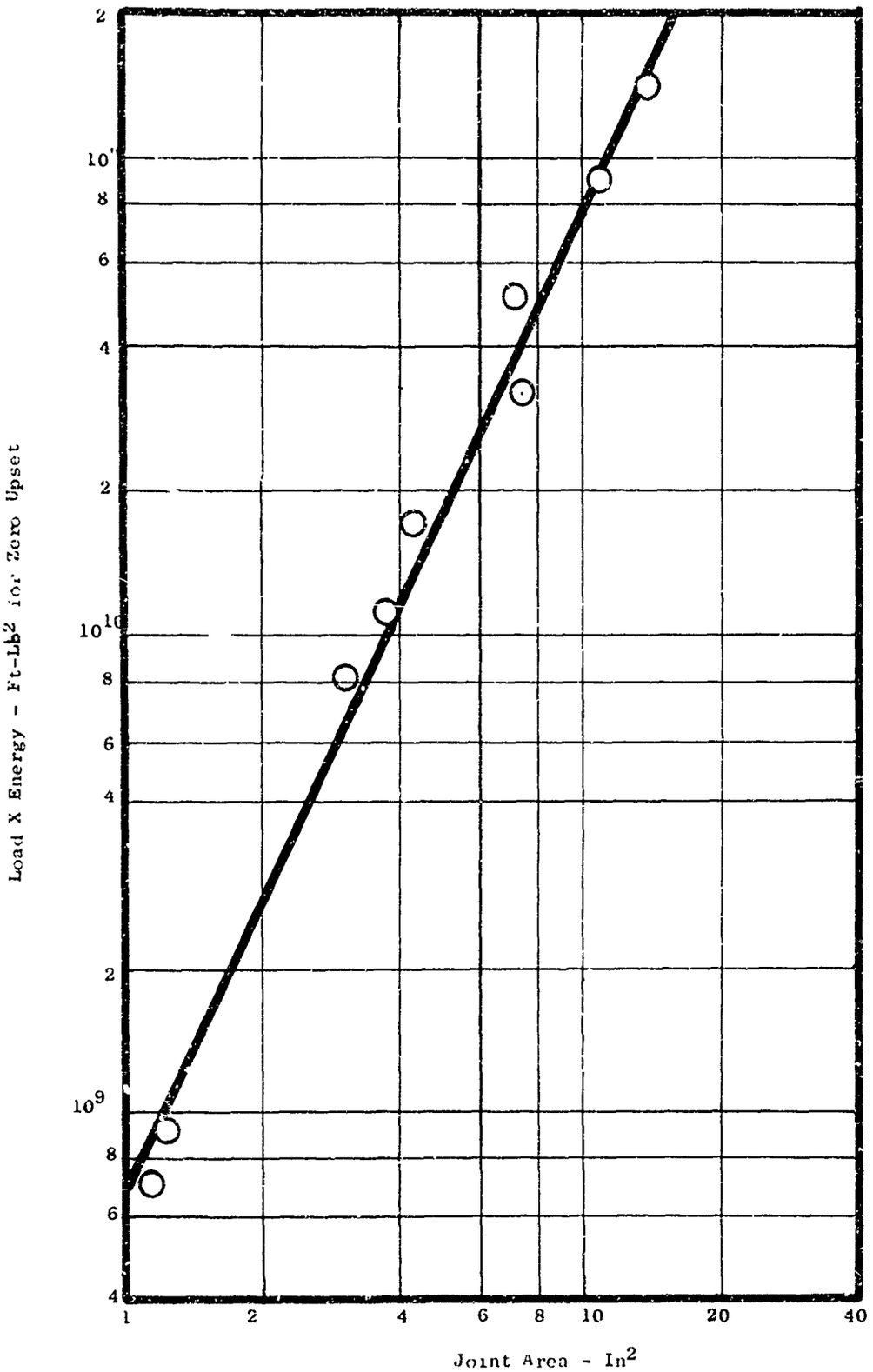

Figure 21 Load X Energy for Zero Upset versus Weld Joint Area-Inconel 718

$$y = kx^n \qquad (2)$$

where y = load total energy for zero upset = $L \cdot E_t$
x = weld joint area = A
k = value of y at x = 1 (6.45×10^8)
n = slope = 1.987

By substituting "y" from equation (2) for "C" in equation (1) a single equation relating upset to joint area and the load and energy product was obtained.

$$L \cdot E_t = k A^n \cdot 10^{mU} \qquad (3)$$

or

$$E_t = \frac{6.45 \times 10^8 A^{1.987}}{L} \cdot 10^{1.4U} \qquad (4)$$

where E_t = total energy input (corrected for efficiency) ft-lbs
L = total ram load - lbs
A = weld joint area - in^2
U = total upset - inch

The values of the constants, k, m, and n, in equation (3) reflect not only Inconel 718 material properties such as strength, thermal conductivity, coefficient of friction, etc., but are also somewhat dependent on the tubular joint geometry including weld prep design which was quite similar for all diameters and wall thicknesses studied. While the general form of equation (3) should be applicable to the inertia welding of materials other than Inconel 718 the values of k, m, and n would have to be determined from welding studies similar to the one herein described.

D. METALLOGRAPHIC STUDIES

Optical metallographic examination of 4, 12 and 24 inch O.D. weldments showed significant differences in the microstructures of the interface zones. In both the 4 and 24 inch O.D. specimens the interface zones were delineated by a dark line after etching, Figure 22. The 12 inch O.D. specimens were free of this etchant effect, Figure 23. In addition the 4 and 24 inch O.D. samples had localized areas with microstructures much different from the surrounding material. As shown in Figure 24, the structures were eutectic - like suggesting that localized melting had occurred in welding.

After repolishing the specimen shown in Figure 22 to remove the etched surface, oblique bright field and phase contrast illumination were used to examine the interface. As shown in Figure 25, the interface zone in the unetched condition is still distinguishable by surface relief effects and effectively highlighted by phase contrast illumination. No voids or cracks were evident in the interface zone except at the outer edges in the flash notches. Electron microscope examination of four inch O.D. samples showed the interface zone to be recrystallized and free of voids or precipitates. The interface zone was observed to run parallel to recrystallized grain boundaries and also pass through the centers of recrystallized grains, Figure 26. No voids or cracks were observed.

Electron beam microprobe traces were made across the joint interfaces of the 4 and 12 inch O.D. specimens. No significant differences in composition between the interface zone and the surrounding material were observed in the 12 inch O.D. specimens. A depletion of columbium, molybdenum and titanium in the interface zone was determined for the four inch

O.D. specimens. This chemical segregation is considered responsible for the preferential etching of the joint interface observed in the 4 and 24 inch O.D. samples. X-ray analysis of the localized eutectic-like areas showed columbium concentrated to 17 percent (vs. 4 to 5 percent in the parent metal) with decreased iron, nickel, chromium and aluminum. This appears to confirm the occurrence of localized or incipient melting with subsequent chemical segregation during resolidification.

None of the 12 inch O.D. samples examined showed any evidence of localized melting or compositional differences across the joint interfaces. The only significantly different parameter used in welding the 4, 12 and 24 inch O.D. samples was surface velocity. The 12 inch O.D. by 0.100 inch wall specimens were welded at 460 to 520 SFM while the 4 and 24 inch O.D. samples were welded at surface velocities from 1000 to 2000 SFM. Apparently at the high surface velocities the rate of heat input into the joint area is sufficiently high to cause overheating which may or may not be visually evidenced by flash spin-off. From the standpoint of weld quality interface overheating is considered undesirable as it may contribute to deterioration in the strength and ductility of the weldment.

Edge A-100X

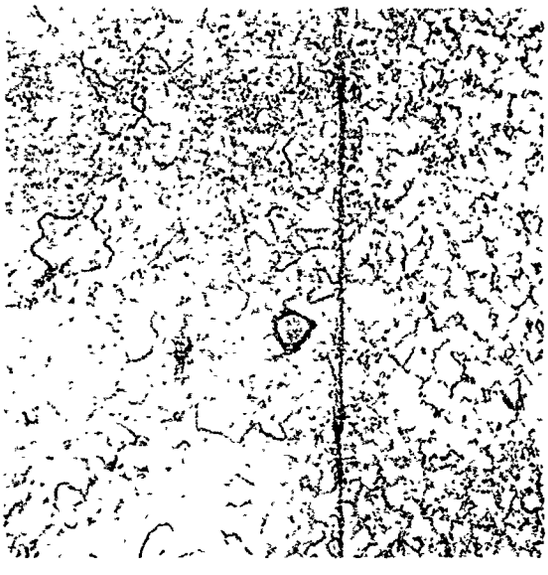

Edge B-500X

Center B-100X

Center B-500X

Figure 22 Microstructure of inertia weld zone in 0.250 inch wall 4 inch OD Inco 718 test specimen 8-28 (0.155 inch upset) showing duplex parent metal structure, sub-layer flow and fine grained structure in weld interface (Hcl, H_2O, H_2O_2 etch).

P9249

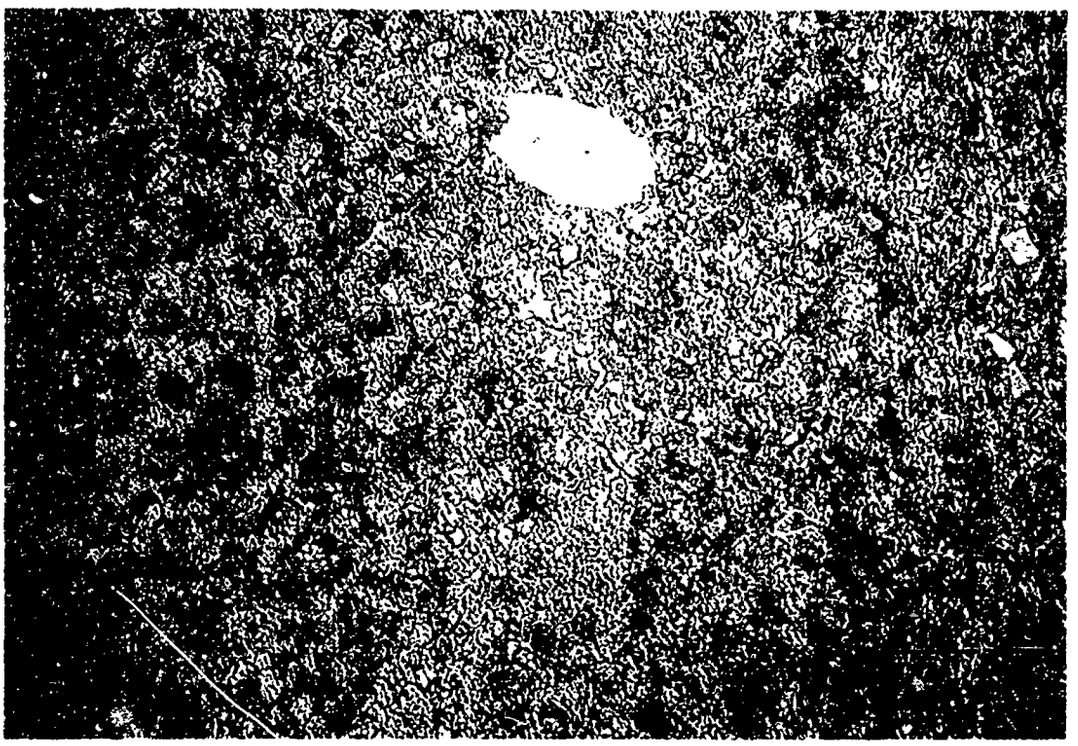

500X ETCHED

Figure 23. Photomicrograph of Inertia Weld Microstructure in center of weld showing equiaxed recrystallized grains in weld interface. Inconel 718 Test Rings 14-35, 12 Inch OD x 0.100 Inch Wall, Run No. 400-8-15, 0.189 Inch Total Upset

100X Etched

Figure 24. Photomicrograph of heat affected zone microstructure of 0.375 inch wall 4 inch OD Inconel 718 test specimen 19-39 (0.134 inch upset) showing liquated phases at the grain boundaries.

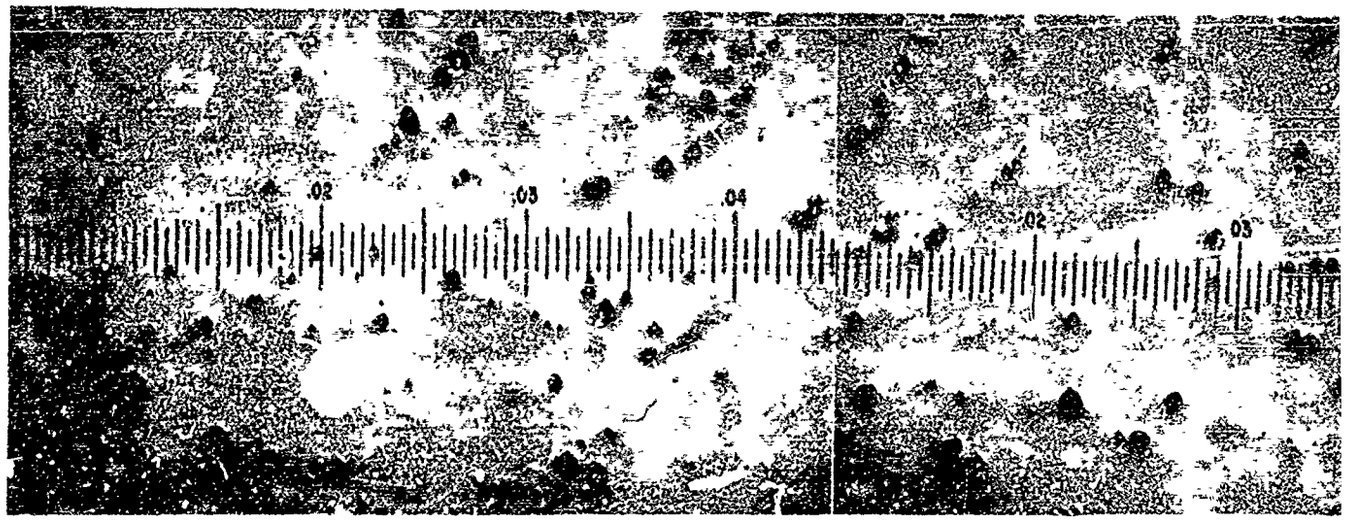
.02
.03
.04
.02
.03

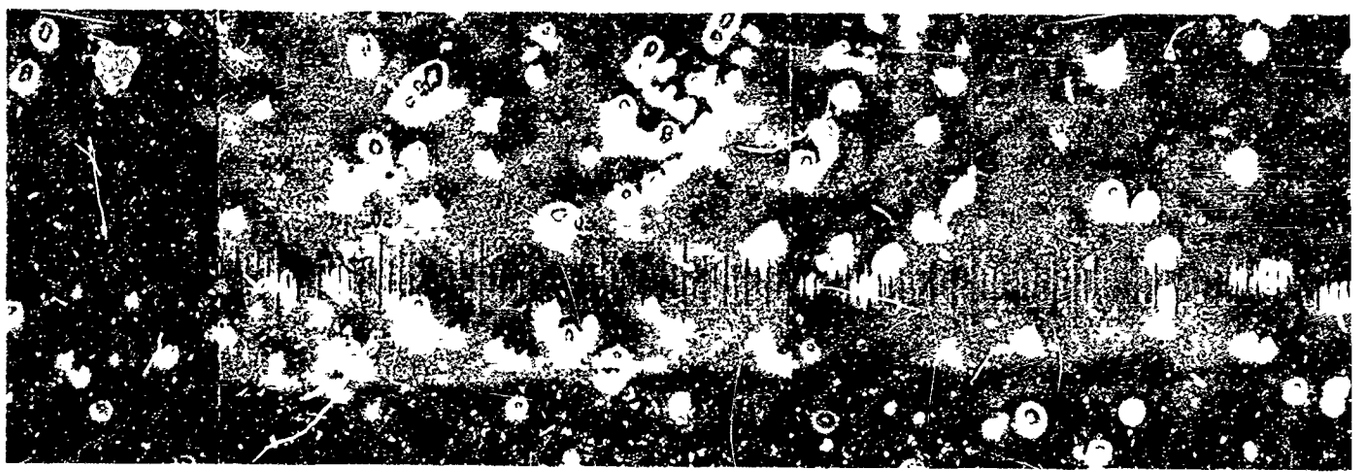

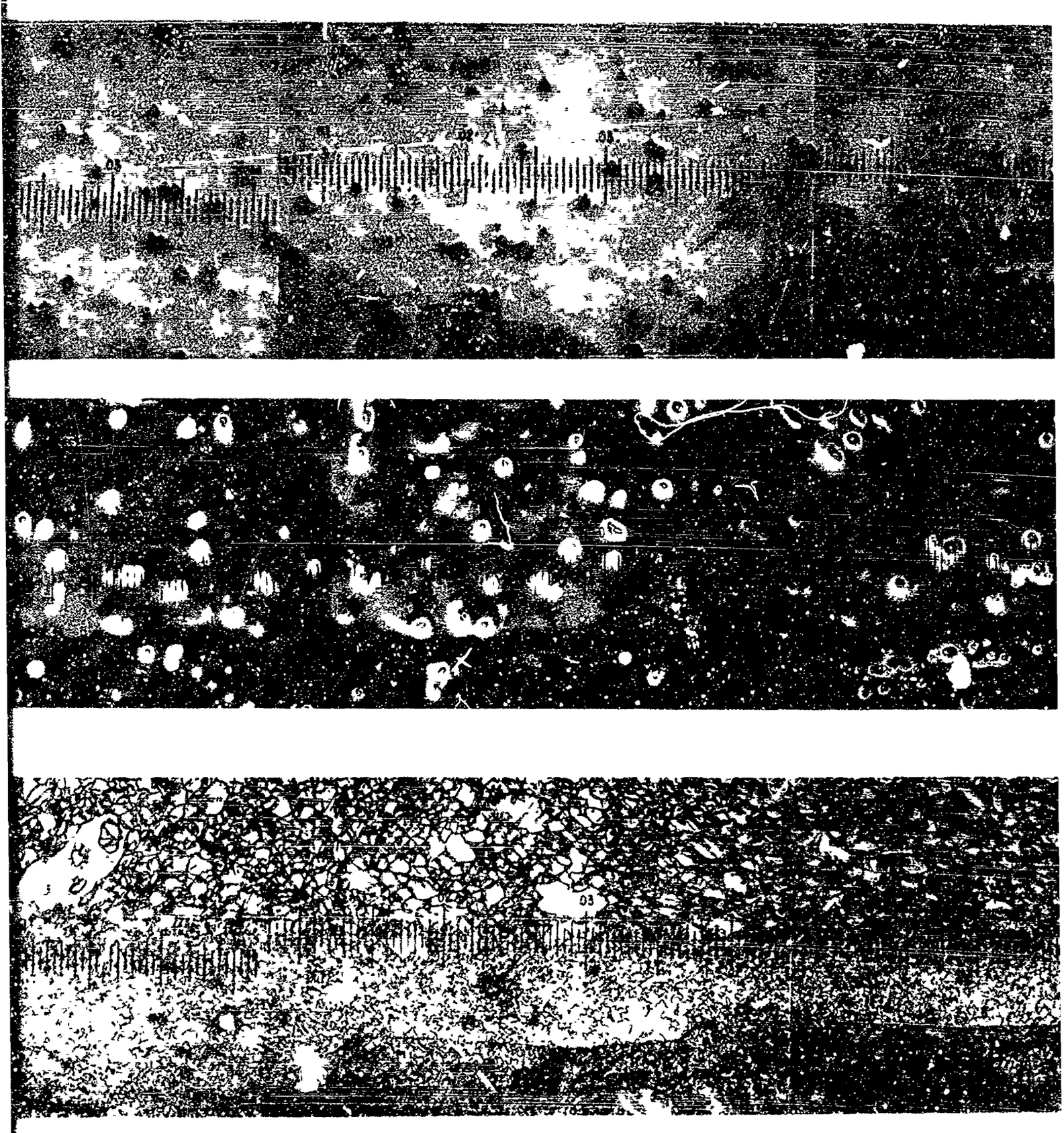

Figure 25 Inertia Welded Joi

As Polished (Oblique - Bright Field)
Interface Zone
100X

As Polished (Phase Contrast)
Interface Zone
100X

As Etched (Bright Field)
Interface Zone
100X

Figure 25 Inertia Welded Joints - Effect of Etching and Surface Lighting

Figure 26 Electron Photomicrograph of Inertia Weld Interface in Inconel 718

SECTION IV

COLD FORMING INCONEL 718 CROSS ROLLED PLATE

A. HEAT-TREATING STUDIES

The goals of this effort were actually two-fold, the first being to determine the optimum heat-treated condition for Inconel 718 to allow maximum cold deformation and the second to develop post heat treatments or combined post heat treatments and mechanical processing sequences to realize the best combination of mechanical properties and uniformity.

In this study Inconel 718 cross rolled plate processed by Universal Cyclops, Specialty Steel Division, from Heat No. K66510K11 was used as the base material. The processing schedule was as follows: Hot rolled at 2050°F from 3.75 inch x 10 inch x 28 inch billet to a 26 inch x 28 inch x 1.4 inch plate. Reheated to 2050°F and cross rolled to 26 inch x 65 inch x 0.625 inch thick plate for a total reduction of approximately 6:1. Metallographic examination of the plate showed a fairly uniform equiaxed grain size with a Rockwell D hardness of 28.

Strips were cut from the plate and annealed in a gradient furnace. The softest section was obtained from the portion that had been heated to approximately 2000°F for one hour. To make a preliminary check on formability, a test specimen was cut from the cross rolled plate, heat-treated for one hour at 2000°F, then air cooled. A wedge indentor, having a profile similar to that proposed for the cold forming of the compressor rotor wheel rim, was mounted in an air hammer and the plate was impacted. A notch over one inch deep was cut in the edge of the plate specimen, Figure 27, with only light surface cracking on the edges. A second set of specimens was prepared from the as-received plate and deformed by the indentor without cracking. It was therefore concluded that as-received plate had sufficient ductility to accept heavy cold working for the compressor wheel forming.

Macroscopic and microscopic examination also indicated the as-received condition more suited to the cold deformation process. This was apparently due to a finer grain size, which allowed more deformation to occur within each grain before the imposed strain was relieved by grain boundry separation. This is indicated in Figure 28, which shows sections of surface replicas taken from equivalent areas of electropolished specimens deformed using the wedge indentor. The slip bands appear much finer and closer together in the as-received material as compared to the coarse slip bands in the annealed structure.

To determine the best combination of cold work and heat treatment, two series of tapered wedges were cut for cold rolling. Both sets of specimens were heated to 2000°F for one hour and air cooled. One group of specimens was cold rolled from 0 to 40% reduction and a second group was cold rolled from 20 to 60% reduction. Neither group had any edge cracking. Microscopic examination of the wedge shaped specimens with various heat treatments showed the following variations in grain size and hardness:

As Rolled 20 to 60% Reduction (Rockwell D 47.5)

20%	ASTM No. 2 to 4
40%	ASTM No. 2 to 5
60%	ASTM No. 2 to 3 (elongated)

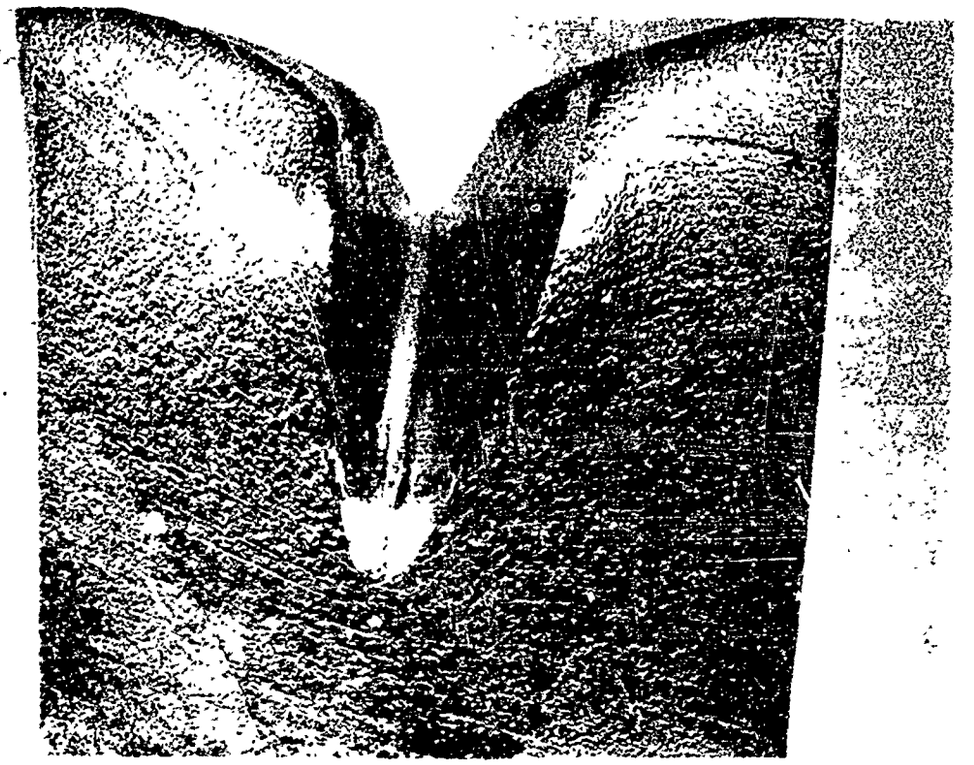

Figure 27 Inco 718 Cold Formed by Impactor

N6286

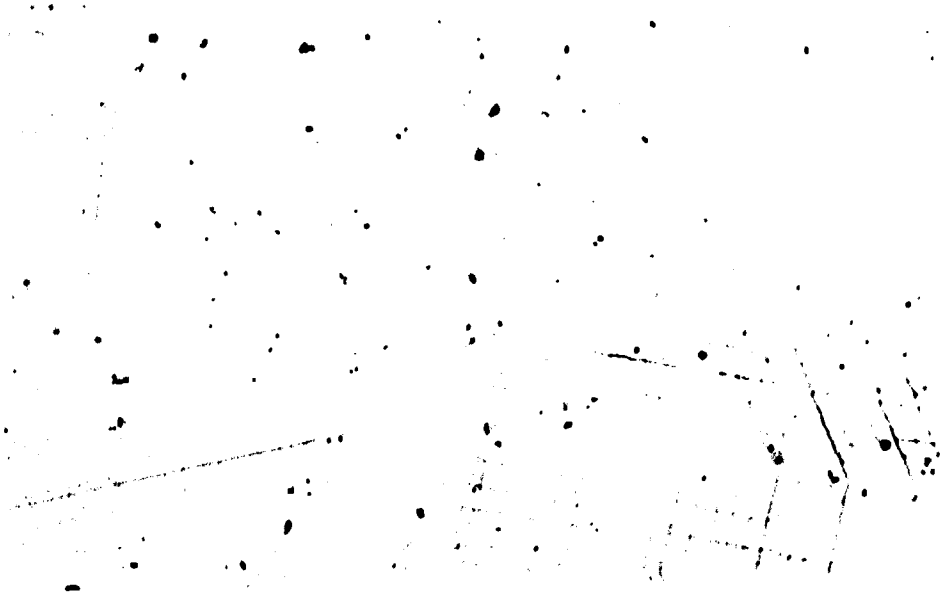

As Received 1000X

+ Cold Deformation

N6280

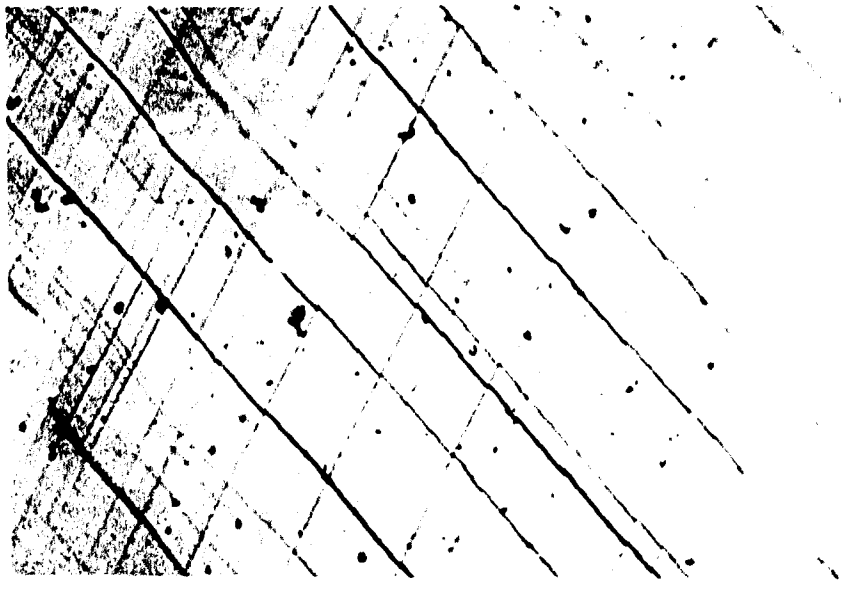

2000°F/Hr/Ac 1000X

+ Cold Deformation

Figure 28 Effort of Annealing on Microstructure of Cold Worked Inconel 718

As Rolled 20 to 60% Reduction + 1200°F/50 hr/AC (Rockwell D 52.5)

20%	ASTM No. 2 to 5
40%	ASTM No. 2 to 5
60%	ASTM No. 2 to 4 (elongated)

As Rolled 20 to 60% Reduction + 2000°F/1 hr/AC (Rockwell D 21.5)

20%	ASTM No. 2 to 4 (Mostly 3 and 4)
40%	ASTM No. 2 to 4
60%	ASTM No. 2 to 4 (Mostly 2 and 3)

Microstructures from each of these specimens are shown in Figure 29. The 2000°F/1 hr/AC was sufficient to completely recrystallize the cold rolled structure. The low temperature (1200°F/50 hr/AC) stabilizing heat treatment had no effect upon grain size and was sufficiently high to assure precipitation as indicated by the increase in Rockwell D hardness.

It was concluded that the application of a low temperature (1200°F/50 hr/AC) stabilizing heat treatment after rolling had no effect upon grain size and that the stabilization temperature was sufficiently high to assure precipitation as indicated by the increase in hardness. It appeared feasible that incorporation of large amounts of cold deformation with a high temperature solution followed by a low temperature stabilization treatment could be used to return the properties of cross rolled Inconel 718 plate to their original levels. A further indication of this was observed in specimens cut from an Inconel 718 plate, solution treated (2000°F/1 hr/AC), cold rolled to 20% reduction, then heat treated and pulled to 0.2% yield at room temperature:

Specimen	Condition	.02% YS (ksi)	.2% YS (ksi)
#1	As cold rolled (20%)	108	133
#2	Cold rolled (20%)+1800°F/1 hr/AC+1325°F/8 hr/FC-100°F/hr to 1150°F+1150°F/8 hr/AC	143	162
#3	Same as #2 +1250°F/16 hr/AC	161	183
GE Average Design Value	1800°F/1 hr/AC+1325°F/8 hr/FC-100°F/hr to 1150°F+1150°F/8 hr/AC	139	167

B. MECHANICAL PROPERTY STUDIES

1. Cross Rolled Plate - The first lot of mechanical property tests was made on Inconel 718 plate in the as rolled, as rolled + 2000°F solution treatment and as cold rolled + 1200°F aging treatment.

Tensile data are tabulated in Table XV and illustrated in Figures 30, 31, and 32. General observations from this data were:

- Tensile strength and ductility were affected by the amount of deformation, the more highly strained specimens showing lower ductility but higher ultimate and yield strengths.

- The alloy in the as-received condition, i.e., as cross rolled and air cooled from 2000°F, while quite ductile at room temperature was extremely weak mechanically, requiring a final heat treatment to raise its properties to acceptable levels.

- The increase in tensile strength and decrease in tensile ductility of the as-received material with increasing temperature indicated that the alloy was in a supersaturated, metastable condition at room temperature. As the test temperature was increased, the alloy moved toward a more stable condition, most probably, through the precipitation and growth of gamma prime (Ni_3Cb) precipitate.

- Longer aging times at 1200°F were very effective in improving tensile strength, particularly yield, but with a considerable loss in tensile ductility.

- The application of longer 1200°F aging heat treatments (64 to 200 hours) was sufficient to reduce both the amount of primary creep as well as the secondary creep rate.

- Material as cold rolled to 25% or 57% reduction showed extremely poor creep behavior, i.e., a high primary creep and an accelerated secondary creep rate.

In summary it was apparent that the application of a backup heat treatment was necessary after cold forming to elevate the properties to that of the specifications and assure mechanical homogeneity within the part. Since the first lot of mechanical property tests had shown the effectiveness of longer aging times at 1200°F in improving strength, a second lot of tests was made on 0%, 25% and 50% cold worked material given a final aging treatment of 64 hours at 1250°F. The results, Table XVI, show this treatment was effective in increasing tensile strength with only a slight reduction in ductility.

2. Cold Rim Formed Discs

(a) Test Specimen Preparation - The Inconel 718 obtained for cold rim forming differed from the first heat of material used to measure initial properties and deformation behavior with respect to both grain size morphology and hardness.

The first heat of material had a fairly uniform, equiaxed grain size and a Rockwell D hardness of about 28, whereas the second heat had a duplex grain structure and a Rockwell D hardness of 44. The cause of this difference was attributed by the vendor to a 1750°F/1 hr/WQ solution heat treatment applied to the first lot of plate. This heat treatment was not applied to the second lot since the purchase order specified an as rolled and air cooled condition. However, the same heat treatment, i.e., 1750°F/1 hr/WQ, applied to sections cut from the second heat of material did not eliminate the duplex grain structure or produce any significant softening. It was found that an 1850°F/90 min/AC heat treatment was required to soften the second set of plates to approximately Rockwell D 32, and cold indentation results showed adequate deformation for cold rim forming.

A completely rim formed compressor wheel used to establish rim forming maching parameters was selected for mechanical property testing. In addition to the precold forming 1850°F heat treatment, the wheel had received an intermediate anneal at 1850°F prior to the finish rim forming operation. Test specimens machined from the rim and web sections were then heat-treated to the schedule: 1850°F/90 min/AC + 1800°F/1 hr/AC + 1325°F/8 hr/FC - 100°F per hour to 1150°F + 1150°F/8 hour/AC + 1250°F/64 hr/AC.

(A) ~ 20% As Rolled

(B) ~ 40% As Rolled

(C) ~ 60% As Rolled

(D) ~ 20% + 1200°F/50 hr/AC

(E) ~ 40% + 1200°F/50 hr/AC

(F) ~ 60% + 1200°F/50 hr/AC

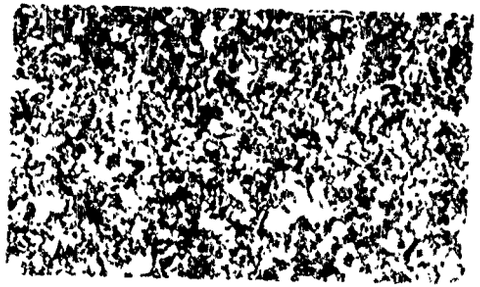

(G) ~ 20% + 2000°F/1 hr/AC

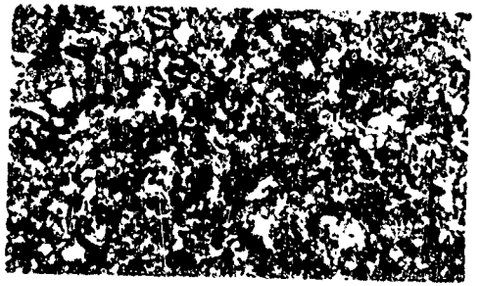

(H) ~ 40% + 2000°F/1 hr/AC

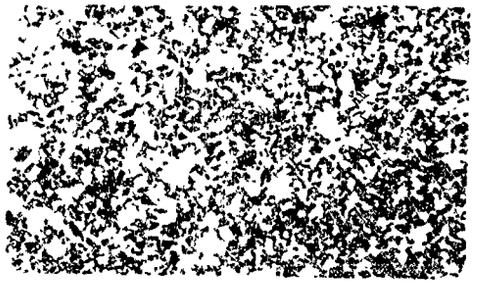

(I) ~ 60% + 2000°F/1 hr/AC

Figure 29 Effect of Various Annealing Treatments on Microstructure of Cold Worked Inconel 718

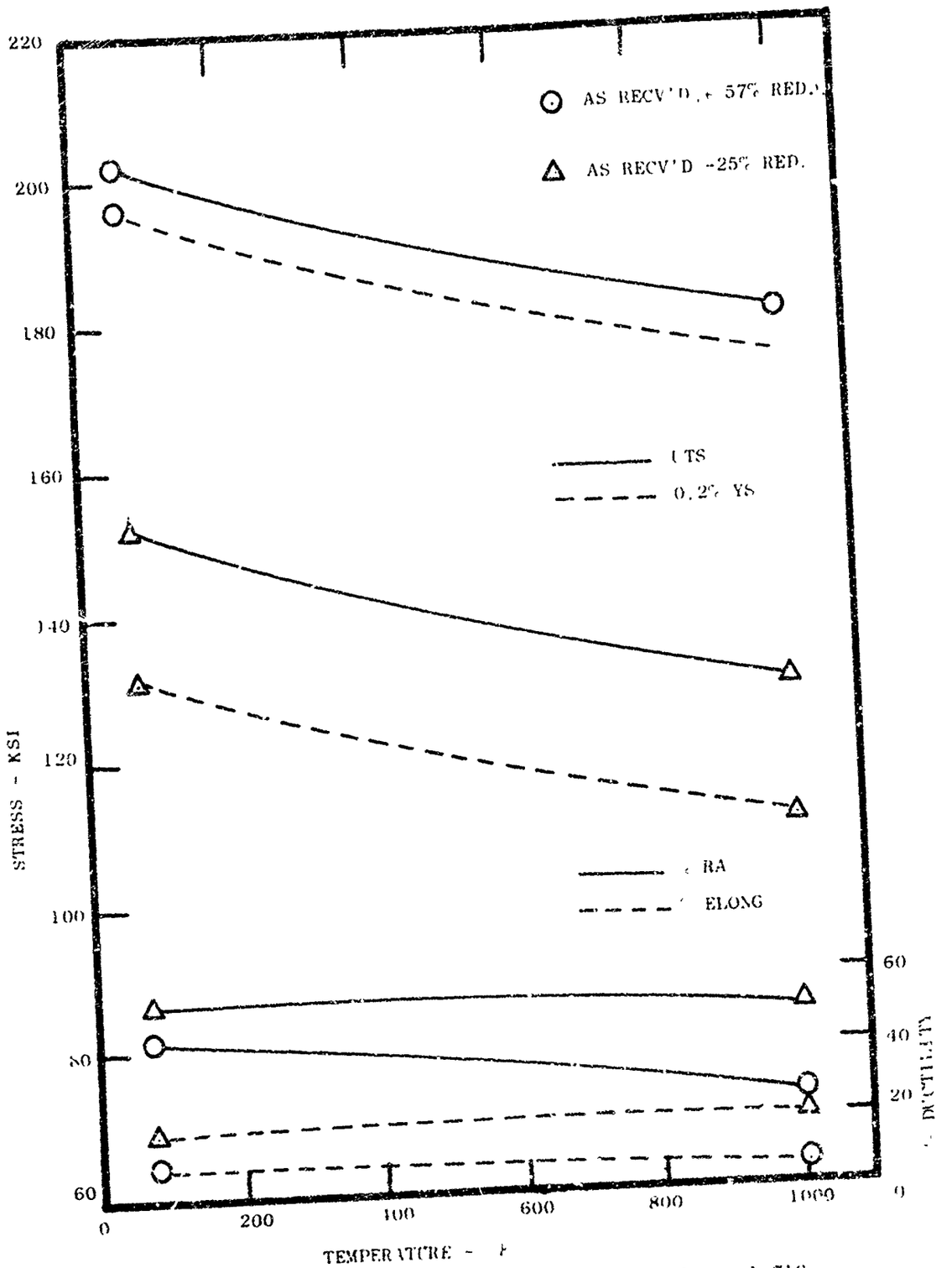

Figure 30 Tensile Properties of Cold Worked Inconel 718 Cross Rolled Plate

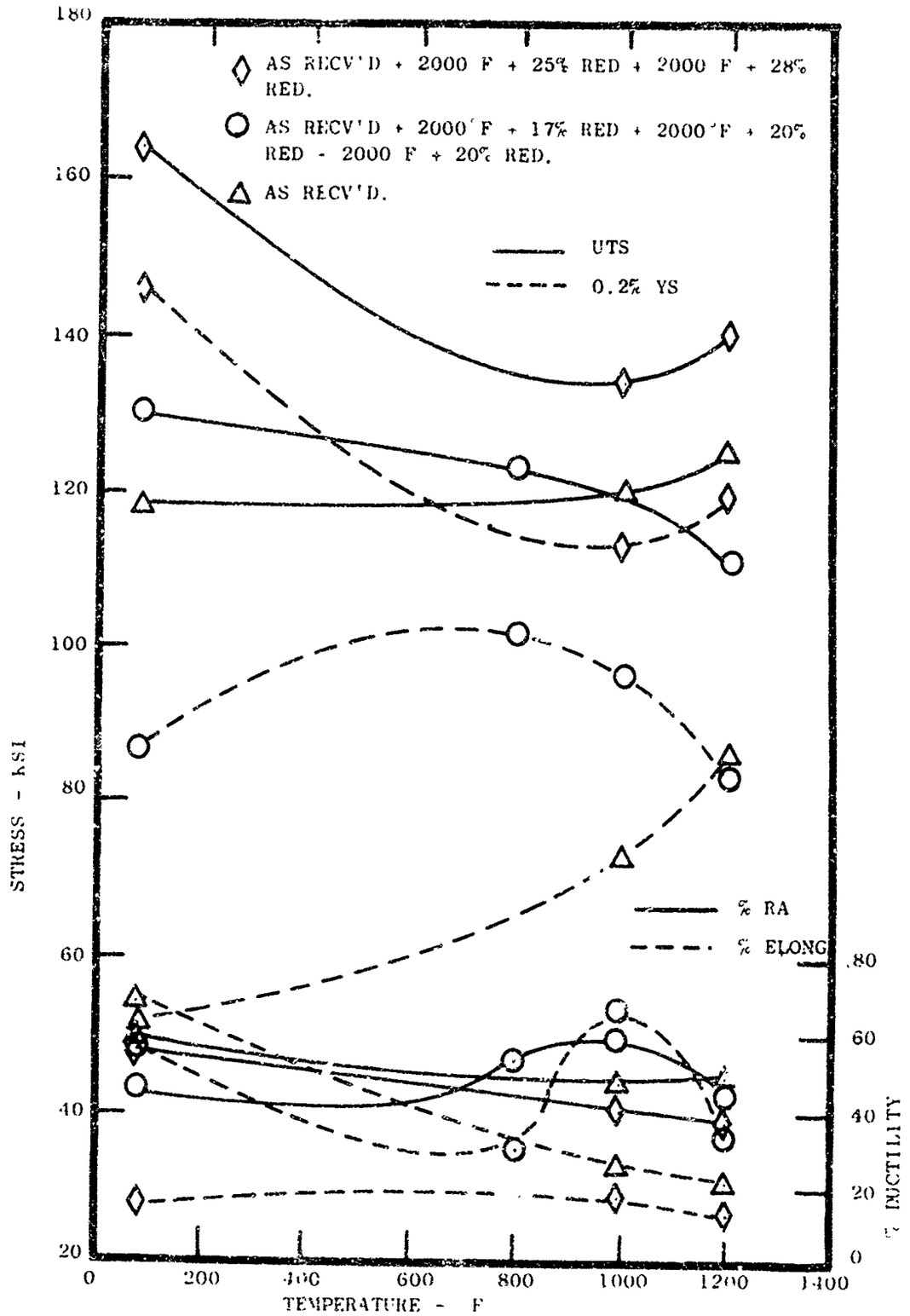

Figure 31 Tensile Properties of Cold Worked and Heat Treated Inconel 718 Cross Rolled Plate

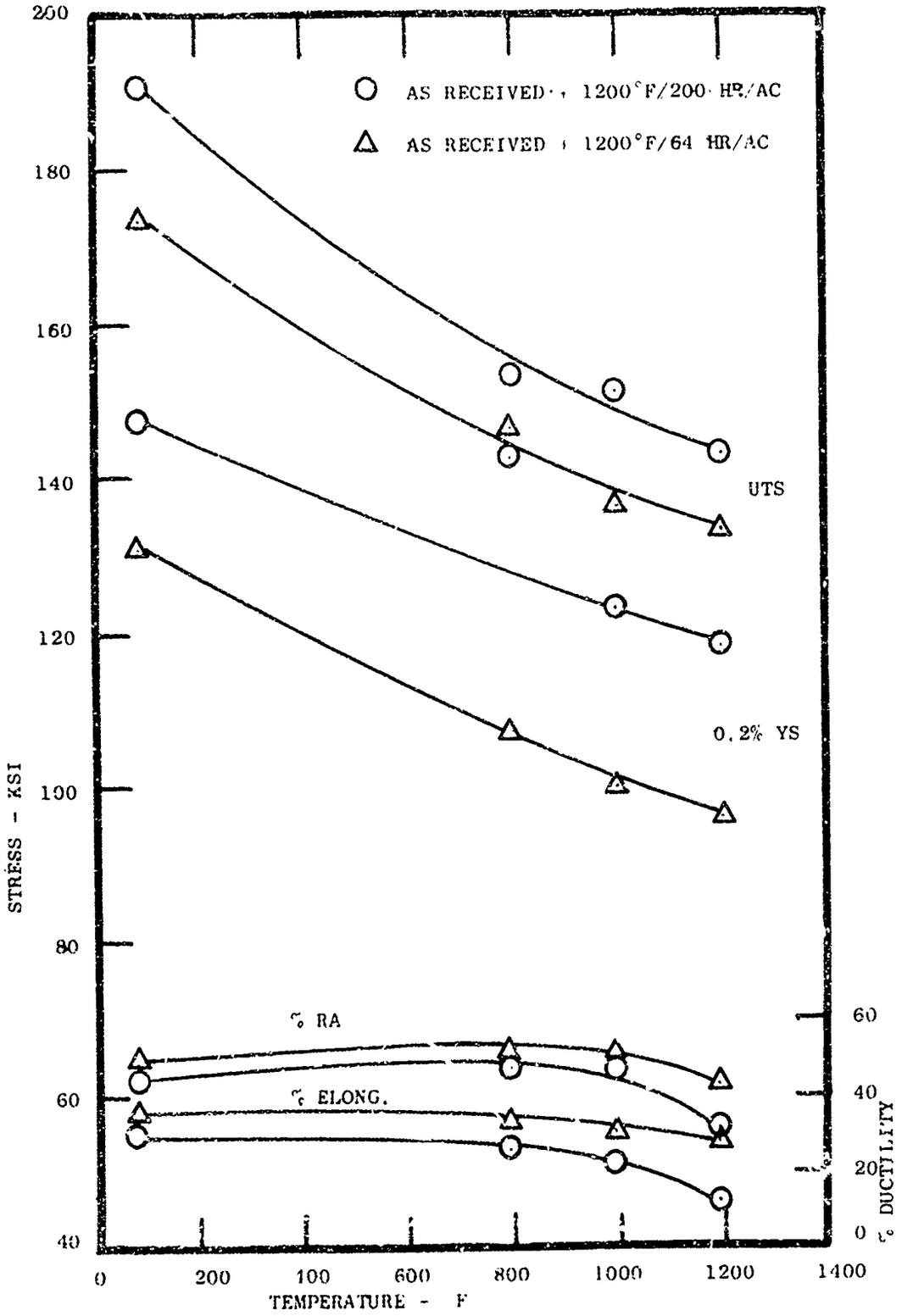

Figure 32 Tensile Properties of Heat Treated Inconel 718 Cross Rolled Plate

(b) Tensile Properties - Smooth and notched bar tensile properties of rim and web sections removed from the cold formed compressor wheel are listed in Table XVII and plotted in Figures 33 and 34. Average GE design book curves are also shown for comparison purposes. The tabulated data show both the rim and web test specimens met the GE minimum strength values and were slightly under the ductility minimums at 1200°F. With respect to the GE average design book curves the web test specimens were slightly below in yield strength and in ductility at 1200°F and above. Specimens from the rim appeared stronger in tensile and yield strength but fell below the ductility curves at 1000°F and above. In summary, the effect of cold rim forming Inconel 718 cross rolled plate appeared to be mainly that of increasing the yield strength with a slight lowering of ductility at 1000°F and above.

(c) Stress Rupture Properties - Stress rupture properties of the rim and web sections are tabulated in Table XVIII and plotted in Figure 35 with average design book curves for comparison. Both the rim and web specimens appeared equivalent to each other and to the average data book properties for Inconel 718. Four of the test specimens from the rim broke in the threads and the data points fell slightly below the lower 3 sigma curve. With respect to stress rupture properties there did not appear to be any significant effect on the cross rolled plate by cold rim forming.

(d) Cyclic Rupture Properties - Cyclic rupture test results using the 10 seconds load - 90 seconds at stress -10 seconds unload cycle are presented in Table XIX and Figure 36. Due to the lack of stock in the rim section, a nonstandard configuration was used to prepare rim specimens with a K_t of 2. As indicated by the data cold rim forming appeared to improve low cycle fatigue strength

(e) Rotating Beam Fatigue Properties - Room temperature rotating beam fatigue test specimens were prepared from the web sections only due to the lack of stock in the rim section. Test results are tabulated in Table XX and plotted in Figure 37. The S/N curve showed run out (1×10^7 cycles) at 50 ksi with testing terminated after 45,370,000 cycles. No comparable data for Inconel 718 was available for comparison purposes.

(f) Mechanical Properties - Standard Double Age - To compare the merit of the standard double aging heat treatment against the single 64 hour age at 1250°F additional specimens were prepared from the web section of another compressor wheel which had been only partially cold formed and therefore had only one 1850°F 90 minute anneal prior to test specimen preparation. The test specimens were then given the following heat treatment: 1900°F/90 min/AC + 1800°F/1 hr/AC + 1325°F/8 hr/FC - 100°F/hr to 1150°F + 1150°F/8 hr/AC + 1325°F/8 hr/FC @ 100°F/hr to 1150°F + 1150°F/8 hr/AC.

The test results are compared to single age results in Tables XXI, XXII, and XXIII and show the standard double age treatment was equivalent to the single 64 hour age at 1250°F. The NTS/UTS ratio for the double aged specimens was between 1.20 and 1.25 which is considered satisfactory for the TF39 rotor application. In view of the additional time and money required by the unique 64 hour treatment with little significant gain in mechanical properties, it was decided to adopt the standard double aging treatment after inertia welding.

C COLD RIM FORMING DEVELOPMENT

1. Process Description - The fabrication of individual compressor rotor wheels or stages from cross rolled plate required the preparation of a starting blank such as illustrated in Figure 38. The periphery of the blank is then split to a predetermined depth

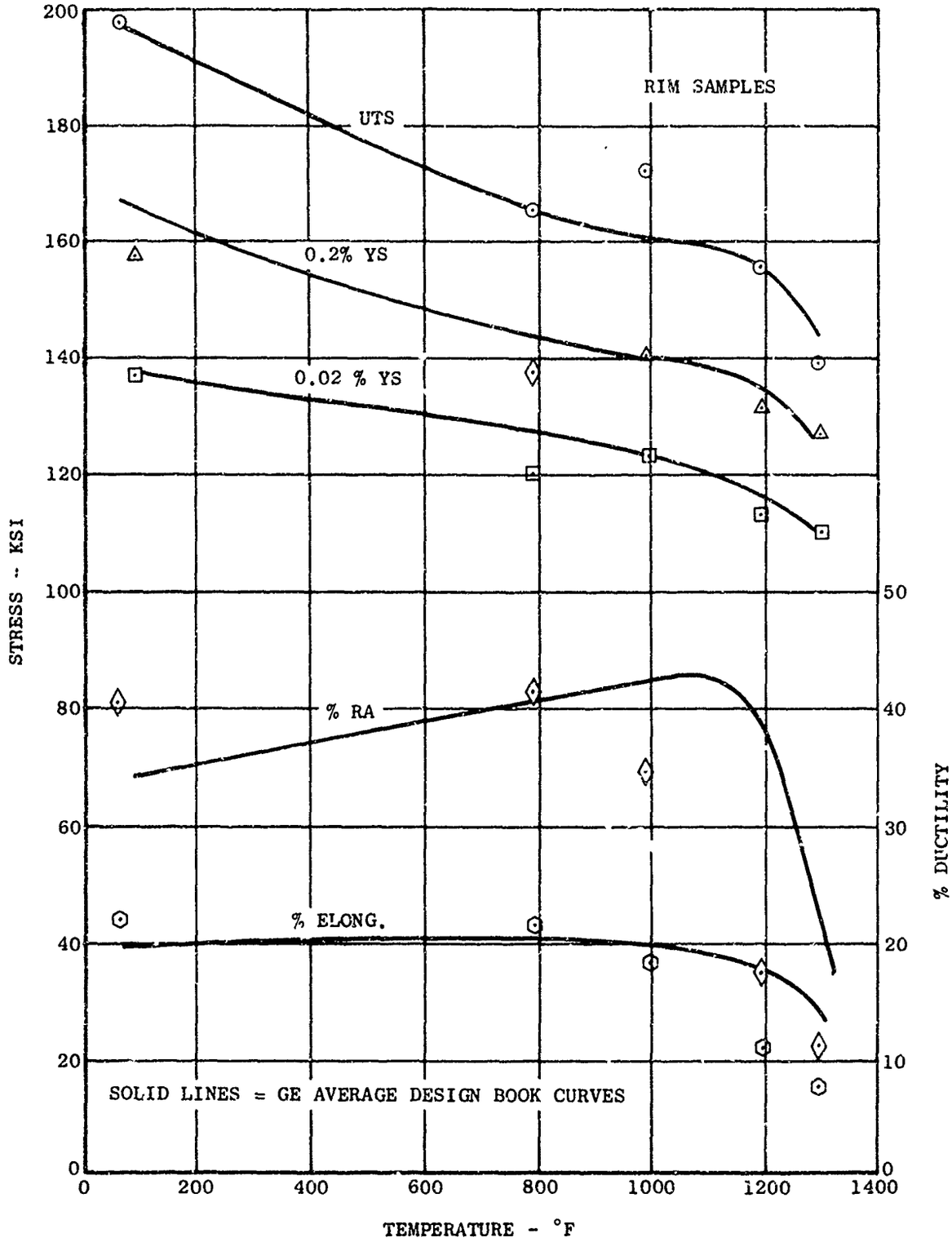

Figure 33 Tensile Properties of Cold Rim Formed (Rim Section) Inconel 718 Cross Rolled Plate.

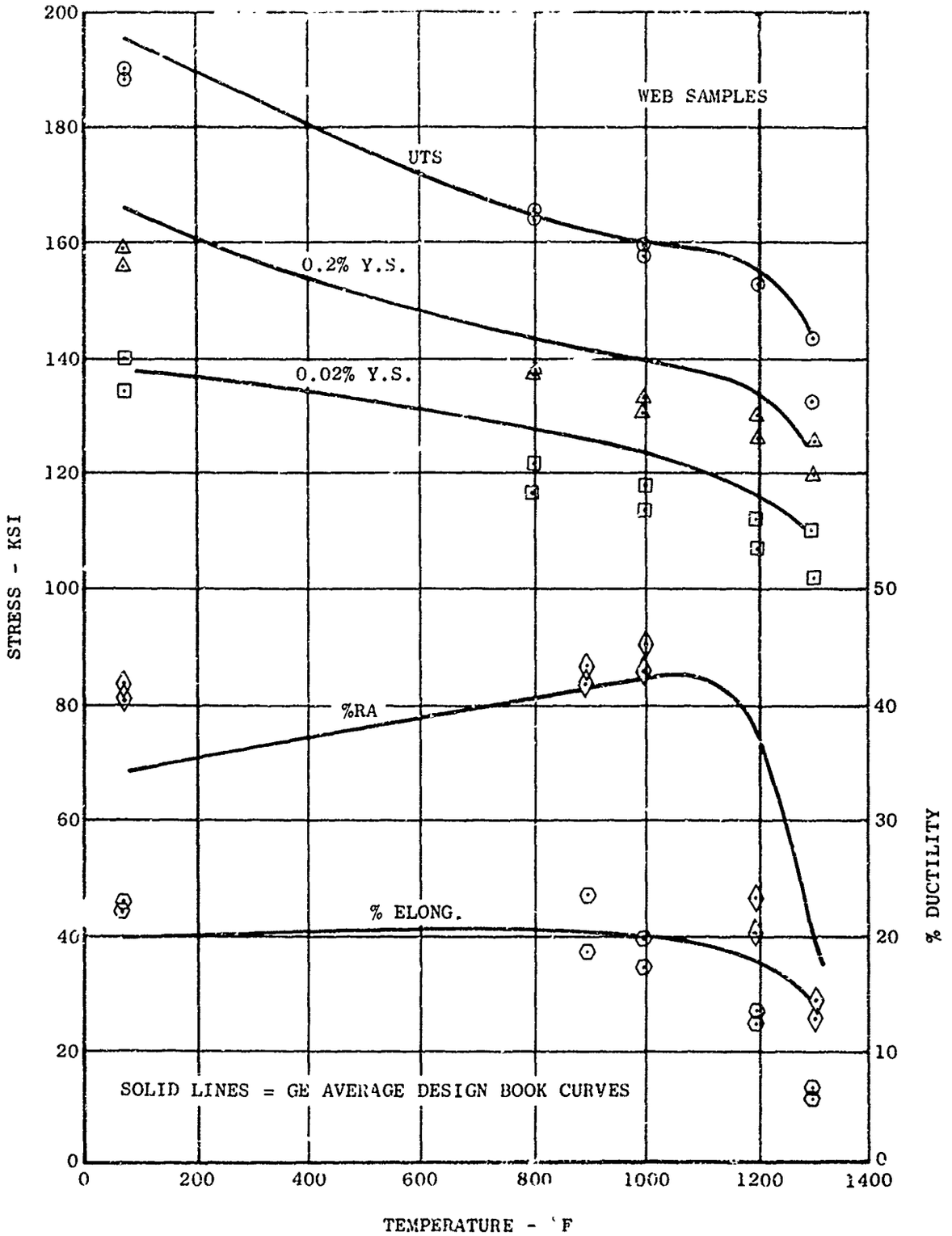

Figure 34 Tensile Properties of Cold Rim Formed (Web Section) Inconel 718 Cross Rolled Plate.

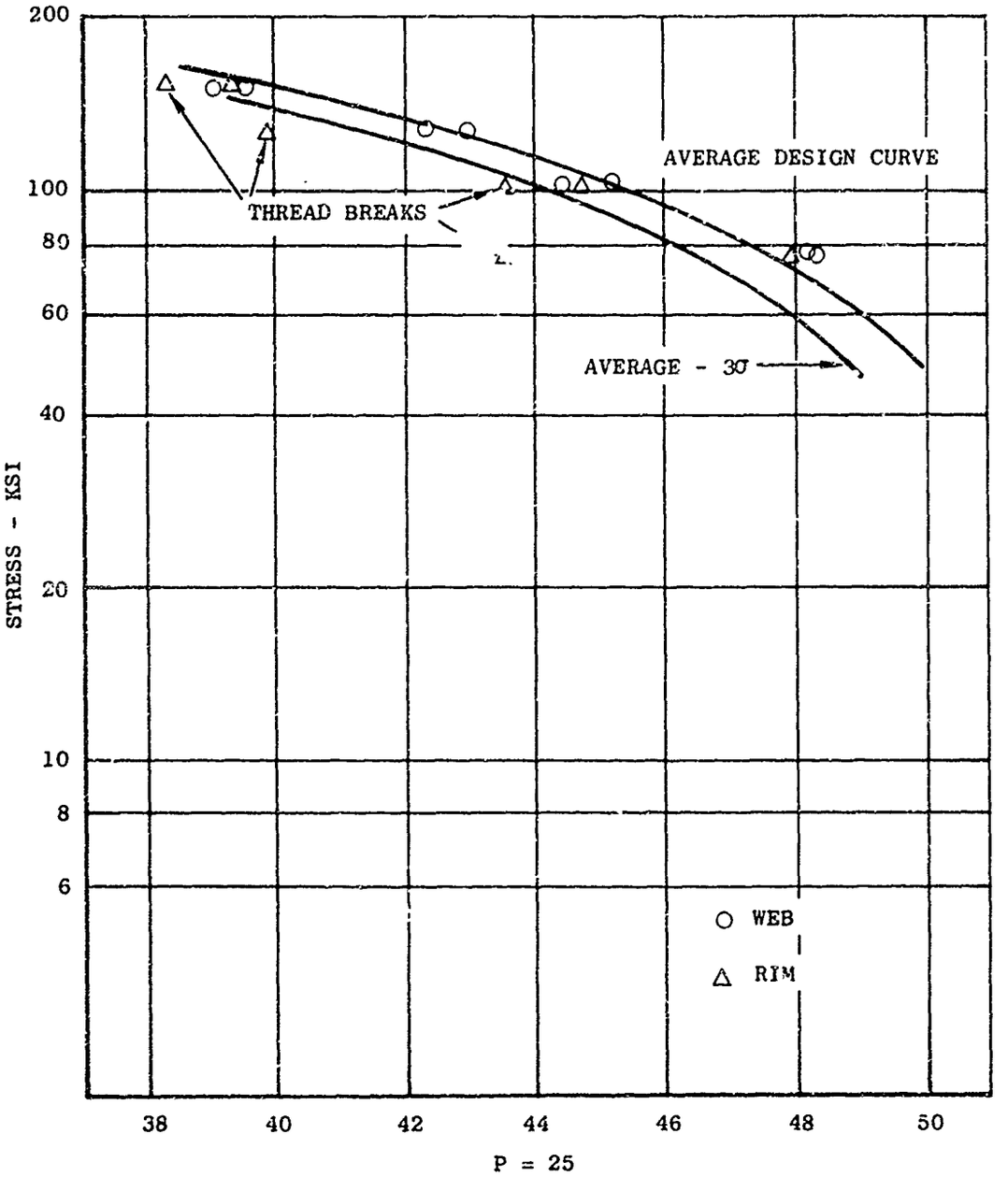

Figure 35 Stress Rupture Properties of Cold Rim Formed Inconel 718 Cross Rolled Plate.

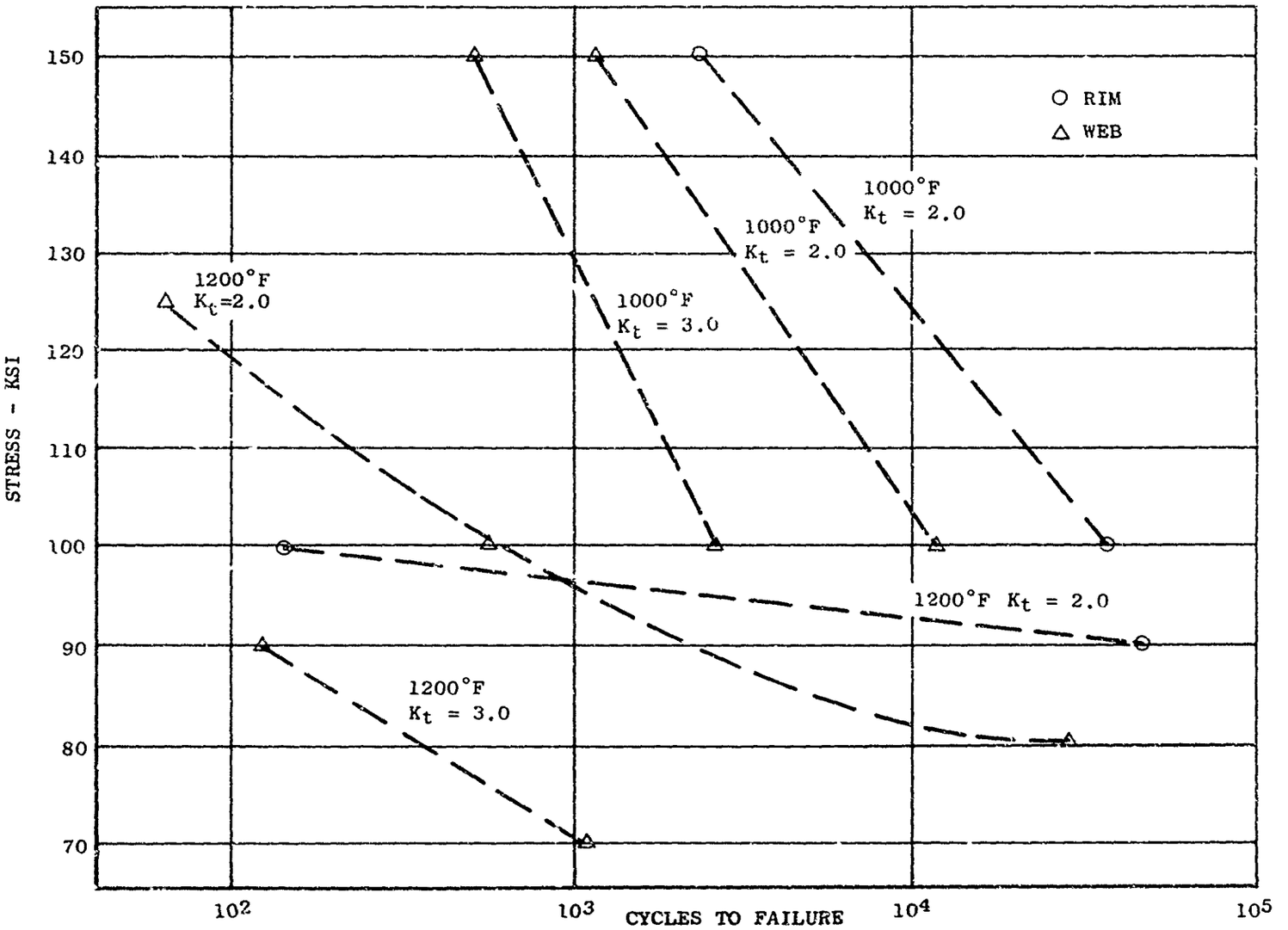

Figure 36 Interrupted Low Cycle Fatigue Properties of Cold Rim Formed Inconel 718 Cross Rolled Plate.

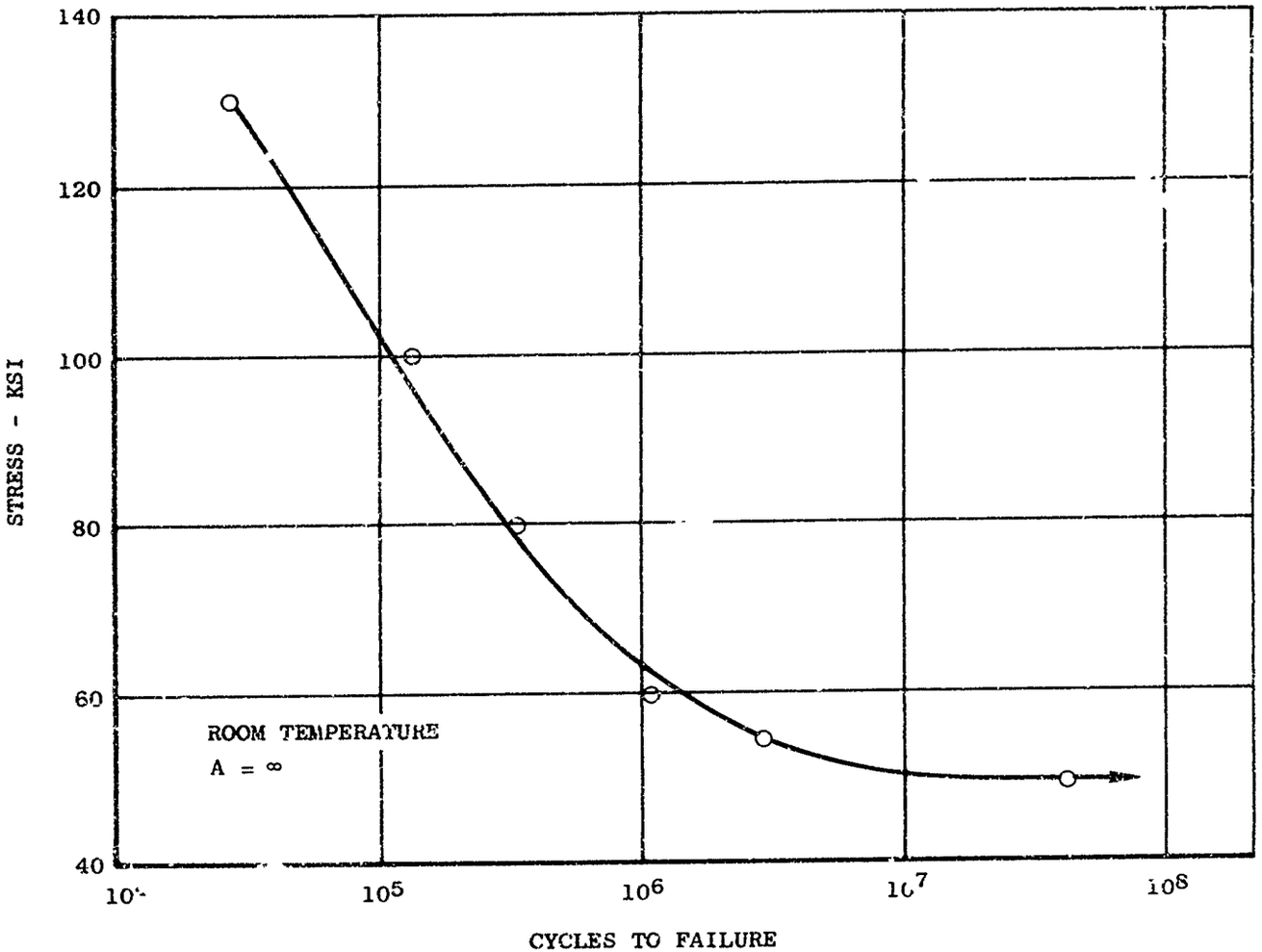

Figure 37 Rotating Beam Fatigue Properties of Cold Rim Formed Inconel 718 Cross Rolled Plate.

Figure 38 Compressor Disc Blank Prior to Cold Forming

forming a circumferential "V" notch. Each leg of the "V" is then flared out 90° to form the rim of the wheel or rotor stage, Figure 39. The sequence of operations is illustrated in Figure 40. A multistage compressor rotor can then be fabricated by inertia welding the rims of individual rotor stages together, Figure 41.

The machine used in the development (and in subsequent fabrication) of the cold rim forming process was a 42 inch x 50 inch horizontal Cincinnati Hydrospin Machine rated at 50,000 lb. force cross slide capability. Because of the unique type of forming, the specific machine parameters developed are for this machine only. The basic process, however, is adaptable to other forming machines of comparable capabilities.

The basic orientation of the tooling and components for cold forming is shown in Figure 42. The basic machine movements for the forming operation are made by the rotating spindle, and the hydraulically actuated cross slides. The deformation of the part is determined by the type of tool rings, Figure 43, mounted in the cross slide adapters. Figure 44 illustrates the cross sectional view of the actual work area. The cross slides are fed in to form the part. The two basic machine parameters for this forming operation are the spindle speed and the cross slide feed rate (measured in inches per minute).

Dimensional control was achieved by controlling the depth of penetration of the tool rings by setting the cross slide micrometer stops. To facilitate measurement, the distance from the end of the micrometer screw to the face of the micrometer dial was used as a process parameter. The cross slide pressure system was maintained at 1200 psi using 8 inch diameter hydraulic cylinders.

The spindle speed was controlled by the use of a potentiometer with a speed indicator in revolutions per minute (RPM).

The axial orientation of the cross slides was controlled by the use of adjustable stop blocks between the mainslide housings and the machine way housings. The mainslide hydraulic pressure system (approximately 1400 psi in 8 inch diameter hydraulic cylinders), was allowed to work against the mechanical stops while rolling, thus assuring no drift in the axial location of the mainslides.

The cross slide feed rate and spindle speed were held constant during the various stages of the process. The deflections on the cross slides, controlled by use of the cross slide stop settings, changed as a function of force. Therefore, a stop setting had to be developed for each machine set up.

These techniques were somewhat individualistic since the design of the machine mainslide and cross slide structures was for primary loading parallel to the machine centerline. When cylindrical or conical shapes are spun on this machine, the deflection of the cross slides along the axis of the machine is not critical. During radial forming, as in this process, axial machine deflections were critical since the formed circumferential envelope had to be located about the disc centerline.

2. Parameter Development

(a) Mild Steel Components - Prior to cold forming cross rolled Inconel 718, fifteen mild steel discs were used to determine the flow tendencies of metal in this particular work configuration. The original process plan included three roll form passes (split,

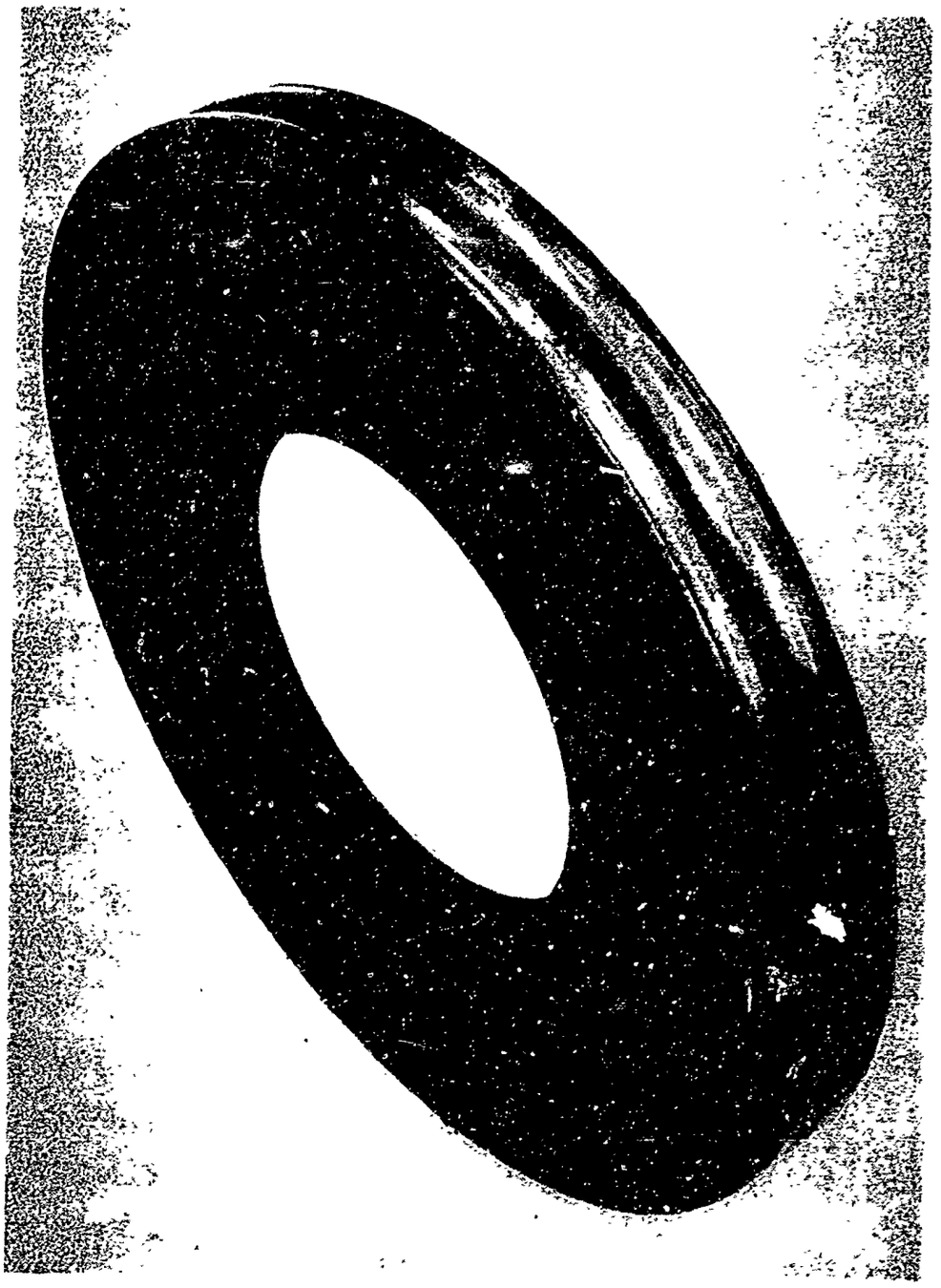

Figure 39 Mild Steel - Compressor Disc after Cold Forming

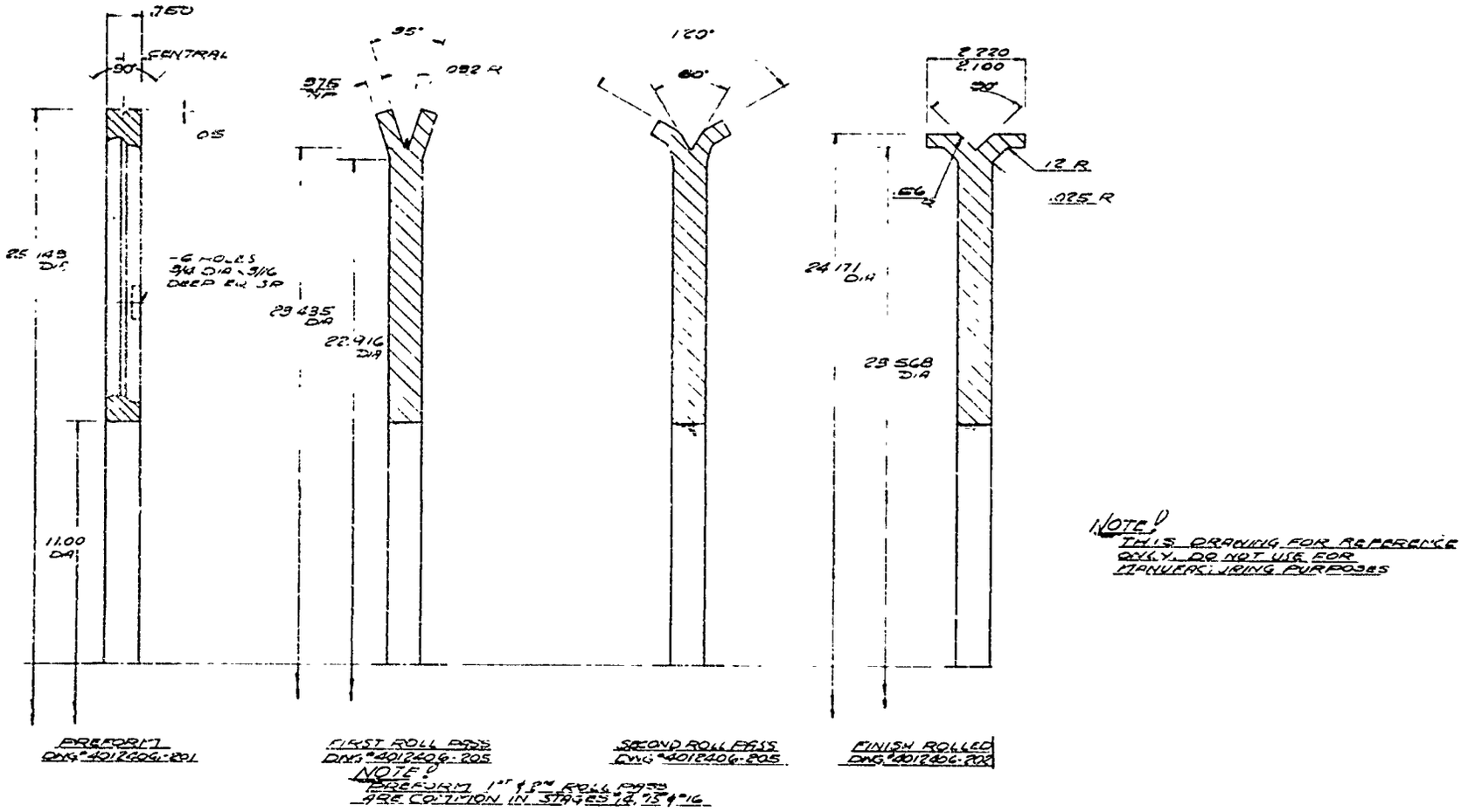

Figure 40 Sequence of Cold Rim Forming Operation

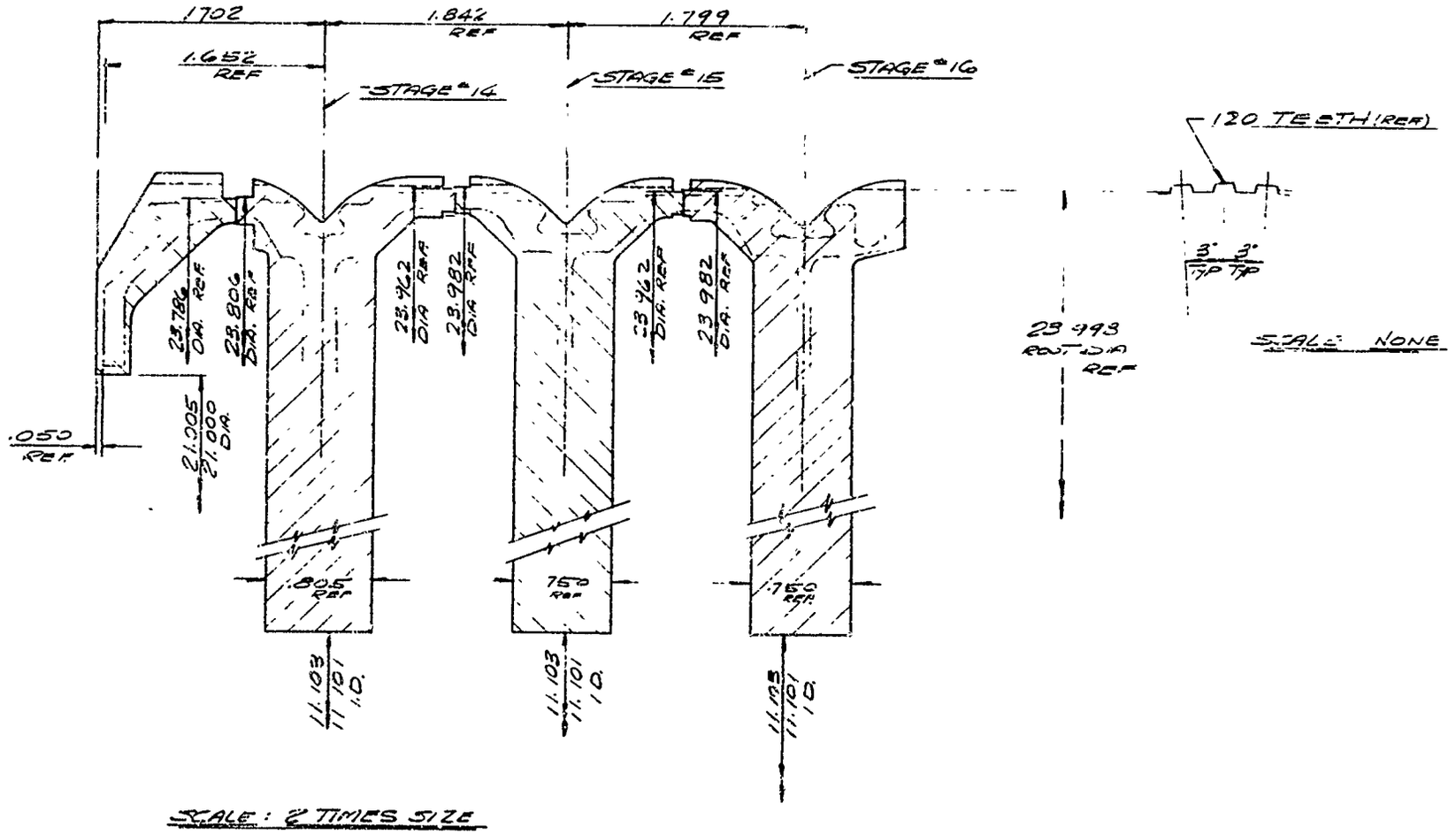

Figure 41 Configuration of Multistage Compressor Rotor Inertia Welded from Cross Rolled Plate

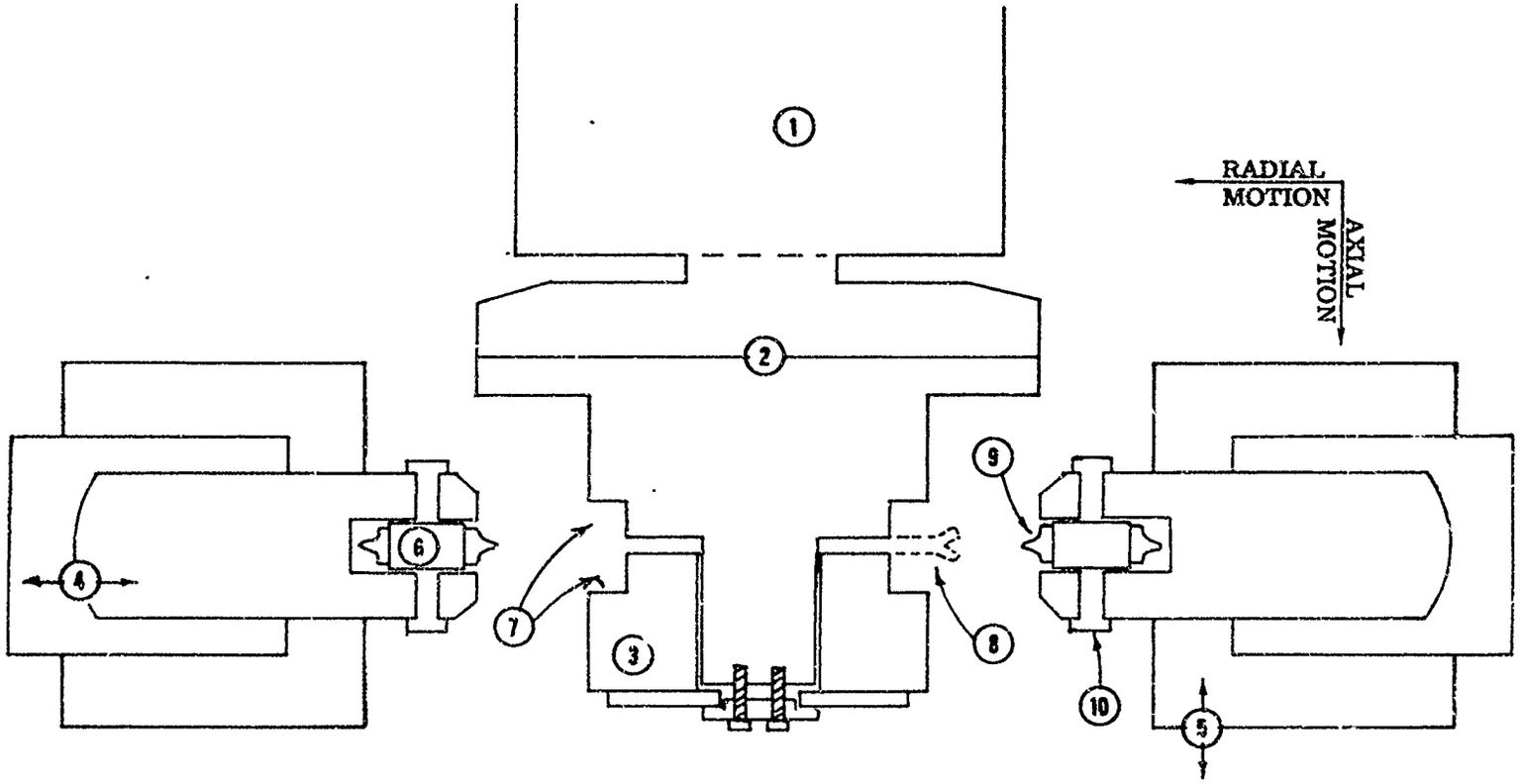

1. Spindle Housing
2. Spindle & Mandrel Interface
3. Rear Mandrel (removable)
4. Cross Slide
5. Main Slide
6. Tool Ring Adapter
7. Location of Back-up Tool Rings
8. Part Mounted on Mandrel
9. Tool Ring (Split)
10. Tool Ring Housing Shaft

Note: Arrows ← (X) → indicate functional direction of component.

Figure 42 Machine Layout - 42" x 50" Hydrospin

Figure 43 Tool Rings for Cold Forming Compressor Disc Rims

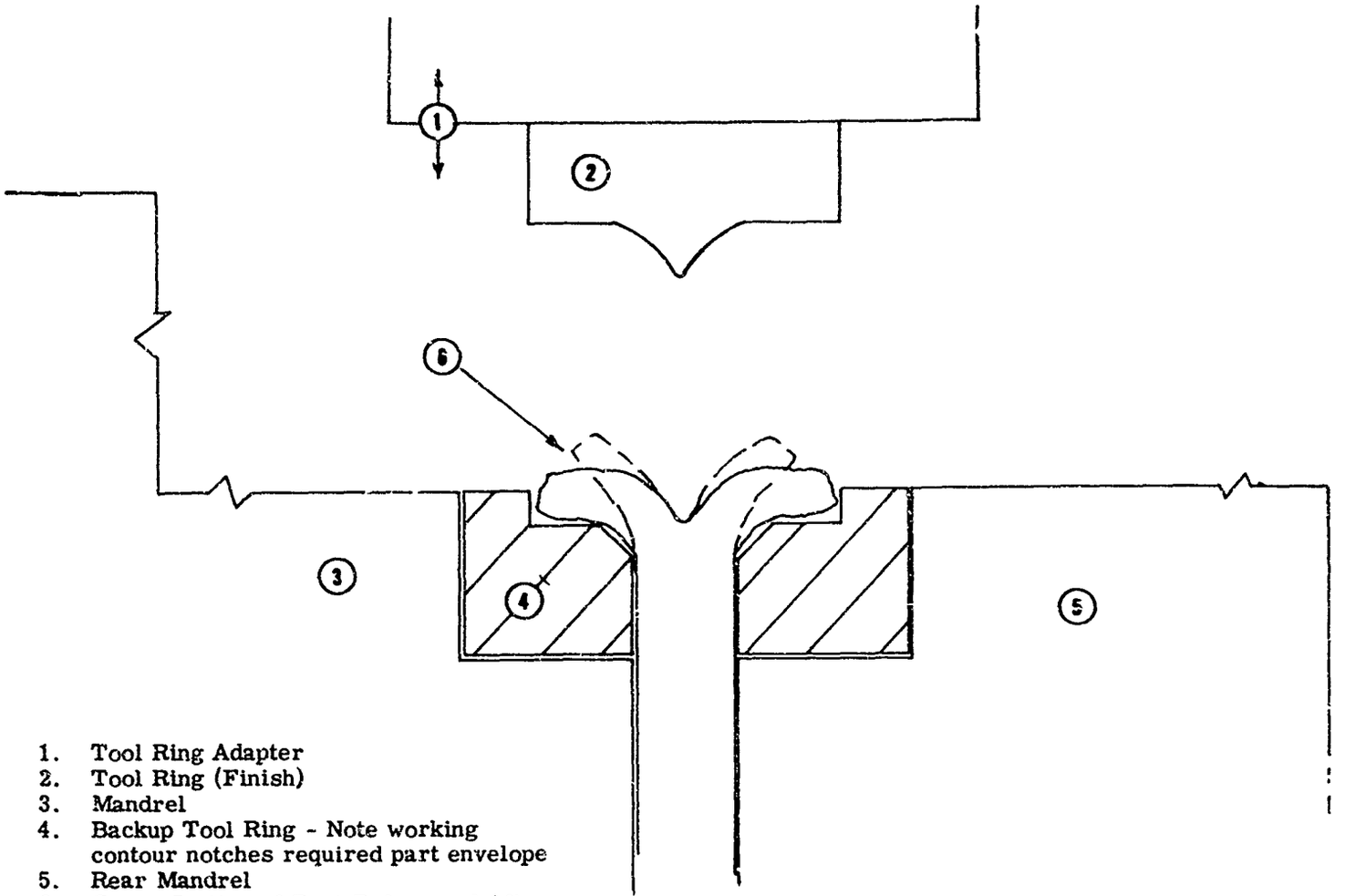

1. Tool Ring Adapter
2. Tool Ring (Finish)
3. Mandrel
4. Backup Tool Ring - Note working contour notches required part envelope
5. Rear Mandrel
6. Cross Section of Part Before and After Forming

Note: Arrows indicate functional direction of component

Figure 44 Cross Section of Work Area Before and After "Finish" Pass

spread, and finish). Initial development procedures on the mild steel components included an attempt to cold form all three passes without an intermediate stress relief, the omission of the "spread" pass and the movement of the stress relief operation to various stages in the process. Table XXIV shows the parameter variations for the mild steel components. The process finally developed with the mild steel discs was as follows:

- Split operation
- Stress relieve (1250°F/1 hr/AC)
- Spread operation
- Finish operation
- Angle operation (stages 14 and 16 only)

Several problems arose during the development of the processing technique for the mild steel parts:

- Improper diameter control of the shear formed groove due to improper selection of a cross slide feed rate. A 3 inch advance per minute feed rate minimized this problem.

- Improper location of the split center line to the part center line: this problem was not resolved until the positive stop technique was developed.

- Severe laminations and cracks at the base of the groove in the root dovetail area: investigation of the failures indicated that laminations and pipes in the base material caused the failures.

- Failure of two splitting rolls during roll forming: laminations and cracks in the groove area caused the failure of two "split" rolls during the latter stages of the development of the process. The first split roll failed while rolling disc S/N S-14. A replacement roll was manufactured. During the last run of the mild steel blanks the second of the original pair of split rolls failed in a manner similar to the first failure. Hardness measurements indicated that the tool rings were in the proper metallurgical condition. Both of the mild steel parts being rolled when the failures occurred had severe laminations in the root area offset from the centerline of the machined part centerline by 0.050 to 0.070 inch. When these laminations opened up during the forming operation, the tool rings experienced rapid fluctuations in resistance pressures from the opposing sides of the part. These rapid variations in the axial loads caused the tool rings to fatigue and ultimately fail in the relieved areas behind the actual work area of the tool ring. Tool ring configurations were altered to strengthen these areas.

(b) Inconel 718 - The failure of the second tool ring immediately before starting the development of the cold form process for Inconel 718 required adjustments in the use of the various tool rings. It was decided to use a "split" roll on one side with an opposing "spread" roll. The first part, S/N 1, was split-spread and was defect free. However, a radical change in the cross slide deflection caused the part to be dimensionally incorrect (the groove diameter was undersize, violating the part envelope at the base of the dovetail slot). This part, S/N 1, was then finish rolled to a stage 15 configuration to determine if the material was capable of withstanding additional forming without intermediate annealing. The finish pass propagated several small surface cracks at the base of the groove diameter, indicating the material would require an intermediate anneal.

Since the initial split-spread operation had been successful, several more parts were processed through this operation. The lot was then annealed, (1850°F/90 min/AC).

Attempts were then made to develop a technique for forming the stage 14 and 16 configurations using a pair of 25°, 0.25 inch radius rolls. The components were difficult to form until the back up tool rings were removed, thus allowing the material to fold without resistance. The stage 14 and 16 component envelopes were then easily formed using the radius rolls and previously developed machine parameters.

The results of processing 13 Inconel 718 discs are listed in Table XXV. Machine parameters used to form the dimensional envelopes are given in Table XXVI.

With respect to the rim forming of Inconel 718, the major problem was cracking in the dovetail groove area. Subsequent investigation of the metallurgical condition of cracked components indicated that they had not received the specified solution treatment (1850°F/90 min/AC) either before cold forming or after the split-spread pass and as a result were still too hard for cold forming.

3. Process Evaluation

(a) The Split Operation - The split operation, first of the four pass process, physically parts the machined disc to create the two rims necessary for inertia welding. This initial operation was the most critical dimensionally since the relative position of the groove to the part centerline and the diameter of the groove, both determined during this pass, are priority dimensions in assuring no violations of the part envelope.

The split-spread technique, using unmatched opposing tool rings, worked satisfactorily, and parts that had been properly annealed prior to forming were defect free after the operation. Dimensionally, the parts exhibited the "spread" configuration, Figure 45, which is the limit of cold forming without surface cracking.

(b) The Spread Operation - This pass increases the included angle of the groove from 49° to 60° in the dovetail slot area and to 120° in the outer flange area. The peripheral part contour matches the contour of the "spread" rolls, Figure 45. Functionally, this configuration separates the flange material so that the subsequent finish pass will produce the axial width required to assure the part envelope.

(c) The Finish Operation - The third roll form pass forms the circumferential contour necessary for the machining and welding of the part, Figure 46. The outer flanges are flattened out so that the inside envelope of the outer flanges can be formed during the subsequent operation.

(d) The Angle Operation - The final pass technique developed to form the required part configuration utilized a pair of 25°, 0.25 inch radius rolls. The depth of penetration with these rolls and the relative alignment of the rolls to the finish part was determined by the stage designation for the particular part being formed. Figures 47 and 48 illustrate the two general techniques, the first being a single ring technique used to "pinch-in" the outer flange edges sufficiently to meet the pre-weld part envelope. The second technique (with matched opposing rings) folded the material in to form the difficult part configurations necessary for stages 14 and 16.

A significant variation for this pass was the removal of back up tooling during the run. The part was formed with little machine deflection since the machine cross slide pressure was working entirely against the material being formed rather than against the part and the back up tooling. During the development program this operation was performed in two steps (one pass for each flange). A production technique could be developed to eliminate the duplicate effort.

Figures 49, 50 and 51 illustrate the finish rolled parts. The critical areas of the part envelope are at the dovetail and the edges of the outer flanges.

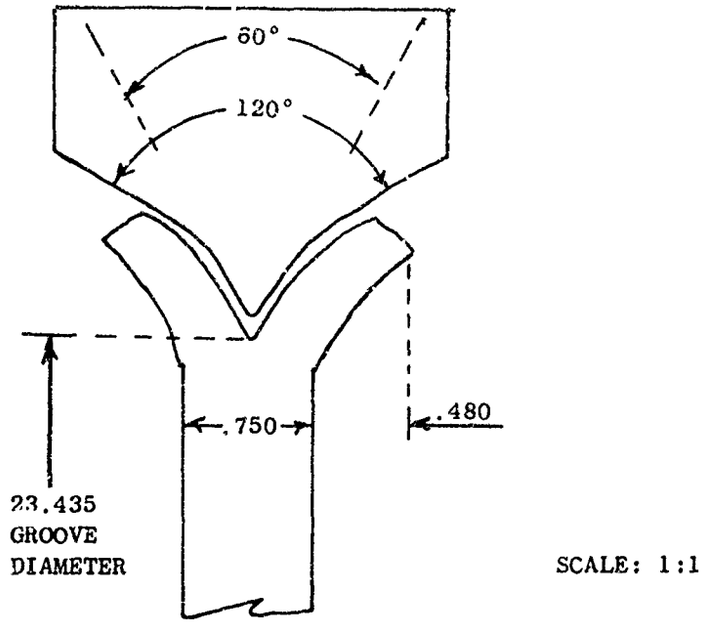

Figure 45 Spread Configuration

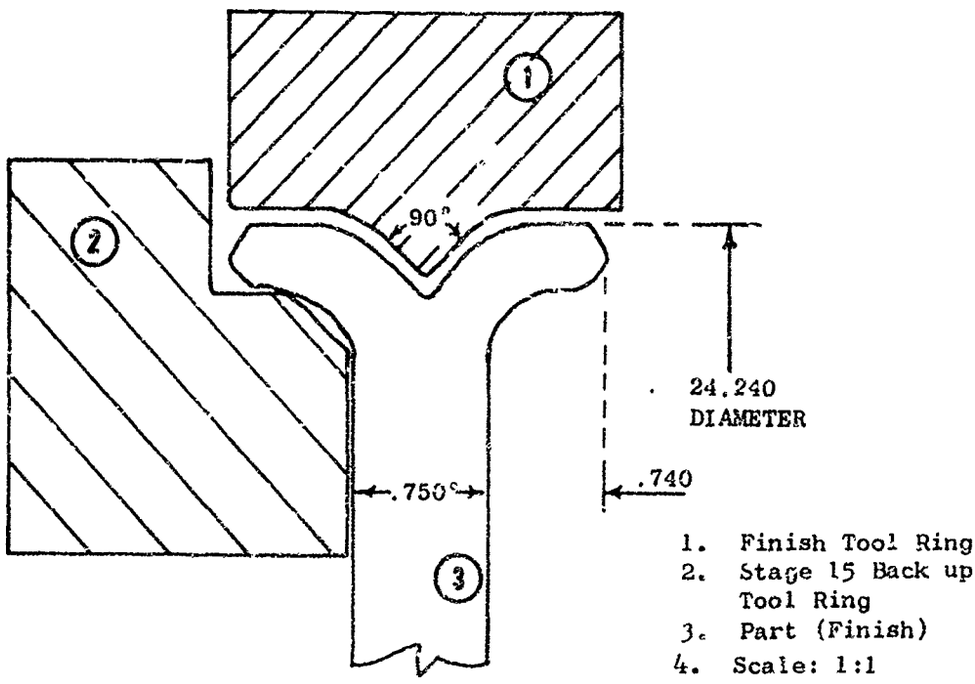

Figure 46 Finish Configuration

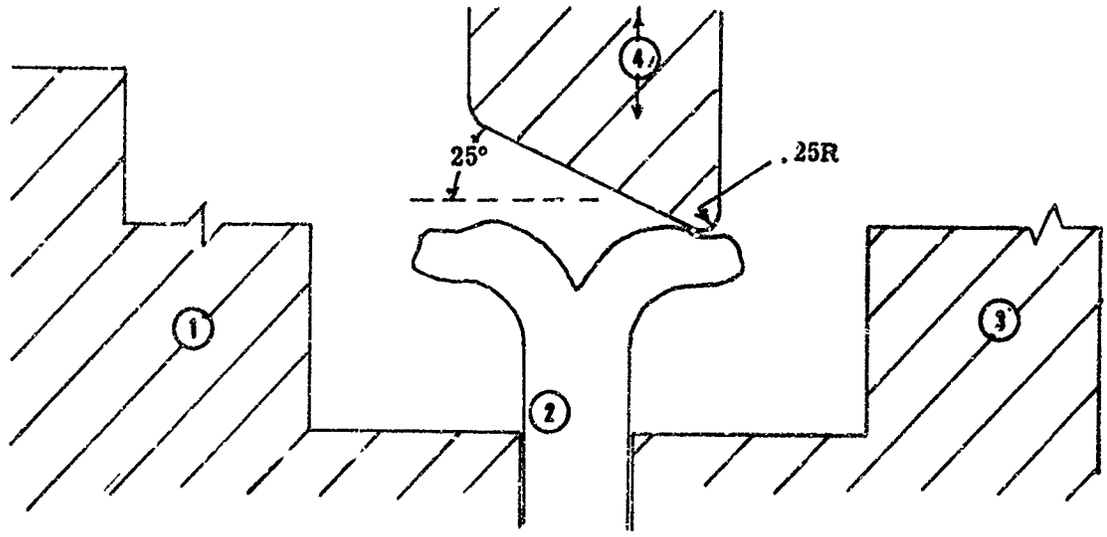

1. Mandrel
2. Stage 15 Component
3. Rear Mandrel
4. Single 25°, .25 Radius Roll

Figure 47 Stage 15 Component During the "Angle" Operation
(Note That Backup Rings have been removed)

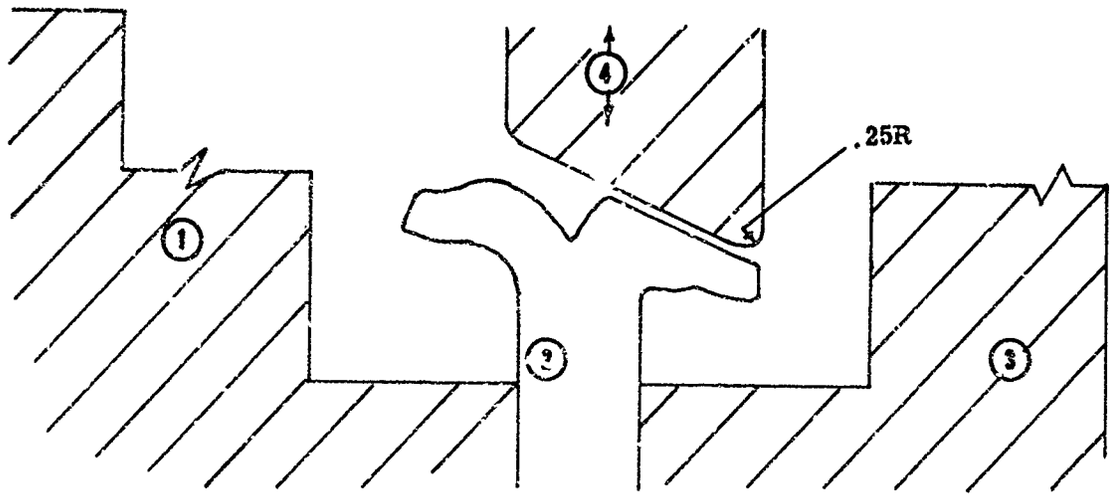

1. Mandrel
2. Stage 16 Component
3. Rear Mandrel
4. Matched Set of 25°, .25 Radius Rolls

Figure 48 Stage 16 Component During "Angle" Operation

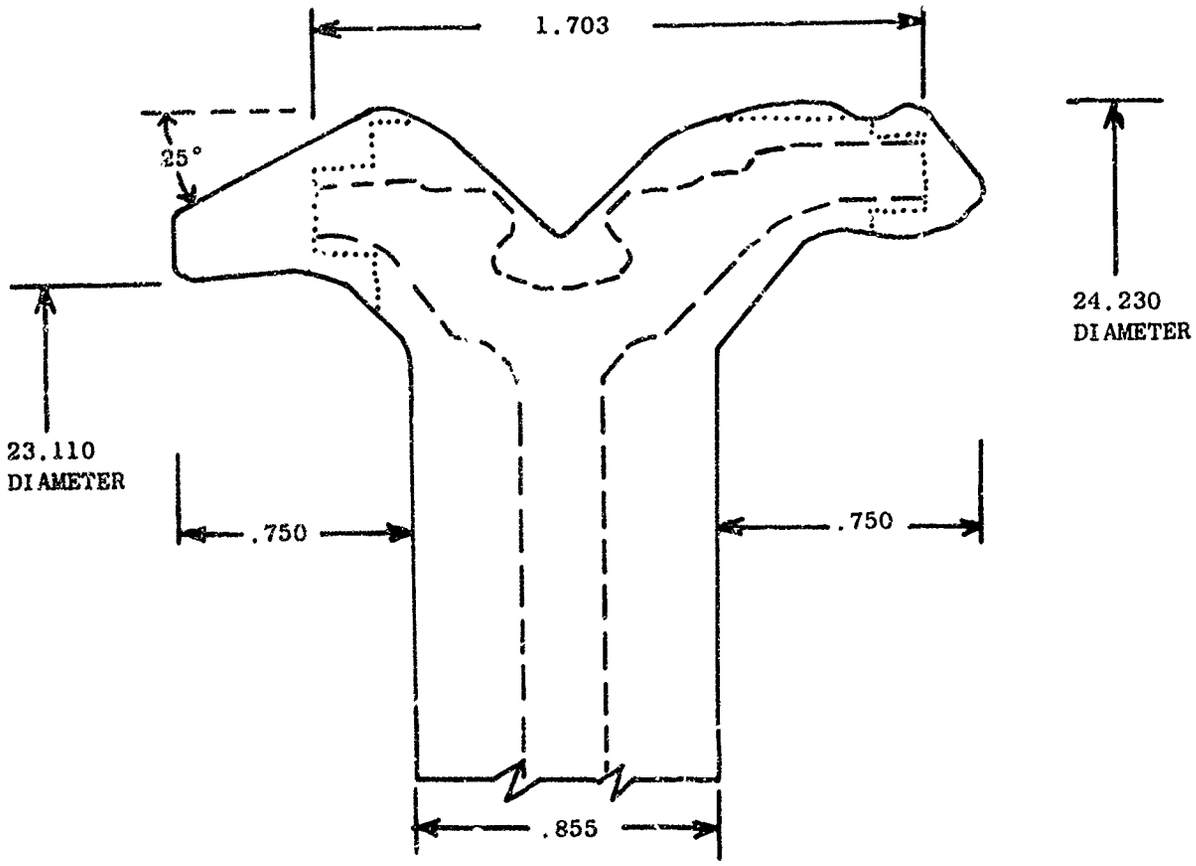

KEY:

1. Scale is 2:1
2. Solid Line Indicates Roll Form Envelope
3. Dashed Line Indicates Finish Machined Envelope
4. Dotted Line Indicates Weld Prep Configuration (Prior to Inertia Weld)

Figure 49 Stage 14 Disc After Rim Forming

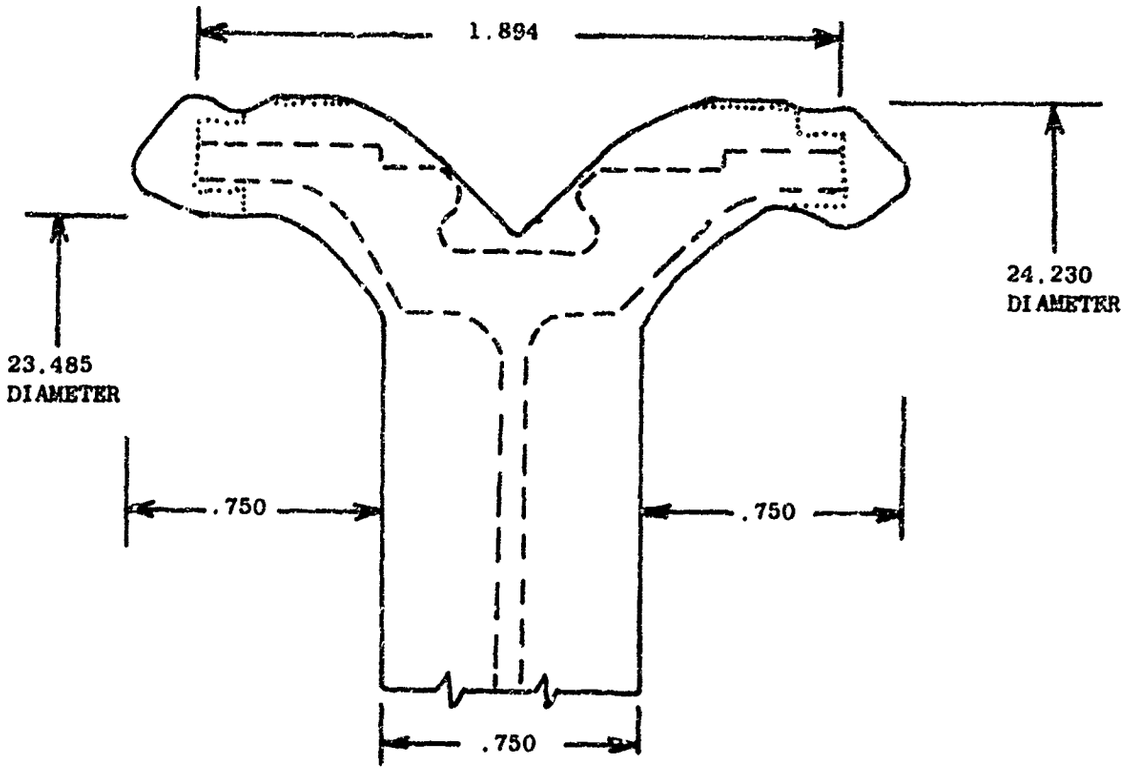

KEY:

1. Scale is 2:1
2. Solid Line is Roll Form Part Envelope
3. Dashed Line is Finish Machined Part Envelope
4. Dotted Line is Weld Prep Envelope (Prior to Inertia Weld)

Figure 50 Stage 15 Disc After Rim Forming

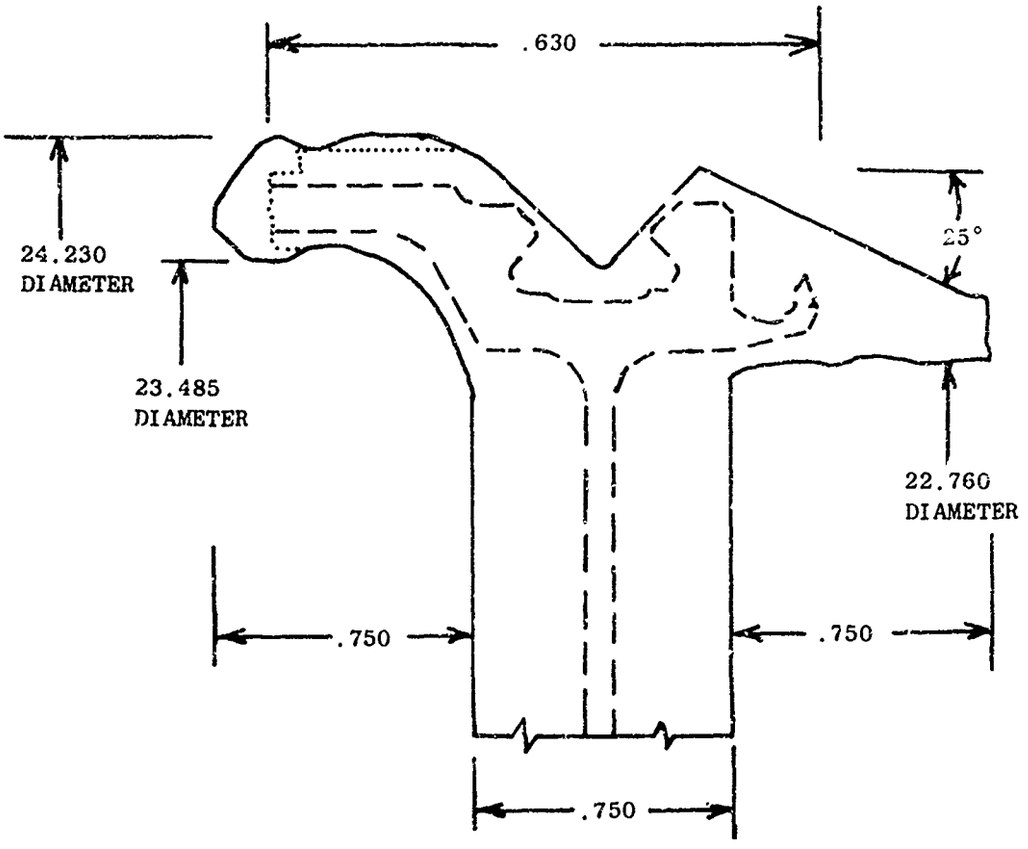

KEY:

1. Scale is 2:1
2. Solid Line is Roll Form Part Envelope
3. Dashed Line is Finish Machine Part Envelope
4. Dotted Line is Weld Prep Part Envelope (Prior to Inertia Weld)

Figure 51 Stage 16 Disc After Rim Forming

SECTION V.

COMPRESSOR ROTOR FABRICATION

A. FABRICATION FROM CROSS ROLLED PLATE

1. Cold Rim Forming - The optimization of the cold rim forming process was discussed in the previous section. Of eight rotor stages accepted for inertia welding, Table XXV, only one was a stage 14 disc. Accordingly five additional plates were procured and processed to allow the fabrication of four complete TF39 Stage 14 - 16 compressor rotors.

Although the certificate test report showed the chemical analysis and mechanical properties of the cross rolled plates to be within GE specifications, Tables XXVII and XXVIII, metallographic examination of test pieces removed from the plates showed them to have a duplex grain structure.

This condition was similar to that of the plates which had cracked in cold rim forming, Figure 52. In addition, the plates had Rockwell D hardness values ranging from 32 to 41, somewhat higher than desirable for successful cold forming.

To achieve a more uniform grain size, and to increase ductility for rim forming without danger of cracking, the plates were heat treated for 90 minutes at 1950° F followed by a rapid air cool. This resulted in a completely recrystallized structure, Figure 53, with a Rockwell D hardness of 25.

The 42 inch Cincinnati Hydrospin machine had been used between forming the initial group of discs and this group. Therefore, several parameters used originally had to be reset and recalculated. Two of the mild steel discs from the initial development program were run to reestablish the necessary parameters. These trials ran well and produced dimensionally correct results. The Inconel 718 discs were then formed and checked. This secondary run of five discs produced:

- 4 acceptable stage 14 discs
- 1 acceptable stage 15 disc

The surface cracking problem of the initial development run did not appear during this supplemental run due to close control of the initial heat treat cycle. An evident problem, however, was that of maintaining the split centerline on the part centerline due to lack of control of the machine's deflections.

Tables XXIX and XXX illustrate the machine parameters used and the dimensional results. Because of the special nature of forming, the specific machine parameters are applicable to this machine only. The basic process of course, is adaptable to other forming machines.

Prior to weld prep machining the five discs were heat treated to the schedule: 1950° F/90 min/AC + 1800° F/1 hr/AC + 1325° F/8 hr/FC - 100° F/hr to 1150° F + 1150° F/8 hr/AC.

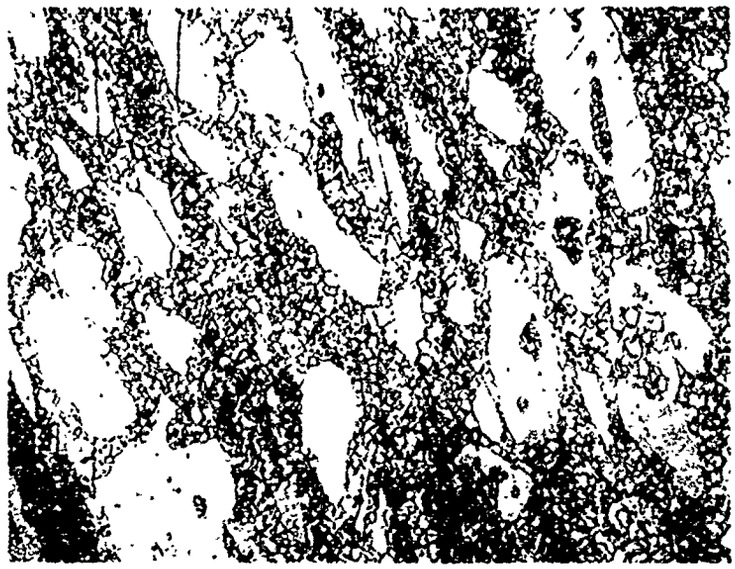

A-100X

Undesirable duplex structure of previous plates in as received condition

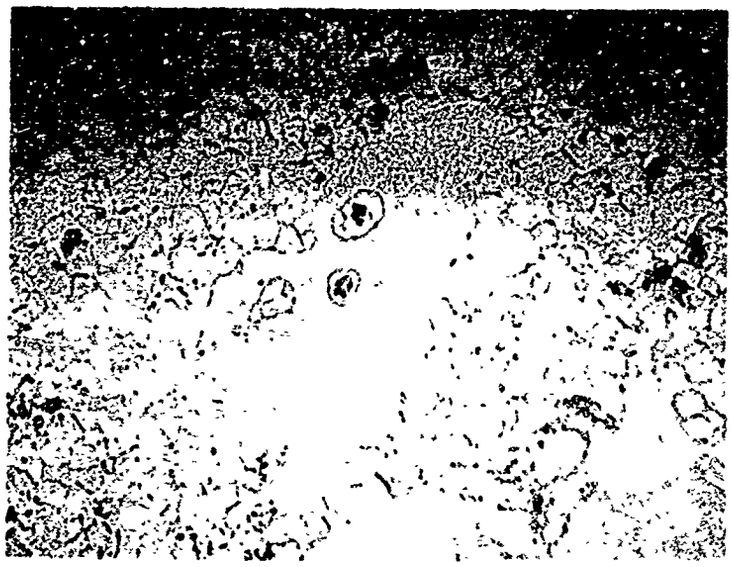

B-100X

Duplex structure in plates #1 #4 in as received condition

Figure 52 Duplex microstructures of as-received Inconel 718 cross rolled plate

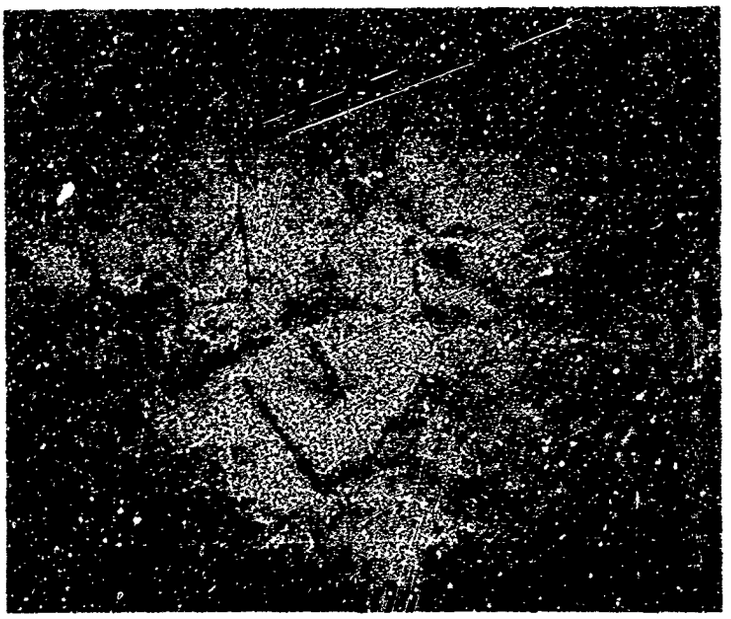

J4872 100X

Figure 53. Recrystallized Structure of Plates after 1950+0-50°F/90 Min/AC Prior to Cold Rim Forming Step

2. Machining and Inspection

(a) Machining - Splining of the outer diameters for holding and driving the rotor stages in inertia welding was selected as the method requiring the least development and offering the greatest degree of confidence in preventing work-piece-tooling slippage from the high torque values anticipated in welding.

In machining the weld prep configuration three problem areas were noted:

- The cold rim formed discs were out of flat making them difficult to set up.
- There appeared to be some hardness variation in the components which decreased machinability.
- The parallelism requirements of the weld prep faces were difficult to meet.

Photographs of a stage 14 attachment ring, a stage 15 and a stage 16 disc are shown in Figures 54, 55 and 56 respectively.

(b) Inspection - All rotor stages including the attach rings made from ring forgings were zyglo and ultrasonically inspected. Three sub-surface cracks 1/8 to 1/2 inch in length and 3/4 inch deep were detected in the dovetail groove of one stage 16 rotor in the same position where cracks were found by zyglo prior to post-form aging. An attempt had been made to hand grind the cracks out prior to aging. In addition to being unsuccessful, the grinding had deepened the dovetail groove to below minimum print diameter. No ultrasonic indications were detected in the rest of the stages.

Zyglo inspection showed numerous indications in and adjacent to the cold formed V-grooves on most of the stages. These appeared to be mainly tears or laps from the rim forming operation which should be cleaned up in subsequent machining.

A complete dimensional inspection was made of all rotor stages to determine their conformance to the pre-weld configurations shown in Figures 57, 58, 59 and 60. A total of 13 stages (4 stage 16's, 4 stage 15's, and 5 stage 14's) and 4 attach rings or flanges made from ring forgings were available for welding.

With respect to machined dimensions, only one part, a flange ring forging, was found out-of-print. The weld prep O.D. had been machined 0.020 inch undersize leaving no stock for flash clean-up and final machining. However, significant deviations were determined in the axial and radial position of the V-grooves with respect to the axial and radial centerlines of the discs. Wax impressions were made of the V-groove contours to establish maximum radial and axial deviations. Layouts at 10X size were made of the finished machined dovetails and the V-groove contours for each rotor part to determine optimum positioning of the dovetail centerlines for clean-up stock both at the dovetail and the hubs of each stage.

This allowed sorting and selection of the best stages to be welded together, then the second, third and fourth best as listed in Table XXXI

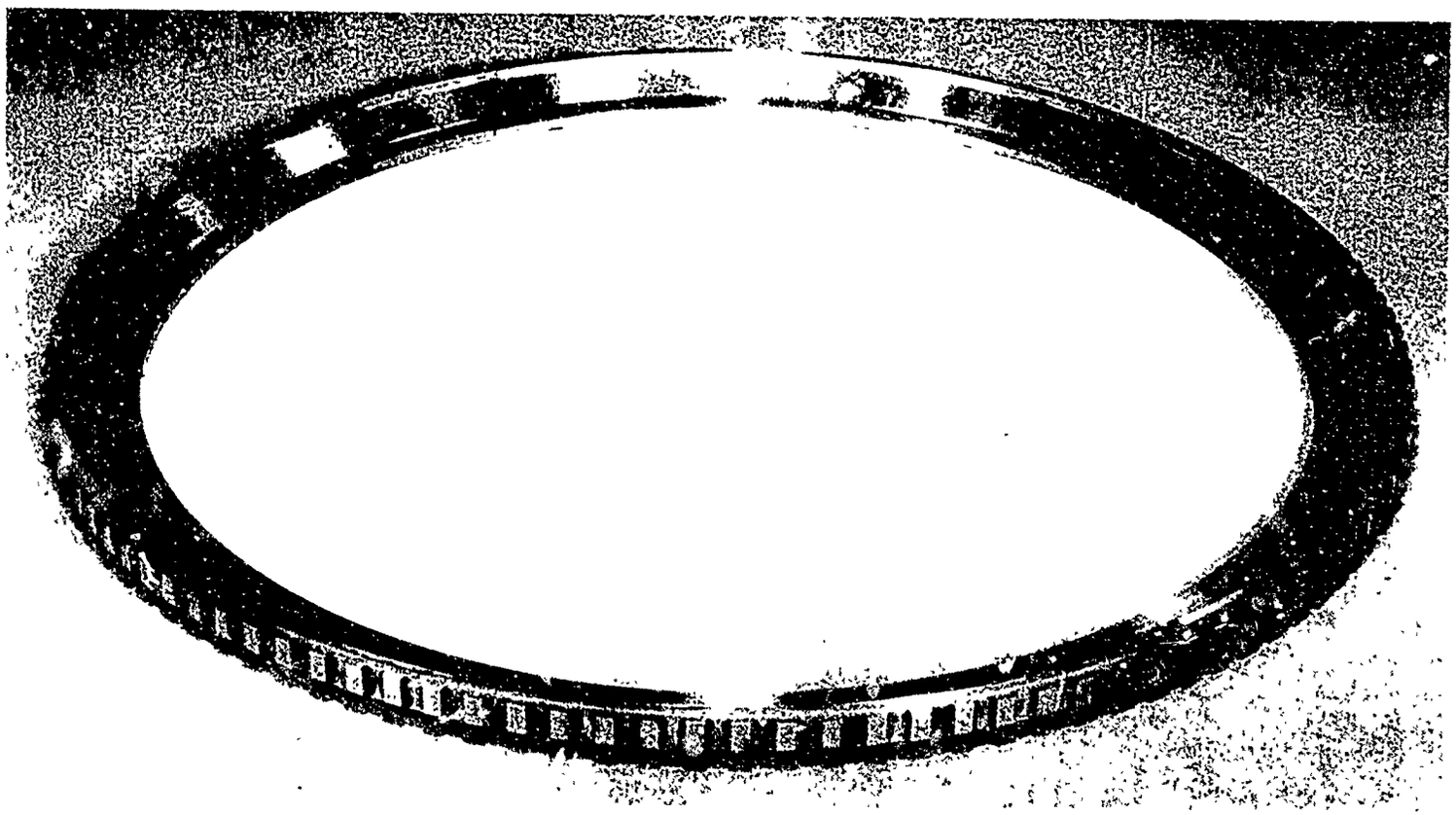

Figure 54. Stage 14 Attachment Ring TF39

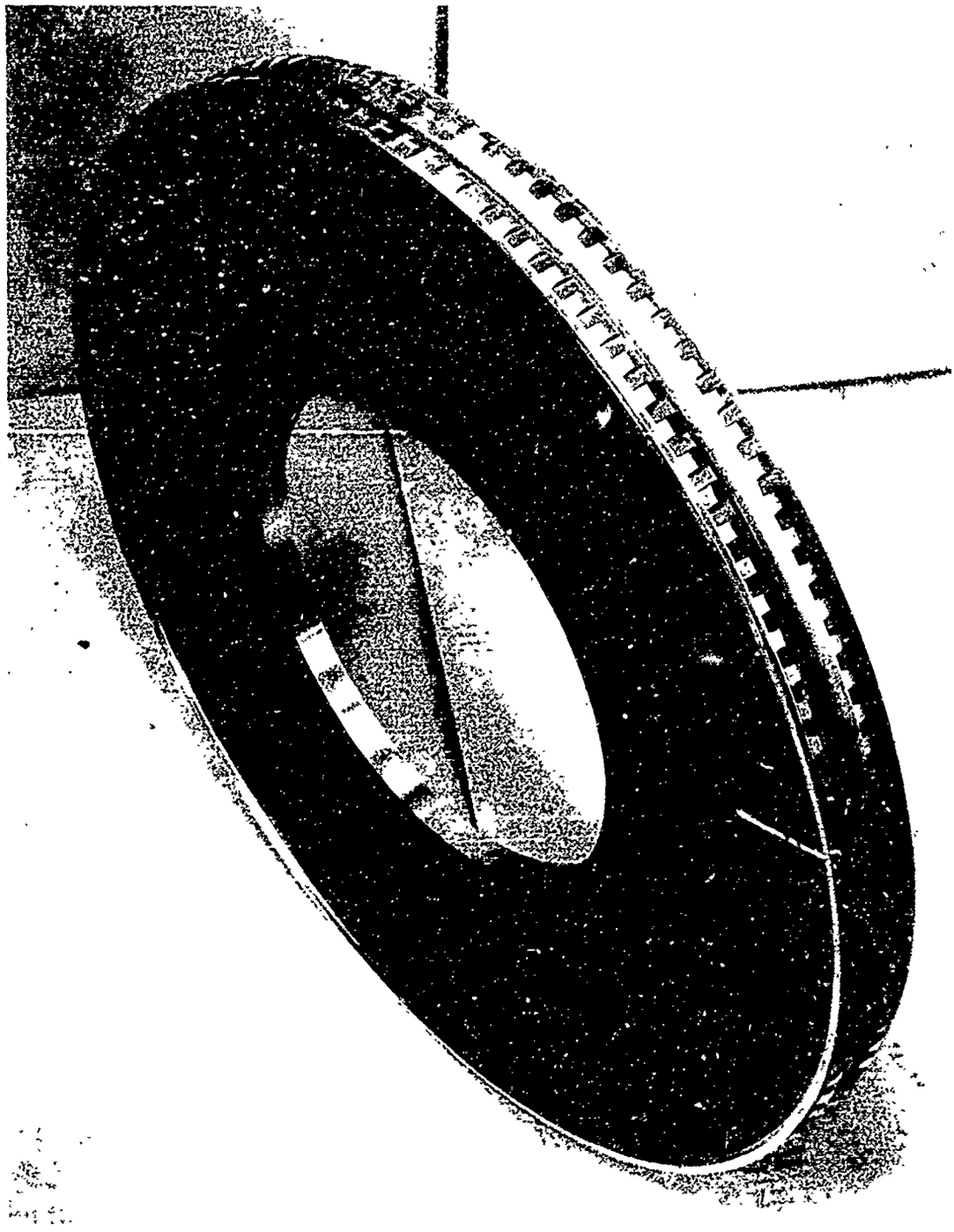

Figure 55. Finish Machined Cold Rim Formed Inco 718 Compressor Rotor Disc Stage 15

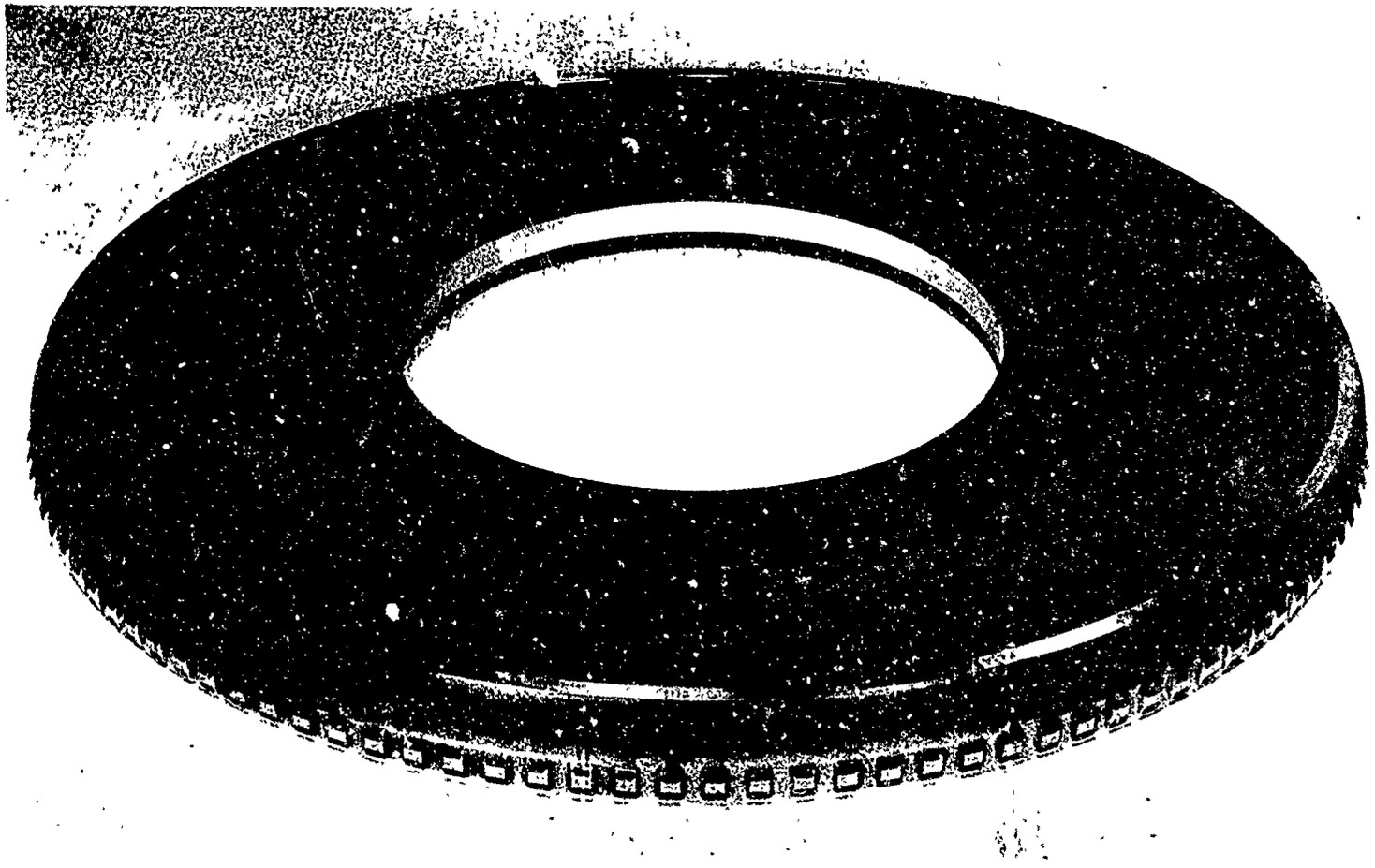

Figure 56. Stage 14 or 16 Disk TF39

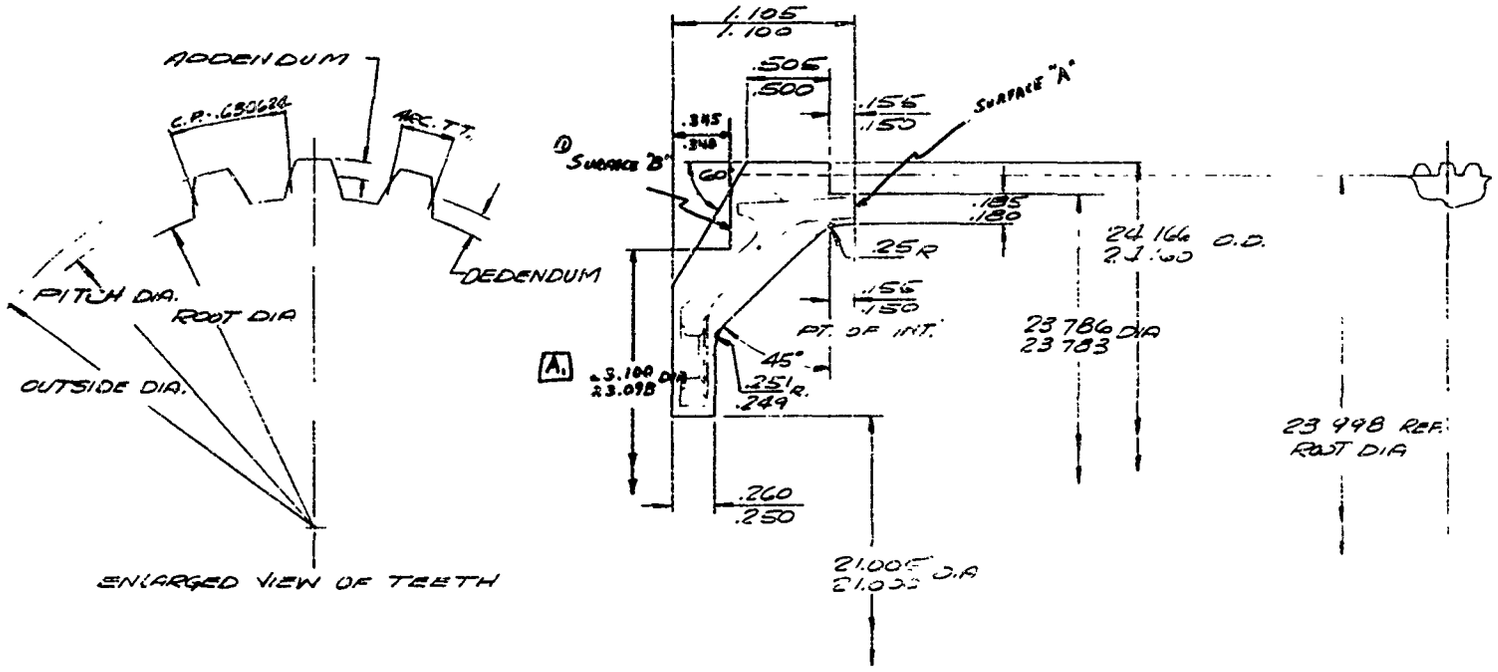

TOOTH DATA

DIA PITCH	6/28
PRES. ANGLE	14½°
OUTSIDE DIA	24.160 +.006 -.000
PITCH DIA.	24.088
ROOT DIA.	23.798 ±.0075
WHOLE DP.	.081
NO. TEETH	120
CIR. PITCH	.0806
ADDENDUM	.036 +.003 -.000
DEDENDUM	.045
ARC T.T.	.3153

A. NOTE:
ALL MACHINED DIA'S MUST BE CONCENTRIC WITH THE SPLINE O.D. WITHIN .003 TOTAL INDICATOR READING.

① SURFACES "A" AND "B" MUST BE FLAT AND PARALLEL WITHIN 0.001.

Figure 57 Pre-Weld Configuration of Attach Ring - Stage 14

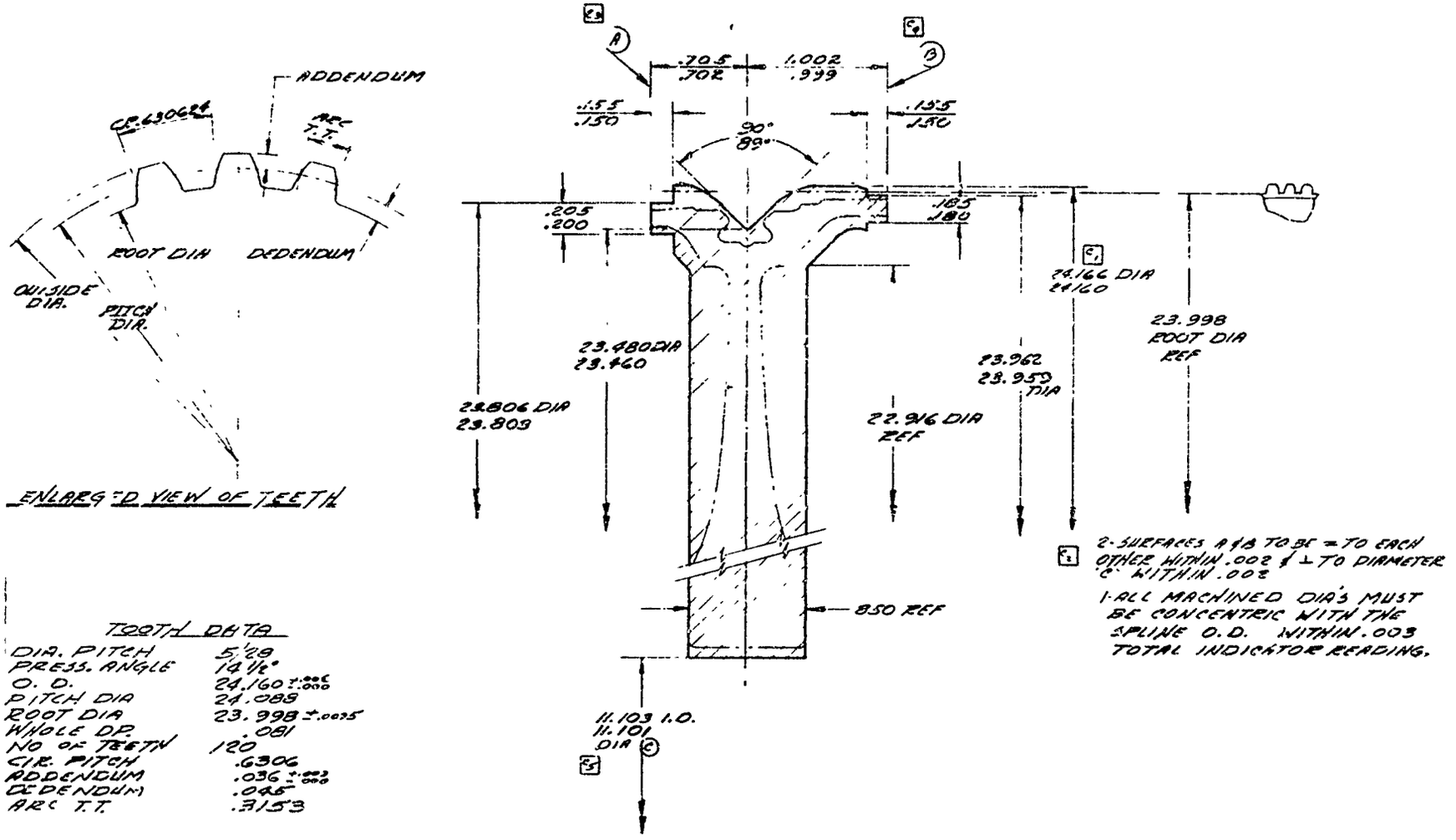

TOOTH DATA

DIA. PITCH	5/20
PRESS. ANGLE	14 1/2°
O. D.	24.160 +.000 -.006
PITCH DIA	24.089
ROOT DIA	23.998 ±.0035
WHOLE DP.	.081
NO OF TEETH	120
CIR. PITCH	.6306
ADDENDUM	.036 +.003 -.000
DEDENDUM	.045
ARC T.T.	.3153

Figure 58 Pre-Weld Configuration - Stage 14

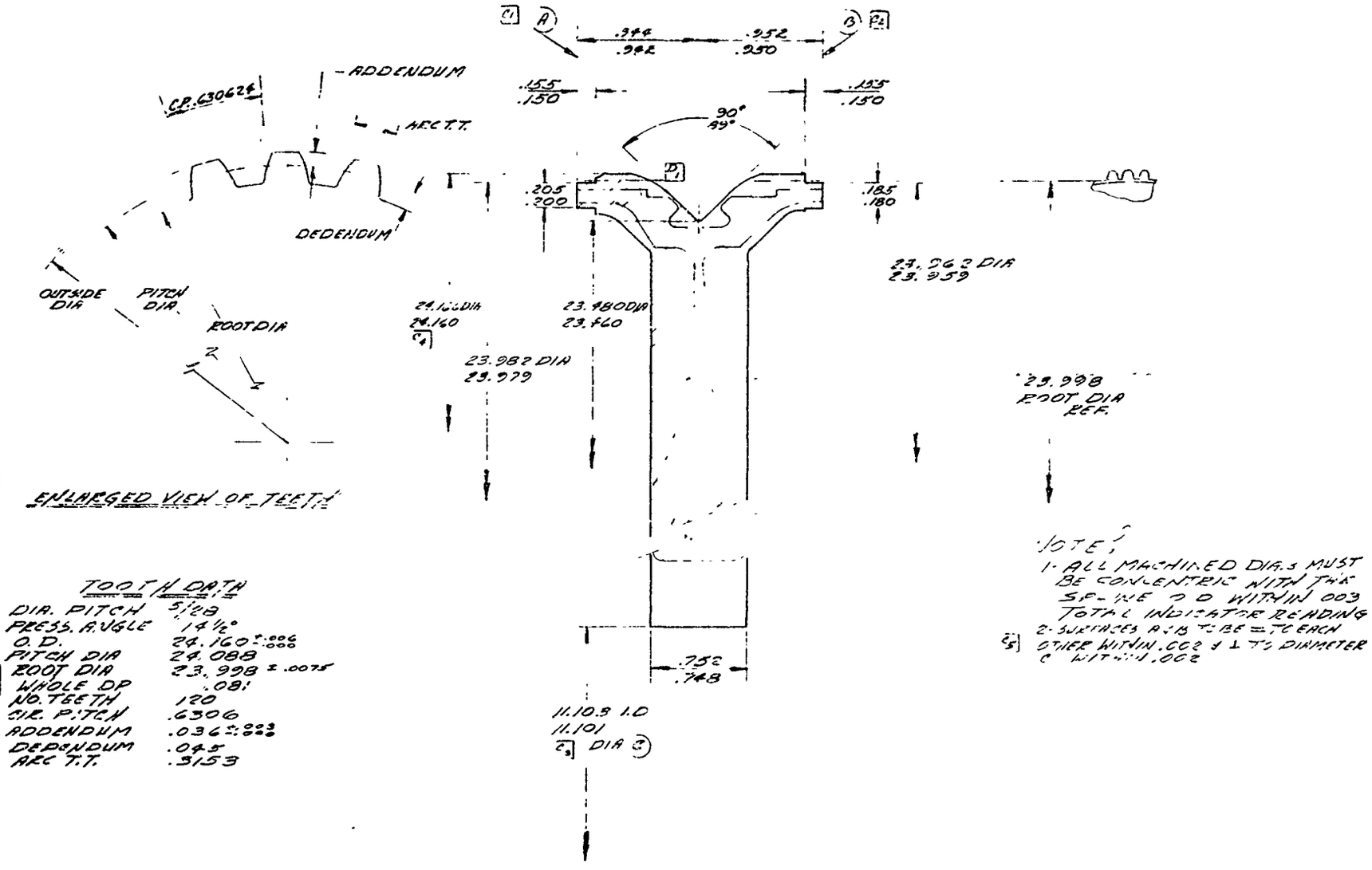

Figure 59 Pre-Weld Configuration - Stage 15

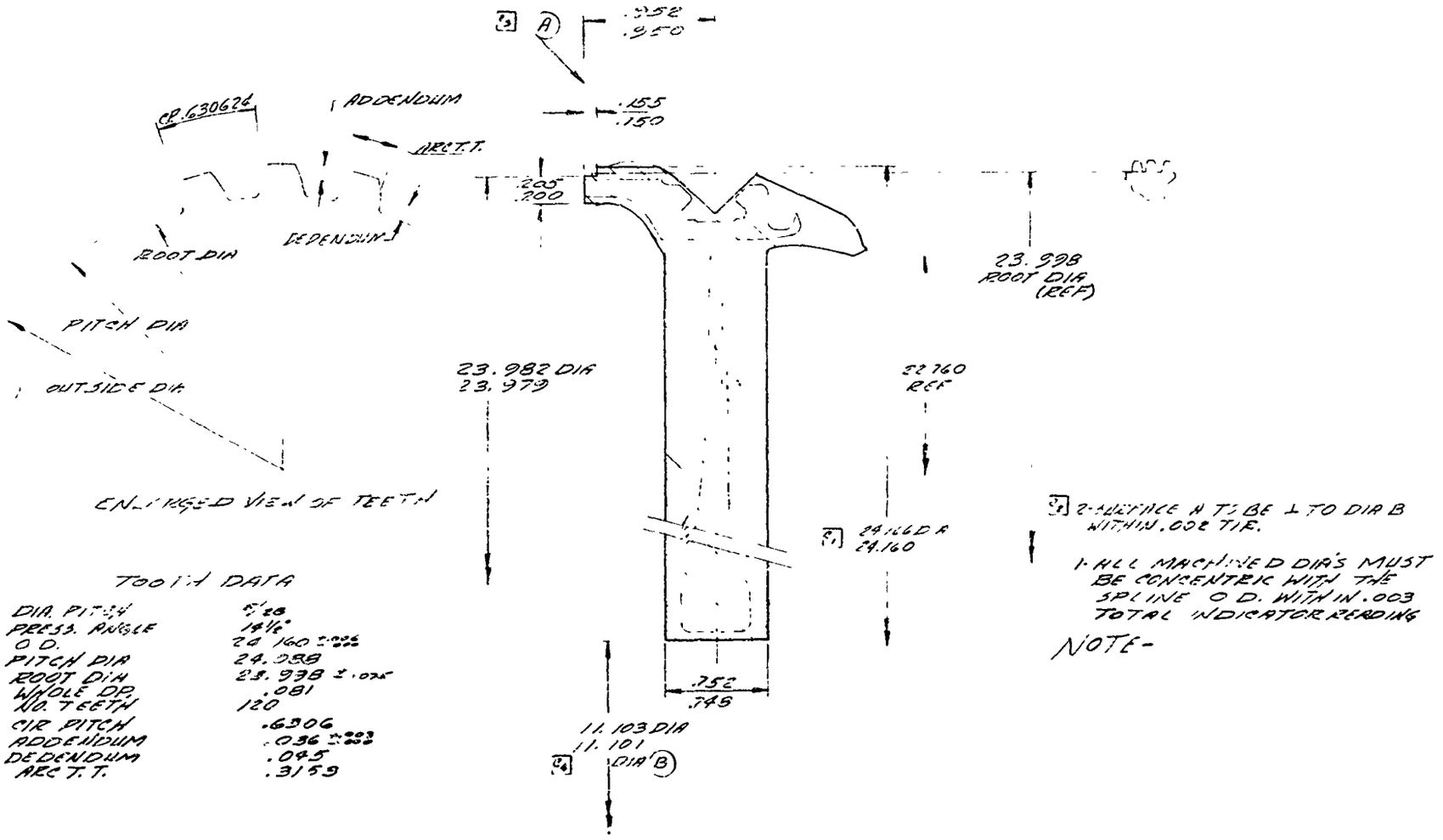

Figure 60 Pre-Weld Configuration - Stage 16

3. Inertia Welding - The welding sequence for each rotor spool is shown in Figures 61, 62 and 63. After weld No. 1 and again after weld No. 2, the subassemblies were ground flat and parallel within 0.002 inch TIR. In certain cases, remachining of weld prep extensions was required to reduce the amount of upset necessary to bring the dovetail centerlines within required axial dimensions. After weld No. 2, filler metal was applied to the bores of stages 14 and 15. They were then rebored concentric to the stage 16 bore within 0.001 inch TIR. After each weld the total upset was plotted as a function of unit energy input. This served as a working guide to the selection of welding speed for the target upset of the next weld. Target upsets for each weld were slightly different due to the relative displacements of the centerlines of the cold formed V-grooves and the disc webs. As shown in Figure 64 all but two of the data points fall within a band representing a spread of 0.022 inch in total upset for a given unit energy input. The two data points outside the band represent energy losses due to bushing - pilot seizure and a changed weld prep geometry. (Run down curves with a tight and a loose bushing showed a 26.2 percent loss in efficiency with the tight bushing).

Rotor No. 1 is shown in Figure 65 after weld No. 2. A close-up view of the weld flash is shown in Figure 66.

Figures 67 and 68 show close-up views of the weld flash of rotors 2 and 3 after weld No. 3. Overall views of the rotors 1, 2 and 3 after weld No. 3 are shown in Figure 69.

The welding of rotor No. 4 proved rather difficult but the experience gained and lessons learned should be very valuable in the future. For weld No. 1, the weld prep face of both stages were machined for a target upset of 0.075 inch, shortening the length of the weld prep extension from 0.150 to 0.100 inch. This apparently increased the heat sink at the weld interfaces and an upset of only 0.047 inch was obtained. It was decided to cut the stages apart and re-weld, using the spare stage 14 disc as a spacer to make up for the material lost in cutting and re-weld prep machining. The first repair attempt failed due to an undersize back-up ring behind the stage 14 spacer in the stationary tooling. Upon pressure application a portion of the stage 14 spacer slipped over the back-up ring resulting in a wedge effect, the upset ranging from 0.078 to 0.023 inch. The weld was cut apart again and the two pieces machined for re-welding. This time a new brass pilot bushing with 0.0005 inch diametral clearance was used. An upset of only 0.007 inch resulted and the bushing was heavily scored. The weldment was cut apart again and the stages machined for a final weld attempt; energy input was purposely increased to insure sufficient upset. This was accomplished but the weld was very hot short. In machining away the stage 14 spacer to serve as a weld prep extension for stage 15, the I.D. weld flash was also machined to bring out the weld line. Zyglo inspection showed no indications and the repair attempt was considered successful. Weld Nos. 2 and 3 were accomplished successfully. An overall view and a close-up view of the weld flash of rotor No. 4 are shown in Figures 70 and 71, respectively.

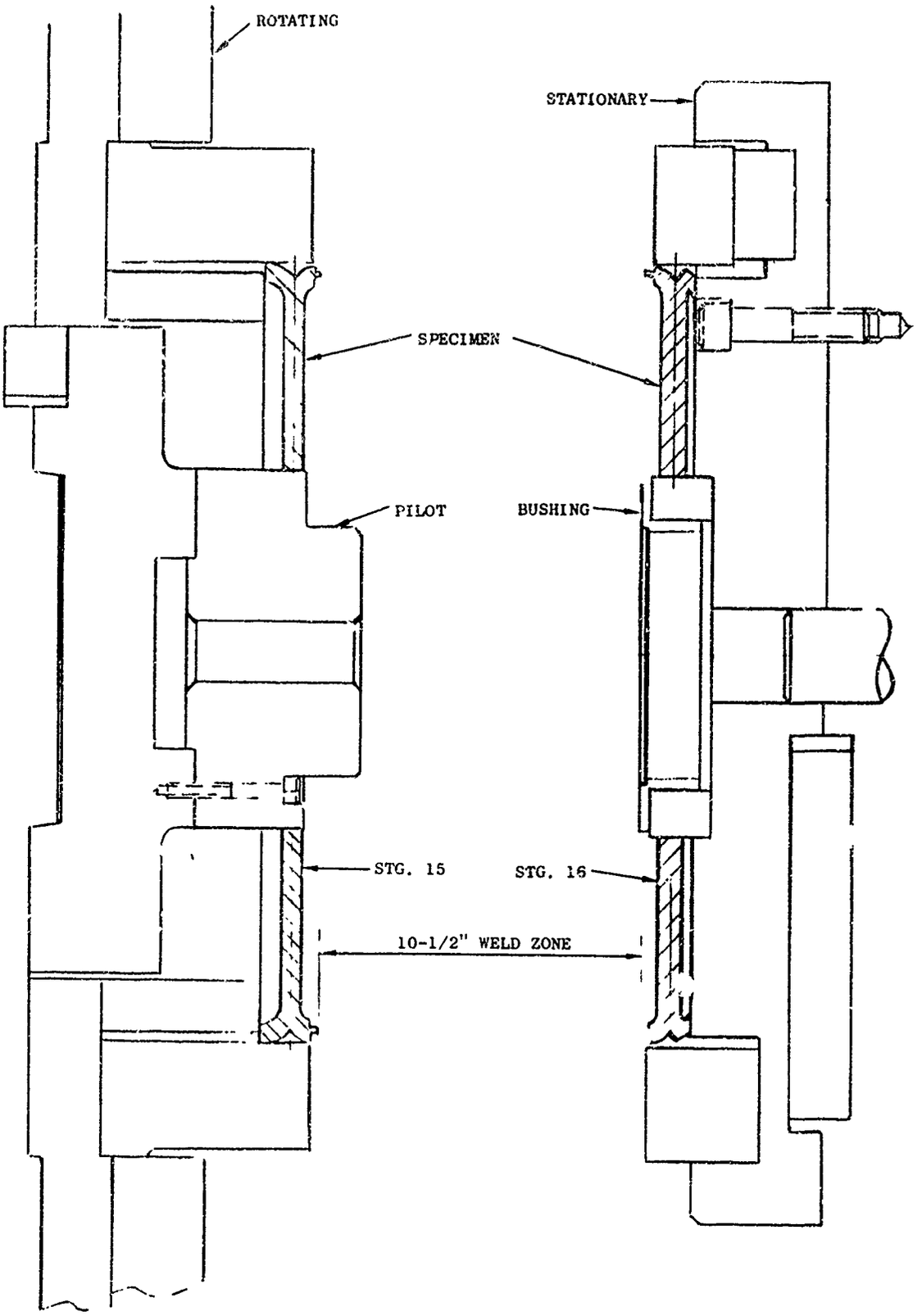

Figure 61 Assembly Layout for Rotor Weld No. 1

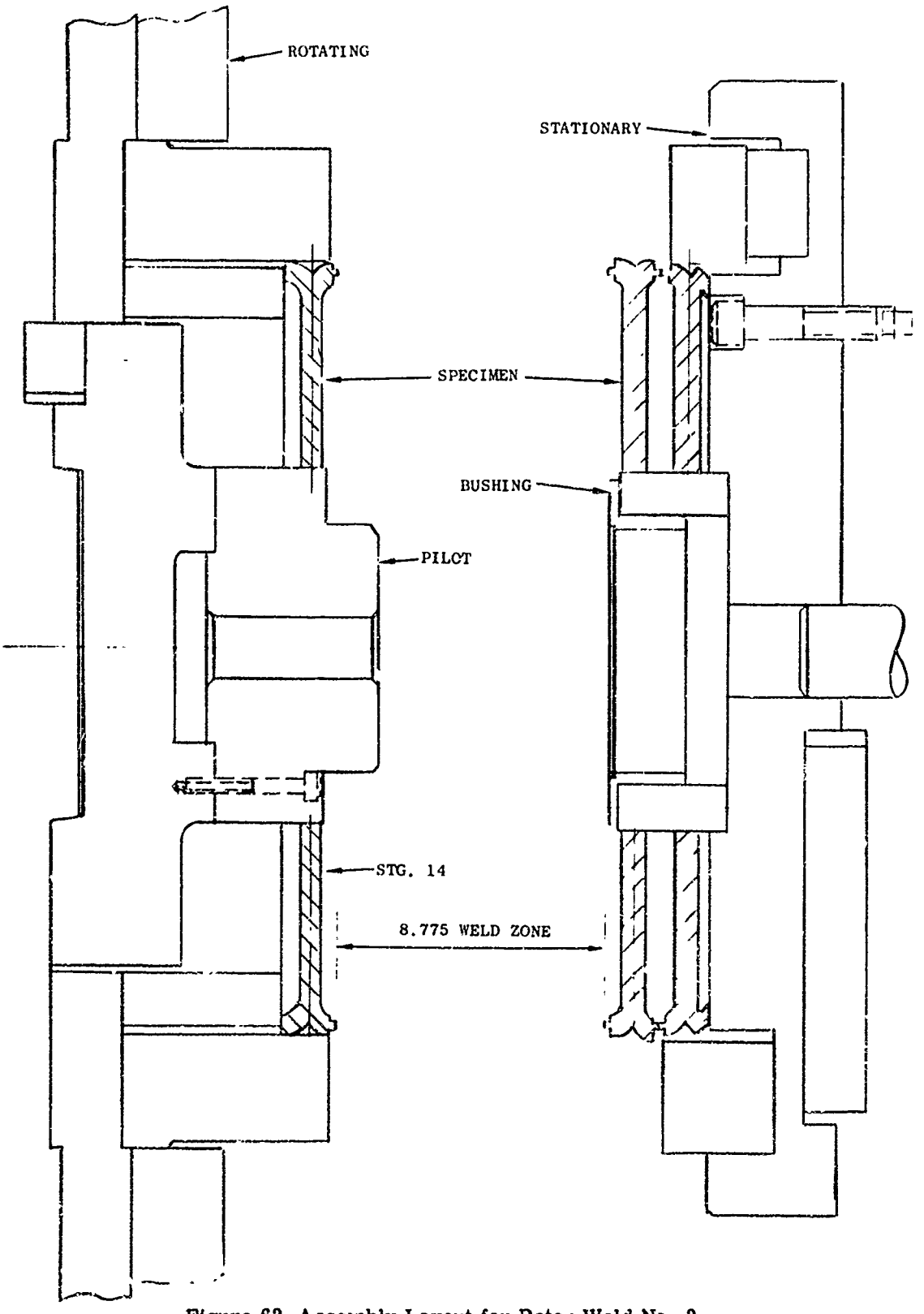

Figure 62 Assembly Layout for Rotor Weld No. 2

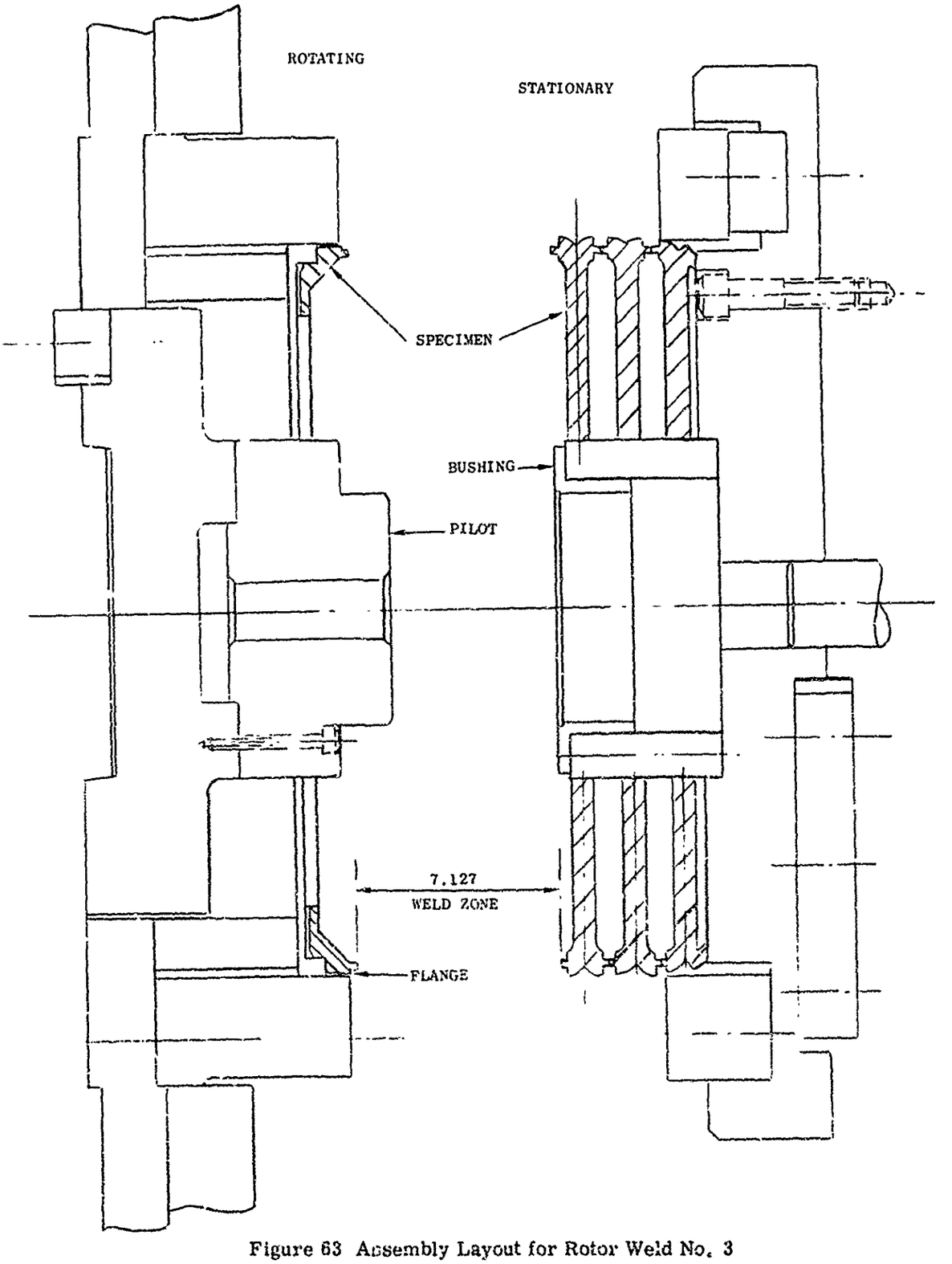

Figure 63 Assembly Layout for Rotor Weld No. 3

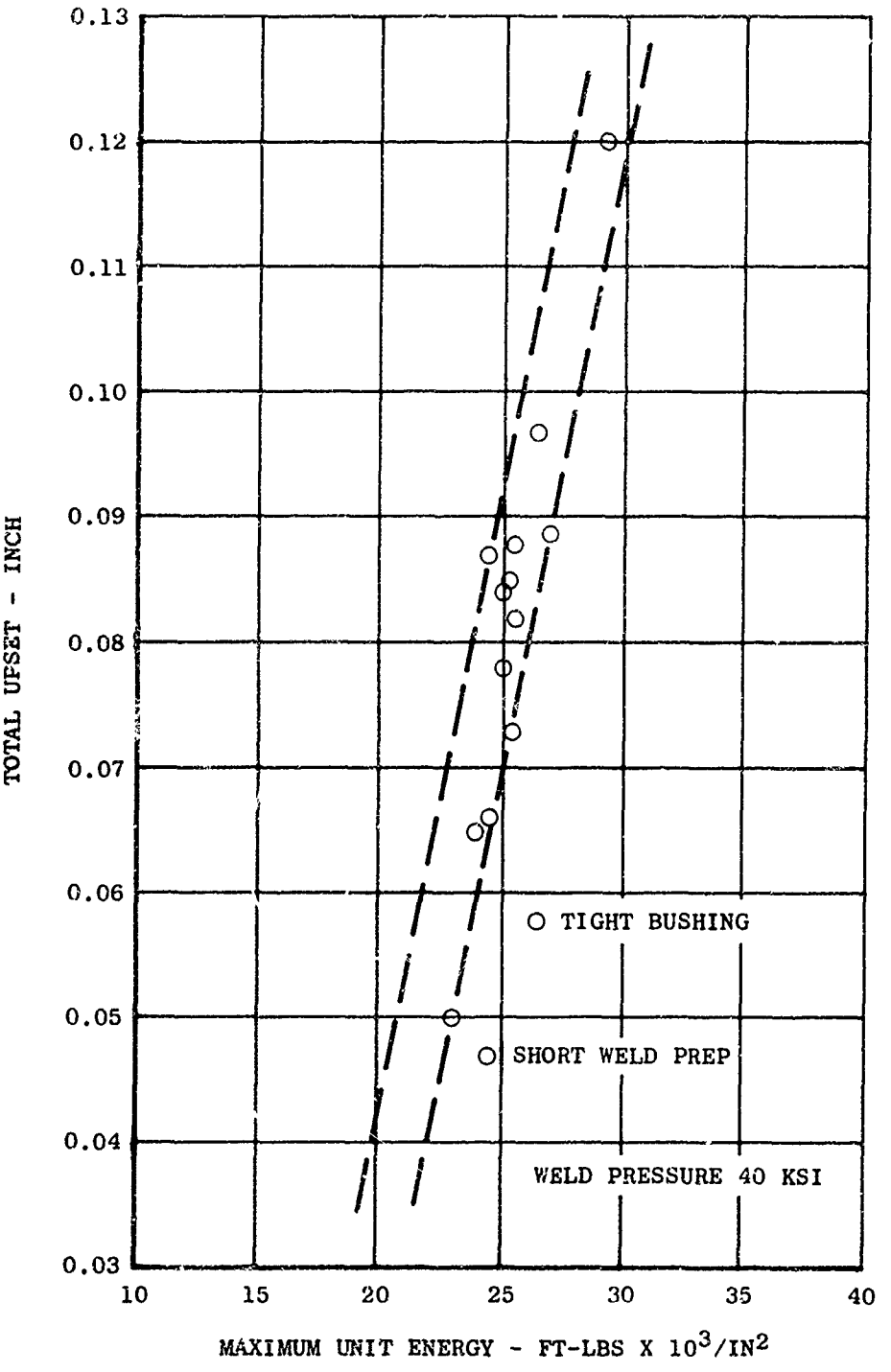

Figure 64 Upset vs. Unit Energy in Inertia Welding
Cold Rim Formed Inconel 718 Cross Rolled Plate

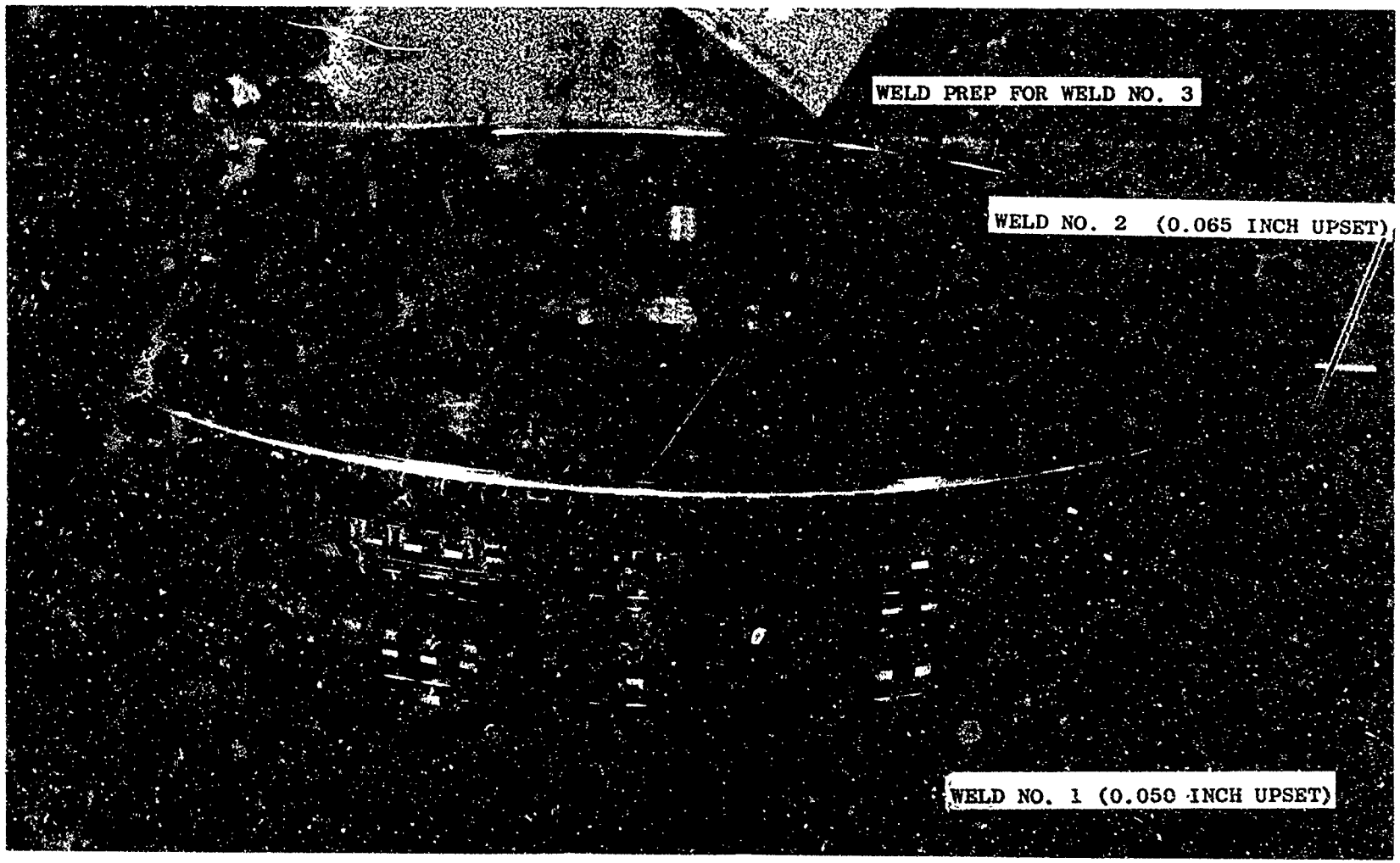

Figure 65 Photograph of Rotor 1 after Weld No. 2
Ready for Dimensional Inspection

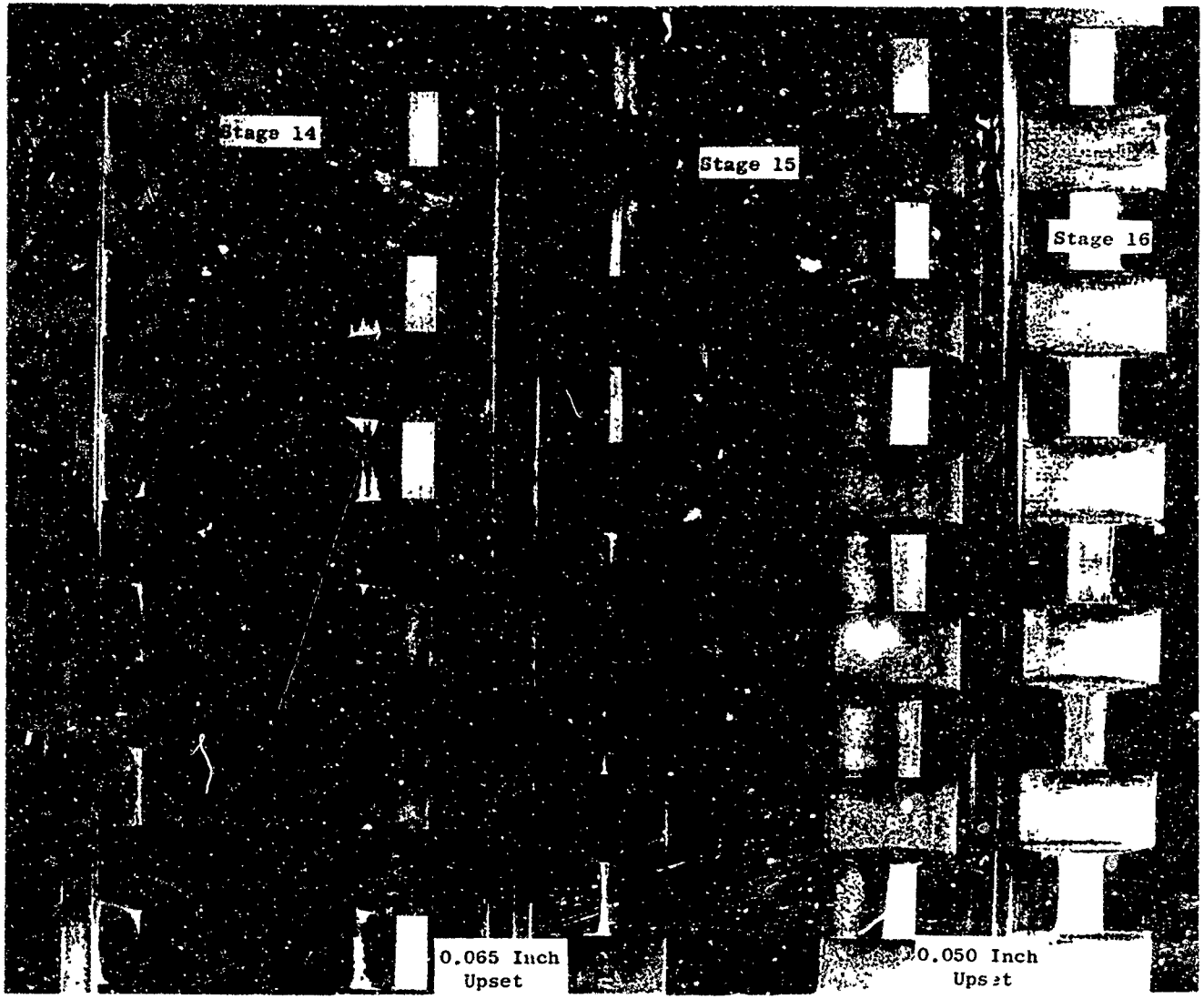

Figure 66. Close-up View of Weld Flash of Rotor 1 after Weld No. 2

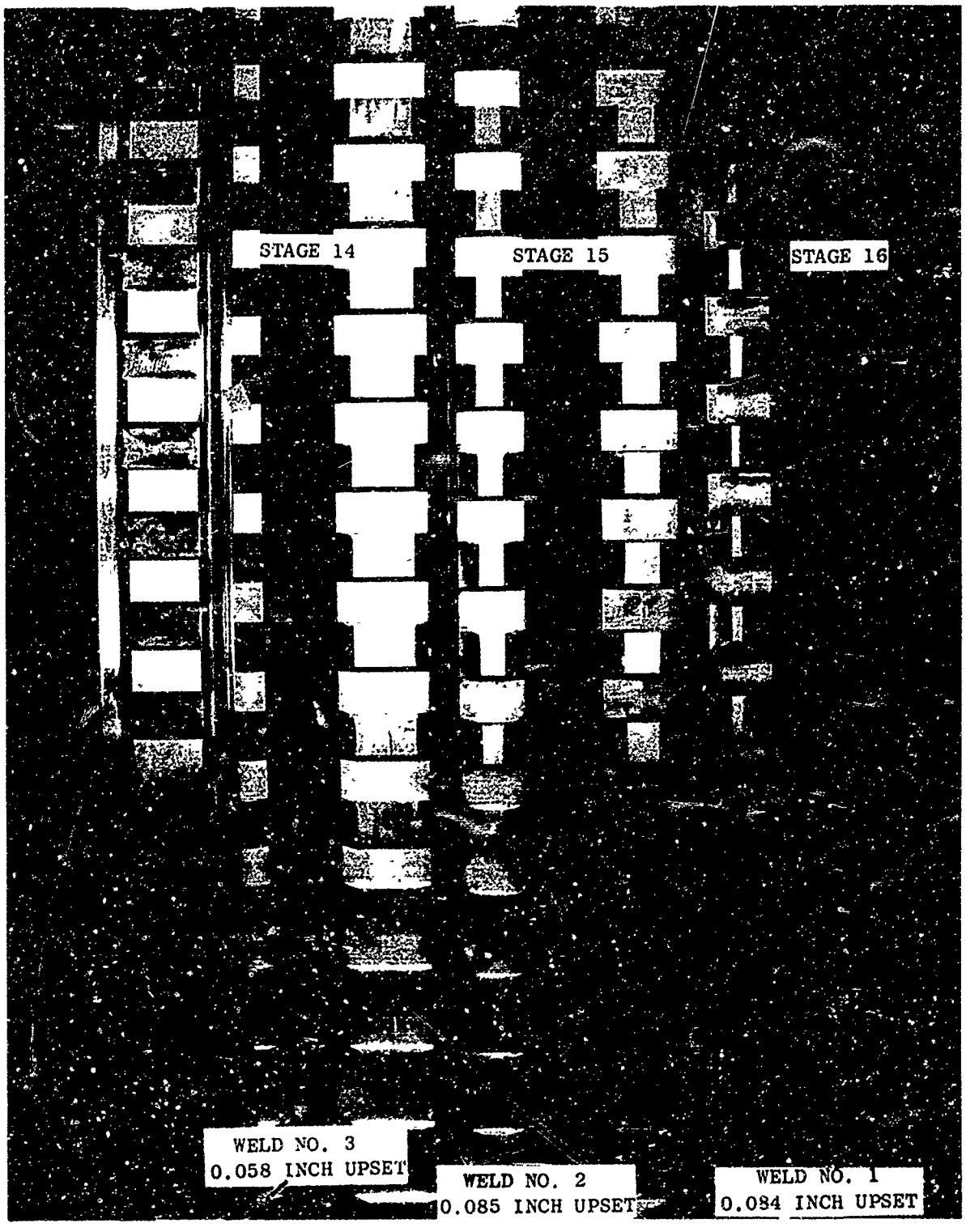

Figure 67 Close-Up View of Weld Flash of Rotor 2 after Weld No. 3

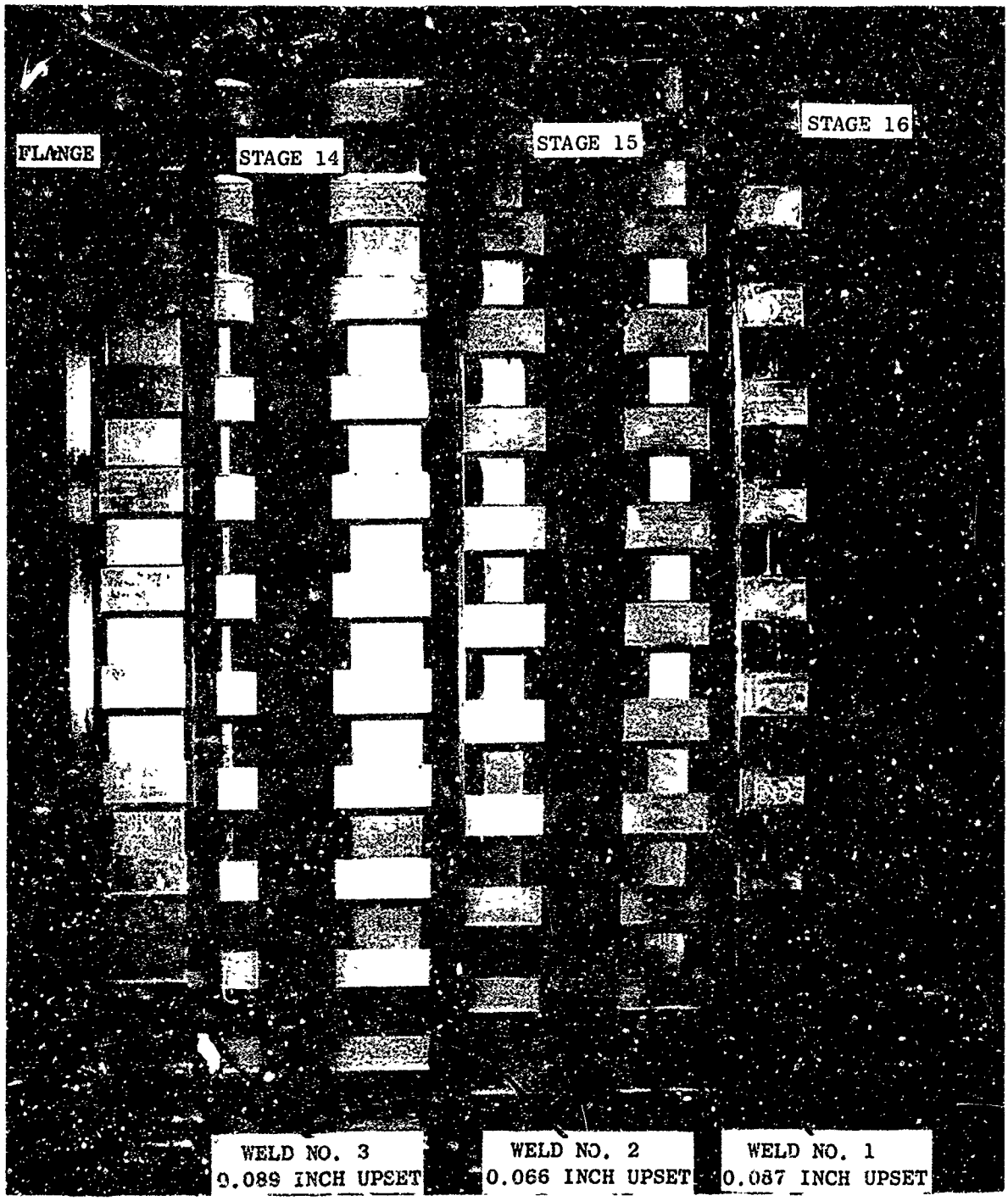

Figure 68 Close-Up View of Weld Flash of Rotor 3 after Weld No. 3

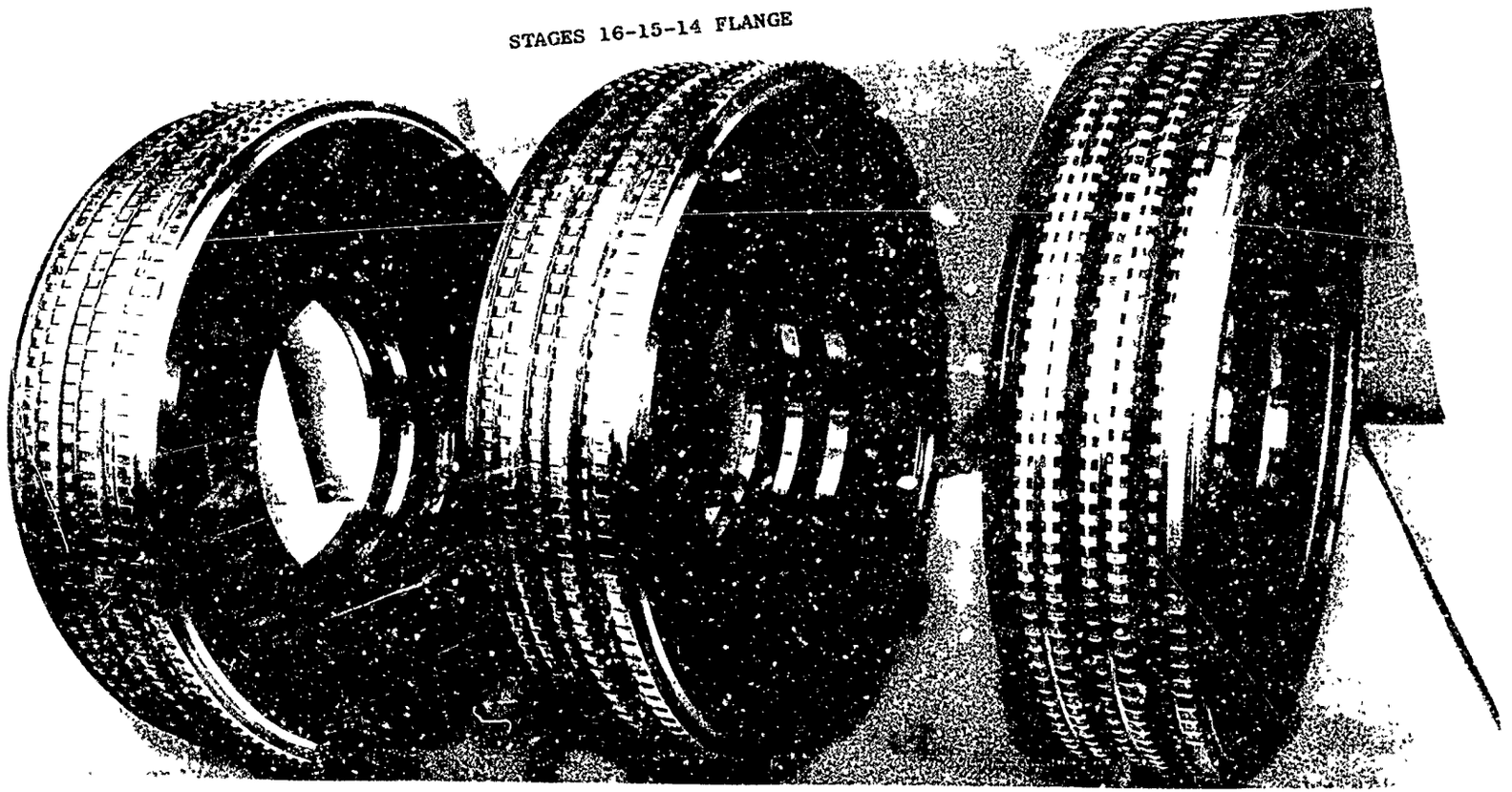

Figure 69 Photographs of Rotors, 1,2, and 3 afterWeld No. 3

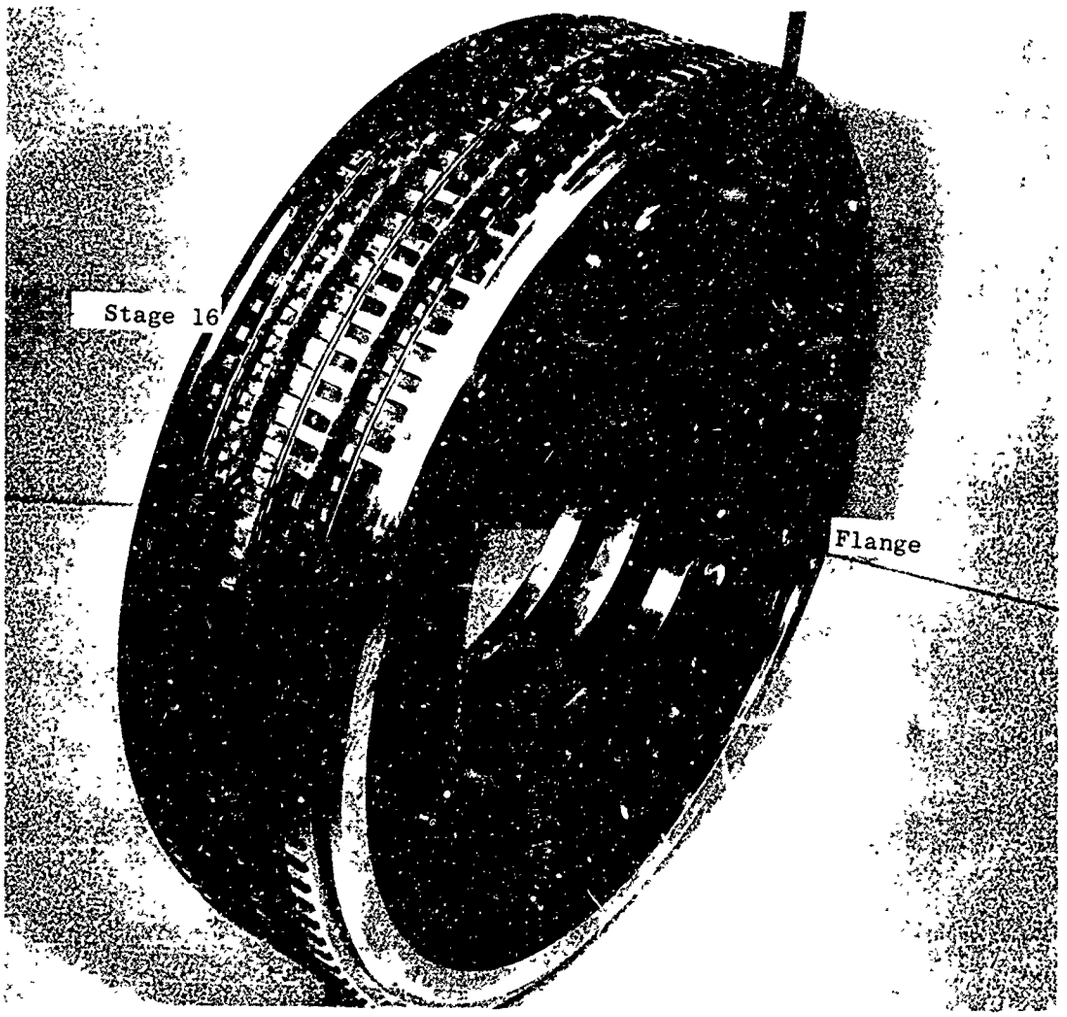

Figure 70. Photograph of Rotor 4 after Weld No. 3

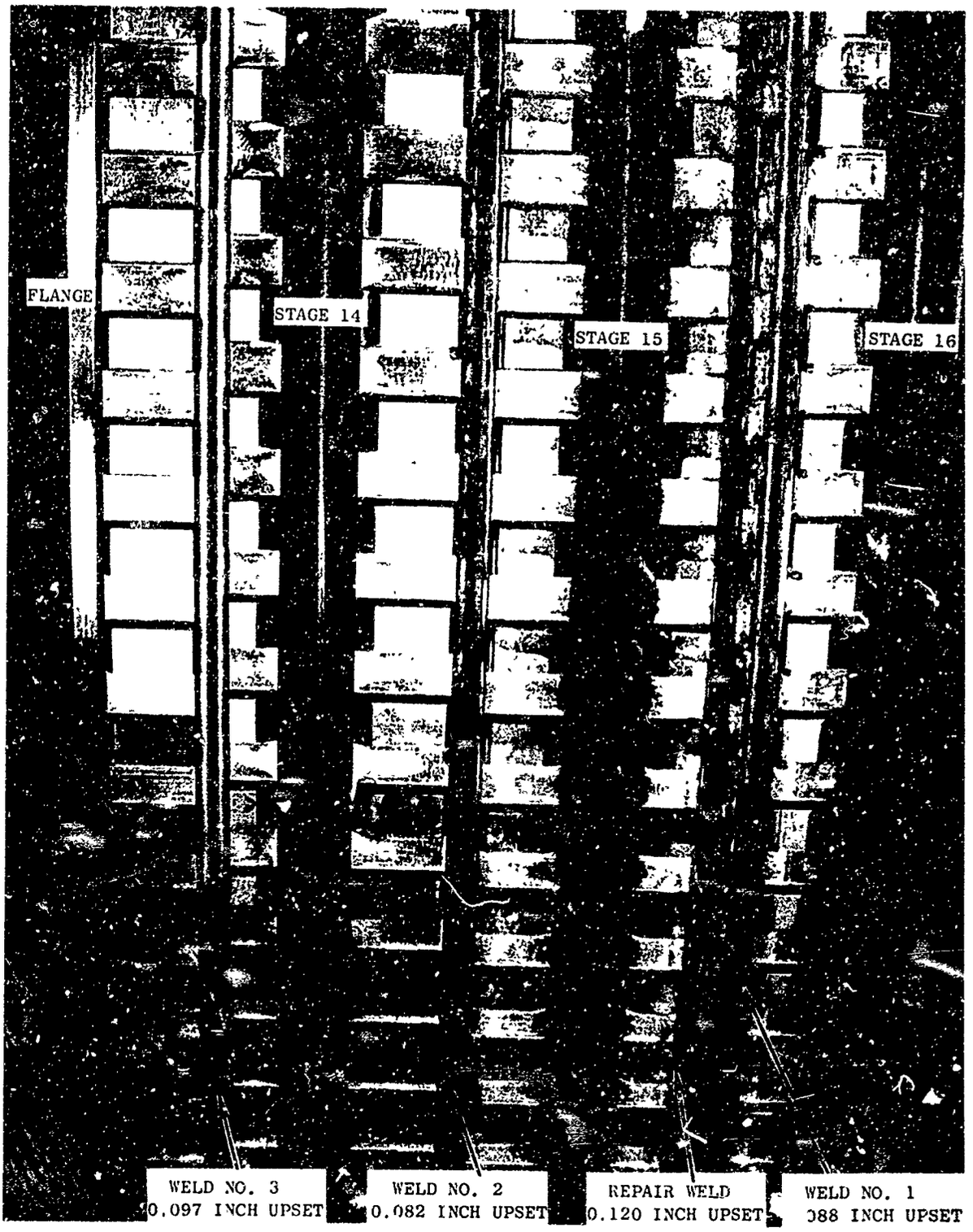

Figure 71 Close-Up View Flasn at Rotor 4 after Weld No. 3

A summary of the inertia welding parameters is given in Table XXXII with dimensional inspection results and explanatory remarks. All the values in the column headed "Max. Radial Shift (Inch)" are with respect to the axial centerline of stage 16. After weld No. 1 and again after weld No. 2 the subassembly was rotated in the stationary fixture to avoid the development of successively higher radial displacement from the axial centerline of stage 16. This was reasonably successful as shown by the plot in Figure 72. Rotating the stationary member after each weld also assisted in controlling parallelism since the weldments were usually thinner at the bottom than at the top.

As shown in Table XXXII for rotor No. 4, the achievement of upsets of 0.082 to 0.097 inch without overheating and the close dimensional control of 0.0075 and 0.002 inch TIR diametral and parallelism runouts respectively, with the maximum radial displacement of 0.004 inch demonstrates the potential of the inertia welding process for fabricating compressor rotors from individual premachined discs.

4. Post Weld Processing

(a) Flash Machining - In view of the potential for machine operator errors in contouring the I.D. configuration of the rotors it was decided to leave the spline teeth on as long as possible through the various machining operations to allow repair welding.

As shown in Figure 73, the weld flash was removed from rotor No. 1 with a square tipped 0.250 inch wide tool. These narrow grooves could not be ultrasonically inspected by any techniques currently available leaving zyglo inspection as the only dependable nondestructive inspection method. In order to remove maximum stock at the weld line and leave as much material as possible on either side, the flash of rotor Nos. 2, 3 and 4 was machined using a 0.100 inch radius tool. Prior to zyglo inspection the machined grooves were etched for 2 to 3 minutes in a heated (125° F) chem-mill solution (50 H_2O: 34 HCl: 16 HNO_3: 27 oz/gal $FeCl_3$) to bring out the weld joints. While this etchant brought out the weld line, surface pitting appeared excessive. Prior to the low temperature aging heat treatment, all weld grooves were remachined to remove as much of the etched surfaces as possible.

Rotor No. 1 required three flash machining steps to remove all zyglo indications. Rotor No. 2 required two and rotor Nos. 3 and 4 showed no indications after the first flash machining. This is summarized in Table XXXIII. The total amount of stock removed from each joint prior to aging is given in Table XXXIV. All rotors were given the standard low temperature double age cycle: 1325° F/8 hr/FC to 1150° F @ 100° F/hr + 1150° F/8 hr/AC.

Since no weld line defects were indicated in the post-heat treat zyglo inspection, rotor Nos. 2, 3 and 4 were processed through rough turning on manual and tracer controlled vertical turret lathes. In general, established production operation sheets were followed but some modifications were required to compensate for the unique geometry of the welded rotors as opposed to production rotors machined from forgings.

Two views of rotor No. 4, Figures 74 and 75, show the extent of machining completed in rough turning. Figure 74 shows the bore of stage 14 opened up and the forward side of the web rough contoured. The I.D.'s of all stages have been rough contoured although only the stage 14 - flange I.D. can be seen in the photograph. Dovetail grooves have been roughed in on stages 14 and 16. The aft side of the stage 16 web has also been rough contoured, Figure 75.

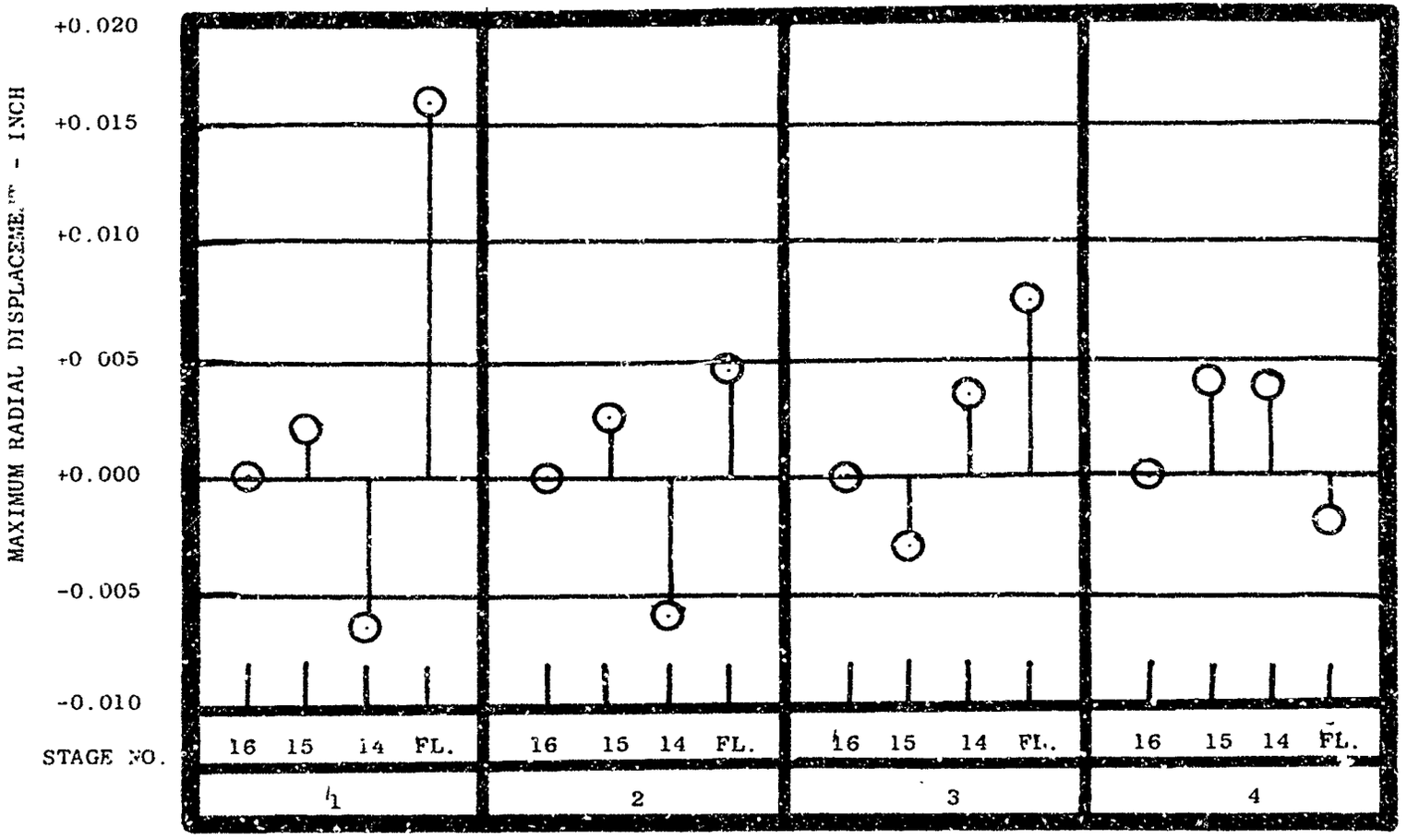

Figure 72 Maximum Radial Displacements of Welded Rotor Stages

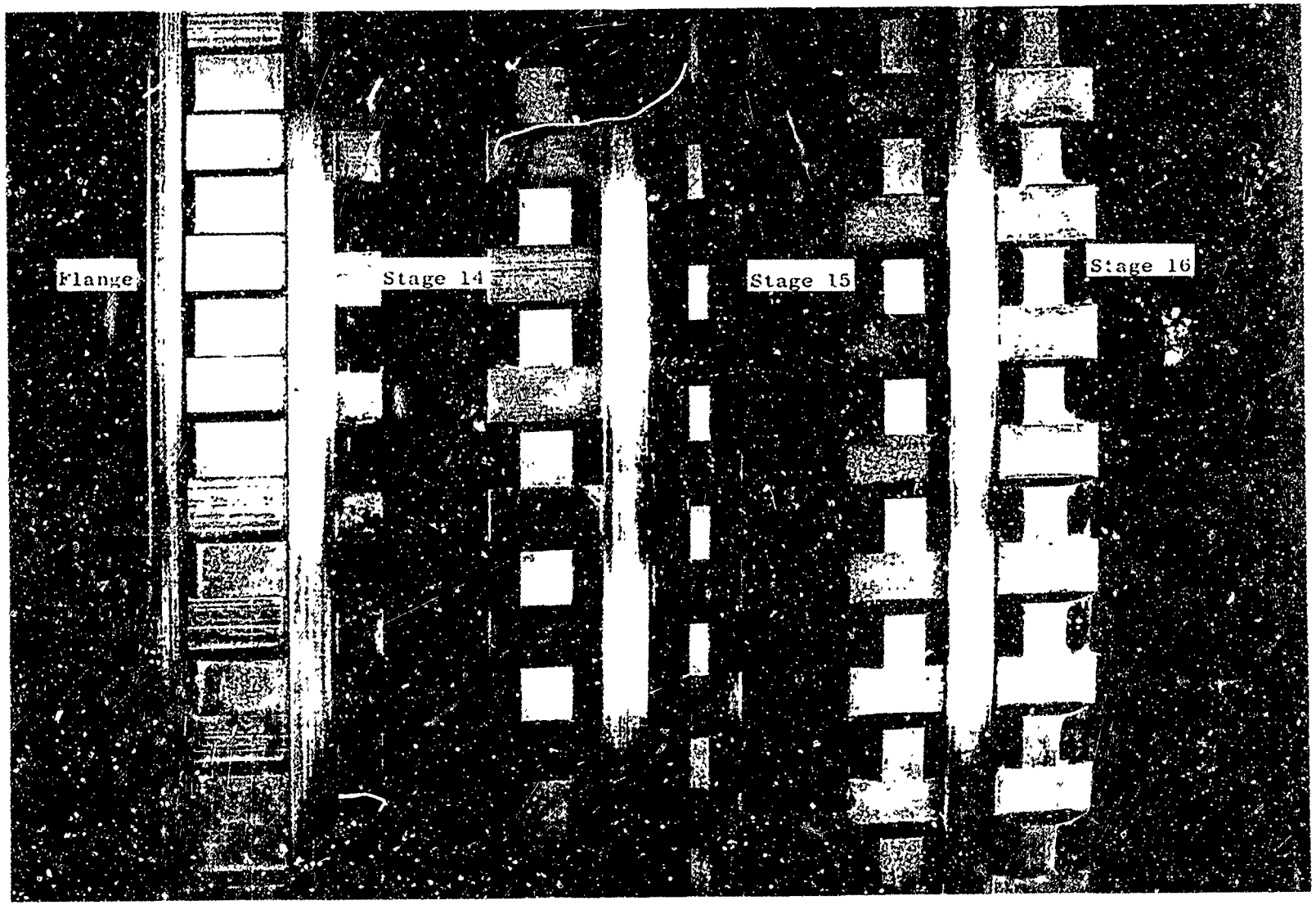

Figure 73. Close-up View of Rotor 1 After Machining Weld Flash

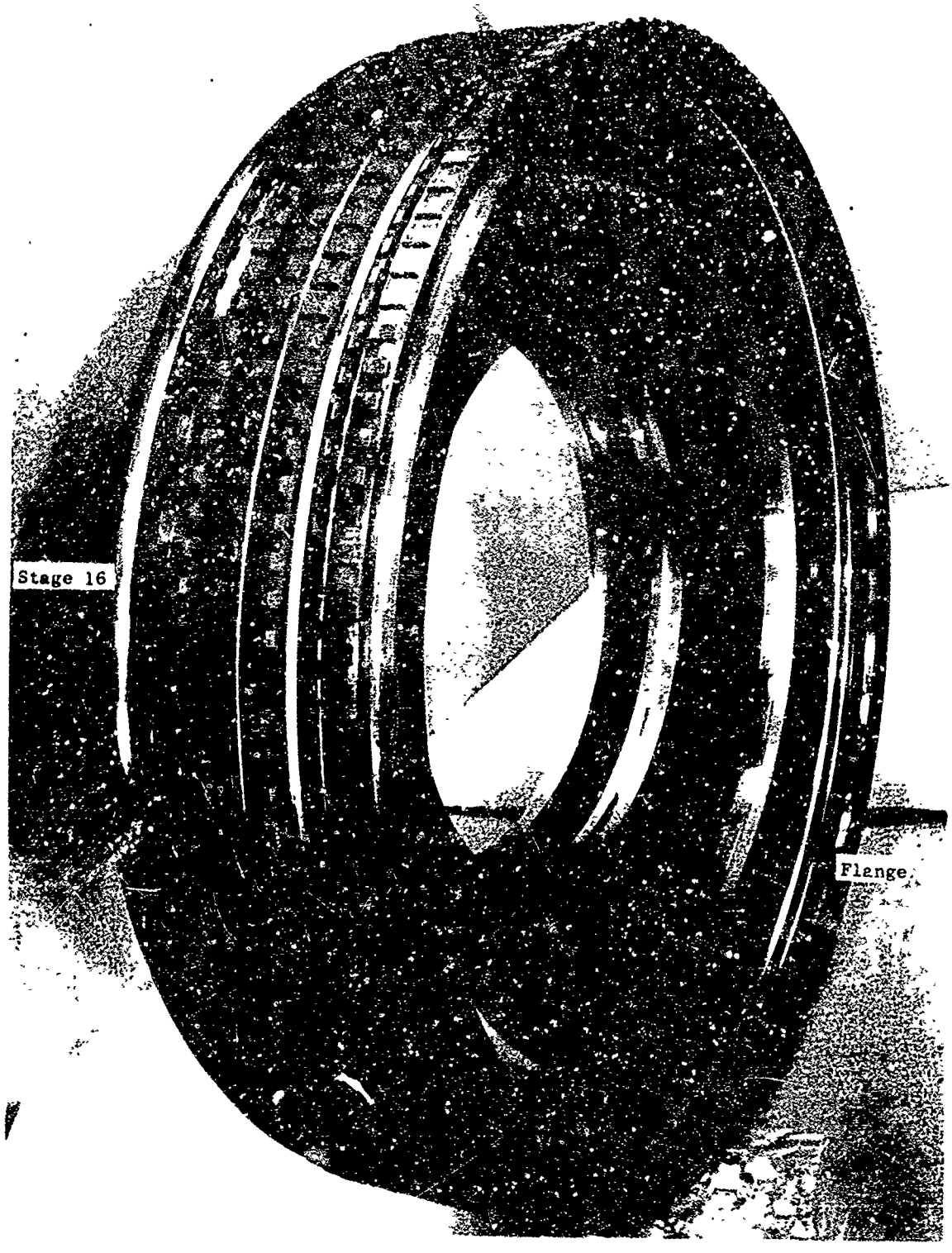

Figure 74. Forward View of Partially Machined Rotor No. 4

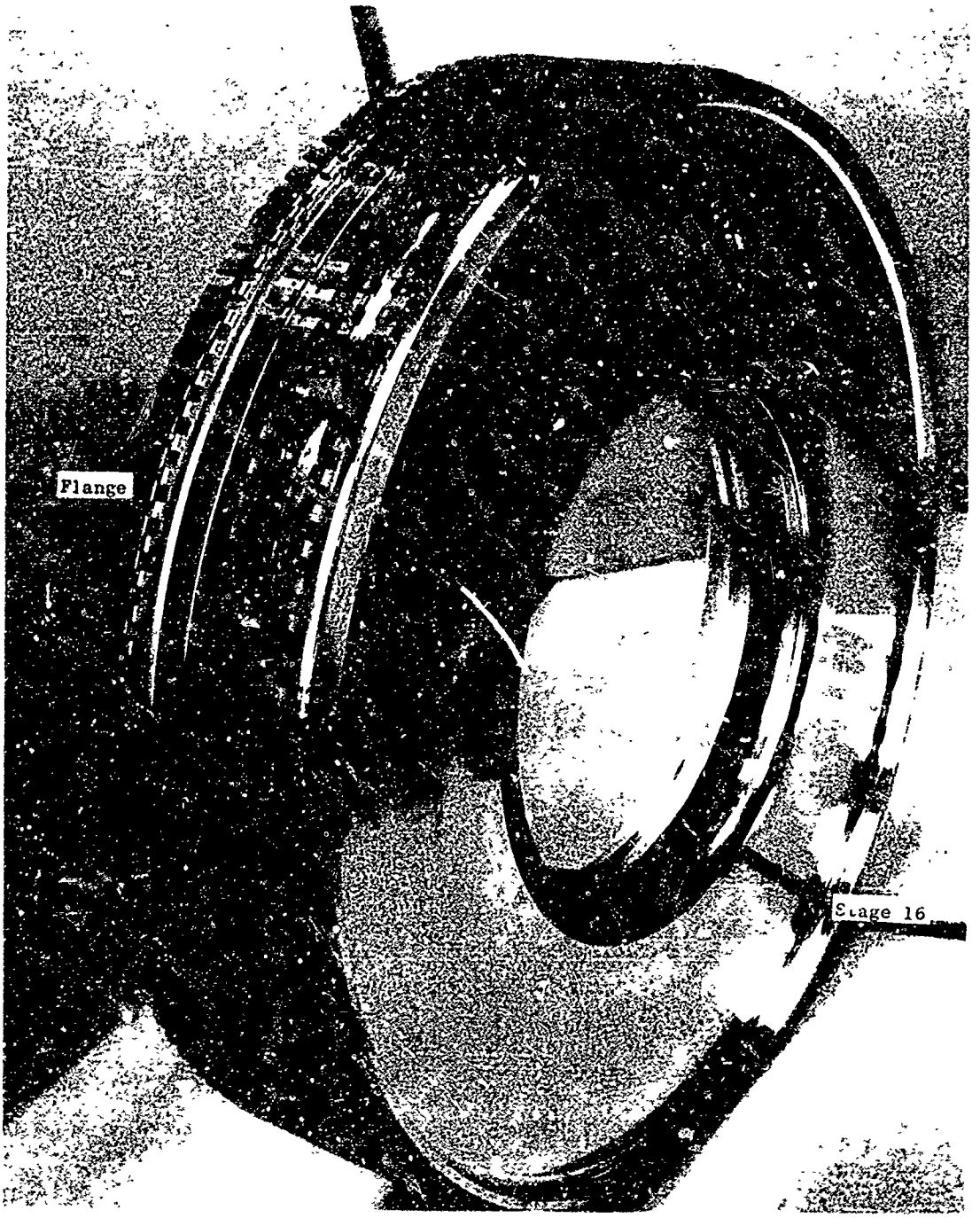

Figure 75. Aft View of Partially Machined Rotor No. 4

All finish turning operations were performed on numerically controlled (N/C) vertical turret lathes and engine lathes equipped with turret heads. Established production process operation sheets were followed. Rotor No. 4 is shown after finish turning in Figures 76 and 77.

After the final finishing operations which included scalloping and drilling bolt holes in the flange and milling loading and locking slots in each circumferential dovetail groove, rotor No. 4 was given the final zyglo inspection.

This inspection revealed numerous cracks on both the O.D. and I.D. adjacent and transverse to the circumferential weld joints. Although none of the cracks appeared to penetrate the weld joints many apparently penetrated completely through the spacer walls. Ultrasonic inspection confirmed the zyglo results. Visual inspection of the O.D.'s of rotor Nos. 2 and 3, which had the spline teeth removed in preparation for finish turning also showed cracks transverse to the weld joints. Again no cracks crossed or penetrated the weld interface itself. In addition each crack was observed to be located at the base of a spline tooth, the spline pattern standing out in relief on the machined surface.

The frequency and severity of the spacer wall cracks eliminated all three rotors from any consideration of cyclic testing. With rotor No. 1 containing undersize and defective parts, no fabricated rotors were available for cyclic testing. In lieu of procuring additional cross rolled plates for fabricating and testing a replacement rotor, which would have extended completion of this program excessively, permission was requested and granted to fabricate and test a replacement from immediately available scrap in-process forgings. At the same time a thorough study of the cracking problem was initiated to determine the causes and prevent future occurrences.

5. Investigation of Spacer Wall Cracking - Initially it was thought that all cracks were associated with the notches at the base of the spline teeth and occurred in the post-weld heat treat cycle by strain-age cracking. The absence of cracking in any of the flanges which were made from ring forgings tended to support this initial conclusion. As discussed in the previous section all the cross rolled plate had of necessity been given several high temperature (1950° F) anneals to correct a duplex grain structure and impart sufficient ductility for cold rim forming without cracking. As a result the ASTM grain size which ranged from 1 to 5 with an average of 2 was excessive for optimum mechanical properties, particularly 1200° F notch ductility. On the other hand, the ring forgings had been solution annealed at 1750° F to 1800° F in accordance with the GE forging specification and had an ASTM grain size of 4 1/2. Accordingly a thermal stress analysis was conducted wherein temperature distributions were found from a heat transfer analysis and from thermocouple data on rotor No. 1 which was specifically instrumented through the post weld heat treat cycle for this purpose. The stress analysis, which included the stress concentration effects at the sharp radius at the base of the spline teeth did not indicate a condition which could be responsible for the cracks. Further visual and ultrasonic inspection of the cracked rotors then showed the cracks were not in all cases specifically associated with the sharp radius at the spline teeth. Many cracks, especially on the inner diameter, were spaced much closer together than the spline tooth pattern.

Rotor No. 3 was then sectioned and samples from the rim were prepared for fracture and metallographic analysis. The results of breaking samples at existing cracks clearly showed

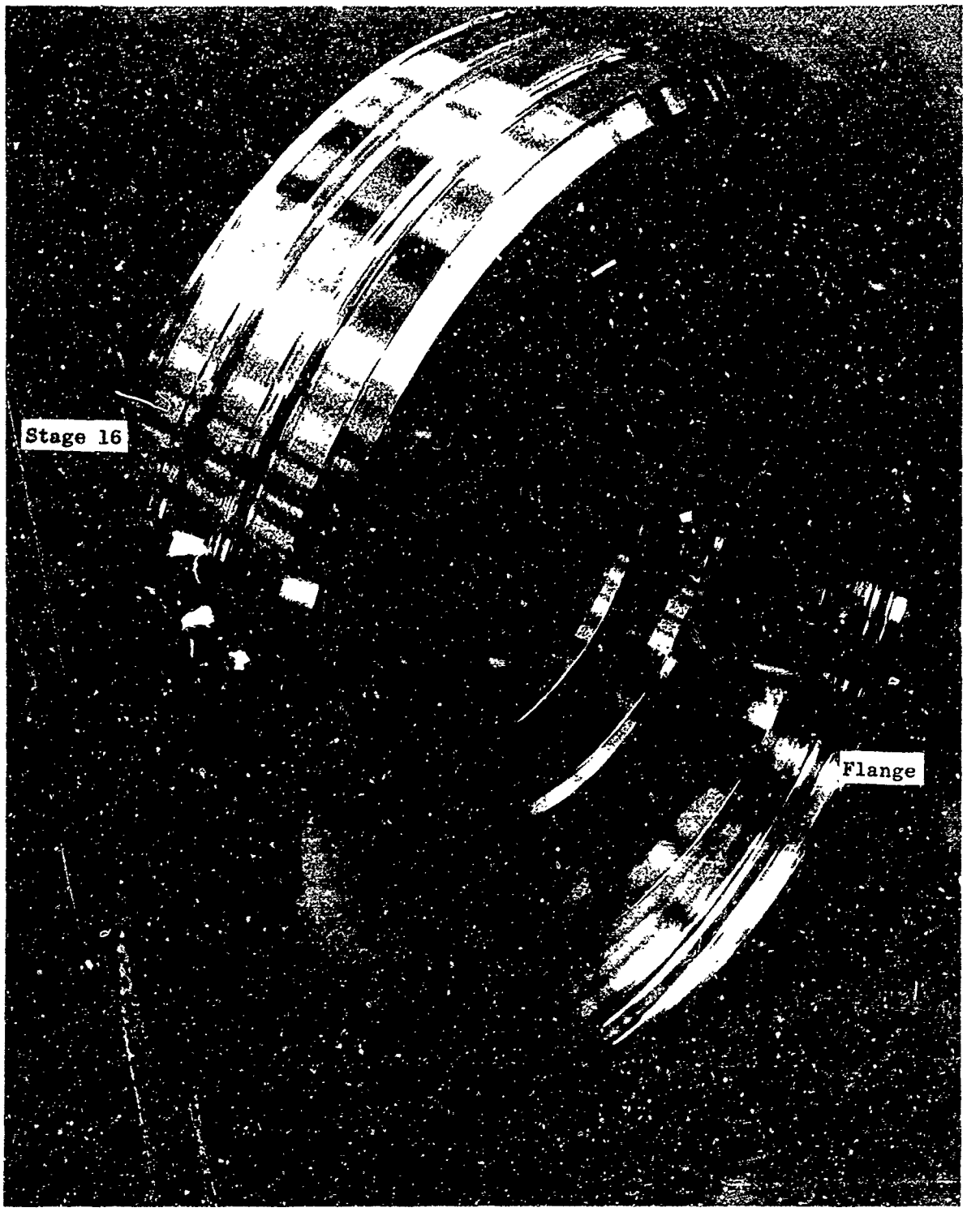

Figure 76. Forward View of Finish Machined Rotor No. 4

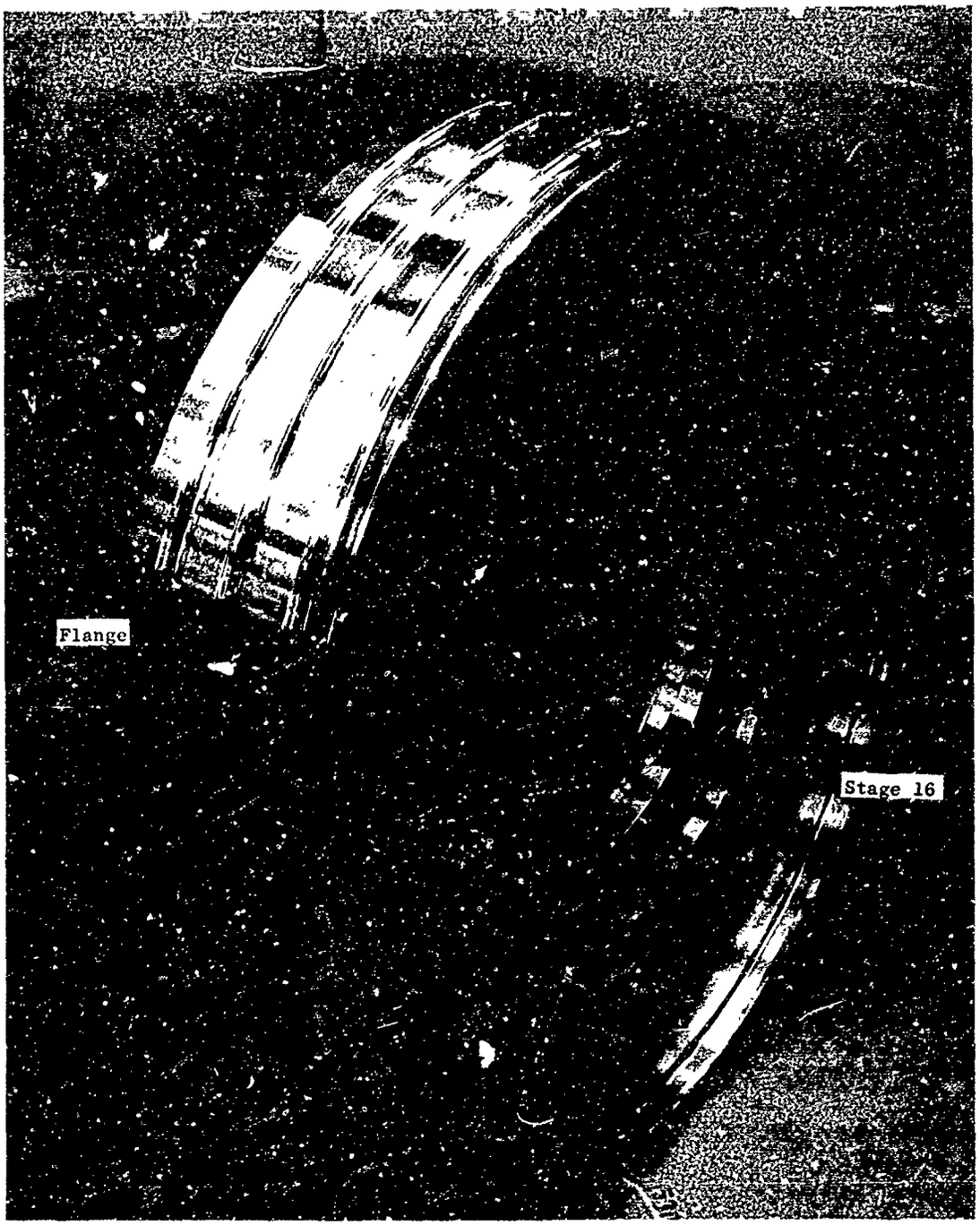

Figure 77. Aft View of Finish Machined Rotor No. 4

the surface at which the cracks originated due to the dark discoloration in the existing cracks. It was found that the cracks originated at either the outer or inner diameter and in many cases completely penetrated the spacer wall, Figures 78, 79 and 80. Outer diameter cracks were associated with the base of the spline teeth while inner diameter cracks occurred in a random pattern. No cracks were observed to cross over the weld interface. X-ray diffraction of a fractured surface was attempted but the black material was too thin to produce a pattern detectable above background. Microexamination showed the cracks to be completely intergranular, Figure 81, which may explain why no cracks crossed over the weld interface. As shown in Figure 81 the crack propagation appears to be blocked by the heavily worked very fine grained zone adjacent to the weld interface. The microstructural appearance of the cracks, i.e., rounded grain edges, was suggestive of a stress-corrosion type mechanism. Electron microprobe analysis of the crack area did not indicate any gross contamination or presence of foreign material although non-metallic particles, probable oxidized carbides, were observed in the cracks.

In attempting to determine when and why the cracking occurred most significance was attached to the discoloration of the cracked surfaces. The post weld heat treat cycle was conducted in a 98 N_2 - 2 Co_2 atmosphere which at most resulted in freshly machined surfaces turning a light straw color. The stress analysis also indicated that cracking did not occur during the heat treat cycle. Since the discoloration was very similar to that produced in chem-mill etching the weld joints it appeared likely that cracking occurred either prior to or during the chem-mill etch and additional propagation occurred in heat treat.

If the cracks existed prior to acid etching they may have been initiated during inertia welding or in flash machining. Of these two possibilities the latter appears more likely especially in view of the nature of the flash and the way flash machining was done. As shown in Figure 82 the flash metal contains entrapped oxidized material, voids, fissures and cracks. The flash was machined by feeding a radius tool directly into the joint as illustrated below.

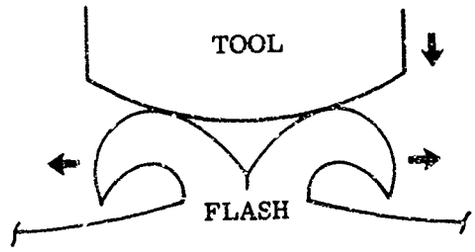

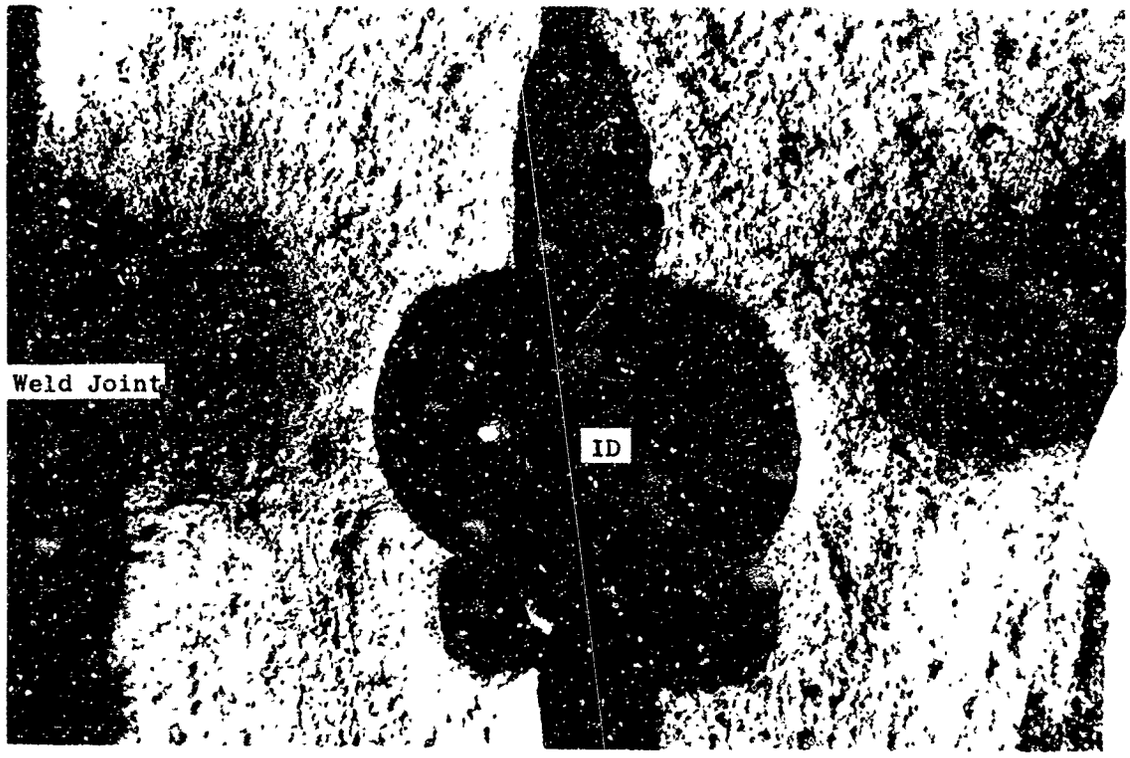

Figure 78. Macrophotograph of Fracture Specimen from Rotor No. 3 Showing Spacer Wall Crack Originating at Outer Diameter

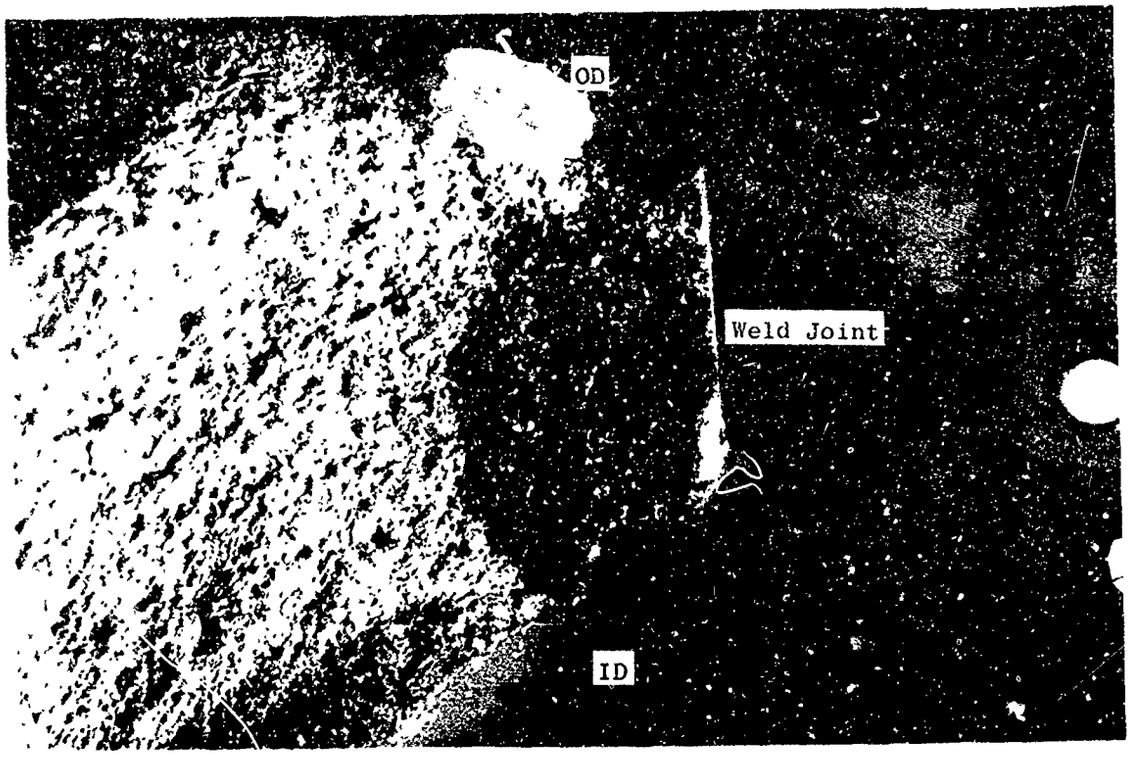

Figure 79. Macrophotograph of Fracture Specimen from Rotor No. 3 Showing Spacer Wall Crack Originating at Inner Diameter

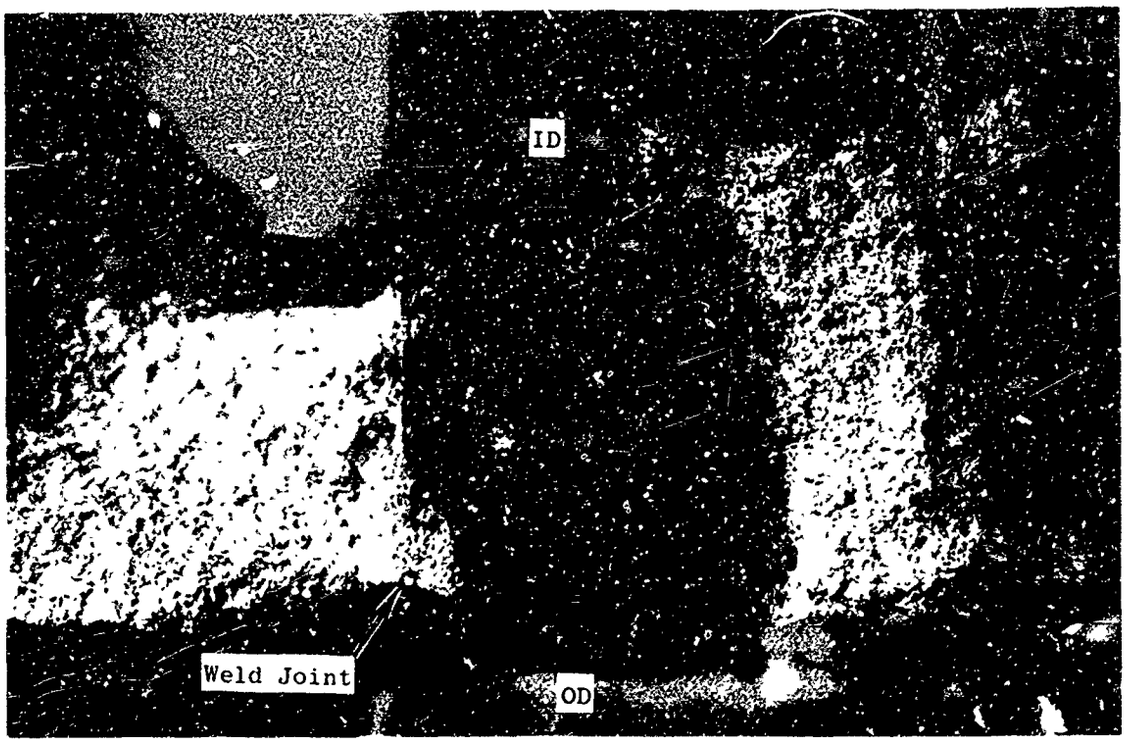

Figure 80. Macrophotograph of Fracture Specimen from Rotor No. 3 Showing Complete Crack Penetration Through Spacer Wall

88869

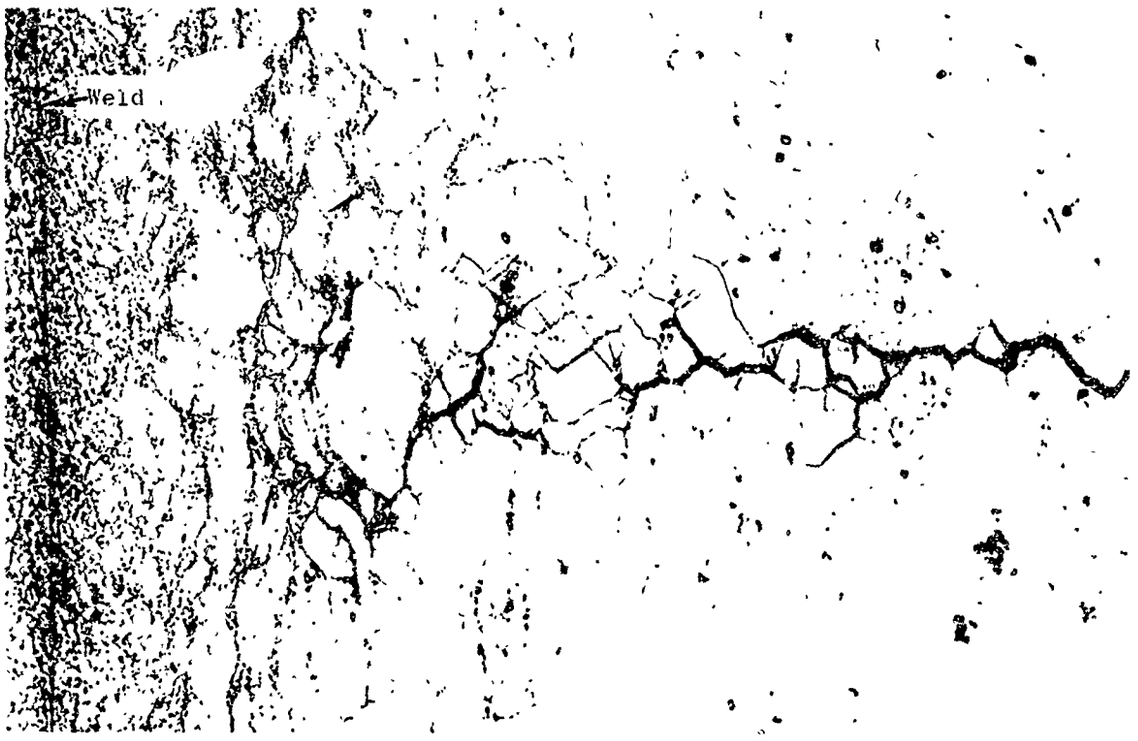

Etched 100X

Figure 81. Photomicrograph of Intergranular Spacer Wall Crack in Rotor No. 3

B9762

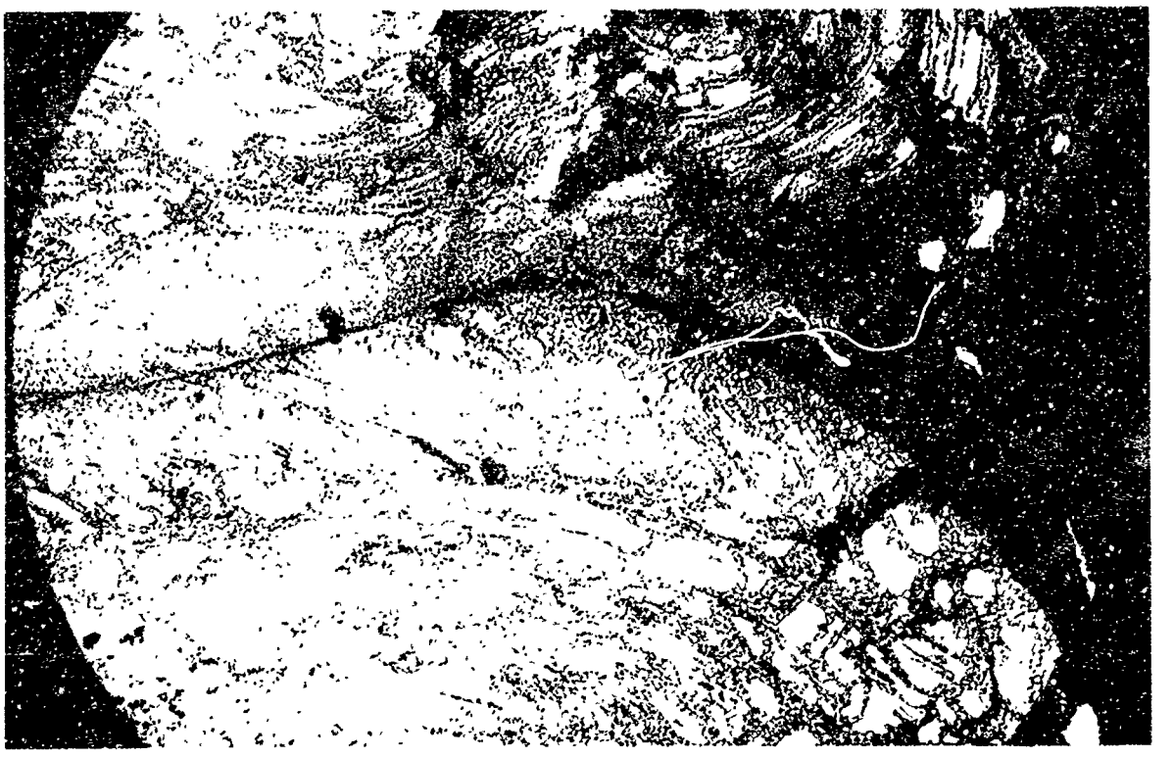

Etched 50X

Figure 82. Photomicrograph of Weld Flash of Test Weld No. 400-9-105 Showing Porosity and Cracks in Flash Curls

As indicated above the tool force tends to spread the flash apart such that existing cracks could be propagated and new ones initiated. Further propagation of these cracks into the coarse grained base metal adjacent to the fine grained weld joints could then have occurred.

Initiation of the cracks during acid etching is also a distinct possibility since all the requirements for stress corrosion were present. These are a corrosive environment, high residual stresses and coarse grained material. Microexamination showed the completely intergranular mode of cracking and the microstructural appearance definitely resembled stress corrosion cracking

In summary although this investigation did not conclusively determine the cause of the spacer wall cracks, several probable causes or contributing factors were identified and are listed below.

- Excessive grain size of the cross rolled plate
- Flash machining by "plunge" cutting
- Excessively strong acid etch solution

All of the factors listed above are subject to control or modification such that spacer wall cracking in future rotor fabrication from cross rolled plate should be prevented.

B. FABRICATION FROM FORGED STOCK

1. Selection of Parts - In production machining TF39 stages 14 to 16 compressor rotors from one piece forgings occasional operator errors or machine malfunctions result in partially machined parts which cannot be finished to blueprint without significant dimensional deviations. The practice is to place such parts on hold while a review is made to determine their disposition. In reviewing such parts two I.D. rough contoured rotors were found with one deviation each in different locations. It was immediately apparent that the good and bad stages could be separated by splitting each rotor into three individual discs. Three discs were then selected for rotor welding as illustrated below.

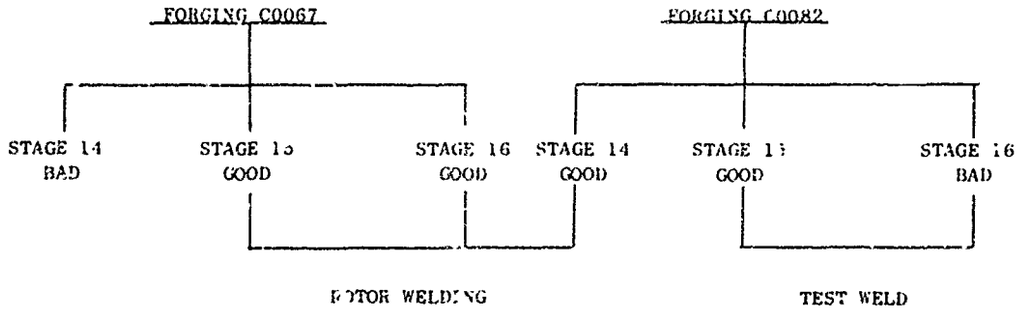

Also, as shown above, two discs were selected for test piece welding to insure that weld parameters previously used for cross rolled plate were applicable to this material.

To utilize as much of the existing weld tooling as possible splines were machined on the outer diameters for driving and holding. The weld prep geometry used in cross rolled plate welding was maintained.

2. Inertia Welding - Since previous metallographic studies had shown the presence of liquated phases in Inconel 718 inertia welds made at high angular velocities, the flywheel moment of inertia was increased from 26,038 to 32,500 lb-ft^2, thereby allowing some reduction in welding speed. Three sets of 24 inch diameter test rings welded in the wall thickness - diameter study were cut apart and remachined for additional test piece welds.

Welding of the three test ring sets and the test discs salvaged from the two forgings showed no significant changes in the welding parameters, maximum input energy and welding pressure, from those used for cross rolled plate. The two rotor welds were then made with good dimensional and upset results. Table XXXV summarizes the parameters and results. Two views of the welded rotor are shown in Figures 83 and 84. As shown in Figure 83 the flange section was an integral part of Stage 14 eliminating one of the welds previously required. A close-up view of the two weld joints is shown in Figure 85.

3. Post Weld Machining - In order to avoid "plunge" cutting the weld flash and possible crack propagation it was decided to machine the rotor to within 0.015 inch of blueprint on both inner and outer diameters prior to inspection and heat treat. As a result the flash was removed in the normal course of machining operations by a single point tool traversing the weld joints. Since some dimensional changes were anticipated in heat treat the dovetail grooves were roughed in only. The fine grained weld joints stood out in such sharp contrast to the coarser grained parent metal that acid etching was not required prior to the zyglo inspection which showed no defect indications. The rotor was then aged in vacuum using controlled heating and cooling rates of 200° F/hr to reduce any possibility of warpage or distortion of the nearly finish machine rotor. The standard Inconel 718 aging cycle of 8 hours at 1325° F + 8 hours at 1150° F was used. Dimensional inspection after aging showed no significant changes or distortion had occurred and zyglo inspection again showed no defect indications.

The rotor was then finish machined, Figures 86, 87 and 88. Final dimensional inspection showed only two out of print dimensions. The stage 15 hub was 0.010 inch under minimum thickness and some of the flange bolt holes were back spot faced out of parallel by 0.0005 inch over the maximum allowed on blueprint. Neither of these deviations were considered excessive for spin pit cyclic testing. After the final zyglo inspection showed no defect indications the rotor was shot peened and delivered to test assembly.

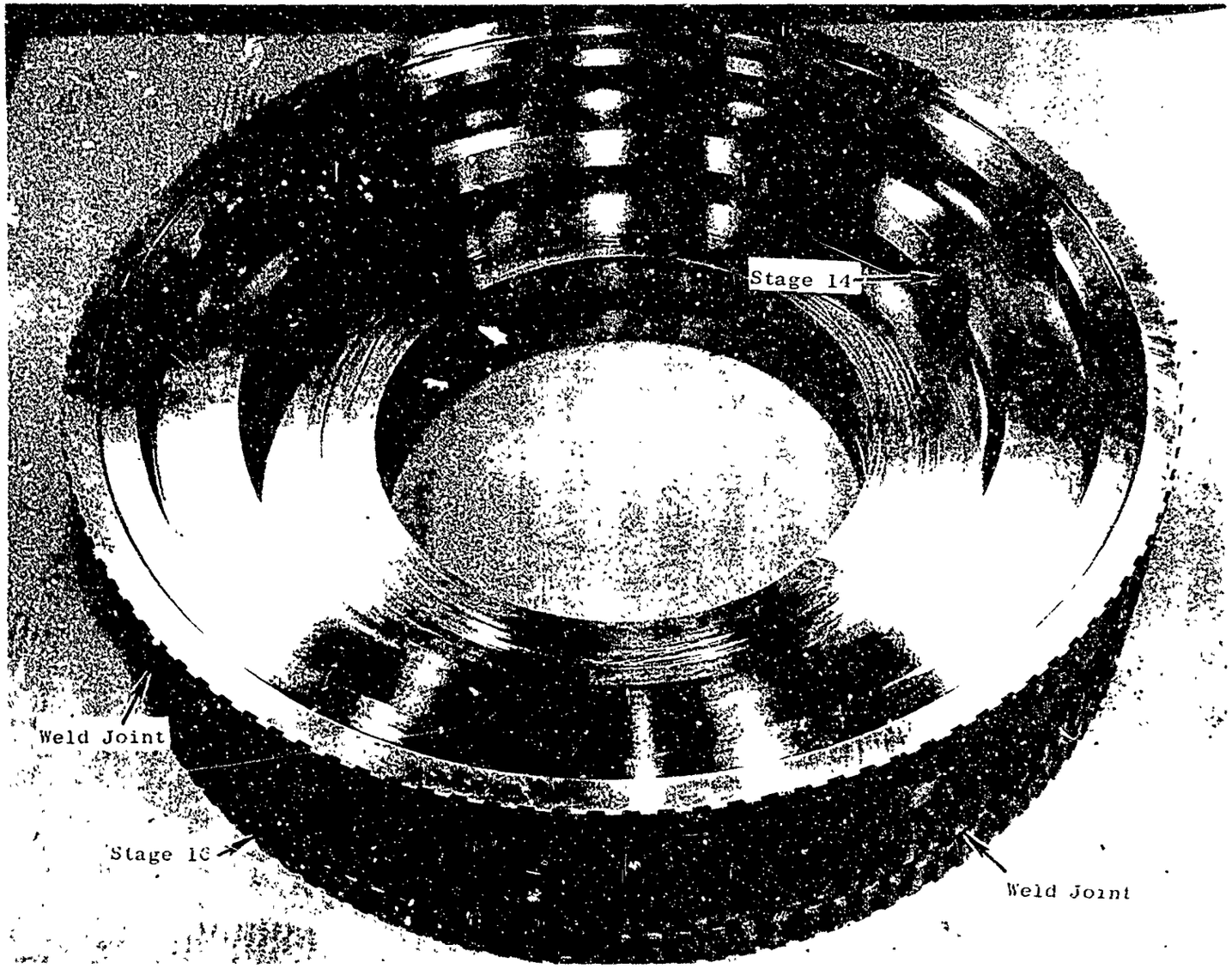

Figure 83. Forward View of Inertia Welded Rotor No. 5

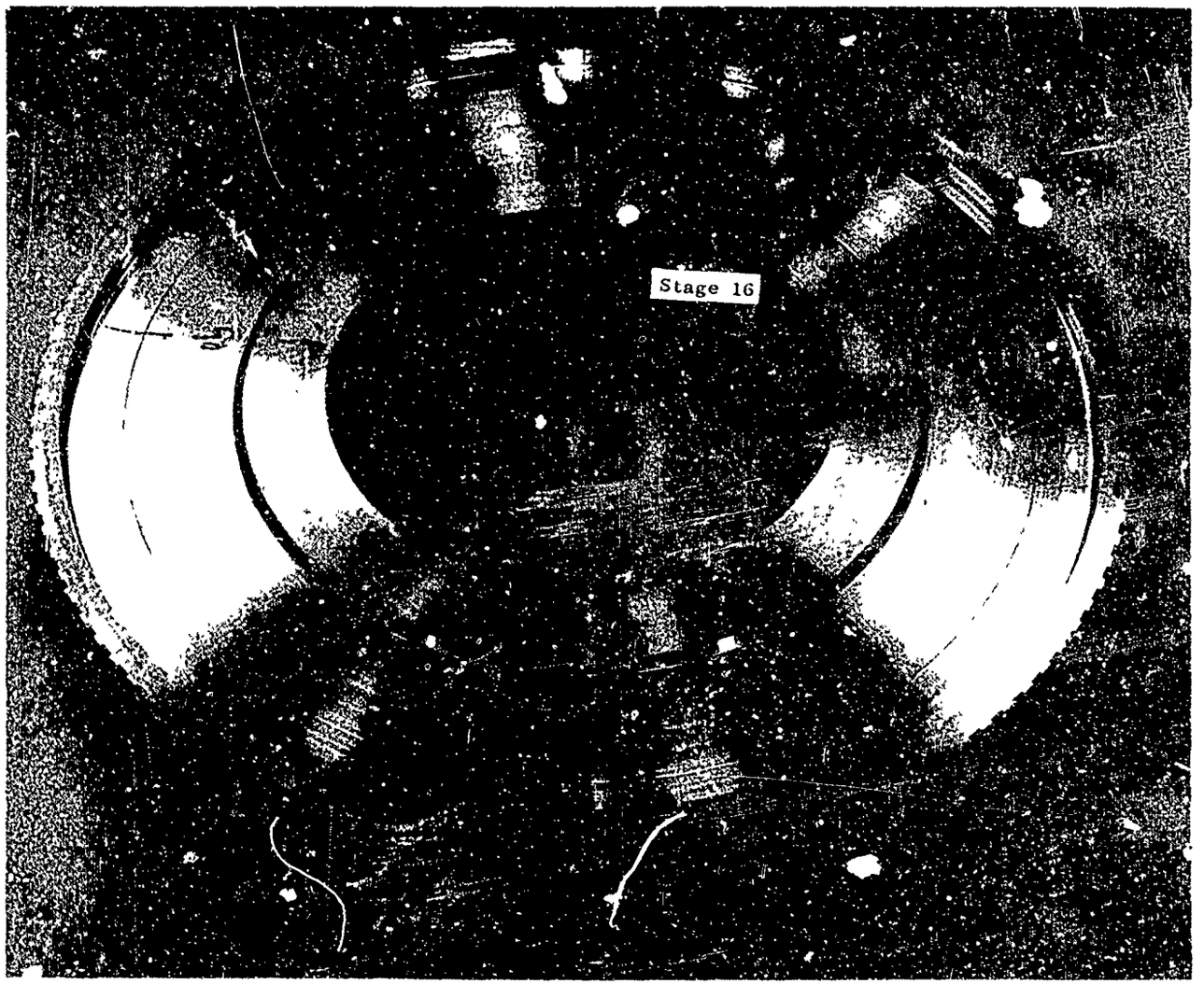

Figure 84. Aft View of Inertia Welded Rotor No. 5

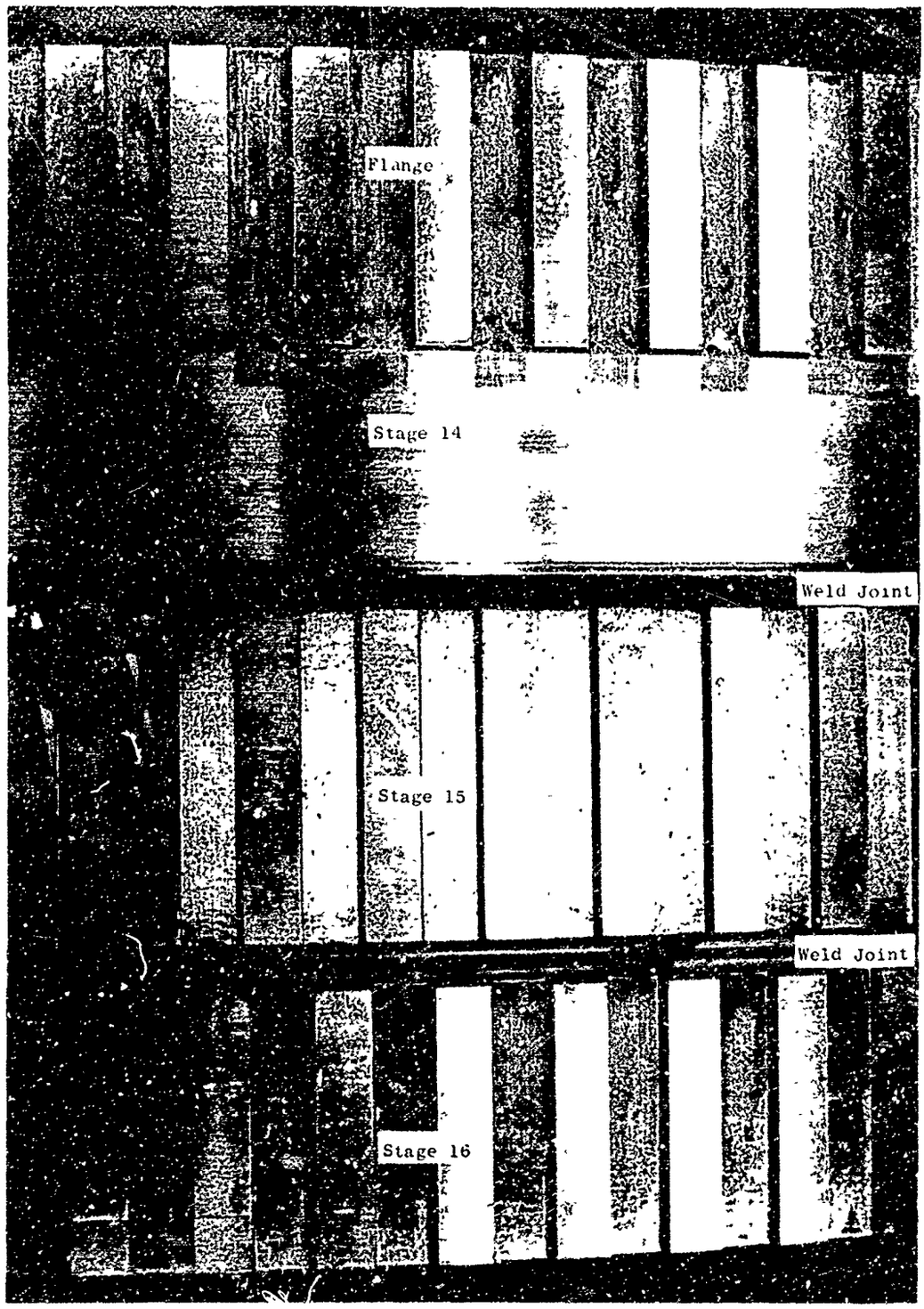

Figure 85. Close-Up View of Weld Joints in Rotor No. 5

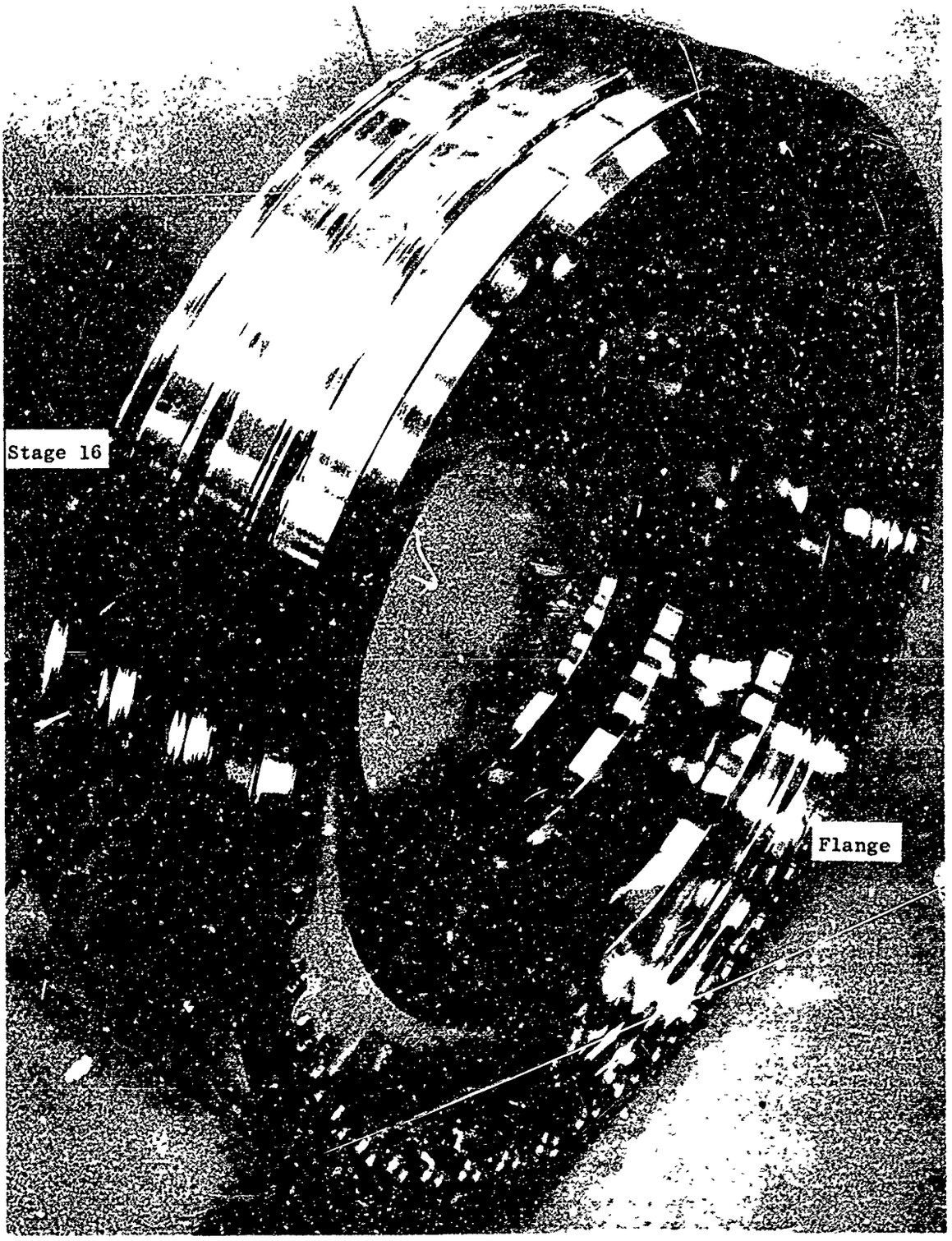

Figure 86. Forward View of Finish Machined Rotor No. 5

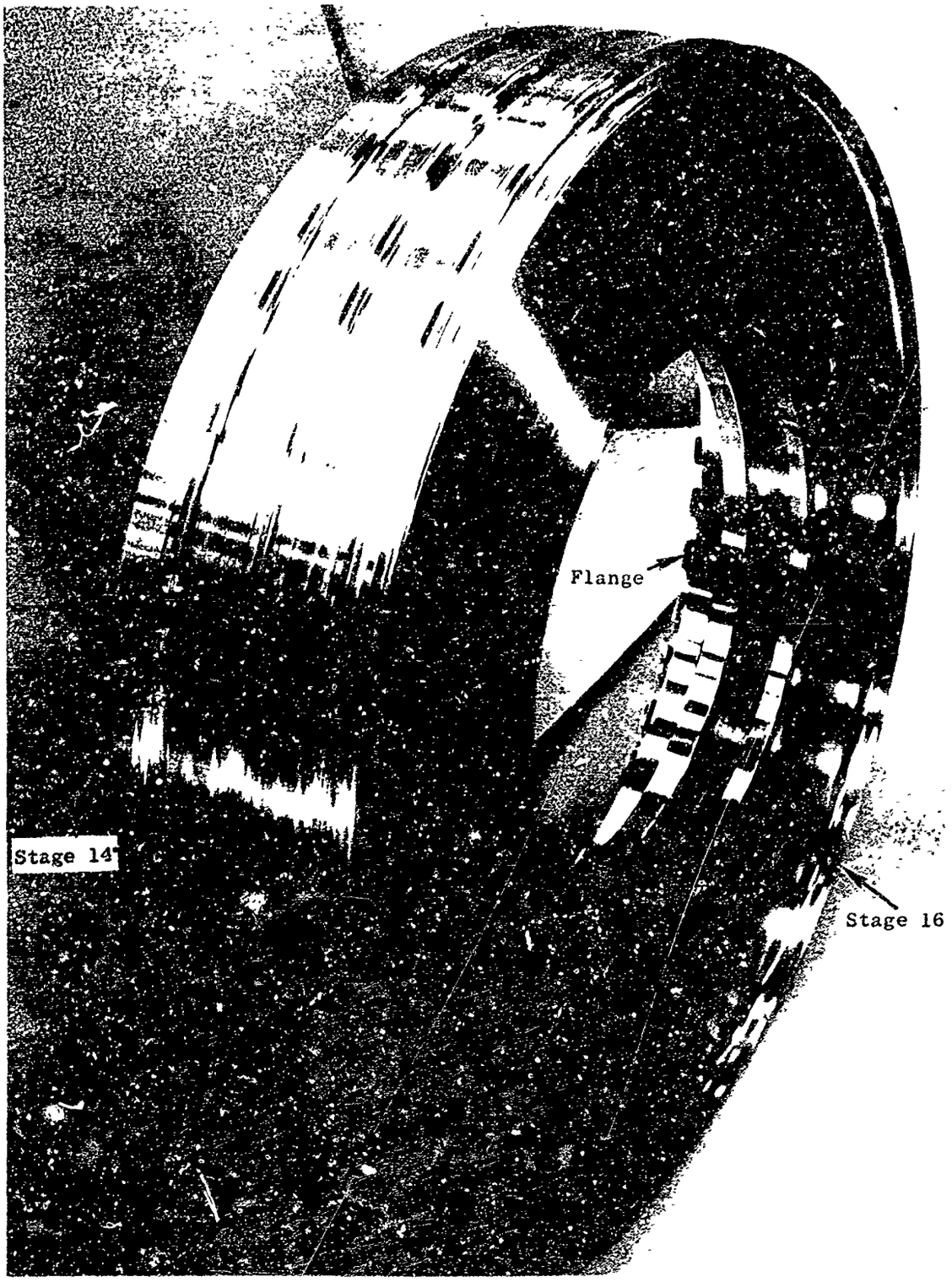

Figure 87. Aft View of Finish Machined Rotor No. 5

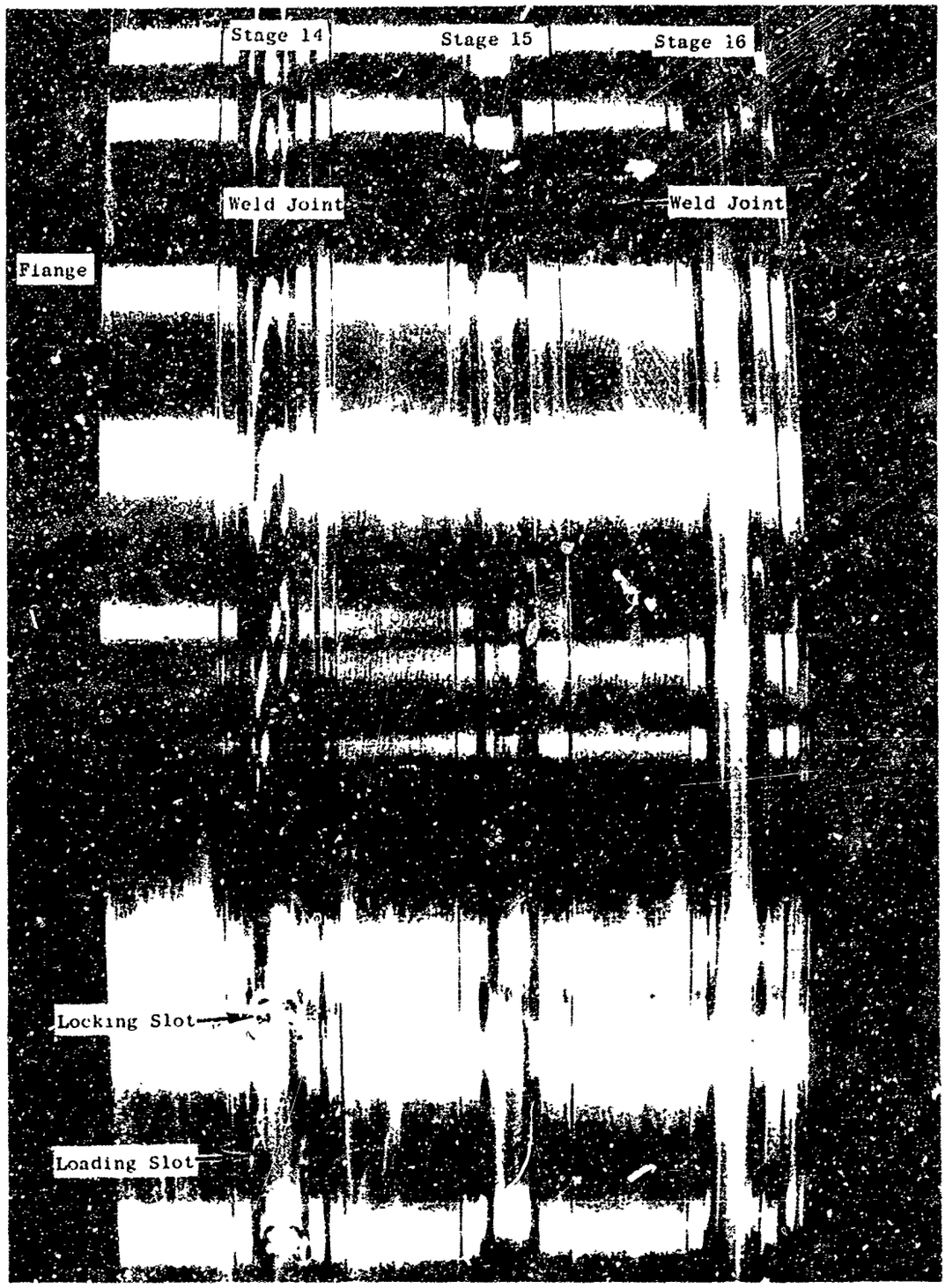

Figure 88. Close-up View of OD of Finish Machined Rotor No. 5

4. Test Weld Evaluation - To obtain property data representative of the welded joints in the rotor, test bars were machined from weld 400-9-105, Table XXXV. As shown in this table, the welding parameters were essentially the same as for the rotor and the material was from one of the forgings (C0082) used in the rotor. Test bars were also machined from forging C0067 for parent metal properties. All specimens were aged in vacuum prior to testing. Parent metal and weld test specimens had the same orientation.

The results of tensile and stress rupture testing, Table XXXVI, showed that except for one specimen, C-9, the welded specimens were equivalent to the parent metal specimens in ultimate and yield strength. Weld ductility values were below both parent metal and minimum specification levels, especially at 1200F. Stress rupture life of the weld test specimen also was lower than parent metal and below the specification minimum. With respect to Larson-Miller parameters the weld test specimen values represented about a 10 percent reduction in rupture strength, Figure 89.

Microexamination of fractured specimens showed that liquated grain boundary phases in the heat affected zones were the most likely cause for the low ductility and rupture life results. The fracture paths in most cases were associated with these grain boundary phases. Microhardness measurements showed the liquated phases were extremely hard (882 VHN) vs 460 VHN in parent metal) and therefore probably very brittle. Electron microprobe analysis of the second phase showed the Cb content ranged from 18 to 20 percent with confirmed that the grain boundary phases were the result of incipient melting during welding.

To determine if the adverse effect of the liquated phase on ductility and rupture properties could be reduced, additional test bars were prepared from the test weld. Three treatments were selected for investigation as shown below.

- AGE + shot peen
- AGE + solution anneal + age
- AGE + shot peen + solution anneal + age + shot peen

Only 1200F tensile and stress rupture tests were made since the influence of the second phase was most evident at elevated temperatures. As shown in Table XXXVII, shot peening had the most beneficial effect but none of the treatments raised the ductility and rupture properties to minimum specifications.

The above mechanical property test data from tensile and stress rupture testing were inadequate to assess the low cycle fatigue (LCF) capability of weld joints containing liquated grain boundary phases, and therefore to predict rotor performance in cyclic testing to the TF39 engine design requirements. However, earlier in this program (Section III-B) LCF data had been generated in evaluating 4 inch OD x 0.290 inch wall test specimen welds. Since liquated grain boundary phases had been identified in the HAZ of these welds it seemed reasonable to expect the 4 inch LCF data to be representative of the 24 inch test and rotor welds. As shown in Figure 90, the two 4 inch weld data points, although well below the LCF average design curve, are above the minimum requirement curve for 10,000 cycle life at 1000F at a maximum stress of 80 ksi. This indicated that the welded rotor had the capability to meet the TF39 cyclic life goal.

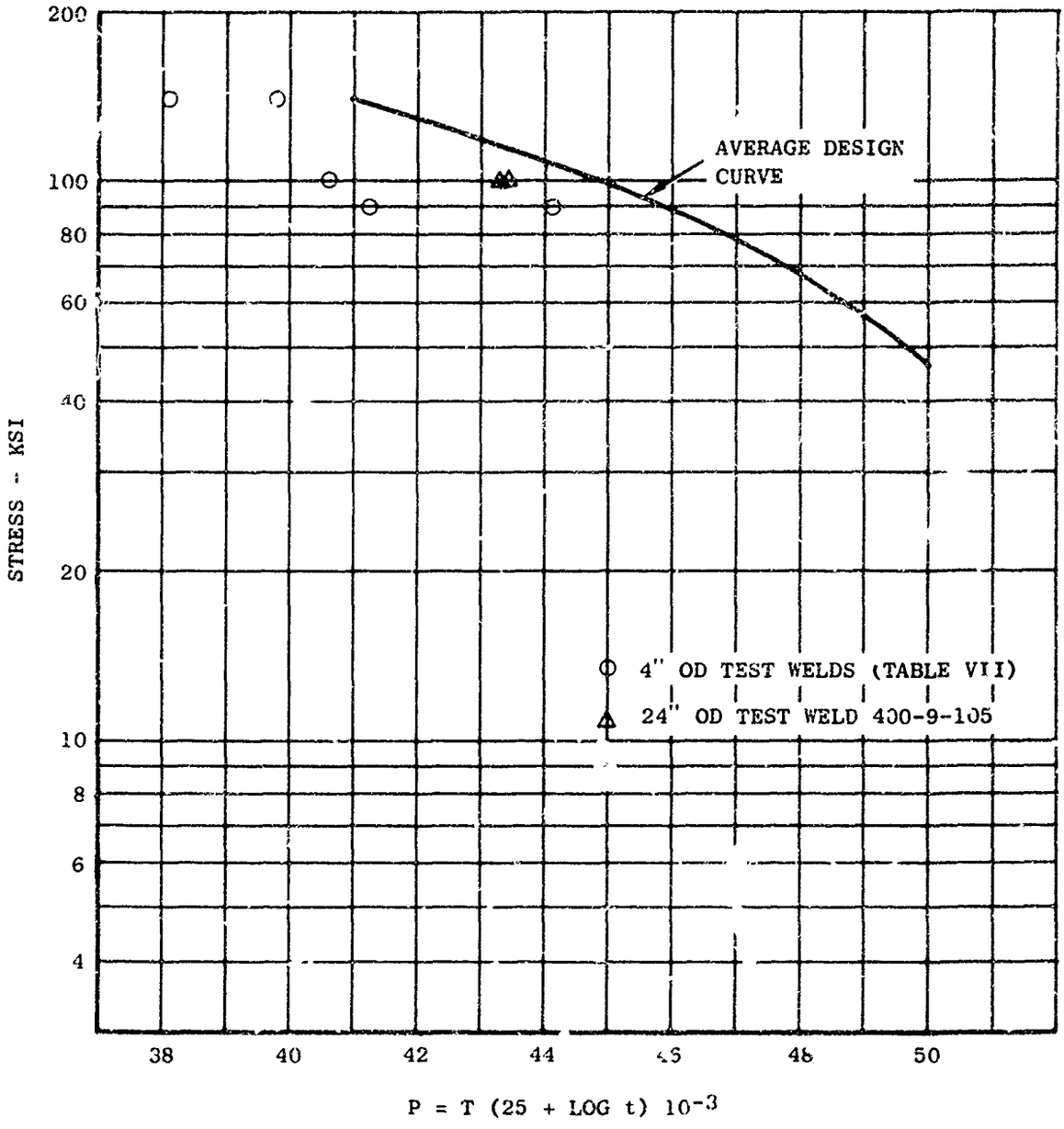

Figure 89 Stress Rupture Properties of 4 and 24 inch Diameter Inconel 718 Test Welds

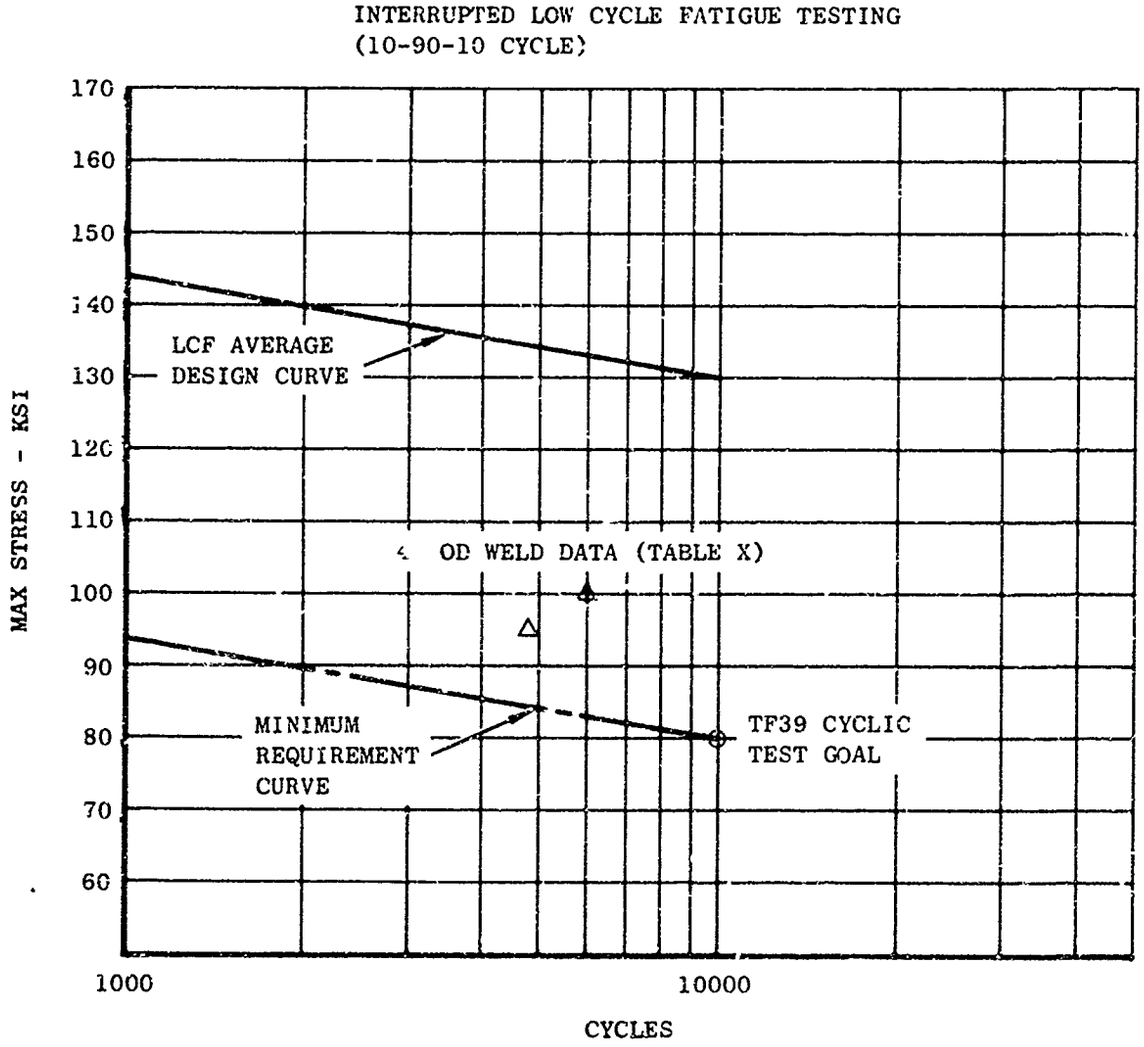

Figure 90 Comparison of Low Cycle Fatigue Test Results of Inertia Welded Inconel 718 With TF33 Cyclic Test Requirements

5. Cyclic Test Decision - At this point in the program a review of the TF39 production schedules showed that due to the reduced C5A procurement and the early cut-off date for material procurement, introduction of the inertia welding process into TF39 compressor rotor manufacture was no longer feasible. In addition sufficient testing time had been accumulated on rotors welded in other programs to amply demonstrate applicability of the process to rotor fabrication. In view of these facts the significance of cycle testing this welded rotor was diminished to such an extent that it was decided rather than test the rotor and possibly damage or destroy it, the objectives of this program would really be served better by retaining it as an example of hardware fabrication by the fabricated rotor process. This decision terminated all further work under this program. See Appendix II, III and IV.

SECTION VI

OVERALL PROGRAM ANALYSIS AND EVALUATION

A. SUMMARY ANALYSIS OF RESULTS

1. Review of Program Objectives

The principal objective of this program was to develop an improved manufacturing method for producing jet engine compressor rotors. There were two new fabrication concepts to be explored, developed and finally proved by the fabrication of a TF39 Stages 14-16 compressor rotor. The first concept was to fabricate single compressor rotor discs or stages from Inconel 718 cross rolled plate by cold forming. The second concept was to join three cold formed stages by inertia welding to form an integral multi-stage compressor rotor. As described within this report both of these unique fabrication methods were successfully developed and proved. In doing this certain studies were required to establish process parameters and material properties. The results of these studies were not always as expected or even as desired but the new knowledge acquired is considered essential for the successful application of both new fabrication methods to the manufacture of jet engine compressor rotors.

2. Cross Rolled Plate Studies

The substitution of rolled plate for forged stock in rotor fabrication required an evaluation of the mechanical properties of the plate in both worked and unworked conditions to establish its acceptance for jet engine use. Room temperature and 1200°F tensile properties and stress rupture properties of a typical lot of TF39 Stage 14-16 forgings are compared with as rolled cross rolled plates heat treated to the forging specification and cold rim formed cross rolled plate given three high temperature (1850 to 1900°F) anneals in cold rim form processing, Tables XXXVIII, XXXIX, XL and XLI and Figures 91, 92 and 93. The data clearly show that as rolled and standard heat treated cross rolled plates meet all GE forging specifications and with respect to the data for the particular lot of forgings shown have better properties than the forgings. As discussed in this report (Section IV-B-2) cold working the disc rims had no significant effect on tensile or stress rupture properties although low cycle fatigue life appeared to be increased. Therefore no distinction is made between worked and non-worked properties in Figures 91, 92 and 93. However the deleterious effect of the high temperature anneals on tensile strength and 1200°F ductility is quite obvious. The lesson learned here is that for optimum strength and elevated temperature ductility cross rolled plate must not be heat treated above 1750°F to 1775°F. Oil or water quenching from this temperature should result in room temperature ductility sufficiently high for crack-free cold forming without sacrificing tensile strength or high temperature ductility.

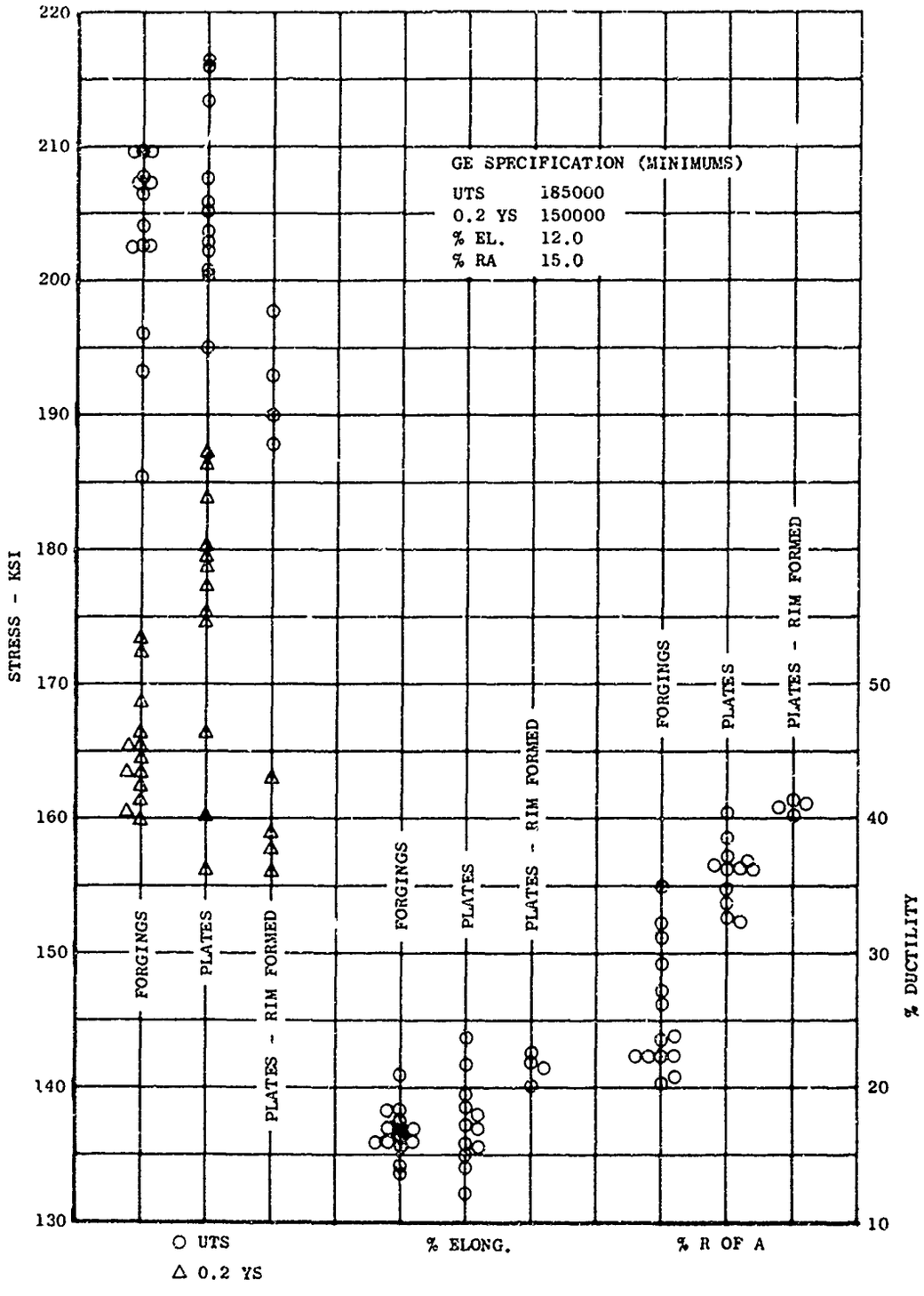

Figure 91. Room Temperature Tensile Properties of Inconel 718 Forgings, As Rolled Plates and Rim Formed Plates

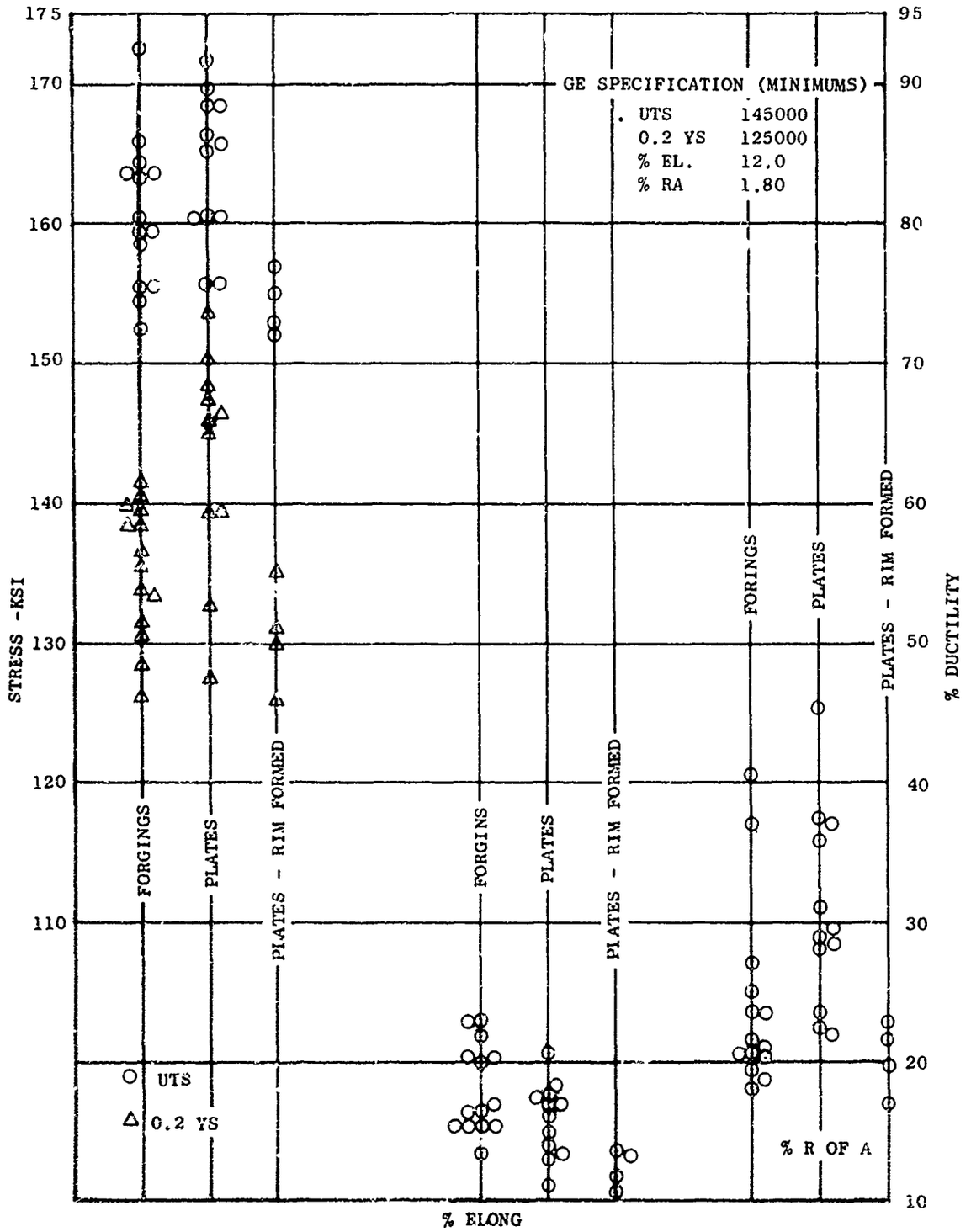

Figure 92 1200°F Tensile Properties of Inconel 718 Forgings, As Rolled Plates and Rim Formed Plates

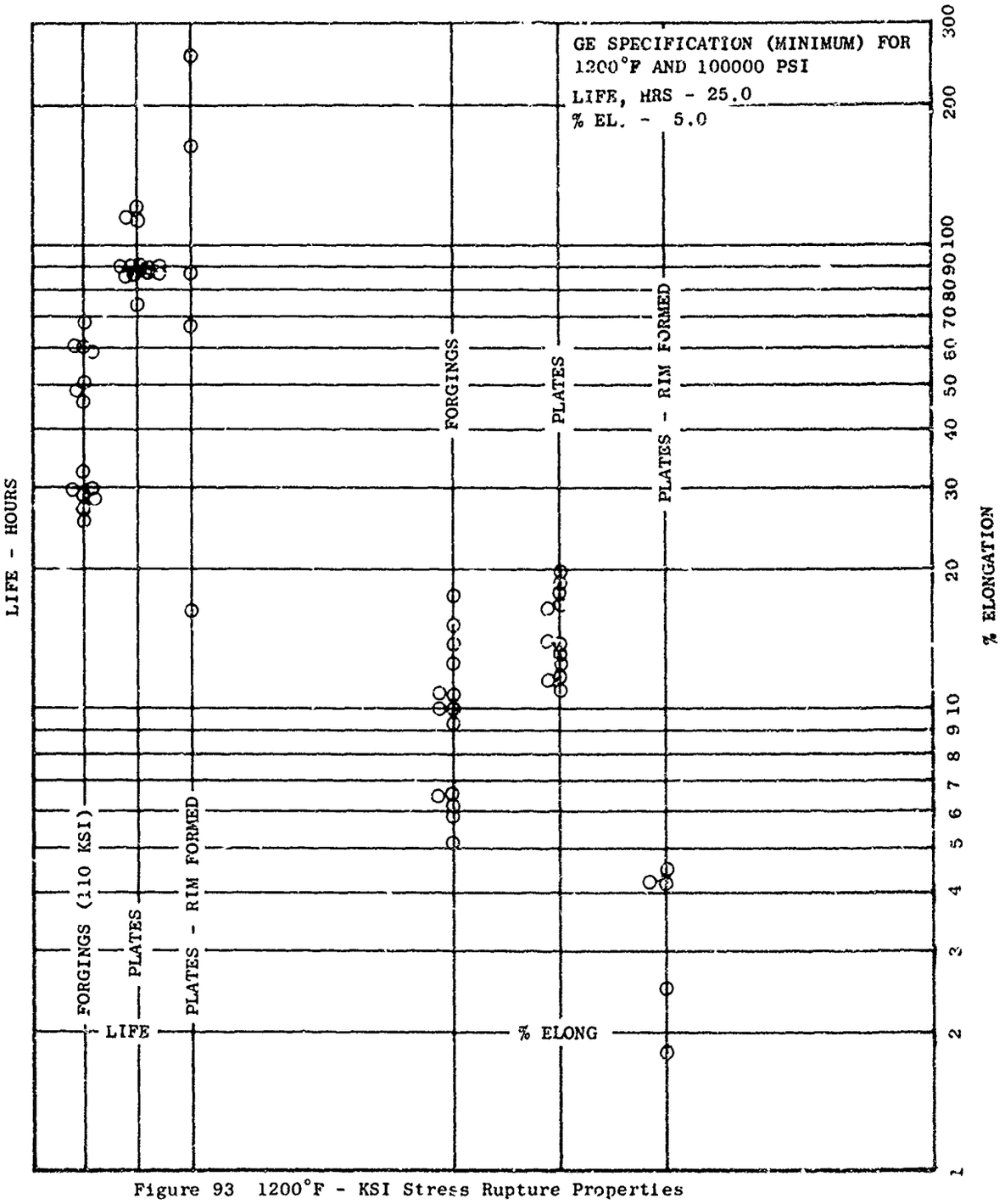

Figure 93 1200°F - KSI Stress Rupture Properties of Forgings, As Rolled Plates and Rim Formed Plates

3. Cold Rim Forming Results

A total of 18 discs machined from cross rolled plates were cold rim formed. The first disc was used to establish machine settings and then intentionally destroyed for metallurgical and mechanical property studies. The tabulation below summarizes the results of forming the remaining 17 discs.

Number of Discs	Cold Rim Forming Results
5	Shear Form Groove Cracks
7	Part Envelope Violated
5	Acceptable Rotor Stages

Although the yield of acceptable rotor stages appear low it must be noted that 11 of the 12 discs with cracks or envelope violations were formed in the first run when roll forming machine deflections and cross rolled plate hardness were not under control. In the second run of five discs four were formed to acceptable rotor stages and the envelope violation of the fifth was due to the eccentricity of the groove machined in the rim for the splitting operation. Given material of the proper hardness and with suitable compensations over machine deflections, cold rim forming of discs into proper geometries for inertia welding should become an established process. Based on the lessons learned in forming the first 18 discs, additional tooling and method sophistications should enable reproducible cold forming to tighter tolerances and narrower part envelopes thereby reducing the material investment still further.

4. Inertia Welding Studies

The inertia welding studies conducted on one-inch diameter Inconel 718 cylinders led to the selection of preliminary parameters to be further explored in scale-up welding to 24-inch diameter cylinders in preparation for welding the actual hardware. Analysis of the results of welding 4, 12 and 24-inch diameter cylinders of various wall thicknesses led to a general empirical equation relating the total upset to joint area and the welding thrust load and energy. It was pointed out that the equation was applicable to the welding of Inconel 718 only within the limits of the joint geometry, diameters and wall thicknesses studied. Within these prescribed limits, the equation does allow the pre-selection of weld parameters for other diameters and wall thicknesses without the need for additional parametric studies.

Metallographic and electron microprobe analyses of test welds led to the identification of incipient melting in the interface, within the grain boundaries of the heat affected zones or in the flash in all welds made at linear velocities above 700 SFM. Greater amounts and more massive concentrations of the liquated phases were observed in welds wherein the parent metal was coarse grained (ASTM 4 to 5) or duplex (ASTM 8 + ASTM 1 to 2) in structure than in fine grained (ASTM 8) material. Mechanical property tests of welds containing liquated phases showed that elevated temperature tensile and stress rupture ductility and stress rupture life of coarse grained or duplex material were lowered significantly. Fractures were observed to initiate at liquated grain boundaries and crack propagation generally followed along the liquated grain boundaries. In uniformly fine grained material welded above 700 SFM the liquated phases were well dispersed and appeared to have no significant effect on the tensile and stress rupture properties. However, low and high cycle fatigue testing of such welds would be required to establish their tolerance for grain boundary liquation.

Based on present knowledge it would appear that welding speeds for Inconel 718 should not exceed 700 SFM but further parametric studies are required to establish the interrelationships and effect of flywheel mass, linear velocity, welding pressure and wall thickness on the amount and location of liquated grain boundary phases. A proper combination of weld parameters may result in displacing the liquated areas to the weld flash in welds made above 700 SFM. This is important in welding joints where the 700 SFM limit would reduce the angular velocity to very low values and require very large flywheels. Such conditions could create insufficient weld zone temperatures and cause excessive twisting of the weld zone following coalescence across the interface, thereby leading to tearing of material at the peripheral edge of the heat affected zone.

5. Rotor Welding Results

Prior to welding the rotor stages a significant amount of effort was expended in 24 inch diameter test ring welding to establish reproducible control over joint parallelism and concentricity. This was finally accomplished by numerous adjustments and modifications to both machine and tooling, and by strict control over the dimensional quality of the parts to be welded.

Five TF39 Stage 14-16 compressor rotors were welded. The first four were made from cold rim formed discs and the fifth from forged stock. Of a total of 18 welds, three were considered unacceptable, two for insufficient upset and one for excessive out-of-parallelism. Of the remaining 15 welds parallelism runouts ranged from 0.001 to 0.011 inch TIR. The diametral runouts of 14 welds ranged from 0.002 to 0.0075 inch TIR with one weld at 0.016 inch TIR. This weld joined two undersize parts in rotor No. 1 (Stage 14 to flange) and the pre-weld concentricity was 0.029 inch TIR. Reproducibility of total upset was determined to be chiefly influenced by weld prep geometry, pilot-bushing clearances and engagement, and thrust load during welding.

In summary, the welding of these five rotors demonstrated that multi-stage compressor rotors can be inertia welded to the close dimensional tolerances necessary for subsequent successful machining to blueprint dimensions. However, with respect to weld quality, test weld data indicated that ductility and rupture life properties were reduced below parent metal values by the presence of liquated grain boundary phases in the heat affected zones. Based on the knowledge gained in the inertia welding studies, much lower welding speeds and/or higher welding pressures would have been required to eliminate or reduce the amount of incipient melting. However, the capacity limits of the Model 400 inertia welder did not permit any significant changes in these parameters.

6. Rotor Machining Results

One very important but costly lesson learned in machining the weld flash of the first four rotors welded from cross rolled plate was that forcing the cutting tool into the cracked flash could initiate and/or propagate cracks into the base metal. Four rotors were scrapped because of spacer wall cracks transverse to the circumferential weld joints. The weld flash of the fifth rotor was machined by traversing a single point tool laterally across the weld joint. This rotor was free of cracks by zyglo inspection before and after aging and after finish machining.

No significant problems were encountered in rough and finish turning the rotors. In the initial rough turning operations manual controlled vertical turret lathes were used. Subsequantly numerically controlled VTL's and lathes were used in contouring to blueprint. Fxcept for minor modifications in the initial rough turning operatings the machine operators were able to follow the standard TF39 Stage 14-16 rotor manufacturing process sheets in finish turning.

B. APPLICABILITY OF THE FABRICATED ROTOR PROCESS

A review was made of General Electric and competitor axial flow compressor rotor designs to determine whether the fabricated rotor process was applicable to only a few or a broad range of jet engine compressor rotors. The analysis showed that compressor rotors for the advanced jet engines being built today are of three basic designs, i.e., the smooth spool type, the disk and spacer construction and the loose spacer, stacked rotor design. These three basic types of rotors are sketched below as presently being built and as they would be fabricated by inertia welding.

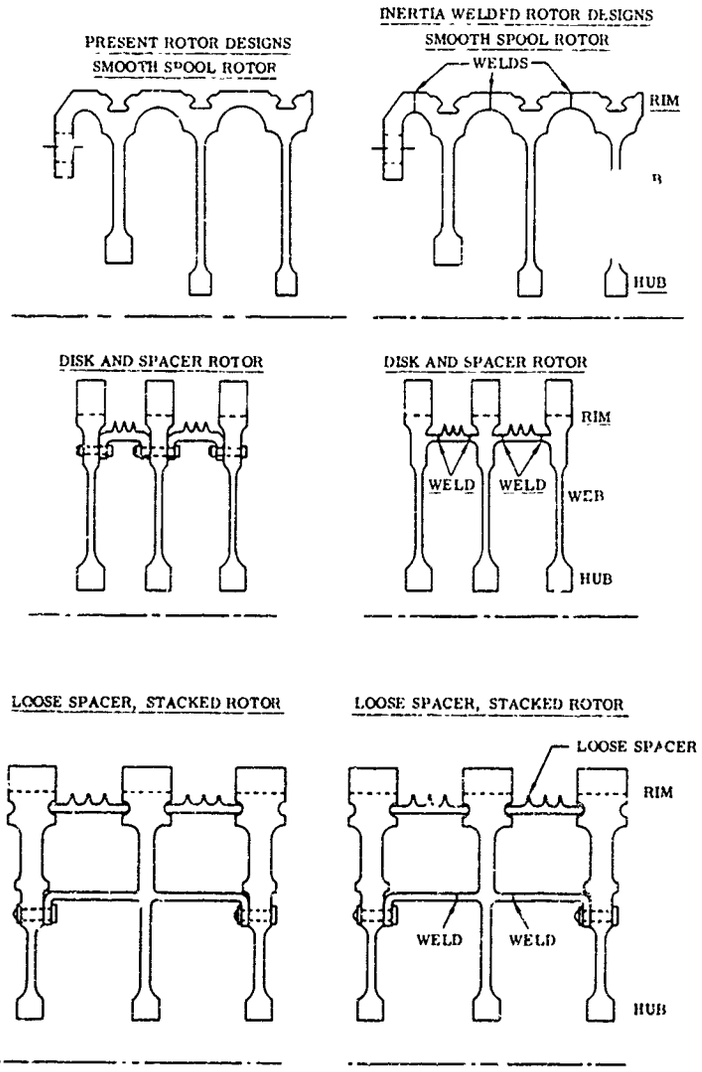

In general, spool type rotors consist of three or more stages machined from one piece forgings. Depending on the particular rotor design a number of such subassemblies are then bolted together to form the complete rotor. As shown in the sketch the rotor blades are mounted in circumferential dovetail slots or tracks.

Disk and spacer type rotors require extensive bolting in their assembly. Each disk or stage is separated by and bolted to a spacer ring. The rotor blades are fitted into axial dovetail slots machined in the disk rims.

The loose spacer, stacked rotor design requires less bolting for assembly than the disk and spacer design but complex forgings are needed for the disks with integral extension arms. This design also utilizes axial dovetail slots in the disk rims.

The application of the fabricated rotor process to these types of rotors is dependent on both material and design factors as discussed below.

Spool Type Rotors

The complete fabricated rotor process, i.e., inertia welding of rim formed disks, was developed specifically for the spool type design. This design was circumferential dovetail slots is naturally suited to the use of rim formed disks. The V-grooves in the disk rims coincide with the dovetail slots and the rolled over extensions serve to form the spacer sections. The application of the cold rim forming process however is limited to materials with adequate cold workability. Titanium base alloys have strong galling tendencies and some of the stronger nickel base superalloys lack the ductility for cold splitting and forming. In such cases the spool type rotor must be fabricated by welding disks and spacer rings together.

The economic application of rim formed disks machined from flat cross rolled plate is dependent on the axial distance between stages and the relative thicknesses of the disk web and hub since both of these factors determine the starting thickness of plate required. As the separation between stages or the hub thickness increase relative to the web thickness the amount of material lost in machining to the thin web may nullify the economic advantages of cross rolled plate. A process is now being developed for cross rolling the web, hub and rim configuration into plate which would increase material utilization significantly, (Air Force Contract F33615-69-C-1853).

Disk and Spacer Type Rotor

The axial dovetail slots of this design make it unsuitable for the use of rim formed disks with their circumferential dovetail slots. The fabricated approach would be to weld the individual disks and spacers together. As with the spool type rotor, the relative thicknesses of the disk hub, web and in this case, the rim, affect the efficiency of material utilization. The axial distance between stages is not a limiting factor since the spacer sections are separate components. However, the welded design requires a spacer diameter smaller than the bottom of the dovetail slot to allow slot machining and blade insertion after welding.

Rotor material in this design is a limiting factor only when adjoining spacer and disk are of dissimilar materials, e.g., titanium base and nickel base alloys. Sound inertia welds between these two materials have not been achieved up to this time and bolted joints must be used.

Loose Spacer Stacked Rotor Design

All of the comments made above about the disk and spacer type rotors also apply to this design except that the spacer diameter in this case is not a limiting factor since the disks are finish machined prior to assembly.

With respect to the spool and disk and spacer types of rotor designs the one absolute requirement for the fabricated rotor process is a bore diameter large enough for tooling access. In addition the ratio of weld joint inner diameter to bore diameter must be such to allow ID weld flash machining and finish contouring.

The bore diameter is not of concern in the loose spacer, stacked rotor design since the disks are welded and finish machined prior to assembly. Although the bolting requirements are not eliminated or reduced, the obvious advantage of the inertia welding approach is to eliminate the need for expensive complex contoured forgings and reduce the material investment and amount of machining required.

Rotor diameter and weld interface area are limiting factors in a time sense only. Where these exceed the capability of existing welding machines, larger inertia welders will have to be designed and built.

Fabrication of a spool type rotor has been accomplished in this program. Several rotors of the disk and spacer design have been inertia welded in another program. Both of these accomplishments demonstrate that the fabricated rotor process, in whole or in part, is applicable to a broad range of jet engine compressor rotors.

C. COST COMPARISON OF FORGED AND MACHINED VS FABRICATED ROTORS

Based on the fabrication procedures developed in this program a labor and material cost comparison with the present forged and machined rotor method was made. Two alternate inertia welding approaches also were evaluated. These were: (1) the use of two plates for Stages 15 and 16 and a forging combining Stage 14 and the flange; and (2) the use of three forgings for Stage 14 plus flange, 15 and 16. A labor summary comparison of the three inertia welding methods to the forged and machined method on a percentage basis is shown in Table XLII. A complete labor breakdown on a percentage basis for the inertia welding methods is tabulated in Table XLIII. Tables XLIV and XLV compare the material inputs, and total cost for the different methods on a percentage basis.

With respect to material costs both cross rolled plate methods are more economical than the forging method. They also require less material input. Inertia welding three contoured forgings requires both the least material input and the least amount of labor but the higher forging costs nullify these advantages. Both of the cross rolled plate methods require more process labor than the present manufacturing method. However, as shown in Tables XLII and XLIII a significant percentage of the labor totals is made up of estimated hours for new operations never before performed on a repetitive basis. Based on industrial experience with learning curves, rapid reductions in labor hours can be expected as repetitive manufacture proceeds. On the other hand, the present manufacturing method has been in production for several years and is well down the learning curve such that additional significant reductions in labor input would not be as rapid.

The learning curve is based on the theory that if the quantity is increased the labor required to produce each individual unit is reduced in some proportion to the increase in quantity. The difference in the degree of learning between types of units or operations is expressed as the "percentage" of the learning curve. The percent of any learning curve is determined by the ratio of the value of any unit to the value of twice that unit. In General Electric jet engine manufacture the 86% learning curve is widely used. This means that every time the total quantity of units produced is doubled, the cumulative average time required to produce the new total quantity is only 86% as great. This is illustrated in Figure 94 which shows the cumulative average time and the unit time reduction as a function of the numbers of units produced using an 86% learning curve. As shown in Figure 94, the forged and machined method is well down the curve and the potential for labor hour reduction in the fabricated methods is obvious.

As shown by Tables XLIV and XLV there is a gross discrepancy between the unit cost of the present TF39 forging and the flange and stage forgings. For example, the flange forging, although only 6% of the weight of the TF39 production forging, costs almost 18% as much. The individual stage forgings show a similar relationship, i.e., 27.7, 21.6 and 20.8% by weight and 55.7, 41.2, and 40.2% of the cost, respectively. These are first order costs and it is reasonable to expect a downward trend with large quantity repetitive procurements. The cross rolled plate costs are based on plate dimensions calculated to ensure adequate material envelopes for meeting finish stage dimensions. With continued learning and experience in rim forming and inertia welding the raw stock dimensions would be reduced resulting in additional material savings.

The significance of the learning curve phenomenon in reducing first unit costs with repetitive manufacture is illustrated in Tables XLII, XLIV, and XLV by the percentage values of Method A^1 (initial production) compared to Method A (after 250 rotors). Since the fabricated approach, even in initial production, is comparable in cost to the present method, repetitive manufacture of fabricated rotors should soon result in significant cost savings.

D. REQUIRED INERTIA WELDING MACHINE SIZES

Since the energy and thrust requirements for inertia welding change rapidly with changing interface areas and differ significantly for different materials the design of a single welding machine to cover a broad range of joint areas and materials becomes impractical.

The machine parameters of greatest interest in welding the tubular joints of compressor rotors are (1) the flywheel or WK^2 capacity, (2) the maximum thrust load and (3) the distance from the spindle centerline to the surface of the machine bed which determines the maximum swing diameter. These parameters are listed in Table XLVI for the inertia welding machines built up to this time.

An analysis of the flywheel and load requirements for welding Inconel 718, Udimet 700 and Ti-6Al-4V compressor rotors was made. The analysis was based on welding joints with 0.200 inch walls using the welding parameters developed for the three alloys in this program. The results, plotted in Figures 95, 96 and 97, show that the four welding machines now available can weld Ti-6Al-4V rotors up to approximately 68 inch diameter. However, the maximum Inconel 718 and Udimet 700 rotor diameters which can be welded are 16.8 and 12.0 inch respectively. Table XLVII lists the maximum rotor diameters for each alloy which can be welded on the four machines available today. The need for a larger inertia

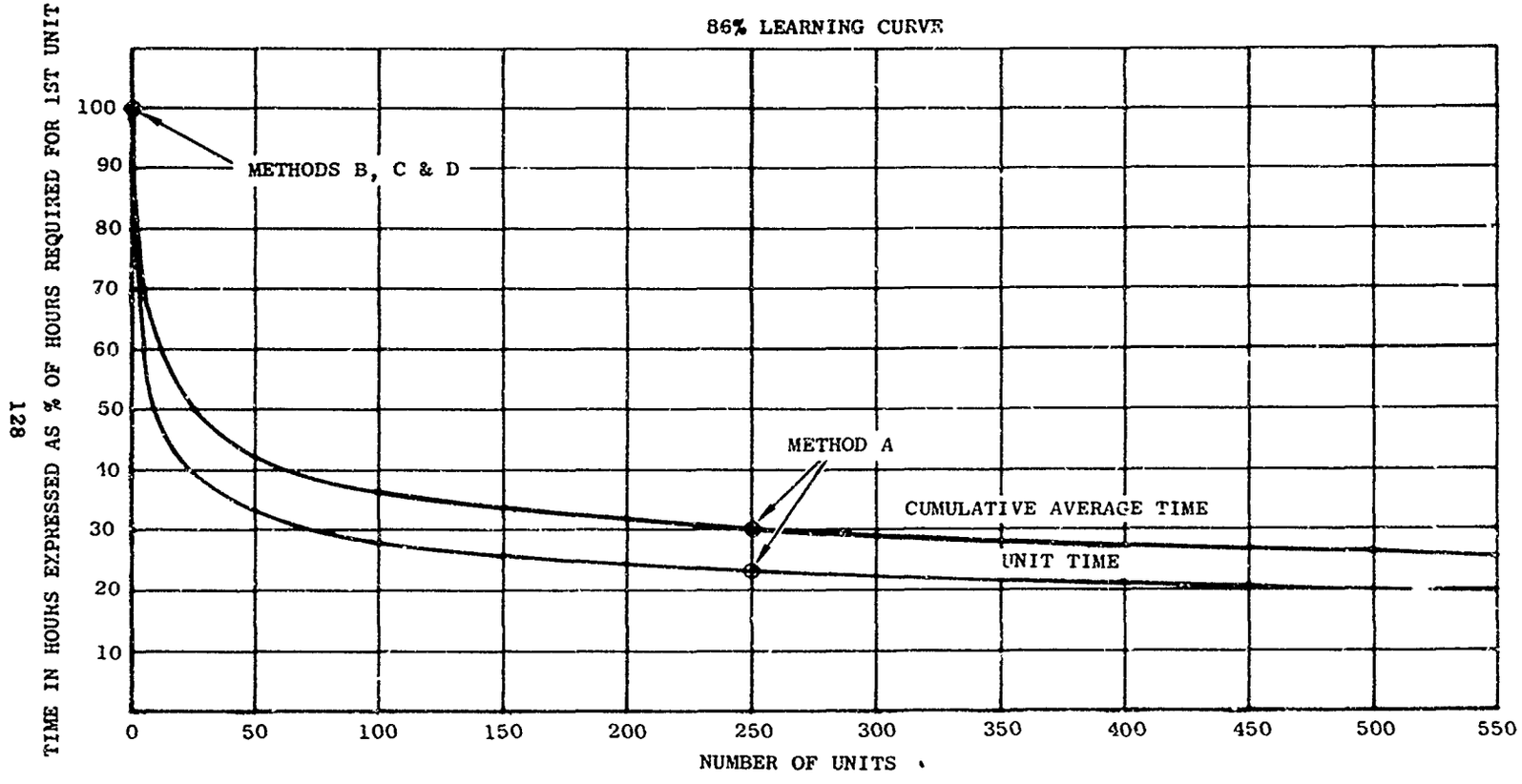

Figure 94 Labor Hour Reduction as a Function of the Learning Curve Phenomenon

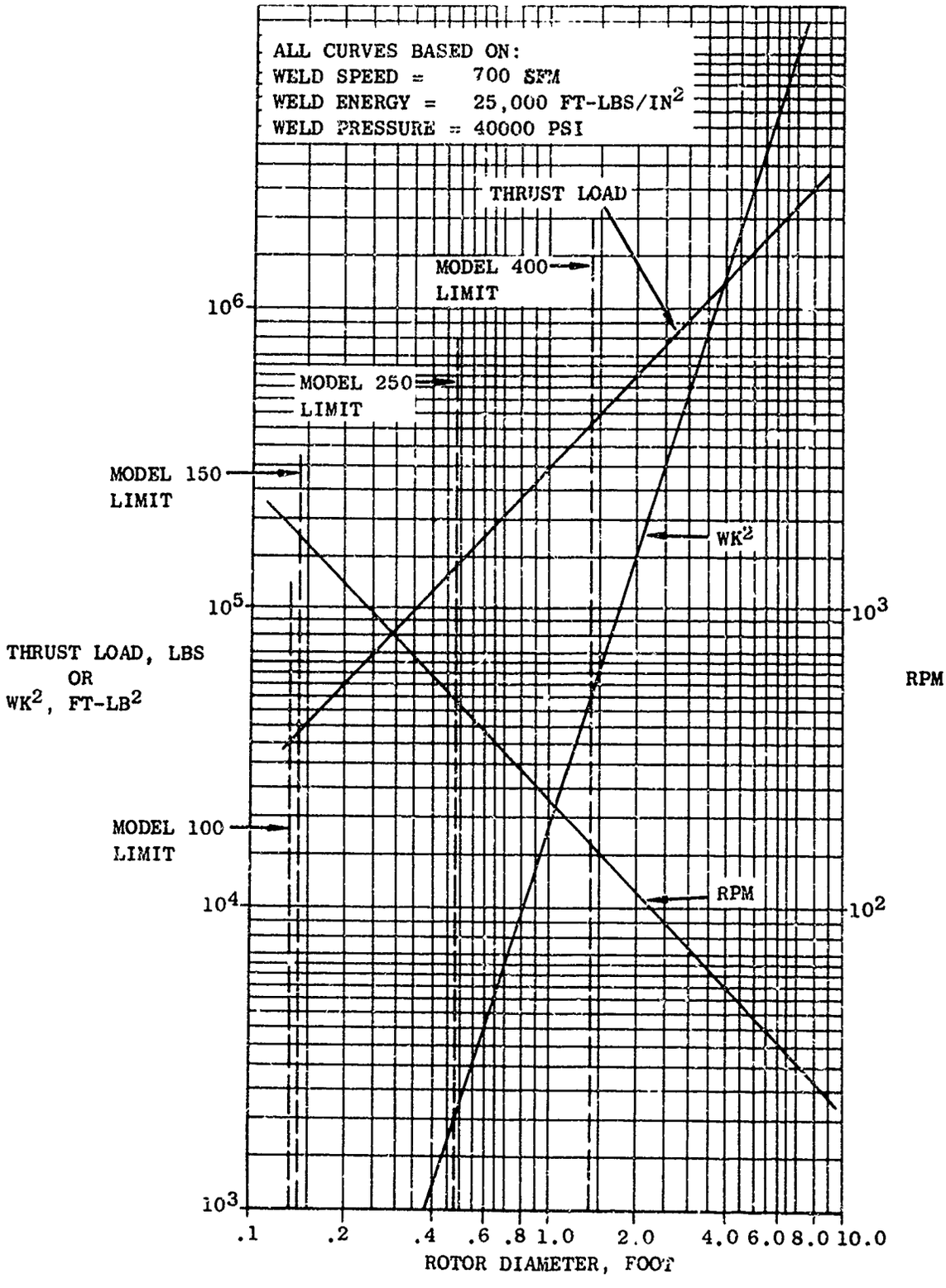

Figure 95 Load and Flywheel Requirements for Welding Inconel 718 Rotors - 0.200 Inch Wall

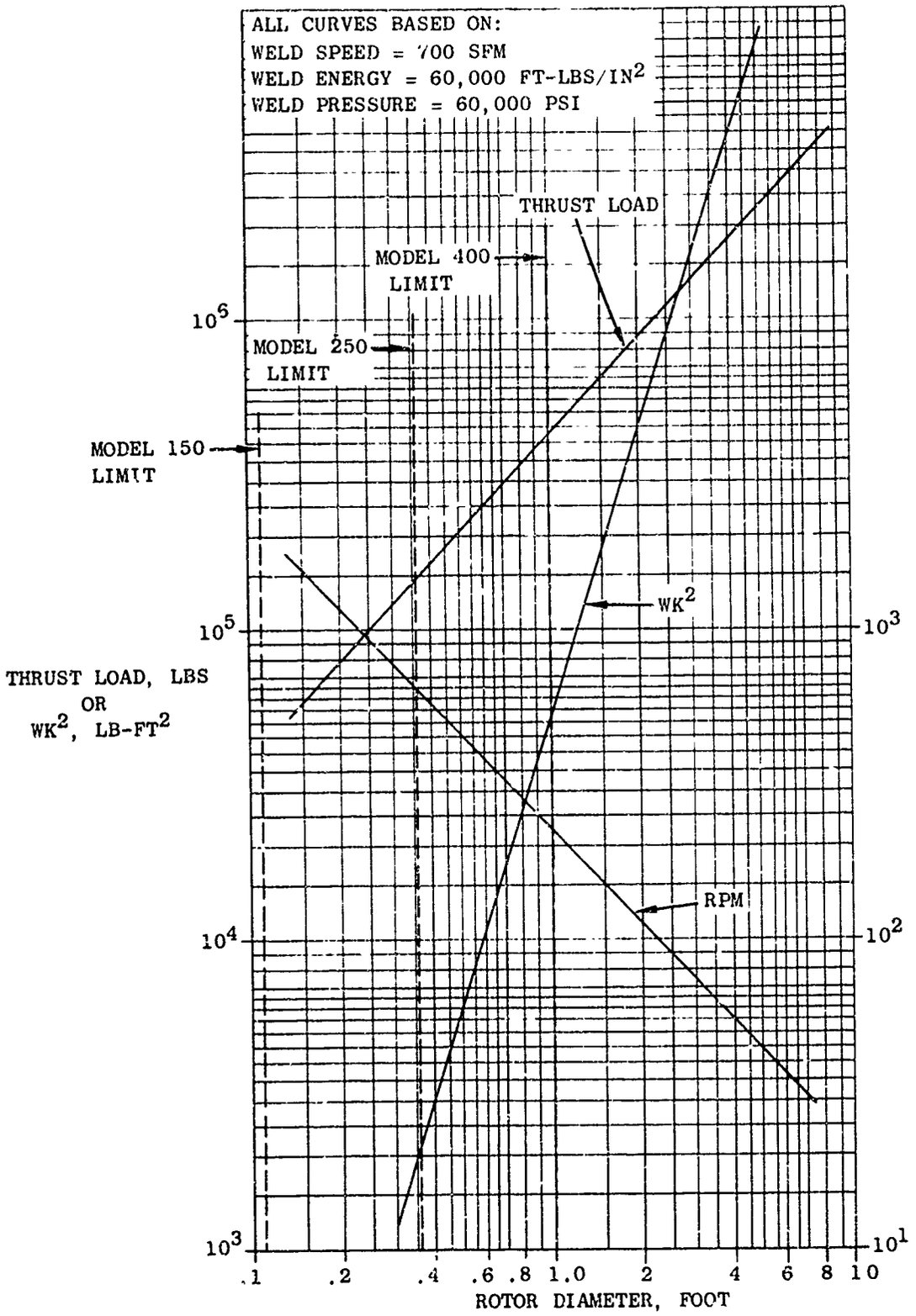

Figure 96 Load and Flywheel Requirements for Welding Udimet 700 Rotors - 0.200 Inch Wall

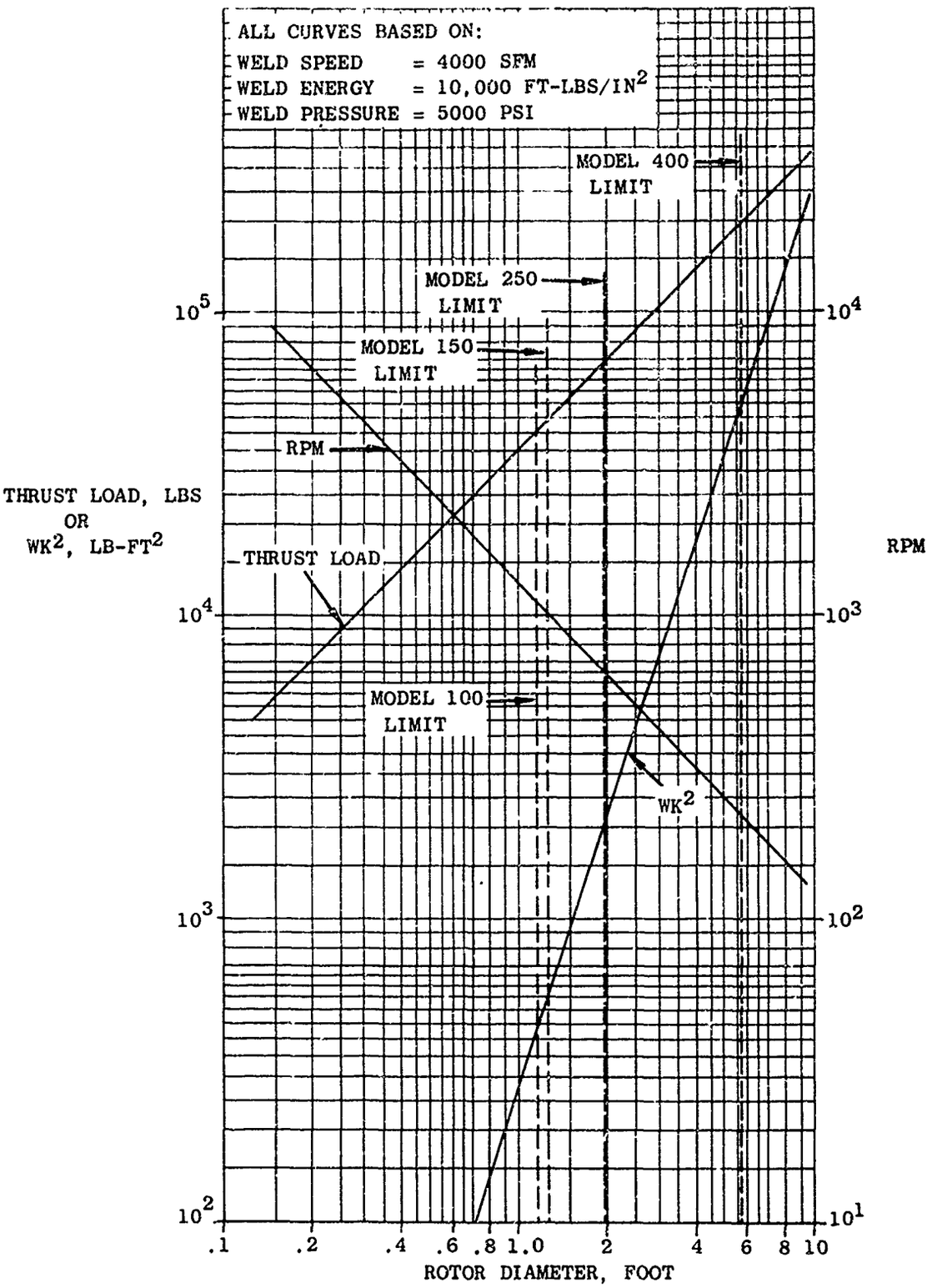

Figure 97 Load and Flywheel Requirements for Welding Ti-6Al-4V Rotors - 0.200 Inch Wall

welder to extend the range of Ni-base superalloy rotor fabrication is obvious. As shown in Figures 95 and 96, a machine with 1,500,000 lb-ft^2 flywheel capacity and 1,500,000 lbs. thrust would allow the welding of 48 inch diameter Inconel 718 rotors and 36 inch diameter Udimet 700 rotors.

The design of a machine with such high thrust and flywheel capabilities, while challenging, is not impractical. Since the moment of inertia is the product of the flywheel weight and the square of gyration increasing the flywheel diameter to 10 or 12 feet would keep the weight within practical limits of support by a properly designed spindle system. In effect, such an inertia welder, while massive in size and construction, would be a scaled-up version of the present horizontal inertia welding machines.

E. IMPACT ON DESIGN FLEXIBILITY

A few examples will suffice to indicate the tremendous impact on design flexibility created by the fabricated rotor approach.

The successive welding of individual stages to form multi-stage rotors can reduce the amount of bolting significantly. In addition to substantial weight savings and improved reliability, compressor and turbine speeds can be raised and the number of engine bearings reduced.

Fabricating individual discs from thin section plates will enhance many materials' responsiveness to heat treatments thereby allowing maximum utilization of their potential properties in addition to reducing material investment and machining costs.

Since the major portion of the disc machining would be done out in the open the design of the rotor bore would not be as dependent on the present state-of-the-art machining capability for grooving out solid forgings.

The fabricated or inertia welding approach can be extended to other engine components besides compressor rotors. These include fan discs, turbine rotors, gears and shaft for various engine applications. The welding of dissimilar materials, such as alloy and maraging steel to Inconel 718 will open additional avenues for design exploitation.

F. IMPACT ON MANUFACTURING EQUIPMENT

Initially the fabricated rotor process as developed in this program would have only a small impact on in-house manufacturing equipment. This is because N/C VTL's are required to contour the webs to some envelope prior to welding, and N/C lathes to finish contour the bores and remove flash after welding. With continued learing in inertia welding, the joining of disks with finish machined webs and hubs should be possible. The need for N/C lathe machining would then be reduced to removing the ID flash and turning the OD, allowing substantial reductions in N/C lathe requirements.

The impact of the fabricated rotor method on the forging and rolling mill industries was analyzed with the following results.

Forging Industry

At the present time there are a total of eight large forging presses and hammers in the 20,000 to 50,000 ton range available to the aircraft industry for producing forgings for large jet engine components. To supply all the forgings for one engine program like the TF39 as it was originally planned (~200 C5A aircraft and 1000 engines), one press full time for five years would be required. This represents a significant portion of the available press capacity being tied up for one engine program alone. By going to the fabricated rotor method for producing compressor rotors and other applicable components, the forging industry load would be reduced and the procurement of additional large forging presses or hammers would not be required.

Rolling Mill Industry

A review of the rolled plate requirements for the TF39 engine program with various vendors showed that the present rolling mill capacity is such that no significant increase in rolling mill workload should be expected. Rolling mill vendors estimate that 1000 plates could be rolled in 8-1/2 turns and 3000 plates could be rolled in 25 turns. They operate 21 turns per week when there is sufficient workload.

G. FACILITY AND DESIGN REQUIREMENTS.

For maximum efficiency in fabricating jet engine compressor rotors by the cold rim forming and inertia welding process an integrated facility composed of roll forming machines, inertia welders and associated supporting machining, heat treating and inspection services would be required.

As discussed within this report the roll forming machine used to develop the rim forming process was not designed for this type of loading. Consequently a forming machine specifically designed for radial forming operations would be required.

In addition to the inertia welding machines (now available) a new welder with increased thrust load capability and flywheel WK^2 capacity would be required to cover a broader range of jet engine compressor rotors.

Manual, tracer and tape controlled vertical turret and engine lathes are required to machine disks for splitting and rim forming, inertia welding, and post-weld machining.

Inert atmosphere and vacuum furnaces are required for in-process heat treating rim formed disks and welded rotors.

Zyglo process tanks and ultrasonic inspection equipment are required for in-process and final inspection of disks and the welded joints.

The introduction of the fabricated rotor process into the manufacture of compressor rotors for any engine program would require a pre-production period wherein soft tooling would be evaluated, operators trained and a sufficient number of rotors welded to establish process capability with respect to yield, tolerances, cycle time, etc. The pre-production period would culminate in the qualification and certification of both the inertia welding machine and welding process for the production of compressor rotors meeting the rigid standards required by the USAF.

APPENDIX I

TABLES

TABLE I

INCONEL 718 TEST SPECIMEN WELD PARAMETERS

Spec. No.	Flywheel WK^2 ($lb\text{-}ft^2$)	Weld Speed RPM	Weld Speed SFM	Max. Energy Input ($ft\text{-}lbs/in^2$)	Upset Pressure (Psi)	Total Upset (inch)
2-5	1240	875	890	50,800	50,500	.060
1-6	1240	925	940	51,500	51,500	.083
3-4	1240	975	990	63,400	51,800	.220

Notes:

1. Test specimen size: 4 inch O.D. x 0.290 inch wall
2. Pre-weld heat treatment: 1775°F/1 hr/AC + 1325°F/8 hr/FC to 1150°F @ 100°F/hr + 1150°F/8 hr/AC
3. Post-weld heat treatment: 1325°F/8 hr/FC to 1150°F @ 100°F/hr + 1150°F/8 hr/AC + 1250°F/64 hr/AC

TABLE II

UDIMET-700 TEST SPECIMENT WELD PARAMETERS

Spec. No.	Preweld Heat-Treat	Flywheel WK^2 (lb-Ft^2)	Weld Speed RPM	Weld Speed SFM	Max. Energy Input (lb.ft/in^2)	Upset Pressure (psi)	Total Upset (inch)	Post Weld Heat-Treat
291	A	19	4200	880	112,000	51,600	.175	C
292	A	19	3900	818	98,000	51,000	.131	C
8-53	B	19	4650	1070	118,000	50,000	.094	D
8-54	A	19	4650	1100	112,000	48,200	.056	C
8-56	A	19	4900	1125	129,000	50,000	.250	C
8-57	A	19	4300	987	100,000	50,000	.170	C
8-58	A	19	4000	920	86,000	50,000	.175	C
8-59	A	19	3900	895	81,800	50,000	.120	C
8-107	A	19	4650	1070	116,000	50,000	.195	D
8-108	A	19	4160	955	93,100	50,000	.171	D
8-109	A	19	3650	837	72,000	50,000	.114	D
8-110	A	19	3650	837	72,000	50,000	.120	D

1. Test specimen size: 0.875 inch diameter solid bar.
2. Heat-Treat Cycles:

   A - As Received
   B - 2100°F/4 hr/Oil quench
   C - 2100°F/4 hr/Oil quench + 1600°F/8 hr/AC +1800°F/4 hr/AC + 1200°F/24 hr/AC + 1400°F/8 hr/AC.
   D - 2100°F/4 hr/Salt quench @ 1000°F/AC + 1600°F/8 hr/AC + 1800°F/4 hr/AC + 1200°F/24 hr/AC + 1400°F/8 hr/AC.

TABLE III

TITANIUM 6Al-4V TEST SPECIMEN WELD PARAMETERS

Specimen Number	Flywheel WK^2 (lb-ft^2)	Weld Speed RPM	Weld Speed SFM	Upset Pressure (psi)	Max. Energy Input (Ft-lbs/in^2)	Spindle Efficiency	Actual Energy Input (Ft-lbs/in^2)	Total Upset (Inch)	Post Weld Heat-Treat
264	1.8	7,600	1,990	7,130	22,500	.40	9,050	.055	B
267	1.8	7,600	1,990	7,130	22,500	.40	9,050	.048	B
269	1.8	7,600	1,990	7,130	22,500	.40	9,050	.048	A
282	1.8	7,600	1,990	7,130	22,500	.40	9,050	.050	B
286	1.8	7,600	1,990	7,130	22,500	.40	9,050	.050	A
287	1.8	7,600	1,990	7,130	22,500	.40	9,050	.054	A
288	1.8	7,600	1,990	7,130	22,500	.40	9,050	.054	A
289	1.8	7,600	1,990	7,130	22,500	.40	9,050	.055	A
8-106	1.8	7,700	2,020	7,020	22,500	.40	9,050	.060	B
8-98	1.8	7,200	1,890	7,650	22,500	.40	9,050	.060	B
208	1.8	7,200	1,890	7,020	20,200	.40	8,070	.050	A
263	1.8	7,600	1,990	7,020	22,500	.40	9,050	.060	B

Notes:
1. Test specimen size: 1.00 inch diameter solid bar.
2. Preweld heat-treat: 1300°F/2 hr/AC.
3. Post weld heat-treat: A - None
   B - 1750°F/1 hr/WQ + 1300°F/2 hr/AC

TABLE IV

TENSILE PROPERTIES OF INERTIA WELDED INCONEL 718

Smooth Bar

Spec. No.	Total Upset (Inch)	Test Temp (°F)	UTS (ksi)	.2% YS (ksi)	.02% YS (ksi)	R.A. (%)	El. (%)	Failure Location
1-PM	--	RT	188	159	141	40.0	24.0	-
2-PM	--	RT	189	160	139	40.0	22.5	-
3-PM	--	1200	151	131	114	16.5	10.5	-
4-PM	--	1200	149	131	114	16.5	10.0	-
1-W	.220	RT	185	150	127	40.4	21.9	Parent Metal
15-W	.083	RT	161	154	129	2.5	0.8	Heat Affected Zone
2-W	.220	1000	152	126	106	45.3	16.4	Parent Metal
16-W	.083	1000	148	129	111	6.5	4.0	Heat Affected Zone
3-W	.220	1200	150	124	98	16.1	9.9	Heat Affected Zone
17-W	.083	1200	82	--	--	4.0	0.4	Weld
4-W	.220	1300	134	118	98	9.1	4.9	Heat Affected Zone
18-W	.083	1300	96	--	--	2.4	0.4	Weld
GE Spec B50TF15-S5		RT	180	150		15.0	12.0	
		1200	145	125		15.0	10.0	

Notched and Radius Bar

Spec. No.	Total Upset (inch)	Test Temp°F	Notch K_t	UTS (ksi)	Failure Location
5	.220	RT	2.5	269	Notch
23	.083	RT	2.5	179	Notch
11	.220	1000	2.5	224	Notch
24	.083	1000	2.5	94	Notch
12	.220	1200	2.5	137	Notch
25	.083	1200	2.5	54	Notch
14	.220	1300	2.5	121	Notch
26	.083	1300	2.5	86	Notch
PM	---	1300	2.5	162	Notch
7	.220	RT	Radius	195	Weld
27	.083	RT	Radius	138	Weld

Heat Treat Cycles:

Inertia Welds - 1775°F/1 hr/AC + 1325°F/8 hr/FC to 1150°F @ 100°F/hr + 1150°F/8 hr/AC + Weld + 1325°F/8 hr/FC to 1150°F @ 100°F/hr + 1150°F/8 hr/AC + 1250°F/64 hr/AC + Test

Parent Metal - Same heat treat as above.

TABLE V

TENSILE PROPERTIES OF INERTIA WELDED UDIMET-700

Smooth Bar

Spec. No.	Total Upset (In.)	Heat Treat Cycle	Test Temp (°F)	UTS (ksi)	.2% YS (ksi)	.02% YS (ksi)	R.A. (%)	El. (%)	Failure Location
291-1	0.175	A	RT	189	135	119	17.0	13.5	Parent Metal
292-1	0.131	A	RT	132	132	121	4.0	1.0	Parent Metal
8-54-3	0.056	A	1200	18	-	-	-	0.4	Weld Area-Quench Crack
8-59-2	0.120	A	1200	28	-	-	-	0.4	Parent Metal-Quench Crack
291-2	0.175	B	1400	144	125	108	24.5	15.0	Parent Metal
292-2	0.131	A	1400	152	122	95	11.5	9.0	Parent Metal
8-54-4	0.056	A	1500	15	-	-	-	1.0	Weld Area-Quench Crack
8-108-2	0.171	B	1500	110	102	82	2.5	2.8	Threads
GE Spec C50TF3-83			RT	185	140		13.0	12.0	
			1400	145	118		15.0	18.0	

Notched and Radius Bar

Spec. No.	Total Upset (Inch)	Heat Treat Cycle	Test Temp (°F)	Notch K_t	UTS (ksi)	Failure Location
8-58-C	0.175	A	RT	3.2	169	Parent Metal-Removed from notch
8-59-B	0.120	A	RT	3.2	203	Notch
8-59-C	0.120	A	1200	3.2	201	Notch
8-107-3	0.195	B	1200	3.2	161	Notch
8-58-D	0.175	A	1400	3.2	28	Parent Metal-Quench Crack
8-59-A	0.120	A	1400	3.2	139	Notch
8-107-1	0.195	B	1500	3.2	147	Parent Metal-Removed from notch
8-59-D	0.120	A	1500	3.2	144	Notch
8-110-1	0.120	B	RT	Radius	195	Weld
8-110-2	0.120	B	RT	Radius	197	Weld

Heat Treat Cycles:

A - Weld + 2100°F/4 hr/Oil Quench + 1600°F/8 hr/AC + 1800°F/4 hr/AC + 1200°F/24 hr/AC + 1400°F/8 hr/AC + Test

B - Weld + 2100°F/4 hr/Salt Quench @ 1000°F/AC + 1600°F/8 hr/AC + 1800°F/4 hr/AC + 1200°F/24 hr/AC + 1400°F/8 hr/AC + Test

TABLE VI

TENSILE PROPERTIES OF INERTIA WELDED Ti 6A1-4V

Smooth Bar Spec. No.	Total Upset (Inch)	Heat Treat Cycle	Test Temp (°F)	UTS (ksi)	.2%YS (ksi)	.02%YS (ksi)	R.A. (%)	El. (%)	Failure Location
208-1	0.050	A	RT	144	131	117	42.5	11.5	Parent Metal
208-2	0.050	A	RT	145	131	120	40.5	13.0	Parent Metal
263-1	0.060	B	RT	135	125	119	40.5	13.0	Parent Metal
263-2	0.060	B	RT	137	125	119	40.0	14.0	Parent Metal
269-A	0.048	A	600	104	84	77	45.2	15.7	Parent Metal
267-A	0.048	B	600	104	83	79	48.9	16.8	Parent Metal
263-B	0.048	A	800	94	78	64	60.7	18.5	Parent Metal
267-B	0.048	B	800	94	76	66	62.3	16.4	Parent Metal
GE Spec C50TF12-S2			RT	130	120		25.0	10.0	

Notched and Radius Bar Spec. No.	Total Upset (Inch)	Heat Treat Cycle	Test Temp (°F)	Notch K_t	UTS (ksi)	Failure Location	NTS/UTS
269-C	0.048	A	RT	3.2	182	Notch	1.26
267-C	0.048	B	RT	3.2	179	Notch	1.31
269-D	0.048	A	600	3.2	132	Parent Metal	1.27
267-D	0.048	B	600	3.2	124	Notch	1.19
269-E	0.048	A	800	3.2	124	Parent Metal	1.31
267-E	0.048	B	800	3.2	124	Parent Metal	1.32
289-B	0.055	A	RT	Radius	163	Weld	-
282-B	0.050	B	RT	Radius	169	Weld	-

Heat Treat Cycles:

A - 1300°F/2 hr/AC + Weld + Test

B - 1300°F/2 hr/AC + Weld + 1750°F/1 hr/WQ + 1300°F/2 hr/AC + Test

TABLE VII

STRESS-RUPTURE PROPERTIES OF INERTIA WELDED INCONEL 718

Spec. No.	Total Upset (Inch)	Test Temp. (°F)	Notch K_t	Stress (ksi)	Life (hrs)	R.A. (%)
13	.220	1000		140	168.73	11.2
19	.083	1000		140	12.60	7.5
6	.220	1200		100	0.29	9.7
20	.083	1200		90	3.80	4.9
21	.220	1300		90	1.05	7.3
22	.083	1300		80	F.O.L.	6.2
10	.220	1200	2.0	100	4.71	-
30	.083	1200	2.0	100	14.58	-
GE Spec B50TF15		1200		100	25.00	-

Heat Treat Cycle: 1775°F/1 hr/AC + 1325°F/8 hr/FC to 1150°F @ 100°F per hr. + 1150°F/ 8 hr/AC + weld + 1325°F/8 hr/FC to 1150°F @ 100°F per hr + 1150°F/ 8 hr/AC + 1250°F/64 hr/AC + test.

TABLE VIII

STRESS-RUPTURE PROPERTIES OF INERTIA WELDED U-700

Spec. No.	Total Upset (inch)	Temp. (°F)	Notch K_t	Stress (ksi)	Life (hrs)	R.A. (%)	Failure Location
8-108-1	0.171	1200	--	120	F.O.L.	5.0	Parent metal
8-110-1	0.120	1200	--	120	618.5	--	Removed - no failure
8-108-3	0.171	1400	--	85	0.7	5.0	Parent metal
8-110-2	0.120	1400	--	70	80.3	6.5	Weld zone
8-109-1	0.114	1400	3.2	85	325.9	--	Notch
8-109-2	0.114	1400	3.2	85	1.9	--	Away from notch
8-110-3	0.120	1500	--	50	23.8	2.5	Weld zone
8-110-4	0.120	1500	--	55	6.9	5.6	Parent metal
GE-C50TF3-S3 Specification		1400	--	85	30.0		

Note:

Heat Treat Cycle: As received + weld + 2100°F/4 hr/salt quench at 1000°F/AC + 1600°F/8 hr/AC + 1800°F/4 hr/AC + 1200°F/24 hr/AC + 1400°F/8 hr/AC + test

TABLE IX

STRESS-RUPTURE PROPERTIES OF INERTIA WELDED Ti 6Al-4V

Spec. No.	Total Upset (Inch)	Heat Treat Cycle	Test Temp (°F)	Notch K_t	Stress (ksi)	Life (hrs)	Remarks
288-A	0.054	A	RT	3.4	155	5.1	-------
264-A	0.055	B	RT	3.4	160	6.0	-------
288-A	0.054	A	600	3.4	120	49.9	Removed - No failure
264-B	0.055	B	600	3.4	120	49.9	Removed - No failure
286-1	0.050	A	800	3.4	115	FOL	-------
282-A	0.050	B	800	3.4	115	0.4	-------
GE Spec C50TF12			RT	—	170	5.0	-------

Heat Treat Cycles: A -1300°F/2 hr/AC + Weld + Test

B -1300°F/2 hr/AC + Weld + 1750°F/1 hr/W.Q. + 1300°F/2 hr/AC + Test

TABLE X

CYCLIC RUPTURE PROPERTIES OF INERTIA WELDED INCONEL 718, UDIMET-700 AND Ti 6A1-4V

Spec. No.	Total Upset (Inch)	Material	Heat Treat Cycle	Test Temp. (°F)	Notch K_t	Stress (ksi)	Life (hrs)	Cycles	Remarks
8	0.220	IN 718	E	1000	2.0	100	183.4	6,008	Failed
28	0.083	IN 718	E	1000	2.0	95	146.1	4,780	Failed
9	0.220	IN 718	E	1200	2.0	75	235.2	7,700	Failed
29	0.083	IN 718	E	1200	2.0	65	14.3	468	Failed
1 PM	-	IN 718	E	1000	2.0	100	1113.2	36,500	Removed
2 PM	-	IN 718	E	1200	2.0	80	1113.2	36,500	Removed
8-106	0.047	Ti 6-4	B	600	3.2	95	70.7	232	Failed
289-A	0.055	Ti 6-4	A	600	3.2	95	60.7	199	Failed
8-108-4	0.114	U-700	D	1400	2.0	80	554.0	18,116	Notch Failure
8-109-3	0.114	U-700	D	1400	2.0	95	27.7	906	Notch Failure
8-53-1	0.094	U-700	C	1400	2.0	80	-	-	Failed in Quench Crack
8-53-2	0.094	U-700	C	1400	2.0	70	-	-	Failed in Quench Crack

Test Cycle: 10 sec. load to stress - 90 sec. hold at stress - 10 sec. unload

Heat Treat Cycles:

A - 1300°F/2 hr/AC + Weld + 1750°F/1 hr/WQ + 1300°F/2 hr/AC + Test

B - 1300°F/2 hr/[illegible] + Weld + Test

C - 2100°F/4 hr/Oil Quench + Weld + 2100°F/4 hr/Salt Quench @ 1000°F/AC + 1600°F/8 hr/AC + 1800°F/4 hr/AC + 1200°F/24 hr/AC + 1400°F/8 hr/AC + Test

D - As received + Weld + 2100°F/4 hr/Salt Quench @ 1000°F/AC + 1600°F/8 hr/AC + 1800°F/4 hr/AC + 1200°F/24 hr/AC + 1400°F/8 hr/AC + Test

E - 1775°F/1 hr/AC + 1325°F/8 hr/FC to 1150°F @ 100°F/hr + 1150°F/8 hr/AC + Weld + 1325°F/8 hr/FC to 1150°F @ 100°F/hr + 1150°F/8 hr/AC + 1250°F/64 hr/AC + Test

TABLE XI

ROOM TEMPERATURE ROTATING BEAM FATIGUE PROPERTIES OF INERTIA WELDED INCONEL 718, UDIMET-700 AND Ti 6A1-4V

Spec. No.	Total Upset (Inch)	Material	Heat Treat Cycle	Stress (ksi)	Life (hrs)	Life (cycles)	Remarks
2-1 PM	-	Inconel 718	D	90	7.50	4.5×10^6	Failed
8-111-1	0.093	Inconel 718	D	90	45.92	2.9×10^7	Run out - step loaded to 96 ksi
8-111-1	0.093	Inconel 718	D	96	32.0	2.0×10^7	Failed
8-111-2	0.093	Inconel 718	D	98	0.78	4.8×10^5	Failed in HAZ
287-1	0.054	Ti 6A1-4V	A	38	47.40	3.0×10^7	Run out
8-98	0.060	Ti 6A1-4V	B	100	0.14	7.3×10^4	Failed in HAZ
8-53-1-B	0.094	U-700	C	75	8.15	5.1×10^6	Failed in HAZ
8-53-1-A	0.094	U-700	C	80	0.59	3.5×10^5	Failed in HAZ

Heat Treat Cycles:

A - 1300°F/2 hr/AC + Weld + Test

B - 1300°F/2 hr/AC + Weld + 1750°F/1 hr/WQ + 1300°F/2 hr/AC + Test

C - 2100°F/4 hr/Salt Quench @ 1000°F/AC + 1600°F/8 hr/AC + 1800°F/4 hr/AC + 1200°F/24 hr/AC + 1400°F/8 hr/AC + Test

D - 1775°F/1 hr/AC + 1325°F/8 hr/FC to 1150°F @ 100°F/hr + 1150°F/8 hr/AC + Weld + 1325°F/8 hr/FC to 1150°F @ 100°F/hr + 1150°F/8 hr/AC + 1250°F/64 hr/AC + Test

TABLE XII

PARAMETERS OF INERTIA WELDING STUDY OF 4-INCH DIAMETER SAMPLES OF INCO 718

Sample Nos.	Flywheel WK^2 ($Lb.Ft^2$)	Max. Speed (RPM)	Ram Load ($Lbsx10^3$)	Max Unit Energy ($Ft-Lbsx10^3/in^2$)	Weld Time (Sec)	Upset Total (Inch)	Surface Speed (SFM)	Maximum Pressure ($PSIx10^3$)	Measured Torque ($Ft-Lbsx10^3$)	Unit Torque ($Ft-Lbsx10^3/in^2$)	Calculated Percent Efficiency	Actual Unit Energy ($Ft-Lbsx10^3/in^2$)	Remarks
							.073 to .093 Inch Wall						
21-22	59.7	1127	57.8	12.8	0.60	.031	1141	37.5	2.89	2.88	85.5	11.0	
1-4	59.7	1315	55.5	17.5	0.73	.113	1345	35.2	2.78	2.76	84.6	14.80	Interface overheated
24-2	59.7	1310	61.9	15.5	0.72	.087	1326	55.0	2.72	2.42	84.6	13.1	Interface overheated
23-6	99.7	1485	18.6	41.8	2.70	.117	1522	20.8	1.18	1.32	72.1	30.0	Interface overheated
3-26	99.7	1315	18.6	32.7	2.55	.033	1348	20.7	1.63	1.81	76.1	24.9	
							.100 Inch Wall						
2-22	59.7	1695	20.95	23.7	1.7	.014	744	25.7	1.79	1.42	76.0	-	Pilot galled in bushing
3-23	59.7	1878	46.6	28.5	1.43	.076	1909	37.3	2.54	2.02	76.5	21.8	Interface overheated
7-27	59.7	1730	45.0	24.1	1.55	.087	1756	36.1	2.54	2.02	78.6	19.0	Interface overheated
6-26	59.7	1525	44.8	19.0	1.3	.031	1557	35.4	2.26	1.80	81.0	15.4	
1-21	59.7	1650	51.0	22.0	1.23	.087	1685	39.8	2.60	2.06	80.9	17.8	Interface overheated
5-25	59.7	1455	56.0	17.3	1.02	.058	1486	45.1	2.86	2.27	83.1	14.3	
4-24	59.7	1486	61.2	17.9	1.02	.079	1506	50.3	2.80	2.22	82.5	14.8	
							.25 Inch Wall						
10-30	99.7	1938	116.0	21.5	2.15	.006	1905	39.1	3.96	1.34	84.4	18.1	
13-33	134.7	1820	128.5	25.6	2.6	.020	1787	43.4	4.20	1.42	86.9	22.2	
11-31	134.7	1810	139.0	26.1	2.38	.025	1780	46.9	4.24	1.44	87.8	22.9	
9-29	174.7	1730	135.0	30.0	3.1	.084	1699	45.5	4.63	1.57	86.5	26.0	
12-32	174.7	1860	129.5	34.7	3.6	.115	1826	43.7	4.18	1.42	85.0	29.4	
8-28	174.7	1955	138.0	38.5	3.14	.155	1920	46.7	4.53	1.53	86.0	33.1	
							.375 Inch Wall						
18-38	359.7	1860	137.0	49.4	7.35	.084	1765	31.9	6.03	1.41	84.0	41.5	
16-36	359.7	1975	127.6	55.7	8.4	.113	1875	29.8	5.42	1.27	81.7	45.5	
17-37	359.7	2055	126.2	60.3	5.9	.020	1951	29.4	6.67	1.56	86.7	-	Pilot stuck in bushing
19-39	359.7	2065	134.0	61.0	9.00	.134	1959	31.3	5.70	1.33	80.9	49.4	
14-34	359.7	2180	160.0	68.0	6.15	.056	2069	37.4	5.95	1.39	86.1	-	Pilot stuck in bushing
15-35	584.7	1750	102.0	70.5	13.0	.145	1680	23.7	5.35	1.25	78.8	55.6	
20-40	584.7	1750	80.0	70.8	14.0	.068	1661	18.6	5.60	1.31	73.3	52.0	

All welds made on Model 250 Inertia Welder.

TABLE XIII

WELDING PARAMETERS AND RESULTS FOR 12 AND 24 INCH OD INCONEL 718 TEST RINGS[1]

Run No.	Sample Nos.	Weld Speed (RPM)	Weld Speed (SFM)	Upset Speed (RPM)	Upset Speed (SFM)	Weld Pressure (PSI x 10^3)	Upset Pressure (PSI x 10^3)	Weld Time (Sec.)	Max. Energy (Ft-Lbs x 10^3/in^2)	Total Upset (Inch)	Total Indicated Run Out Face (Inch)	Total Indicated Run Out Dia (Inch)	Remarks
							12 Inch O.D. x 0.100/0.115 Inch Wall						
400-B-13	15-33	148	461	-	-	32.2	-	1.4	26.9	0.137	0.003	0.016	Smooth Adherent Flash
400-B-14	13-32	149	464	-	-	36.0	-	2.0	26.3	0.102	0.002	0.007	Smooth Adherent Flash
400-B-15	14-35	167	520	-	-	36.0	-	2.6	33.8	0.189	0.002	0.025	Smooth Adherent Flash
400-B-16	3-34	149	464	-	-	35.8	-	2.0	26.1	0.100	0.001	0.025	Smooth Adherent Flash
							24 Inch O.D. x 0.100/0.115 Inch Wall						
400-B-9	23-31	280	1755	-	-	32.0	-	-	49.4	0.187	0.010	0.043	Rough Non-Adherent Flash
400-B-17	21-22	209	1305	-	-	32.8	-	1.8	36.2	0.126	0.003	0.021	Rough Non-Adherent Flash
400-B-19	10-25	180	1124	-	-	31.4	-	1.4	19.0	0.045	0.008	0.036	Low Upset - Little Flash
400-B-26	1-2	201	1260	-	-	36.1	-	1.9	25.1	0.154	0.002	0.042	Equal (0.100 Inch)Walls-Flash Ejection
							24 Inch O.D. x 0.150 0.165 Inch wall						
400-B-10	18-28	280	1755	-	-	41.2	-	-	31.7	0.040	0.008	0.029	Low Upset - Little Flash
400-B-20	19-29	254	1583	-	-	35.3	-	2.2	25.9	0.121	0.005	0.029	Flash Ejection
400-B-22	16-26	224	1396	-	-	39.8	-	1.6	19.7	0.066	0.009	0.042	Intermittent Rough Flash
400-B-28	20-30	312	1960	80	498	15.9	41.0	5.4	39.1	0.158	0.002	0.054	Equal (0.150 Inch)Walls-Flash Ejection
							24 Inch O.D. x 0.180 0.200 Inch Wall						
400-B-29	11-18	298	1855	121	753	21.7	47.0	3.6	33.6	0.088	0.002	0.023	Smooth Adherent Flash
400-B-31	22-23	286	1790	113	708	20.6	41.6	3.8	27.-	0.081	0.006	0.033	Intermittent Rough Flash
400-B-32	10-19	294	1830	118	734	21.1	42.2	3.7	30.6	0.062	0.009	0.031	Rough Flash in One Area
400-B-33	16-21	316	1970	95	592	25.0	44.-	4.1	32.2	0.100	0.004	0.062	Bad Mismatch - Flash Sheared Off

[1]All welds made on Model 400 Inertia Welder with flywheel WK^2 = 26038 lb-ft^2

TABLE XIV

WELDING PARAMETERS AND RESULTS FOR 12 AND 24 INCH OD INCONEL 718 TEST DISKS[1]

Run No.	Sample Nos.	Weld Speed (RPM) (SFM)	Weld Pressure (PSI x 10^3)	Weld Time (Sec.)	Max. Energy (ft.-lbs x 10^3 in^2)	Total Upset (Inch)	Total Indicated Run Out Face (Inch)	Dia. (Inch)	Remarks
				12 Inch O.D. x 0.180/0.200 Inch Wall					
400-8-37	13-32	263 826	37.5	-	42.5	0.106	0.007	0.008	No overheating; smooth flash curls; steel pilot scored cast iron bushing
400-8-38	4-14	263 826	39.3		44.7	0.158	0.0035	0.013	No overheating; smooth flash curls; Mo coated pilot-br ss bushing-no scoring
400-9-2	3-35	259 815	37.8	4.6	42.6	0.146	0.003	0.006	No overheating; smooth flash curls; pilot and bushing same as Run 400-8-38.
400-9-3	15-34	247 777	38.7	4.3	39.5	0.111	0.001	0.0045	Same remarks as Run 400-9-2
400-9-24	12-33	246 773	40.8	3.9	39.5	0.123	0.000	0.004	Same remarks as Run 400-9-2
				24 Inch O.D. x 0.180/0.200 Inch Wall					
400-8-34	28-31	307 1915	36.9	3.0	31.2	0.003	0.002	0.017	Electronic Control inoperative-contact RPM estimated-brass bushing scored
400-8-35	24-26	350 2190	19.4	3.0	39.7	0.005	0.002	0.012	Electronic Control inoperative-two step weld-upset pressure applied after zero RPM
400-8-36	25-27	346 2170	38.0	3.1	38.6	0.066	0.012	0.030	Two step weld-no overheating, steel pilot scored b ass bushing
400-8-39	16-21	330 2050	38.9	3.4	35.7	0.152	0.005	0.019	Very hot short
400-8-40	1-2	310 1925	38.8	3.6	32.0	0.127	0.011	0.0145	Hot short
400-8-41	30-30	288 1810	38.8	3.5	27.3	0.122	0.0115	0.0145	Hot short
400-8-42	11-19	274 1710	39.5	3.8	25.0	0.068	0.005	0.035	No overheating-smooth flash
400-9-1	24-26	296 1858	38.5	3.2	28.4	0.109	0.008	0.026	Two step weld-hot short when upset pressure applied at 130 RPM
400-9-4	22-25	278 1745	38.3	3.8	24.9	0.090	0.005	0.034	Very hot short
400-9-5	1-29	294 1845	37.8	3.9	27.7	0.088	0.002	0.040	Two step weld-hot short when upset pressure applied at 125 RPM
400-9-6	17-31	257 1600	38.5	-	21.5	0.040	0.009	0.018	Test disks machined flat and parallel within 0.002 inch. No overheating
400-9-7	10-18	273 1695	39.9	3.8	25.0	0.077	0.0025	0.021	Same remarks as Run 400-9-6
400-9-8	26-27	277 1735	39.5	3.8	25.0	0.103	0.006	0.018	Test disks machined flat and parallel within 0.002 in. No overheating
400-9-9	16-21	273 1695	40.2	3.8	25.0	0.096	0.008	0.018	Same remarks as Run 400-9-8
400-9-10	23-28	266 1655	39.4	3.6	23.0	0.073	0.004	0.016	Same remarks as Run 400-9-6

[1]All welds made on Model 400 Inertia Welder with Flywheel Wk^2 = 26,038 lb-ft^2

TABLE XV

TENSILE PROPERTIES OF INCONEL 718 CROSS ROLLED PLATE

Specimen No.	Temp (°F)	0.02% Y.S. (ksi)	0.2% Y.S. (ksi)	U.T.S. (ksi)	R.A. (%)	El (%)
1	RT	108.4	129.6	173.0	49.3	35.0
2	800	89.0	107.6	146.2	50.0	32.4
3	1000	89.4	100.3	136.2	51.7	30.6
4	1200	80.5	96.5	132.3	42.0	27.9
9	1200	-	104.2	NB	5.2	11.3
10	1200	-	106.4	NB	5.08	10.7
11	RT	128.0	147.8	189.5	45.5	28.5
12	800	126.0	143.2	153.3	46.6	25.0
13	1000	108.4	123.0	151.2	46.3	23.4
14	1200	100.5	118.3	143.0	29.3	12.3
19	1200	-	125.2	NB	5.8	10.7
20	1200	-	118.5	NB	7.2	12.6
21	RT	40.0	50.6	118.0	59.7	66.4
22	1000	72.5	91.7	120.5	46.9	24.9
23	1200	84.0	100.0	125.0	46.9	20.3
27	RT	115.2	145.8	163.5	48.0	15.7
28	1000	111.1	113.2	134.3	39.8	16.9
29	1200	94.3	119.3	140.4	35.0	12.3
33	RT	101.8	131.9	133.8	55.4	18.7
34	1000	101.5	110.8	129.1	50.6	20.6
38	RT	164.8	196.8	202.0	43.8	10.0
43	1000	-	-	181.0	26.1	7.0
45	RT	66.8	87.0	130.0	60.8	45.6
46	800	86.0	101.4	123.0	50.0	29.8
47	1000	38.3	43.0	95.2	58.6	64.7
48	1200	64.1	83.0	111.0	44.5	34.8
53	1200	-	81.25	NB	5.7	5.1
54	1200	-	62.90	NB	8.9	9.3

Specimen Condition:

#1 → 10 As Received + 1200°F/64 hr./AC
#11 → 20 As Received + 1200°F/200 hr./AC
#21 → 26 As Received + 2000°F/1 hr./AC + 17% Red + 2000°F/1 hr./AC + 20% Red + 2000°F/ 1 hr./AC + 20% Red.
#27 → 32 As Received + 2000°F/1 hr./AC + 25% Red + 2000°F/1 hr./AC + 20% Red
#33 → 38 As Received + 25% Red
#39 → 44 As Received + 57% Red
#45 → 54 As Received

TABLE XVI

TENSILE PROPERTIES OF INCONEL 718 CROSS ROLLED PLATE
AGED AT 1250°F FOR 64 HOURS

	(R.T.)				(1000°F)			
	A	B	C	D	A	B	C	D
U.T.S. (ksi)	189	203	204	198	168	183	186.5	161
.2% YS (ksi)	157.5	156	158	168	131	136	139	140
.02% YS (ksi)	137	130	142	139	115	119	118	123
El (%)	22.1	17.0	17.7	20	18.1	13.4	15.7	20
R.A. (%)	41.5	25.4	26.4	35	43.8	25.4	25.2	41.5

(A) - 1850°F/90 Min/AC - (2 cycles) + 1850°F/90 min/AC + 1800°F/1 hr/AC +1325°F/8 hr/FC - 100°F/hr to 1150°F + 1150°F/8 hr/AC + 1250°F/64 hr/AC

(B) - As Received + 25% Red + 1800°F/1 hr/AC + 1325°F/8 hr/FC - 100°F/hr to 1150°F + 1150°F/8 hr/AC + 1250°F/64 hr/AC

(C) - As Received + 57% Red + 1800°F/1 hr/AC +1325°F/8 hr/FC - 100°F/hr to 1150°F + 1150°F/8 hr/AC + 1250°F/64 hr/AC

(D) - DATA BOOK Inco 718 - 1800°F/1 hr/AC + 1325°F/8 hr/FC - 100°F/hr to 1150°F + 1150°F/8 hr/AC

TABLE XVII

TENSILE PROPERTIES OF COLD WORKED INCONEL 718 CROSS ROLLED PLATE

Tensile Data - From Disk Web. 0.25 Inch Dia. Gauge

	Smooth Bar						Notched Bar K_t = 2.5		
Specimen No.	Temp (°F)	Uts (ksi)	.2%Y.S. (ksi)	.02% Y.S. (ksi)	El (%)	R.A. (%)	S/N	Temp (°F)	Uts (Ksi)
5	R.T.	188	156	134	22.4	41.7	20	R.T.	270
6	R.T.	190	159	140	21.9	41.4	21	R.T.	273
7	800	162	137	116	18.2	43.6	23	800	230
15	800	165	138	122	22.9	42.2	24	800	232
2	1000	157	130	113	19.4	45.1	22	1000	222
8	1000	159	133	118	16.8	42.5	26	1000	224
1	1200	152	126	107	13.2	22.8	19	1200	212
3	1200	153	130	112	11.9	19.9	25	1200	233
16	1300	133	120	102	5.3	13.3	27	1300	195
17	1300	144	126	110	6.3	14.1	28	1300	186

Tensile Data - From Disk Rim - 0.16 Inch Dia. Gauge

	Smooth Bar						Notched Bar K_t = 2.5		
1	R.T.	198	152	137	21.7	40.4	9	R.T.	280
2	800	166	138	120	21.5	41.4	10	800	238
3	1000	172	140	123	18.0	34.4	11	1000	234
4	1200	155	131	113	10.8	17.0	12	1200	222
5	1300	139	127	110	7.3	11.1	13	1300	182
GE Spec.	R.T.	185	150	-	12.0	15.0			
(MIN.)	1200	145	125	-	12.0	18.0			

Processing History. 1850°F/90 min/AC + Cold Work Rim + 1850°F/90 min/AC + Finish Form Rim + 1850°F/90 min/AC + 1800°F/1 hr/AC + 1325°F/8 hr/FC - 100°F/hr to 1150°F + 1150°F/8 hr/AC + 1250°F/64 hr/AC.

TABLE XVIII

STRESS RUPTURE PROPERTIES OF COLD WORKED INCONEL 718 CROSS ROLLED PLATE

Temp (°F)	Stress (ksi)	Rupture Life (hr)	R.A. (%)	El (%)	Remarks
1000	150	126.3	9.4	6.5	1/4" dia from Web
1000	150	55.0	8.7	5.3	" " " "
1100	125	372.8	8.7	4.0	" " " "
1100	125	113.8	6.4	3.1	" " " "
1200	100	66.7	8.5	2.5	" " " "
1200	100	165.0	10.0	4.5	" " " "
1300	75	240.1	14.0	7.3	" " " "
1300	75	228.4	13.4	6.0	" " " "
1000	150	75.9	6.2	4.3	1/8" dia from Rim
1100	125	1.1	Failed in Threads		" " " "
1200	100	1.05	Premature Failure at Pre-existing Crack		" " " "
1000	150	77.69	28.2	8.9	" " " "
1000	150	16.01	7.65	10.3	" " " " (Broke in Threads)
1100	125	94.55	15.8	3.2	" " " "
1100	125	3.30	1.27	2.8	" " " " (Broke in Threads)
1200	100	16.32	5.0	1.8	" " " " (Broke in Threads)
1200	100	86.94	12.2	4.2	" " " "
1300	75	144.73	15.8	5.7	" " " "
1300	75	0.48	1.27	1.2	" " " " (Broke in Threads
GE Spec Min					
1200	100	25.0	-	5.0	

TABLE XIX

CYCLIC RUPTURE PROPERTIES - COLD WORKED INCONEL 718 CROSS ROLLED PLATE

10-90-10 Cycle

Specimen Configuration I

Rim Section $K_t = 2.0$

Temp (°F)	Stress (ksi)	Life (hrs)	Life (cycles)
1000	150	71.58	2,331
1000	100	1144.73	36,800
1200	100	4.84	142
1200	90	1318.25	43,977

Specimen Configuration II

Web Section $K_t = 2.0$

Temp (°F)	Stress (ksi)	Life (hrs)	Life (cycles)
1000	150	32.70	1,221
1000	100	353.00	11,624
1000	80	17.35	522
1200	125	1.97	65
1200	100	16.00	587
1200	80	911.50	27,547

Specimen Configuration II

Web Section $K_t = 3.0$

Temp (°F)	Stress (ksi)	Life (hrs)	Life (cycles)
1000	150	15.66	511
1000	100	76.57	2,671
1200	90	4.04	128
1200	70	34.40	1,135

TABLE XX

ROTATING BEAM FATIGUE PROPERTIES - COLD WORKED INCONEL 718 CROSS ROLLED PLATE

Rotating Beam Fatigue - Room Temperature - A = °°

Stress (ksi)	Cycles To Failure
130	27,900
100	120,000
80	267,000
60	1,093,000
55	2,183,000
50	45,370,000 (Ran Out)

TABLE XXI

COMPARISON OF TENSILE PROPERTIES OF DOUBLE AND SINGLE AGED INCONEL 718

Smooth Bar											Notched Bar (K_t = 2.5)		
Temp. (°F)	UTS (ksi) Double	UTS (ksi) Single	0.2%YS (ksi) Double	0.2%YS (ksi) Single	0.02%YS (ksi) Double	0.02%YS (ksi) Single	El.(%) Double	El.(%) Single	RA.(%) Double	RA.(%) Single	Temp. (°F)	UTS (ksi) Double	UTS (ksi) Single
RT	193	188	163	156	138	134	20.2	22.4	41.0	41.7	RT	240	270
RT		190		159		140		21.9		41.4	RT		273
800	169	162	143	137	121	116	17.6	18.2	42.2	43.6	800	204	230
800		165		138		122		22.9		42.2	800		232
1000	162	157	137	130	118	113	18.7	19.4	30.5	45.1	1000	203	222
1000		159		133		118		16.8		42.5	1000		224
1200	157	152	135	126	116	107	13.7	13.2	21.8	22.8	1200	190	212
1200		153		130		112		11.9		19.9	1200		233
1300	133	133	122	120	108	102	6.0	5.3	13.8	13.3	1300	165	195
1300		144		126		110		6.3		14.1	1300		186

Heat Treat History: Double Age - 1850°F/90 min/AC + 1900°F/90 min/AC + 1800°F/1 hr/AC + 1325°F/8 hr/FC-100°F/hr to 1150°F + 1150°F/8 hr/AC + 1325°F/8 hr/FC-100°F/hr to 1150°F + 1150°F/8 hr/AC.

Single Age - 1850°F/90 min/AC (3 cycles) + 1800°F/1 hr/AC + 1325°F/8 hr/FC-100°F/hr to 1150°F + 1150°F/8 hr/AC + 1250°F/64 hr/AC.

TABLE XXII

COMPARISON OF SINGLE AND DOUBLE AGED INCONEL 718 STRESS-RUPTURE PROPERTIES

Temp. (°F)	Stress (ksi)	Rupture Life (hrs) Double	Rupture Life (hrs) Single	R.A. (%) Double	R.A. (%) Single	El. (%) Double	El. (%) Single	Remarks
1000	150	111.1	126.3	16.0	9.4	4.6	6.5	
1000	150		55.0		8.7		5.3	
1100	125	25.3	372.8		8.7		4.0	Thread break - double
1100	125		113.8		6.4		3.1	
1200	100	255.4	66.7	10.9	8.5	4.2	2.5	
1200	100		165.0		10.0		4.5	
1300	75	1.3	240.1		14.0		7.3	Thread break - double
1300	75		228.4		13.4		6.0	

Heat Treat History: Double Age - 1850°F/90 min/AC + 1900°F/90 min/AC + 1800°F/1 hr/AC + 1325°F/8 hr/FC-100°F/hr to 1150°F + 1150°F/8 hr/AC + 1325°F/8 hr/FC-100°F/hr to 1150°F + 1150°F/8 hr/AC.

Single Age - 1850°F/90 min/AC (3 cycles) + 1800°F/1 hr/AC + 1325°F/8 hr/FC-100°F/hr to 1150°F + 1150°F/8 hr/AC + 1250°F/64 hr/AC.

TABLE XXIII

COMPARISON OF CYCLIC RUPTURE PROPERTIES OF DOUBLE AND SINGLE AGED INCONEL 718

Temp. (°F)	Stress, (ksi)		Life, (hrs)		Life, (cycles)	
	Double	Single	Double	Single	Double	Single
1000	150	150	106.47	32.7	1260(1)	1221
1200	100	100	6.70	16.0	192	587
1200	90	80	7.64	911.5	253	27547

(1) Low number of cycles due to malfunction in test stand cycling mechanism.

Heat Treat History: Double Age - 1850°F/90 min/AC + 1900°F/90 min/AC + 1800°F/1 hr/AC + 1325°F/8 hr/FC-100°F/hr to 1150°F + 1150°F/8 hr/AC + 1325°F/8 hr/FC-100°F/hr to 1150°F + 1150°F/8 hr/AC.

Single Age - 1850°F/90 min/AC (3 cycles) + 1800°F/1 hr/AC + 1325°F/8 hr/FC-100°F/hr to 1150°F + 1150°F/8 hr/AC + 1250°F/64 hr/AC.

TABLE XXIV

MILD STEEL COMPONENT PROCESS DEVELOPMENT

Part No.	Process Sequence and Pertinent Results
1, 2, 3, 4	Split only - these components were used during the development of set up procedures for control of the mainslides during forming. Since the machine is designed for forming while the mainslides are moving axially, the initial attempts to control the axial location of the "split" were not successful.
5	Split (groove diameter oversize, cross slide feed rate incorrect - 1"/minute too slow). Angle operation (25°) attempted after split to develop technique for Stage 16 configuration.
6	Split (groove diameter correct, cross slide feed rate incorrect - machine vibrated severely during run), stress relieve, spread, finish (good Stage 15 configuration), later angle (25°) operation for Stage 16 resulted in undersize diameter.
7	Spread (no split) - severe laminations - machine vibration - determined that cannot split with the "spread" rings.
8	Split, spread, finish (surface failures), stress relieve, finish, angle (developed "pinching" technique).
9	Split, stress relieve, angle (15°, part envelope incorrect).
10	Split (groove diameter good), stress relieve, spread, finish (acceptable Stage 15 configuration without angle hit).
11	Split, stress relieve, spread, finish (acceptable Stage 15 configuration), angle (25°, good stage 14 envelope).
12	Split, stress relieve, finish (oversize - can not eliminate spread operation).
13	Split, stress relieve, spread, finish, angle (good Stage 16 configuration).
14	Split (tool ring failed during run, part had severe surface laminations), stress relieve, spread, finish, angle (good Stage 14 component).
15	Split (tool ring failed during run, severe laminations), finish (oversize), stress relieve, finish (good Stage 15), angle (25°, good Stage 16).

TABLE XXV

INCONEL 718 PROCESS DEVELOPMENT RESULTS (continued)

Part No.	Stage Configuration	Groove Diameter (inch)	Results
1	--	23.350	Groove diameter undersize after Split-Spread hit no crack failures. Finish hit without solution treatment, propogated light surface cracks, used to develop proper machine settings for remaining parts, later destroyed for metallurgical evaluation.
2	16	23.480	Groove .050" off part centerline, no surface failures. Selected for rotor fabrication.
3	15	23.460	Groove .030" off centerline, no surface failures. Selected for rotor fabrication.
4	15	23.460	Groove .025" off centerline, no surface failures. Selected for rotor fabrication.
5	16	23.475	Groove .020" off centerline, .030" grindout required to remove surface failures. Selected for rotor fabrication.
6	15	23.455	Groove .015" off centerline, no surface failures, best of entire lot of components dimensionally. Selected for rotor fabrication.
7	16	23.435	Part .706" thick, status marginal since removal of surface defects nearly violates part envelope. Selected for rotor fabrication.
8	--	--	Part cracked severely during Split-Spread operation, used for metallurgical evaluation, resulting in discovery of improper solution treatment.

TABLE XXV

INCONEL 718 PROCESS DEVELOPMENT RESULTS (concluded)

Part No.	Stage Configuration	Groove Diameter (inch)	Results
9	--	--	Split only, severe surface failures.
10	16	23.425	Part had cracks after Split operation, failures removed, stage 16 envelope maintained. Selected for rotor fabrication.
11	14	23.430	Light surface cracks after Split-Spread, defects removed. Selected for rotor fabrication.
12	14	23.430	Severe cracks during Split-Spread resulted in part being scrapped for part envelope violations.
13	14	--	Part failed during Split-Spread operation, violating part envelope.

TABLE XXVI

COLD FORM PARAMETERS -- 42 INCH X 50 INCH CINCINNATI HYDROSPIN

Cross Slide Feed Rate (All passes): 2 Inches/minute

Spindle Speed (All passes): 160 RPM

Part Configuration	Pass	Mainslide Gap (inch)	Cross Slide Stop Setting (inch)
14 (.855 Inch thick)	Split	1.305	19.315
15, 16 (.750 Inch thick)	Split	1.250	19.315
14	Spread	1.305	19.315
15, 16	Spread	1.250	19.315
14	Finish	1.305	19.200
15, 16	Finish	1.250	19.225
14	Angle (Fwd. Flange)	1.515	19.290
14	Angle (Aft Flange)	1.515	19.390
15	Angle	1.415	19.390
16	Angle (Fwd. Flange)	1.415	19.390
16	Angle (Aft Flange)	1.515	19.065

TABLE XXVII

CERTIFICATE OF CHEMICAL ANALYSIS INCONEL 718 CROSS ROLLED PLATE

Elements	Heat No. K67483K12	GE Spec. Range
Carbon	0.050	0.02 - 0.08
Manganese	0.080	0.35 Max.
Silicon	0.250	0.35 Max.
Chromium	17.82	17.00 - 21.00
Nickel	53.87	50.00 - 55.00
Cobalt	0.11	1.00 Max.
Iron	Bal.	16.50 - 20.50
Molybdenum	3.03	2.80 - 3.30
Titanium	1.03	0.75 - 1.15
Aluminum	0.47	0.30 - 0.70
Boron	0.005	0.006 Max.
Zirconium	0.01	-------
Sulfur	0.010	0.015 Max.
Columbium	5.33	4.75 - 5.50
Copper	<0.05	0.30 Max.
Phosphorous	0.002	0.015 Max.

TABLE XXVIII

CERTIFICATE OF TEST MECHANICAL PROPERTIES [1] INCONEL 718 CROSS ROLLED PLATE

Material[2]	Test Temp. (°F)	UTS (ksi)	0.2% YS (ksi)	%EL	%RA	Stress (ksi)	Life (hr)	%EL
Ht K67483K12	R.T.	200.4	179.3	19.6	41.8			
"	R.T.	194.5	171.5	19.2	38.0			
"	1200	158.4	140.6	12.5	18.9	100.0	69.0	5.6
"	1200	165.2	142.3	12.0	20.5	100.0	67.6	8.9
GE Spec.	R.T.	185.0	150.0	12.0	15.0			
C50TF6	1200	145.0	125.0	12.0	18.0	100.0	25.0	5.0

[1] Duplicate test results at R.T. and 1200°F represent test specimens removed from the plate parallel and transverse to the final direction of rolling.

[2] Material tested in heat treated condition: 1750° - 1800°F/1 hr./AC + 1325°F/8 hr./FC -100°F/hr. to 1150°F + 1150°F/8 hr./AC

TABLE XXIX

INCONEL 718 COLD FORM PARAMETERS - 42 INCH X 50 INCH CINCINNATI HYDROSPIN

Cross Slide Feed Rate (All passes): 2 Inch/minute

Spindle Speed (All passes): 160 RPM

Part Configuration	Pass	Mainslide Gap (inch)		Cross Slide Stop Setting (inch)	
		Front	Rear	Front	Rear
14-15	Split	1.425	1.495	18.073	17.948
14-15	Spread	1.380	1.490	18.090	17.985
14-15	Finish	1.380	1.490	17.958	17.833
14	Angle (Fwd. Flange)	1.635	1.700	18.065	17.940
14	Angle (Aft Flange)	--	1.700	--	18.050
15	Angle	--	1.700	--	18.050

TABLE XXX

INCONEL 718 COLD FORMING RESULTS

Part No.	Stage Configuration	Groove Diameter (inch)	Comments
100	14	23.490	Groove .015 inch off center line. No surface failures.
101	14	23.480	Groove .035 inch off center line. No surface failures.
102	15	23.450	Groove on center line. No surface failures.
103	14	23.484	Groove .050 inch off center line. The premachined O.D. groove was .030 inch off center line. No surface failures.
104	14	23.475	Groove .005 inch off center line. The premachined O.D. groove was remachined to center line.

TABLE XXXI

SELECTION OF ROTOR STAGES FOR SPOOL ASSEMBLIES

Rotor No.	Stage No.	Serial No.	Minimum Stock[1] (Inch) For: Dovetail Fwd.	Dovetail Aft.	Hub Fwd.	Hub Aft.	Remarks
1	16	7	0.020	0.005	0.160	0.060	Cracks in Dovetail V-Groove
	15	3	0.020	0.025	0.020	0.000	
	14	11	0.025	0.050	(0.005)	(0.010)	No stock for Hub
	Flange	36	-	-	-	-	Undersize on Weld Prep O.D.
2	16	5	0.015	(0.045)	0.130	0.065	
	15	4	0.010	0.020	(0.034)	0.055	
	14	101	0.030	0.100	0.000	0.060	
	Flange	39	-	-	-	-	
3	16	10	0.010	(0.030)	0.130	0.135	
	15	6	0.035	0.020	(0.017)	0.065	
	14	100	0.045	0.060	0.000	0.060	
	Flange	37	-	-	-	-	
4	16	2	0.020	(0.010)	0.076	0.000	
	15	102	0.030	0.030	0.020	0.025	
	14	104	0.050	0.075	0.000	0.050	
	Flange	38	-	-	-	-	
Spare	14	103	0.052	0.045	(0.027)	0.071	

[1]Forward and Aft are in reference to air flow direction

Lack of stock indicated by ( )

TABLE XXXII

WELDING PARAMETERS AND RESULTS FOR TF39 STAGES 14-16 ROTOR SPOOLS[1]

Run No.	Rotor No.	Stage Nos.	Weld Speed RPM - SFM	Weld Pressure (PSI x 10^3)	Weld Time (Sec)	Max. Energy (ft.-lbs x 10^3/in^2)	Total Upset (Inch) Target	Actual	Total Indicated Run Out Face(Inch)	Dia.(Inch)	Max. Radial Shift (Inch)	Remarks
400-9-11	1	16-15	266 - 1665	39.4	2.6	21.0	0.070	0.050	0.0035	0.003	0.002	No overheating; used test disk parameters-low upset indicative of higher strength of rim section.
400-9-12	1	15-14	273 - 1715	39.2	2.8	24.0	0.065	0.065	0.0065	0.012	0.0065	No overheating
400-9-14	2	16-15	278 - 1742	39.4	2.7	23.0	0.088	0.084	0.005	0.0035	0.0025	No overheating
400-9-15	3	16-15	275 - 1730	39.4	2.5	24.5	0.075	0.087	0.003	0.004	0.003	Some flash spin off just before seizure
400-9-16	4	16-15	277 - 1740	38.8	2.8	24.5	0.075	0.047	0.004	0.0065	0.006	No overheating; low upset believed due to short(0.100 inch) weld prep length
400-9-17	2	15-14	280 - 1760	39.5	2.7	25.3	0.085	0.085	0.004	0.0105	0.006	Some flash spin off just before seizure
400-9-18	3	15-14	277 - 1740	39.6	-	24.5	0.070	0.066	0.004	0.0045	0.0035	No overheating
400-9-19	1	14-Flange	278 - 1750	39.5	2.7	25.3	0.085	0.073	0.007	0.027	0.016	Hot short; pre-weld eccentricity high-(0.029 TIR)
400-9-20	4	15-Spacer	277 - 1737	39.5	4.2	24.9	0.080	0.078 Max.	0.055	-	-	Repair weld-spacer slipped over back-up tooling causing extreme out-of-parallelism
400-9-22	4	15-Spacer	289 - 1810	40.8	1.7	24.1	0.080	0.097	-	-	-	Second repair attempt-new brass bushing seized on pilot-low upset-short weld time
400-9-23	2	14-Flange	281 - 1750	40.7	2.4	26.7	0.095	0.078	0.001	0.0045	0.0045	Used another brass bushing with more clearance than above-still had some seizure on pilot
400-9-25	3	14-Flange	289 - 1800	40.0	2.9	27.0	0.100	0.089	0.002	0.0125	0.0075	No overheating-used old brass bushing with 0.003 in. clearance
400-9-27	4	15-Spacer	316 - 1990	36.7	2.9	28.7	0.130	0.130	-	-	-	Hot short-third repair attempt successful-no concentricity or parallel checks made
400-9-28	4	16-15	282 - 1770	40.2	2.5	25.5	0.085	0.088	0.002	0.0075	0.004	No overheating
400-9-29	4	15-14	283 - 1775	40.6	2.6	25.5	0.085	0.082	0.002	0.007	0.004	No overheating
400-9-30	4	14-Flange	286 - 1780	40.0	2.4	26.4	0.100	0.097	0.001	0.003	0.002	No overheating

[1]All welds made on Model 400 Inertia Welder with Flywheel Wk^2 = 36,038 lb.-ft.^{2}

TABLE XXXIII

SUMMARY OF ZYGLO INSPECTION RESULTS

Rotor No.		After 1st Machining	After 2nd Machining	After 3rd Machining
1	I.D.: All Joints:	No indications	No indications	Not inspected
	O.D.: 16/15 Joint:	2 Ind.-12 to 18 inches long	No indications	Not inspected
	15/14 Joint:	1 Ind.-1/2 inch long	No indications	Not inspected
	14/F1 Joint:	1 Ind.-2 inch long	1 Ind.-2 inch long	No indications[1]
2	I.D.: All Joints:	No indications	Not inspected	
	O.D.: 15/14 Joint:	1 Ind.-3 inch long	No indications[1]	
3	I.D.: All Joints:	No indications		
	O.D.: All Joints:	No indications		
4	I.D.: All Joints:	No indications		
	O.D.: All Joints:	No indications		

[1] Defective area was electro-etched with rotor in machine.

TABLE XXXIV

STOCK REMOVAL AT WELD JOINTS PRIOR TO AGING HEAT TREATMENT

Rotor No.	Stg./Stg. Weld	Flash Groove Dimension, (inch) O.D.	I.D.	Wall Thickness (inch)	Upset (inch)	Total Stock Removed on Side, (Inch)[1] 0.200 inch Wall O.D.	I.D.	0.180 inch Wall O.D.	I.D.
1	16/15	23.904	23.679	0.112	0.050	0.036	0.052	0.029	0.042
	15/14	23.906	23.622	0.142	0.065	0.038	0.023	0.027	0.015
	14/Fl.	23.730	23.492	0.119	0.073	0.038	0.046	0.018	0.046
2	16/15	23.939	23.639	0.150	0.084	0.020	0.030	0.011	0.022
	15/14	23.941	23.619	0.161	0.085	0.021	0.022	0.009	0.013
	14/Fl.	23.770	23.444	0.163	0.058	0.022	0.022	0.005	0.017
3	16/15	23.926	23.620	0.153	0.087	0.026	0.024	0.018	0.012
	15/14	23.940	23.618	0.161	0.066	0.022	0.022	0.014	0.011
	14/Fl.	23.777	23.433	0.172	0.089	0.015	0.018	0.002	0.012
4	16/15	23.933	23.641	0.146	0.088	0.024	0.030	0.012	0.026
	15/Spacer	23.933	23.600	0.172	0.120	0.024	0.012	0.024	0.005
	15/14	23.932	23.612	C 158	0.082	0.026	0.021	0.014	0.013
	14/Fl.	23.772	23.421	0.169	0.097	0.017	0.019	0.005	0.012

TF39 Stages 14-16 Rotor Spool Dimensions[2], (Inch)

	O.D. (Min)	I.D. (Max)	Wall (Min)
16/15	23.9265	23.7465	0.090
15/14	23.9265	23.6665	0.130
14/Fl.-Rotor 1	23.744	23.484	0.130
2	23.750	23.490	0.130
3	23.748	23.488	0.130
4	23.744	23.484	0.130

[1]Figures based on pre-weld diameters and are minimum amount removed as weld joint thickens during upset.

[2]Dimension of Stage 14/Flange weld depend on weld joint position relative to forward surface of machined flange due to taper.

TABLE XXXV

SUMMARY OF WELD PARAMETERS AND RESULTS FOR ROTOR NO. 5

Run No.	Stage Nos.	Weld RPM	Speed SFM	Weld Pressure PSI	Weld Time Sec.	Max. Energy Ft-Lbs/in^2	Total Upset Inch	Total Indicated Face (in)	Run Out Dia. (in)
400-0-102	Test Rings	246	1550	35,800	2.8	25,200	0.091	0.0055	0.005
400-9-103	Test Rings	245	1540	35,100	2.5	24,500	0.069	0.004	0.020
400-9-104	Test Rings	250	1570	35,200	2.6	25,600	0.092	0.007	0.020
400-9-105	Test Rings	252	1585	36,000	2.9	26,300	0.092	0.007	0.012
400-9-106	14-15	251	1580	35,500	2.8	26,000	0.084	0.002	0.0065
400-9-107	14+15-16	249	1560	37,500	2.8	25,500	0.072	0.011	0.004

Flywheel WK^2 = 32,500 lb-ft^2

Table XXXVI

Tensile and Stress Rupture Properties of Parent Metal[1] and Weld Specimens[2] - Forged Stock

Tensile						Stress Rupture					
Sample	Temp °F	UTS ksi	0.2%YS ksi	El %	Failure Location	Sample	Temp °F	Stress ksi	Life hrs.	El %	Failure Location
B-3(Parent Metal)	RT	191	169	13		B-2(Parent Metal)	1200	100	72	3	
B-5 " "	RT	192	171	15		B-8 " "	1200	100	78	4	
C01 Weld	RT	192	170	11	HAZ	C-8 Weld	1200	100	14	2	Weld line
D-6 Weld	RT	194	171	10	HAZ	C-10 Weld	1200	100	8	2	Weld line
C-9 Weld	RT	132	102	8	HAZ	D-10 Weld	1200	100	9	3	Weld line
B-6 (Parent Metal)	1200	158	146	14		GE Specification	1200	100	25	5	
D-7 Weld	1200	154	146	4	HAZ	C50TF6					
D-9 Weld	1200	159	144	4	Weld line						
GE Specification	RT	185	150	12							
C50TF6	1200	145	125	12							

1 Parent metal specimens from forging C0067

2 Weld specimens from forging C0082

3 Nominal gage section = 0.090 x 0.125 x 0.500 inch

Table XXXVII

Effect of Post-Weld Treatments on 1200F Tensile and Stress Rupture

Sample	UTS ksi	0.2YS ksi	El. %	Failure	Sample	Life	El.	Failure	Post-Weld Treatment[1]
C-2	160.0	138.7	9.4	P.M.	C-4	11.9	1.4	Weld	Age + shot peen
D-2	160.4	135.2	10.0	P.M.	D-8	14.7	1.6	Weld	Age + shot peen
D-4	153.8	111.8	8.9	HAZ	C-7	11.4	4.4	Weld	Age + solution + age
C-3	150.9	109.0	9.0	HAZ	D-11	10.7	7.2	Weld	Age + solution + age
D-12	151.8	120.8	10.4	HAZ	D-13	29.2	4.8	Weld	Age + shot peen + solution + age + shot peen
D-14	156.3	123.1	8.4	HAZ	D-15	15.0	4.8	Weld	Age + shot peen + solution + age + shot peen
Parent Metal	157.5	146.4	14.0			77.8	3.7		
Parent Metal						72.2	2.7		
GE Spec. C50TF6	145.0	125.0	12.0			25.0	5.0		

[1] Post-Weld Treatment:

Age (vacuum) - 1325F/8 hr/FC @ 100F/hr to 1150F + 1150F/8 hr/FC
Solution (vacuum) - 200F/hr to 1750F + 1750F/1 hr/FC @ 200F/hr
Shot peen - No. 110 steel shot - 8 to 10 A2 intensity - 125% saturation
100% coverage of gage section

TABLE XXXVIII

Tensile Properties of TF39 Stg. 14-16 Forgings[1]

Forging Serial No.	Room Temperature UTS Ksi	0.2 YS Ksi	El %	RA %	1200F UTS Ksi	0.2 YS Ksi	El %	RA %
0046	206.5	163.6	15.7	22.4	163	138.6	15.4	19.6
0059	207.3	160.4	17.0	27.2	163.6	139.6	16.4	18.1
0062	209.7	173.3	14.2	20.3	160.4	136.8	20.0	21.7
0064	202.7	166.2	13.5	21.0	166.0	140.4	20.2	23.1
0065	207.3	172.4	17.5	23.6	158.4	135.6	13.5	17.8
0067	193.3	162.4	16.0	35.1	163.6	133.9	23.0	40.7
0068	203.7	166.4	21.0	31.2	159.2	133.3	20.2	23.7
0069	202.5	166.4	18.5	26.5	164.4	141.6	22.0	27.2
0070	196.1	160.8	17.0	22.3	159.6	139.8	16.4	18.9
0071	199.7	163.6	18.4	22.5	155.6	126.3	23.0	37.0
0075	192.9	131.2	15.9	29.2	172.4	138.4	15.5	21.0
0079	197.7	164.4	16.5	22.4	155.2	130.8	15.5	20.7
0080	185.5	160.0	16.9	23.8	154.5	131.8	16.1	20.9
0082	204.1	168.8	16.0	22.4	152.4	128.3	15.5	20.3
GE Specification C50TF6	185.0	150.0	12.0	15.0	145.0	145.0	12.0	18.0

[1] Heat Treatment - 1750F/1 Hr/W.Q. + 1325F/8 Hr/FC @ 100F/Hr to 1150F + 1150F/8 Hr/AC

TABLE XXXIX

1200F Stress Rupture Properties of TF39 Forgings

Forging Serial No.	Stress Ksi	Life Hours	El %
0046	110	25.7	5.1
0059	110	29.1	6.5
0062	110	61.1	15.1
0064	110	67.7	13.8
0065	110	45.9	10.0
0067	110	50.6	10.7
0068	110	59.2	12.7
0069	110	48.7	17.6
0070	110	26.6	10.8
0071	110	28.4	6.5
0075	110	62.3	9.2
0079	105	29.4	6.1
0080	105	29.5	5.8
0082	110	32.7	9.9
GE Specification C50TF6	100	25.0	5.0

Table XL

Tensile Properties of Cross Rolled Plate

	Room Temperature				1200F			
As Rolled[1] Heat No.	UTS Ksi	0.2 YS Ksi	El %	RA %	UTS Ksi	0.2 YS Ksi	El %	RA %
K67440K12	207.8	166.8	18.6	40.7	171.7	148.4	17.7	28.9
K67440K12	216.0	184.0	16.1	36.3	169.7	145.0	20.7	37.4
K67547K13	202.8	160.8	21.8	36.2	160.7	132.9	17.0	22.4
K67547K13	195.1	156.7	23.9	37.2	155.7	127.7	15.0	21.9
K67231K12	202.2	180.2	12.1	38.9	165.1	150.4	14.0	37.0
K67231K12	205.2	186.3	15.8	36.6	165.7	153.8	11.2	29.5
K67231K12	206.5	187.3	14.1	34.9	155.8	139.4	17.3	31.5
K67231K12	203.9	175.3	15.1	36.7	160.5	145.8	13.4	28.3
K67444K12	200.2	179.2	17.2	36.6	160.3	147.5	16.1	35.8
K67444K12	200.4	179.8	19.5	33.9	156.2	146.3	17.0	45.2
K67448K12	216.1	177.6	15.8	32.9	168.3	139.3	18.2	28.0
K67448K12	213.6	174.8	17.7	33.3	168.3	145.6	13.0	23.4
RIM Formed Plate[2]								
WEB	188.0	156.0	22.4	41.7	152.0	126.0	13.2	22.8
WEB	190.0	159.0	21.9	41.4	153.0	130.0	11.9	19.9
RIM	198.0	158.0	21.7	40.4	155.0	131.0	10.8	17.0
WEB	193.0	163.0	20.2	41.0	157.0	135.0	13.7	21.8
GE Specification C50TF6	185.0	150.0	12.0	15.0	145.0	125.0	12.0	18.0

[1] Heat Treatment - 1750-1775F/1 Hr/AC + 1325F/8 Hr/FC @ 100F/Hr to 1150F + 1150F/8 Hr/AC
Duplicate Tests for Each Heat Represent Specimen Orientation Parallel and Transverse to Final Rolling Direction

[2] Heat Treatment - 1850-1 0F/90 Min/AC + 1850F/90 Min/AC + 1850-1900F/90 Min/AC + 1800F/1 Hr/AC
+ 1325F/8 Hr/FC @ 100F/Hr to 1150F + 1150F/8 Hr/AC + 1250F/64 Hr/AC

TABLE XLI

1200F-100 Ksi Stress Rupture Properties of Cross Rolled Plate

Heat No.	Life Hrs.	El %	
K67440K12	88.0	17.7	
K67440K12	88.7	16.8	
K67547K13	112.5	19.7	
K67547K13	93.5	18.6	
K67231K12	90.3	12.5	
K67231K12	90.2	13.1	
K67231K12	90.3	13.7	
K67231K12	90.3	11.7	
K67444K12	116.5	11.5	
K67444K12	120.6	10.9	
K67448K12	87.8	14.1	
K67448K12	75.3	16.6	
RIM Formed Plate			
WEB	66.7	2.5	
WEB	165.0	4.5	
RIM	16.3	1.8	- Thread Break
RIM	86.9	4.2	
RIM	255.4	4.2	
GE Specification C50TF6	25.0	5.0	

TABLE XLII

Labor Summary Fabricated Vs. Forged Rotors on a Percentage Basis

(Method A = 100%)

Operation	% by Method[1]				
	A	A^1	B	C	D
Standard Machining	100.0	238.0	51.2	51.2	51.2
Non-Std. Machining	-	-	42.2	32.6	20.4
Rim Forming	-	-	5.2	3.5	0.0
Inertia Welding	-	-	8.7	6.1	6.1
Heat Treat & Zyglo	-	-	14.9	14.2	5.0
Total Direct Labor	100.0	238.0	122.2	107.6	82.7

[1]Method A - Forged and Machined (0 welds) after 250 rotors

A^1 - Forged and Machined (0 welds)

B - Three Plates + 1 Forging (3 welds)

C - Two Plates + 1 Forging (2 welds)

D - Three Contoured Forgings (2 welds)

} Initial Productio

TABLE XLIII

Labor Breakdown by Operation for Fabricated Rotors on Percentage Basis

(Method B = 100%)

Operation	% By Method[1]		
	B	C	D
1. Turn OD & Bore ID	14.8	9.9	0.0
2. Split OD	1.6	0.6	0.0
3. Anneal	1.3	1.3	0.0
4. Spread	2.1	1.3	0.0
5. Form	1.6	0.6	0.0
6. Zyglo	0.7	0.5	0.0
7. Solution and Age	5.3	5.3	0.0
8. Zyglo	0.7	0.5	0.0
9. Rough Contour & Weld Prep-Stg. 16	5.3	5.3	5.3
10. Rough Contour & Weld Prep-Stg. 15	5.7	5.7	5.7
11. Rough Contour & Weld Prep-Stg. 14	5.7	5.7	5.7
12. Rough Contour & Weld Prep-Stg. FL.	2.8	0.0	0.0
13. Weld Stg. 16 to Stg. 15	1.3	1.3	1.3
14. Weld Prep. Stg. 15	0.6	0.6	0.6
15. Weld Stgs. 16 + 16 to Stg. 14	1.3	1.3	1.3
16. Weld Prep Stg. 14	0.6	0.0	0.0
17. Weld Stgs. 16 + 15 + 14 to FL.	1.3	0.0	0.0
18. Remove Weld Flash	1.3	1.3	1.3
19. Zyglo	0.4	0.4	0.4
20. Vacuum Age	3.5	3.5	3.5
21. Zyglo	0.4	0.4	0.4
Direct Labor Sub-Total	58.3	45.5	25.5
22. Standard Finish Turn	24.4	24.4	24.4
23. Standard Finish Machine	14.3	14.3	14.3
24. Standard Process Room	1.5	1.5	1.5
25. Standard Spray Coat	1.5	1.5	1.5
Total Direct Labor	100.0	87.2	67.2

[1] Method B - 3 plates + 1 forging (3 welds)
C - 2 plates + 1 forging (2 welds)
D - 3 contoured forgings (2 welds)

TABLE XLIV

Comparison of Material Inputs-Fabricated Rotors vs. Forged Rotors on a Percentage Basis

(Method A = 100%)

Stage[2]	% by Method[1] A	A[1]	B	C	D
Flange + 14 + 15 + 16 (F)	100.0	157.0	-	-	-
Flange + 14 (F)	-	-	-	27.7	27.7
Flange (F)	-	-	6.9	-	-
15 (F)	-	-	-	-	21.6
16 (F)	-	-	-	-	20.3
14 (P)	-	-	29.4	-	-
15 (P)	-	-	26.4	26.4	-
16 (P)	-	-	20.8	20.8	-
TOTAL	100.0	157.0	83.5	74.9	70.1

[1]Method A - Forged and machined (0 welds) after 250 rotors

A[1] - Forged and machined (0 welds)

B - 3 plates + 1 forging (3 welds) Initial Production

C - 2 plates + 1 forging (2 welds)

D - 3 contoured forgings (2 welds)

[2]

(F) - Forging

(P) - Plate

TABLE XLV

Comparison of Material Costs-Fabricated Rotors vs. Forged Rotors on a Percentage Basis

(Method A=100%)

Stage[2]	% by Method[1]				
	A	A[1]	B	C	D
Flange + 14 +15 +16(F)	100.0	359.0	-	-	-
Flange + 14 (F)	-	-	-	55.7	55.7
Flange (F)	-	-	17.8	-	-
[illegible]	-	-	-	-	41.2
[illegible] (F)	-	-	-	-	40.2
14 (P)	-	-	27.0	-	-
15 (P)	-	-	24.4	24.4	-
16 (P)	-	-	19.3	19.3	-
TOTAL	100.0	359.0	88.5	99.4	137.1

[1]Method A - Forged and Machined (0 welds) After 250 rotors

A[1]- Forged and Machined (0 welds)

B - 3 plates + 1 forging (3 welds)

C - 2 plates + 1 forging (2 welds) Initial Production

D - 3 contoured forgings (2 welds)

[2]
(F) Forging

(P) Plate

Table XLVI

Inertia Welding Machine Parameters

Inertia Welder Model No.	WK^2 lb-ft^2, max.	Load Lbs, max.	Swing Dia. Inch, max.	RPM, max.
100	40	30,000	11.8	8000
150	50	46,000	11.8	9000
250	2000	175,000	31.8	5130
400	50,000	539,000	71.8	3000

Table XLVII

Inertia Welding Machine Capabilities

Inertia Welder Model No.	Maximum Rotor Diameter, Inch[1]		
	Inconel 718	Udimet 700	Ti 6Al-4V
100	1.6	1.2	13.8
150	1.7	1.3	15.0
250	5.8	4.3	23.4
400	16.8	12.0	67.8

[1] All joints with 0.200 inch walls; for thinner or thicker walls the maximum rotor diameter will increase or decrease respectively.

APPENDIX II

STATISTICAL ANALYSIS OF PARAMETRIC WELDING STUDIES

The statistical analysis of the data generated in the parametric studies was based on an experimental design of 3 x 2 x 3 factorial experiment with the factors tested at unequally spacer levels. The variables selected were 3 levels of flywheel moment of inertia with 2 levels of surface speed and 3 levels of pressure. This required 18 tests for the analysis.

To statistically analyze the data, it was necessary to calculate the following:

1. The Contrast Sum (CS)
2. The orthagonal polynomial sums of squares (Σx^2)
3. The Adjusted Contrast Sums (CS adj)
4. The significant coefficients
5. The inverse calculation to yield the actual data point in contrast to the observed data point.

The procedure used to determine these factors is:

1. The data points (y_o) are tabulated in columnar form and separated into triplets. For a 3 x 2 x 3 experiment there are 6 such triplets.
2. The calculations to determine the contrast sums may be represented by the following table:

	(a)	(b)	(c)
(a')	1	-1	1
(b')	1	0	-2
(c')	1	1	1

where b and c represent linear and quadratic effects, respectively.

In the forward calculations to determine the contrast sums and significant coefficients, the triplets are operated on by the number in colums a, b, and c. For a 3 x 2 x 3 experiment the process must be repeated 3 times.

3. The orthagonal polynomial sums of squares represents the orthagonal polynomial cross product and is dependent upon the number of levels of the experiment and the number of factors per level.

4. The adjusted constract sum is determined by:

$$CS / \sqrt{\Sigma x^2}$$

This value is plotted on half normal probability paper and is used to determine significant factors. Any term affected by a random error only will plot along a straight line while those affected significantly by the experimental factors plot clearly above the line.

5. The significant coefficients for those terms affected by the factors are determined by:

$$CS / \Sigma x^2$$

6. To determine the best fit equation. the inverse calculations are applied to the significant coefficients. Zeroes are substituted for those terms found not to be significant. The inverse calculations use the same sequence as is used to determine the contrast sums (CS) except that the multipliers in rows a', b', and c' are used to operate on the significant coefficient triplets. After applying the sequence 3 times, $\hat{y}$ is obtained and represents the calculated value for the data points.

7. $Y_0 - \hat{y}$ represents the difference between the observed and calculated values and serves as a means to determine the quality of the data.

In the experimental analysis, the factors are identified as A, B, and C which represent the following:

A - Load

B - Energy level

C - Flywheel moment of inertia corrected for efficiency

Some variations between calculated and observed upsets were expected because of the variance between the assigned and actual efficiency between welds within each group The actual efficiency variations can be attributed to by the variation in specimen counterbores and the piloting plugs used causing some specimens to have higher frictional losses than others.

1. TEST RESULTS FOR INCONEL 718

Tables XLVIII and XLIX give the statistical analysis programs for Inconel 718 with the statistical rankings included.

The forward and inverse calculations for the statistical analysis are given in Tables L to LIII. The half normal probability plots for significant factors are given in Figures 98, 99, 100, and 101. In all cases points A and B (load and energy level) plot clearly above the line indicating their significance. Figures 102, 103, 104, and 105 plot the observed and calculated values for upset and quality ranking. Disregarding the effect of variations resulting from efficiency, the plots for the calculated and observed upsets and quality rankings show general agreement. Generally, the better quality welds were obtained with the 2400 ft-lbs/in^2 energy level and 32,000 psi pressure.

2. TEST RESULTS FOR UDIMET-700

Table LIV shows the statistical analysis program for Udimet-700 with the ranking shown in the last column. Table LV and LVI shows the forward and inverse calculations for the statistical analysis in relation to upset and quality. Figure 106 and 107 are the half normal probability plots for the significant factors. In each case, points A and B (load and energy level) plot clearly above the line indicating their significance. C (Flywheel Moment of Inertia) is less significant.

Figures 108 and 109 plot the observed and calculated values for upset and quality ranking. Disregarding the effect of variations resulting from efficiency, the plots for the calculated and observed upsets and quality rankings show general agreement. The best quality welds were obtained with 25000 ft-lb/in^2 energy level and a 32,000 to 38,000 psi pressure range.

3. TEST RESULTS FOR TI-6AL-4V

Table LVII shows the statistical analysis program for Ti-6Al-4V with the ranking shown in the last column. Tables LVIII and LIX shows the forward and inverse calculations for the statistical analysis in relation to upset and quality. Figures 40 and 41 are the half normal probability plots for the significant factors. In each case B and C (Energy and Flywheel Moment of Inertia) plot clearly above the line indicating their significants. A (Load) is less significant. This is different than the results obtained for the super alloys Udimet 700 and Inconel 718. Figures 112 and 113 plots the observed and calculated values for upset and quality ranking. Disregarding the effect of variations resulting from efficiency, the plots for the calculated and observed upsets and quality rankings show general agreement. The best quality welds were obtained with 6700 to 12,800 ft-lbs/in^2 and 4,500 psi.

TABLE XLVIII

INCONEL 718 INERTIA WELDING PARAMETRIC STUDIES

(1.0 inch O.D.. X 0.1 inch Wall)

Flywheel Moment Of Inertia	Welding Speed RPM	SFM	Upset Pressure (psi)	Spindle Efficiency	Actual Unit Energy ($ft\text{-}lbs/in^2$)	Upset (inch)	Visual Results	Ranking
19.5	1,600	420	32,000	.80	24,000	.084	Good weld - no cracks	3
19.5	1,600	420	38,000	.80	24,000	.154	Smooth weld - some expulsion	5
19.5	1,600	420	48,000	.80	24,000	.184	Smooth weld - some expulsion	7
19.5	2,000	525	32,000	.80	38,200	.242	Flash slightly cracked	13
19.5	2,000	525	38,000	.80	38,200	.220	Flash slightly cracked - some expulsion	10
19.5	2,000	525	48,000	.80	38,200	.318	Smooth flash - excessive upset	17
9.5	2,400	630	32,000	.70	23,300	.110	Good weld - no cracks	2
9.5	2,400	630	38,000	.70	23,300	.145	Good weld	6
9.5	2,400	630	48,000	.70	23,300	.193	Very good weld - smooth flash	8
9.5	3,100	810	32,000	.70	38,900	.219	Flash excessively cracked - some expulsion	14
9.5	3,100	810	38,000	.70	38,900	.220	Smooth flash - some expulsion	11
9.5	3,100	810	48,000	.70	38,900	.261	Smooth flash - some expulsion	16
4.4	4,200	1,100	32,000	.50	23,700	.094	Good weld - no cracks	1
4.4	4,200	1,100	38,000	.50	23,700	.128	Good weld - no cracks	4
4.4	4,200	1,100	48,000	.50	23,700	.160	Good weld	9
4.4	5,300	1,400	32,000	.50	37,400	.140	Flash highly cracked	15
4.4	5,300	1,400	38,000	.50	37,400	.192	Good weld	12
4.4	5,300	1,400	48,000	.50	37,400	.307	Good weld - excessive upset	18

TABLE XLIX

INCONEL 718 INERTIA WELDING PARAMETRIC STUDIES

(1.0 inch O.D. X 0.2 inch Wall)

Flywheel Moment Of Inertia	Welding Speed RPM	SFM	Upset Pressure (psi)	Spindle Efficiency	Actual Unit Energy (ft-lbs/in^2)	Upset (inch)	Visual Results	Ranking
19.5	2,100	550	32,000	.80	23,400	.052	Smooth weld - not enough upset	16
19.5	2,100	550	38,000	.80	23,400	.066	Fair weld - minimal upset	9
19.5	2,100	550	48,000	.80	23,400	.117	Good weld - no cracks	4
19.5	2,700	710	32,000	.80	38,400	.148	Flash cracked slightly	11
19.5	2,700	710	38,000	.80	38,400	.147	Flash cracked slightly	10
19.5	2,700	710	48,000	.80	38,400	.188	Very good weld - small cracks present	15
9.5	3,300	865	32,000	.70	24,400	.006	Poor weld - no upset	18
9.5	3,300	865	38,000	.70	24,400	.076	Good weld - no cracks	3
9.5	3,300	865	48,000	.70	24,400	.099	Very good weld - small cracks	2
9.5	3,900	1020	32,000	.70	35,000	.125	Flash cracked slightly	7
9.5	3,900	1020	38,000	.70	35,000	.156	Flash cracked slightly	12
9.5	3,900	1020	48,000	.70	35,000	.168	Flash cracked slightly	13
4.4	5,700	1500	32,000	.50	24,300	.072	Fair weld - no cracks	5
4.4	5,700	1500	38,000	.50	24,300	.074	Fair weld - no cracks	6
4.4	5,700	1500	48,000	.50	24,300	.100	Very good weld - no cracks	1
4.4	7,200	1900	32,000	.50	38,800	.126	Flash heavily cracked	8
4.4	7,200	1900	38,000	.50	38,800	.180	Fair weld - not concentric	14
4.4	7,200	1900	48,000	.50	38,800	.252	Fair weld - excessive upset	17

TABLE L

INCONEL 718 - 1.0 INCH O.D. X 0.1 INCH WALL UPSET MEASUREMENTS

Method: Yates algorithm

y_o	1	2	CS	Term	Σx^2	$\sqrt{\Sigma x^2}$	CS adj	Rank	Coeff	1	2	$\hat{y}$	$\hat{y}$ adj	$y_o - \hat{y}$ adj.
84	426	1206	3375	yo	18	----	-----		187.50	143	95.06	110.48	112.3	-28.3
158	780	1148	534	A	12	3.464	154.2	16	44.50	47.94	-15.42	154.98	146.0	8
184	448	1021	186	A^2	36	6	31.0	10	0	-15.42	0	199.48	202.1	-18.1
242	700	176	863	B	18	4.242	203.4	17	47.94	0	139.56	206.36	208.2	33.8
220	382	125	36	AB	12	3.464	10.4	4	0	0	-15.42	250.86	241.8	-21.8
318	639	233	260	A^2B	36	6	43.3	13	0	0	0	295.36	298.0	20
110	100	72	-185	C	12	3.464	53.4	15	-15.42	187.50	186.06	95.06	101.1	8.9
145	76	53	57	AC	8	2.828	20.2	7	0	47.94	-15.42	139.56	134.8	10.2
193	83	61	-9	A^2C	24	4.898	1.84	2	0	-15.42	0	184.06	190.9	2.1
219	42	354	-97	BC	12	3.464	28.0	9	0	0	190.94	190.94	197.0	22
220	66	252	125	ABC	8	2.828	44.2	14	0	0	-15.42	235.44	230.7	-10.7
261	167	257	-103	A^2BC	24	4.895	21.0	8	0	0	0	279.94	286.8	-25.8
94	-48	-24	-69	C^2	36	6	11.5	5	0	232.0	235.44	79.64	81.8	12.2
128	120	-41	159	AC^2	24	4.898	32.46	11	0	47.94	-15.42	124.14	115.5	12.5
160	13	101	27	A^2C^2	72	8.484	.38	1	0	-15.42	0	168.64	171.6	-11.6
140	40	168	107	BC^2	36	6	17.83	6	0	0	279.94	175.52	177.7	-37.7
192	-2	27	159	ABC^2	24	4.898	32.46	12	0	0	-15.42	220.02	211.4	-19.4
307	63	65	179	A^2BC^2	72	8.484	2.48	3	0	0	0	264.52	267.5	-40.5

TABLE LI

INCONEL 718 - 1.0 INCH O.D. X 0.2 INCH WALL UPSET MEASUREMENTS

y_o	1	2	CS	Term	$\sum x^2$	$\sqrt{\sum x^2}$	CS adj.	Rank	Coe.'s	(1)	(2)	$\hat{y}$	$\hat{y}$ adj	$y_o - \hat{y}$ adj.
52	235	718	2172	yo	18				120.7	85.2	38.1	24.2	26.9	25.1
66	483	650	415	A	12	3.464	122.7	16	35.5	47.1	20.1	72.6	66.9	-.9
117	181	804	75	A^2	36	6	12.5	8	0	7.2	6.2	121.0	124.0	-7
148	469	105	848	B	18	4.242	199.9	17	47.1	-12.9	73.6	144.2	149.3	-1.3
147	246	156	53	AB	12	3.464	12.4	7	0	6.2	7.2	167.0	161.1	-14.1
188	558	154	47	A^2B	36	6	7.8	4	0	0	6.2	189.4	190.0	-2
6	65	79	86	C	12	3.464	24.8	11	7.2	120.7	109.1	25.7	29.7	23.7
76	40	-46	49	AC	8	2.828	20.86	10	0	47.1	-5.7	61.2	55.6	20.4
99	93	42	-37	A^2C	24	4.898	-7.55	3	0	7.2	6.2	96.7	98.6	.4
125	63	248	64	BC	12	3.464	18.48	9	0	0	132.3	119.4	123.9	1.1
156	28	288	113	ABC	8	2.828	36.4	14	12.9	6.2	-5.7	155.4	149.8	6.2
188	126	312	-11	A^2BC	24	4.898	-2.25	1	0	0	6.2	190.9	192.8	-4.8
72	37	-15	222	C^2	36	6	37	15	6.2	156.2	167.8	64.4	69.5	2.5
74	42	-30	-43	AC^2	24	4.898	-8.77	5	0	47.1	7.2	87.0	81.3	-7.3
100	-47	98	213	A^2C^2	72	8.484	25.11	12	0	7.2	6.2	109.6	110.2	-10.2
126	1	5	-16	BC^2	36	6	-2.67	2	0	12.9	203.3	132.8	135.5	-9.5
180	24	48	143	ABC^2	24	4.898	27.2	13	0	6.2	20.1	181.2	175.5	4.5
252	18	-6	97	A^2BC^2	72	8.484	-11.4	6	0	0	6.2	229.6	232.6	19.4

TABLE LII

INCONEL 718 - 1.0 INCH O.D. X 0.2 INCH WALL QUALITY RANKING

y_o	1	2	CS	Term	Σx^2	$\sqrt{\Sigma x^2}$	CS adj	R	Coeff.	1	2	$\hat{y}$	$y_o-\hat{y}$
3	15	55	171		18				9.50	8.00	2	2	1
5	40	57	27	A	12	3.464	7.79	16	2.25	6.00	0	5	0
7	16	59	27	A^2	36	6	4.50	14	.75	0	0	8	-1
13	41	8	81	B	18	4.242	19.09	17	4.50	0	5	14	-1
10	14	8	-9	AB	12	3.464	2.60	13	-.75	0	0	11	-1
17	45	11	27	A^2B	36	6	4.50	15	.75	0	0	17	0
2	4	10	4	C	12	3.464	1.15	10	0	8.00	8	2	0
6	4	6	3	AC	8	2.828	1.06	9	0	3.00	(	5	1
8	6	11	1	A^2C	24	4.898	.20	2	0	0	0	8	0
14	2	25	6	BC	12	3.464	1.73	11	0	0	14	14	0
11	8	25	-5	ABC	8	2.828	1.77	12	0	0	0	11	0
16	3	31	-3	A^2BC	24	4.898	.61	6	0	0	0	17	-1
1	0	0	0	C^2	36	6	0	1	0	12.50	11	2	-1
4	10	-4	3	AC^2	24	4.898	.61	5	0	4.50	0	5	-1
9	-2	-5	9	A^2C^2	72	8.484	1.06	8	0	0	0	8	1
15	8	10	6	BC^2	36	6	1.00	7	0	0	17	14	1
12	2	10	3	ABC^2	24	4.898	.61	4	0	0	0	11	1
18	9	7	-3	A^2BC^2	72	8.484	.35	3	0	0	0	17	1

TABLE LIII

INCONEL 718 - 1.0 INCH O.D. X 0.2 INCH WALL QUALITY RATING

Method: Yates algorithm

y_o	(1)	(2)	CS	Term	Σx^2	$\sqrt{\Sigma x^2}$	CS adj.	Rank	Coeff.	1	2	$\hat{y}$	$y_o - \hat{y}$
16	29	55	171	yo	18	----			9.50	8.42	10.26	10.26	5.74
9	36	55	-13	A	12	3.64	3.75	11	-1.08	-1.84	0	7.10	1.90
4	23	51	9	A^2	36	6	1.50	4	0	0	0	3.94	.06
11	32	-8	43	B	18	4.242	10.14	16	2.4	0	7.10	6.58	4.42
10	12	-10	51	AB	12	3.464	14.7	17	4.24	0	0	11.90	-1.90
15	39	5	-11	A^2B	36	6	1.83	5	0	0	0	17.22	-2.22
18	-12	8	-14	C	12	3.464	4.04	12	0	9.5	3.94	10.26	7.74
3	4	10	13	AC	8	2.828	4.6	13	0	2.4	0	7.10	-4.10
2	-16	-9	-17	A^2C	24	4.898	3.48	10	0	0	0	3.94	-1.94
7	6	7	20	BC	12	3.464	5.77	15	0	0	6.58	6.58	.42
12	-4	9	-3	ABC	8	2.828	1.06	3	0	0	0	11.90	.10
13	9	27	-1	A^2BC	24	4.898	.2	1	0	0	0	17.22	-4.22
5	2	16	6	C^2	36	6	1.	2	0	10.58	11.90	10.26	-5.26
6	6	22	17	AC^2	24	4.898	3.48	9	0	6.64	0	7.10	-1.10
1	14	13	-21	A^2C^2	72	8.485	2.48	6	0	0	0	3.94	-2.94
8	-4	4	16	BC^2	36	6	2.67	7	0	0	17.22	6.58	1.42
14	-6	-18	-15	ABC^2	24	4.898	3.06	8	0	0	0	11.90	2.10
17	-3	3	43	A^2BC^2	72	8.484	5.07	14	0	0	0	17.22	-.22

TABLE LIV

UDIMET-700 INERTIA WELDING PARAMETRIC STUDIES

(1.0 inch O.D. X 0.1 inch Wall)

Flywheel Moment Of Inertia	Welding Speed RPM	SFM	Upset Pressure (psi)	Spindle Efficiency	Actual Unit Energy (ft-lbs/in^2)	Upset (inch)	Visual Results	Ranking
19.0	1,600	420	32,000	.85	25,200	.122	Smooth flash - some expulsion	3
19.0	1,600	420	38,000	.85	25,200	.150	Smooth flash - some expulsion	8
19.0	1,600	420	48,000	.85	25,200	.138	Smooth flash - some expulsion	7
19.0	2,000	525	32,000	.85	38,800	.220	Flash cracked	10
19.0	2,000	525	38,000	.85	38,800	.230	Flash cracked radially	14
19.0	2,000	525	48,000	.85	38,800	.274	Flash cracked radially - some expulsion - sheet like in appearance	16
9.0	2,400	630	32,000	.75	25,100	.086	Smooth weld - minimum upset	5
9.0	2,400	630	38,000	.75	25,100	.095	Good weld - no cracks	2
9.0	2,400	630	48,000	.75	25,100	.147	Rough flash - cracked radially	15
9.0	3,100	810	32,000	.75	39,000	.200	Good weld - no cracks	11
9.0	3,100	810	38,000	.75	39,000	.150	Flash cracked moderately	9
9.0	3,100	810	48,000	.75	39,000	.256	Excessive upset - flash sheet like in appearance	18
3.9	4,200	1,100	32,000	.60	25,100	.062	Smooth flash - minimum upset	6
3.9	4,200	1,100	38,000	.60	25,100	.100	Good weld - no cracks	1
3.9	4,200	1,100	48,000	.60	25,100	.100	Flash heavily cracked radially	12
3.9	5,200	1,400	32,000	.60	38,300	.143	Flash slightly cracked	4
3.9	5,200	1,400	38,000	.60	38,300	.209	Flash cracked radially	13
3.9	5,200	1,400	48,000	.60	38,300	.264	Excessive upset - flash severly cracked radially - sheet like in appearance	17

TABLE LV

UDIMET-700 1.0 INCH O.D. X 0.1 INCH WALL UPSET MEASUREMENTS

Yo	(1)	(2)	CS	Term	ΣX^2	$\sqrt{\Sigma X^2}$	CS adj	Rank	Coeff	(1)	(2)	$\hat{Y}$	$\hat{Y}$ adj	Yo-$\hat{Y}$ adj
122	410	1134	2926		18				162.6	132.1	78.4	99.7	105.4	16.6
150	726	914	366	A	12	3.464	105.7	16	30.5	53.7	-21.3	130.2	128.5	21.5
138	308	978	124	A^2	36	6	20.7	8	0	-21.3	0	160.7	166.7	-28.9
220	606	70	966	B	18	4.242	227.7	17	53.7	0	108.7	207.1	212.8	7.2
230	262	137	96	AB	12	3.464	27.7	9	0	0	-21.3	237.6	235.9	-5.9
274	616	159	234	A^2B	36	6	39.0	13	0	0	0	268.1	274.3	-.3
66	16	-6	-256	C	12	3.464	-73.9	15	-21.3	162.6	139.4	78.4	75.8	-7.2
95	54	179	89	AC	8	2.828	31.5	11	0	53.7	-21.3	108.9	98.9	-3.9
147	81	-49	-43	A^2C	24	4.898	-8.8	1	0	-21.3	0	139.4	137.3	9.7
200	56	314	40	BC	12	3.464	11.5	4	0	0	185.8	185.8	183.2	16.8
150	38	208	45	ABC	8	2.828	15.9	6	0	0	-21.3	216.3	206.3	-56.3
256	121	354	-47	A^2BC	24	4.898	-9.6	3	0	0	0	246.8	244.7	11.3
62	-40	38	184	C^2	36	6	30.7	10	0	193.1	216.3	57.1	61.0	1.0
100	34	-25	-45	AC^2	24	4.898	-9.2	2	0	53.7	-21.3	87.6	84.1	15.9
100	23	83	-413	A^2C^2	72	8.498	-48.7	14	0	-21.3	0	118.1	122.5	-22.5
143	156	74	72	BC^2	36	6	12	5	0	0	246.8	164.5	168.4	-25.4
209	-38	133	171	ABC^2	24	4.898	34.9	12	0	0	-21.3	195.0	191.5	17.5
264	-11	27	-165	A^2BC^2	72	8.484	-19.5	7	0	0	0	225.5	229.9	34.1

TABLE LVI

UDIMET-700 1.0 INCH O.D. X 0.. INCH WALL QUALITY RANKING

Yo	(1)	(2)	CS	Term	ΣX^2	$\sqrt{\Sigma X^2}$	CS adj	Rank	Coeff.	(1)	(2)	$\hat{Y}$	Yo - $\hat{Y}$
3	18	58	171		18	---	---	--	9.5	5.67	2.73	2.73	.27
8	40	60	46	A	12	3.464	13.3	17	3.83	2.94	0	6.56	1.44
7	22	53	30	A^2	36	6	5.0	13	0	0	0	10.39	-3.39
10	38	10	53	B	18	4.242	12.5	16	2.94	0	6.56	8.61	1.39
14	19	17	6	AB	12	3.464	1.7	6	0	0	0	12.44	1.56
16	34	19	-22	A^2B	36	6	-3.7	11	0	0	0	16.27	-.27
5	4	-8	-5	C	12	3.464	-1.4	4	0	9.5	10.39	2.73	2.27
2	6	27	9	AC	8	2.828	3.2	10	0	2.94	0	6.56	-4.56
15	10	11	19	A^2C	24	4.898	3.9		0	0	0	10.39	4.61
11	7	22	-7	BC	12	3.464	-2.0		0	0	8.61	8.61	2.39
9	6	16	5	ABC	8	2.828	1.8	7	0	0	0	12.44	-3.44
18	13	15	-25	A^2BC	24	4.898	-5.1	14	0	0	0	16.27	1.73
6	-6	2	-9	C^2	36	6	-1.5	5	0	13.33	12.44	2.73	3.27
1	-2	-3	-5	AC^2	24	4.898	-1.0	3	0	2.94	0	6.56	-5.56
12	16	7	-51	A^2C^2	72	8.484	-6.0	15	0	0	0	10.39	1.61
4	11	4	5	BC^2	36	6	0.8	1	0	0	16.27	8.61	-4.61
13	16	-5	15	ABC^2	24	4.898	3.0	9	0	0	0	12.44	.56
17	-5	-21	-7	A^2BC^2	72	8.484	-0.8	2	0	0	0	16.27	.73

TABLE LVII

TITANIUM 6AL-4V INERTIA WELDING PARAMETRIC STUDIES

(1.0 inch O.D. X 0.3 inch Wall)

Flywheel Moment Of Inertia	Welding Speed RPM	SFM	Upset Pressure (psi)	Spindle Efficiency	Actual Unit Energy ($ft\text{-}lbs/in^2$)	Upset (inch)	Visual Results	Ranking
3.9	5,000	1,310	4,500	.80	20,100	.150	Good weld	5
3.9	5,000	1,310	6,800	.80	20,100	.184	Good weld - excessive upset	10
3.9	5,000	1,310	9,000	.80	20,100	.175	Excessive upset	13
3.9	8,000	2,100	4,500	.80	30,400	.304	Excessive upset	14
3.9	8,000	2,100	6,800	.80	30,400	X		
3.9	8,000	2,100	9,000	.80	30,400	X		
2.3	5,000	1,310	4,500	.75	6,700	.048	Good weld - minimum upset	6
2.3	5,000	1,310	9,000	.75	6,700	.075	Good weld	2
2.3	8,000	2,100	4,500	.75	17,000	.180	Good weld - excessive upset	7
2.3	8,000	2,100	6,800	.75	17,000	.186	Good weld - excessive upset	8
2.3	8,000	2,100	9,000	.75	17,000	.204	Excessive upset	12
1.8	5,000	1,310	4,500	.70	4,800	.025	Poor weld - flash on one side only	15
1.8	5,000	1,310	6,800	.70	4,800	.030	Poor weld - not concentric	16
1.8	5,000	1,310	9,000	.70	4,800	.042	Good weld - minimum flash	11
1.8	8,000	2,100	4,500	.70	12,800	.090	Good weld	1
1.8	8,000	2,100	6,800	.70	12,800	.124	Good weld	3
1.8	8,000	2,100	9,000	.70	12,800	.180	Good weld - excessive upset	9

TABLE LVIII

TITANIUM 6AL-4V 1.0 INCH O.D. X 0.3 INCH WALL UPSET MEASUREMENTS

Yo	(1)	(2)	CS	Term	ΣX^2	$\sqrt{\Sigma X^2}$	CS adj	Rank	Coeff	(1)	(2)	$\hat{Y}$	$\hat{Y}$ adj	Yo-$\hat{Y}$ adj
150	505	1417	2653		18				147.39	132.14	71.08	148.69	157.2	-7.2
180	912	745	183	A	12	3.464	52.8	14	15.25	61.06	-66.0	165.94	170.6	9.4
175	175	461	25	A^2	36	6	4.2	2	0	-87.42	11.61	183.19	191.5	-16.5
304	570	25	1099	B	18	4.242	259.1	16	61.06	-21.42	86.33	313.65	303.8	.2
304	97	51	45	AB	12	3.464	13.0	8	0	11.61	-68.0	306.40	292.3	11.2
304	334	107	43	A^2B	36	6	7.2	4	0	0	11.61	299 15	289.3	14.7
48	25	-35	-962	C	12	3.464	-267.3	17	-77.17	147.39	101.58	47.86	55.0	-7.0
52	0	31	82	AC	8	2.828	29.0	11	10.25	61.06	-70.0	63.11	66.4	-14.4
75	27	29	64	A^2C	24	4.898	13.1	9	0	-77.17	11.61	78.36	85.3	-10.3
180	24	407	-110	BC	12	3.464	-31.8	12	-9.17	-9.17	193.2	169.98	177.2	2.8
186	17	395	98	ABC	8	2.824	34.7	13	12.25	11.61	-108.84	185.23	188.6	-2.6
204	90	297	-20	A^2BC	24	4.898	-4.1	1	0	0	11.61	200.48	207.5	-3.5
25	-35	-25	418	C^2	36	6	69.7	15	11.61	162.64	208.45	16.69	5.0	20.0
30	0	-3	30	AC^2	24	4.898	6.1	3	0	61.06	-86.34	29.94	14.4	15.6
42	19	73	-68	A^2C^2	72	8.484	-8.0	6	0	-66.92	11.61	43.19	31.3	8.7
90	12	35	-86	BC^2	36	6	-14.3	10	0	3.08	223.70	95.97	102.8	-12.8
124	7	-7	54	ABC^2	24	4.898	11.0	7	0	11.61	-63.84	133.72	136.6	-12.6
180	22	15	64	A^2BC^2	72	8.484	7.5	5	0	0	11.64	171.47	177.9	2.1

TABLE LIX

TITANIUM 6AL-4V 1.0 INCH O.D. X 0.3 INCH WALL QUALITY RANKING

Yo	(1)	(2)	CS	Term	ΣX^2	$\sqrt{\Sigma X^2}$	CS adj.	Rank	Coeff.	(1)	(2)	$\hat{Y}$	Yo - $\hat{Y}$
5	28	77	171		18				9.500	8.083	9.500	7.722	-2.722
10	49	39	17	A	12	3.464	4.91	11	1.417	-1.417	4.334	9.722	.278
13	12	55	-3	A^2	36	6.0	-.50	3	0	-1.833	2.556	11.722	1.278
14	27	12	7	B	18	4.242	1.65	5	0	-6.167	9.500	15.110	-1.110
17	42	1	17	AB	12	3.464	4.91	12	1.417	1.500	2.334	15.994	1.006
18	13	4	13	A^2B	36	5.0	2.17	8	0	-1.056	2.556	16.778	1.222
6	8	-4	-22	C	12	3.464	-6.35	15	-1.833	9.500	9.500	4.388	1.612
4	4	3	-8	AC	8	2.828	-2.83	9	0	0	.334	4.388	-.388
2	-4	-2	2	A^2C	24	4.898	.41	1	0	-1.833	2.556	4.388	-2.388
7	5	21	-50	BC	12	3.464	-14.43	17	-4.167	-4.167	6.666	5.778	1.222
8	-4	15	16	ABC	8	2.828	5.66	13	2.000	1.500	-8.000	8.612	-.612
12	8	-29	10	A^2BC	24	4.898	2.04	6	0	-1.056	.444	11.446	.554
15	-2	-4	53	C^2	36	6	9.00	16	1.500	10.917	9.500	16.390	-1.390
16	-2	9	14	AC^2	24	4.898	2.86	10	0	1.417	-6.000	14.390	1.610
11	0	12	-12	A^2C^2	72	8.484	-1.42	4	0	-1.833	.444	12.390	-1.390
1	3	0	-38	BC^2	36	6	-6.33	14	-1.056	-2.167	12.334	-.890	1.890
3	-6	3	-10	ABC^2	24	4.898	-2.04	7	0	1.500	-4.000	3.944	-.944
9	4	10	4	A^2BC^2	72	8.484	.47	2	0	-1.056	.444	8.778	.222

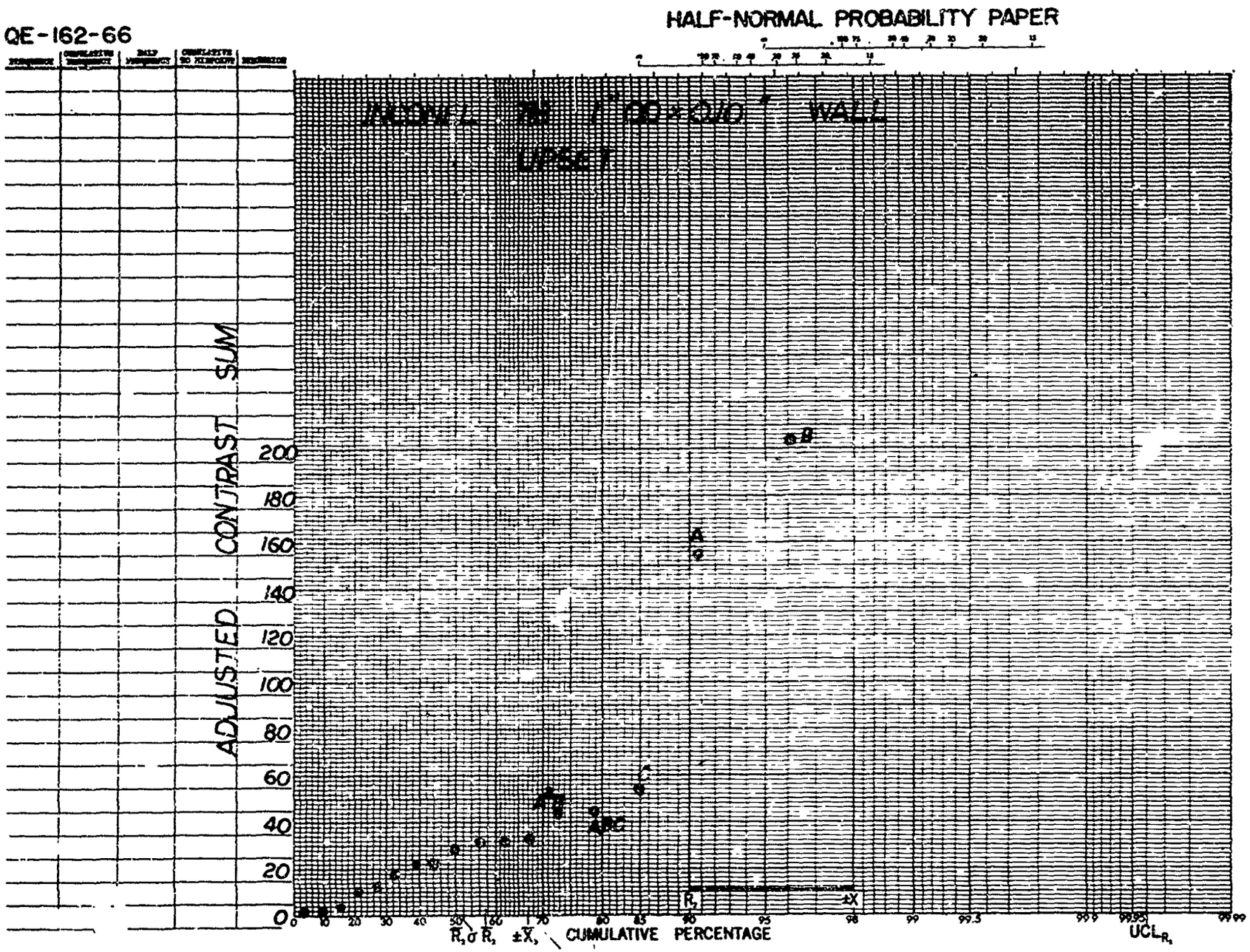

Figure 98 Half Normal Probability Plot for Upset of Inconel 718 0.100 Inch Wall

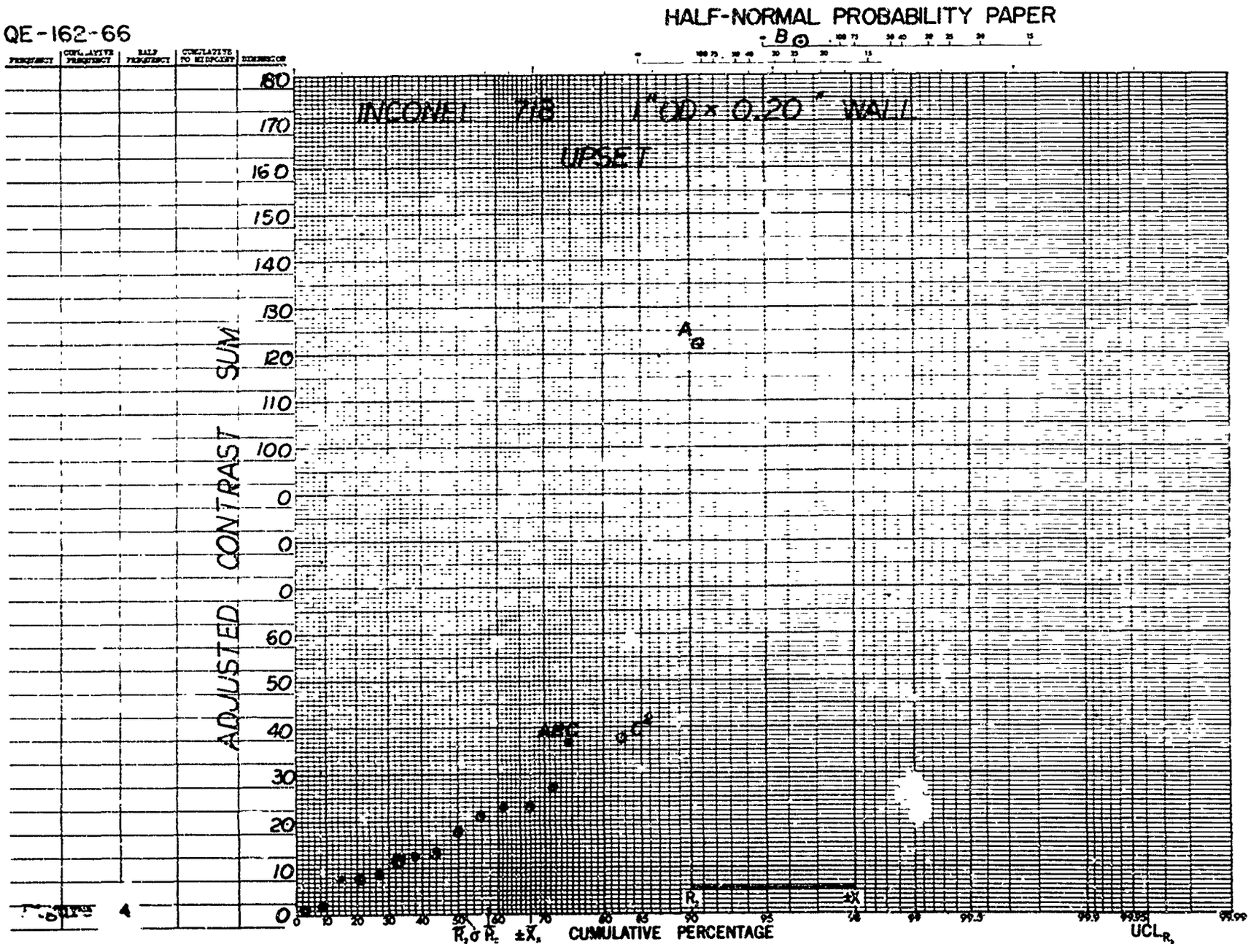

Figure 99 Half Normal Probability Plot for Upset of Inconel 718 0.200 Inch Wall

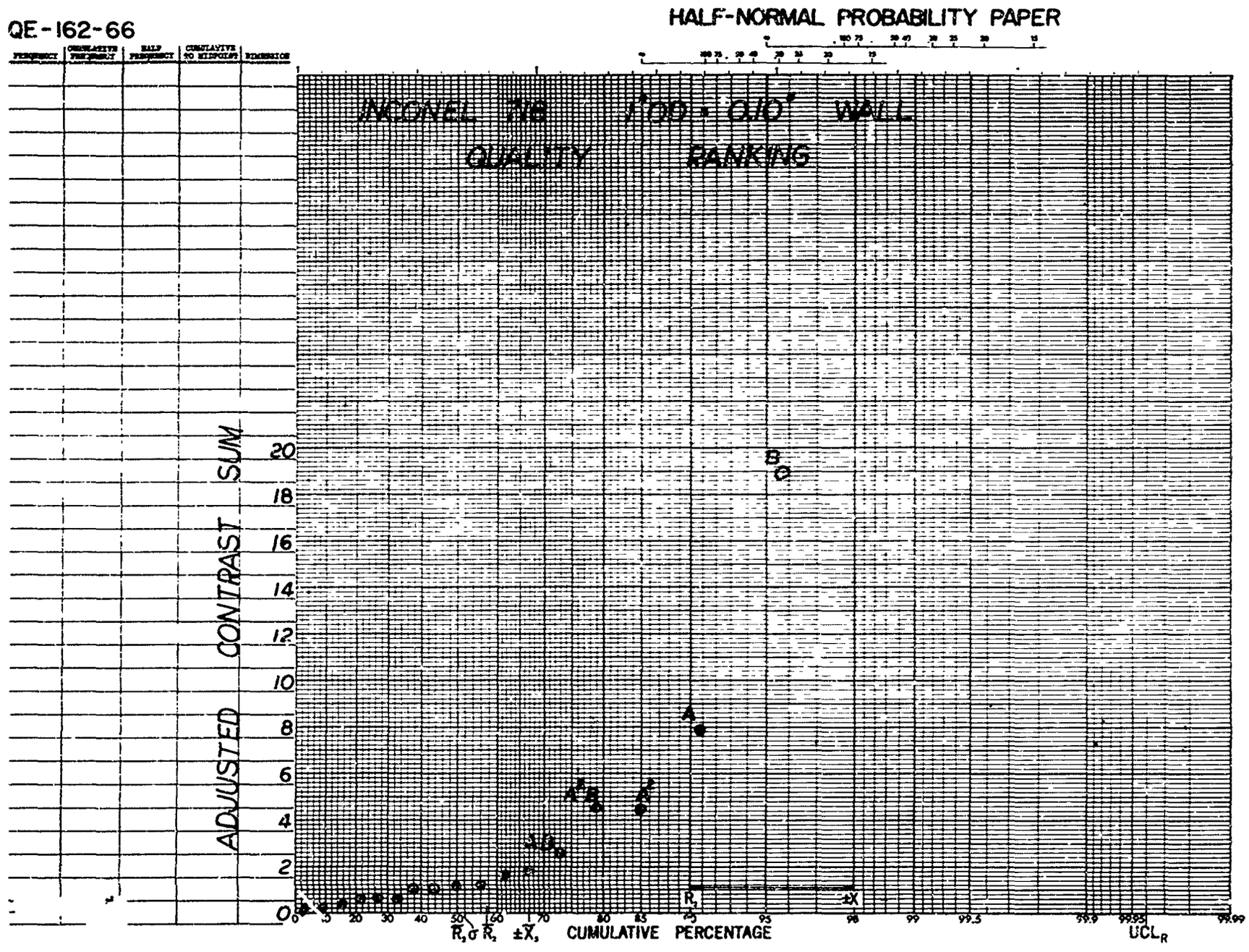

Figure 100 Half Normal Probability Plot for Quality of Inconel 718 0.100 Inch Wall

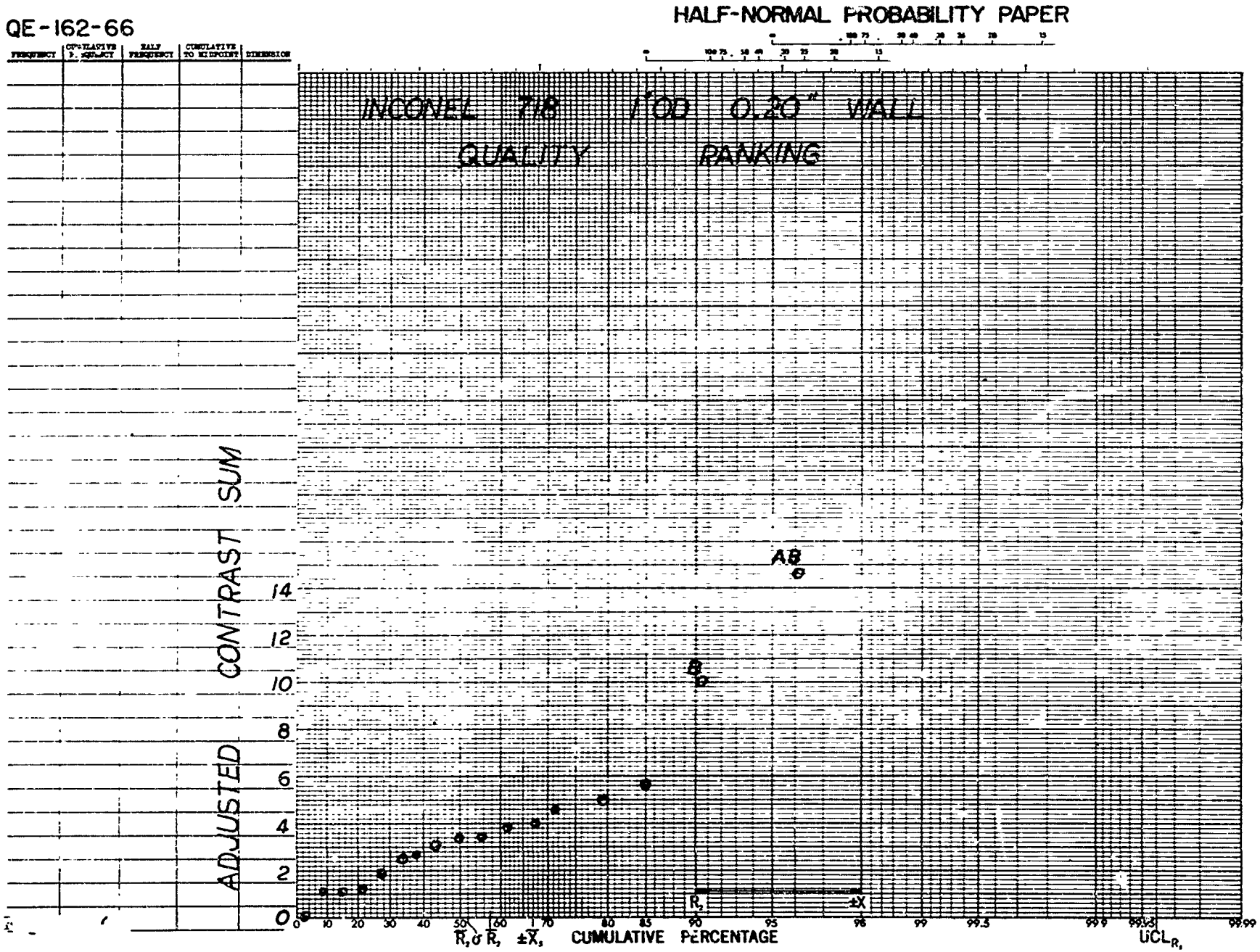

Figure 101 Half Normal Probability Plot for Quality of Inconel 718 0.200 Inch Wall

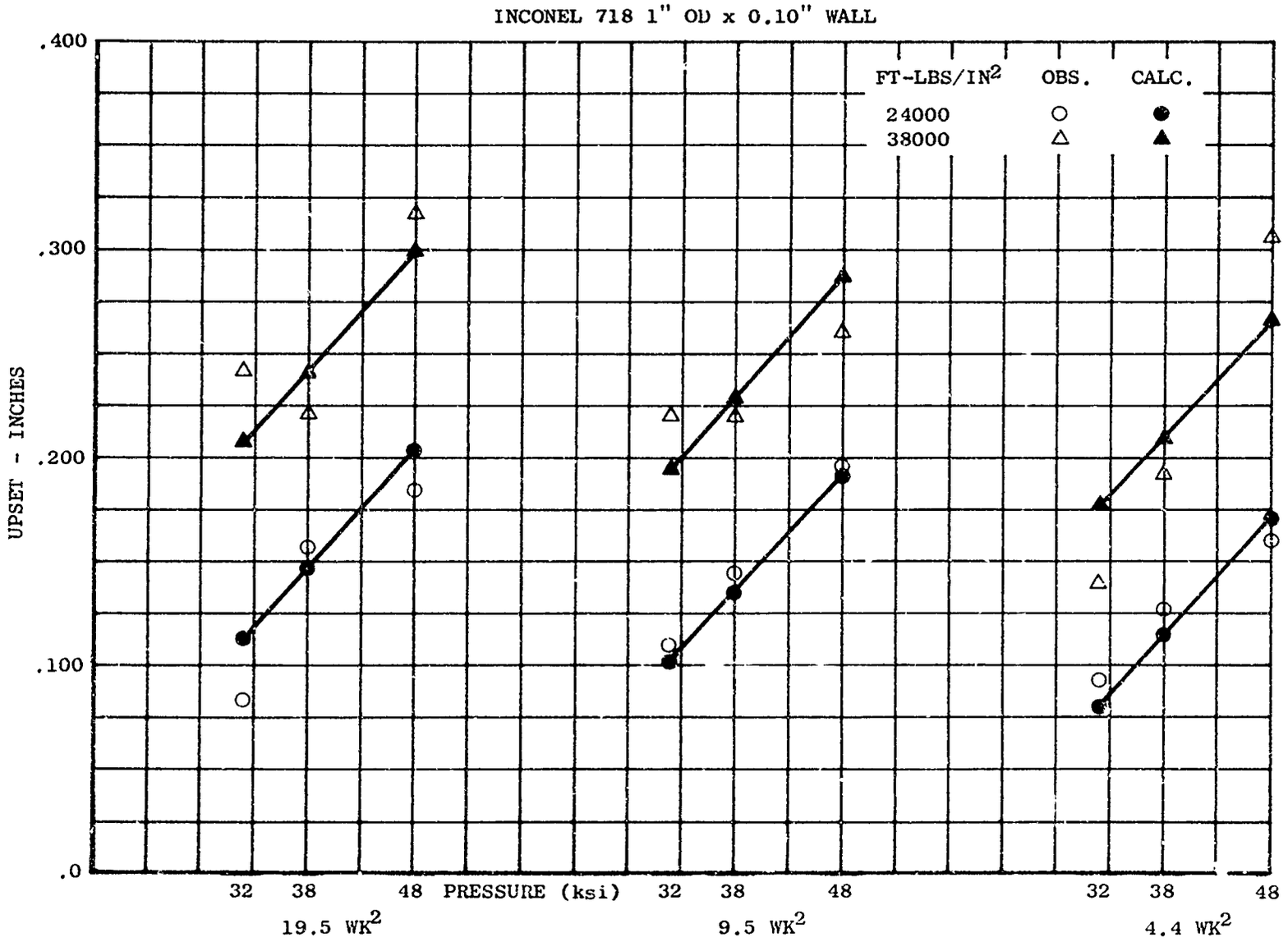

Figure 102 Observed and Calculated Upset Values - Inconel 718 0.100 Inch Wall

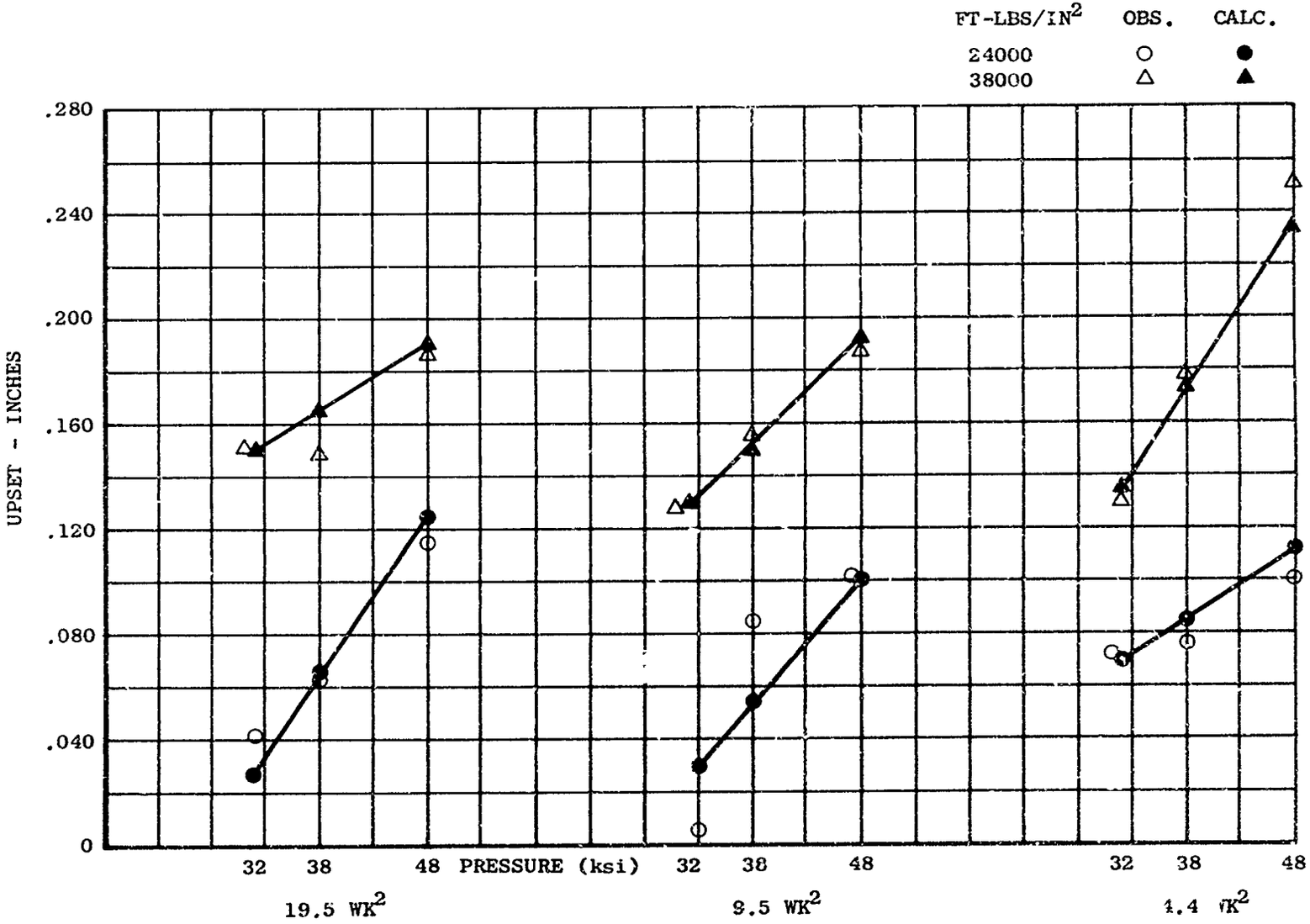

Figure 103 Observed and Calculated Upset Values - Inconel 718 0.200 Inch Wall

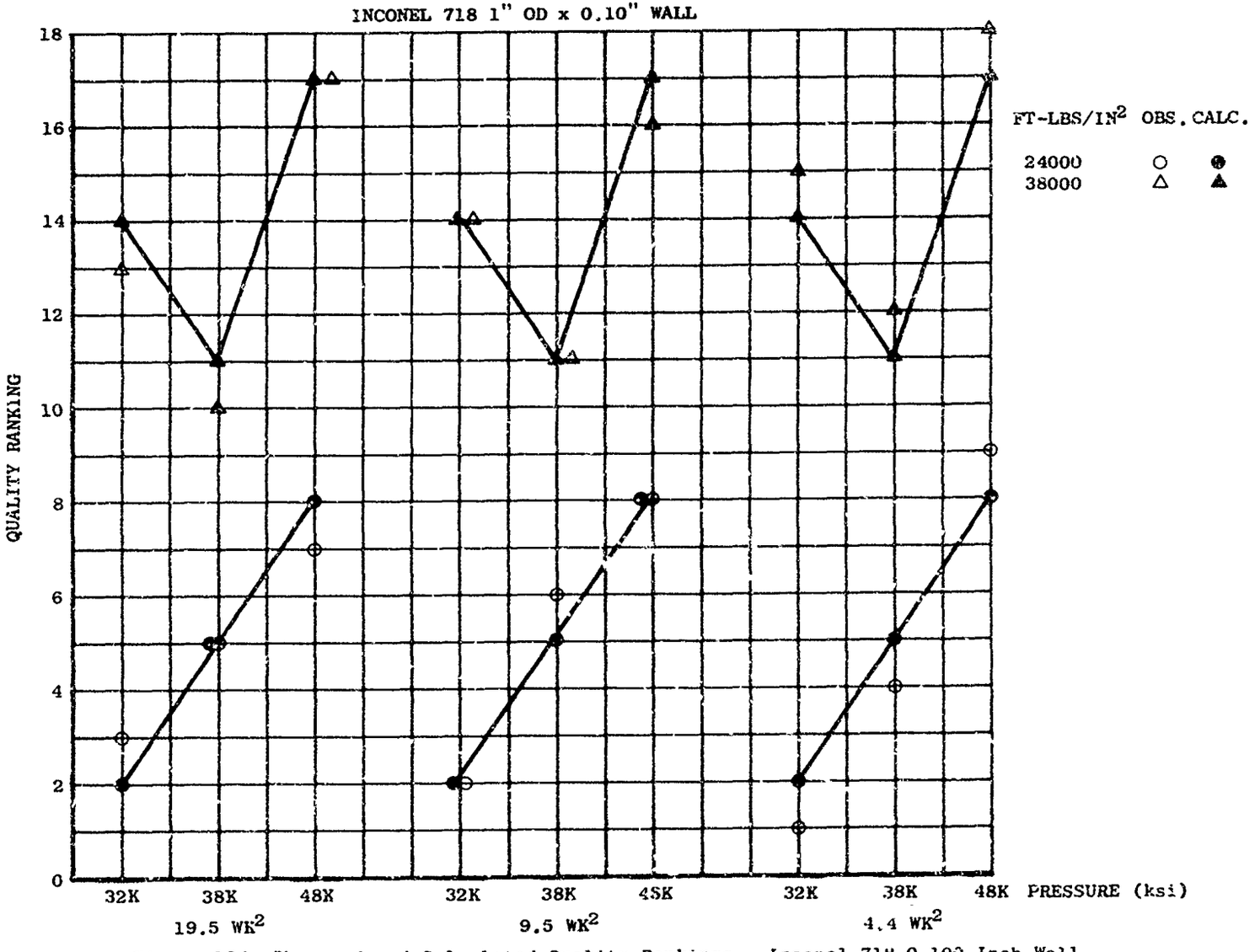

Figure 104 Observed and Calculated Quality Rankings - Inconel 718 0.100 Inch Wall

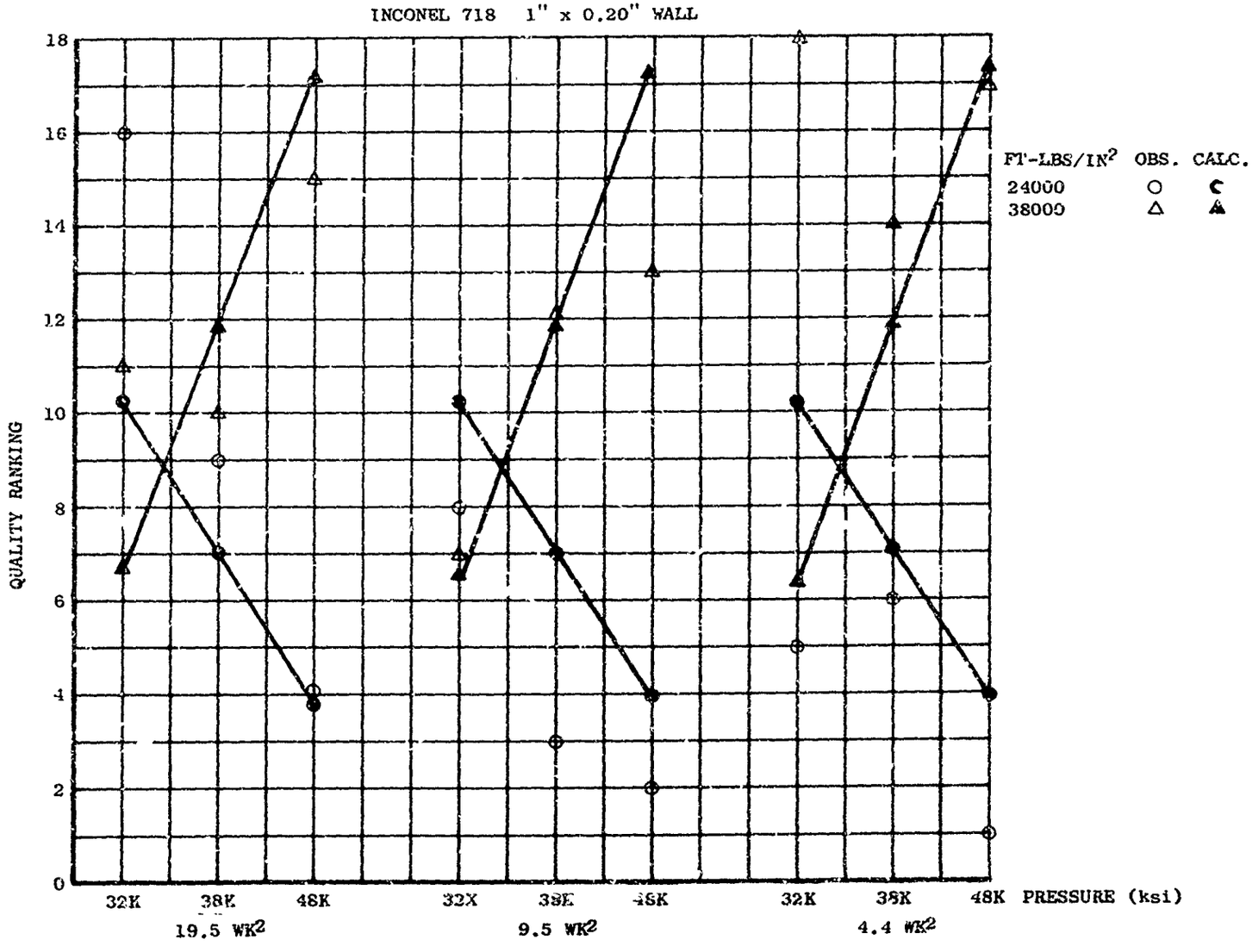

Figure 105 Observed and Calculated Quality Rankings - Inconel 718 0.200 INCH WALL

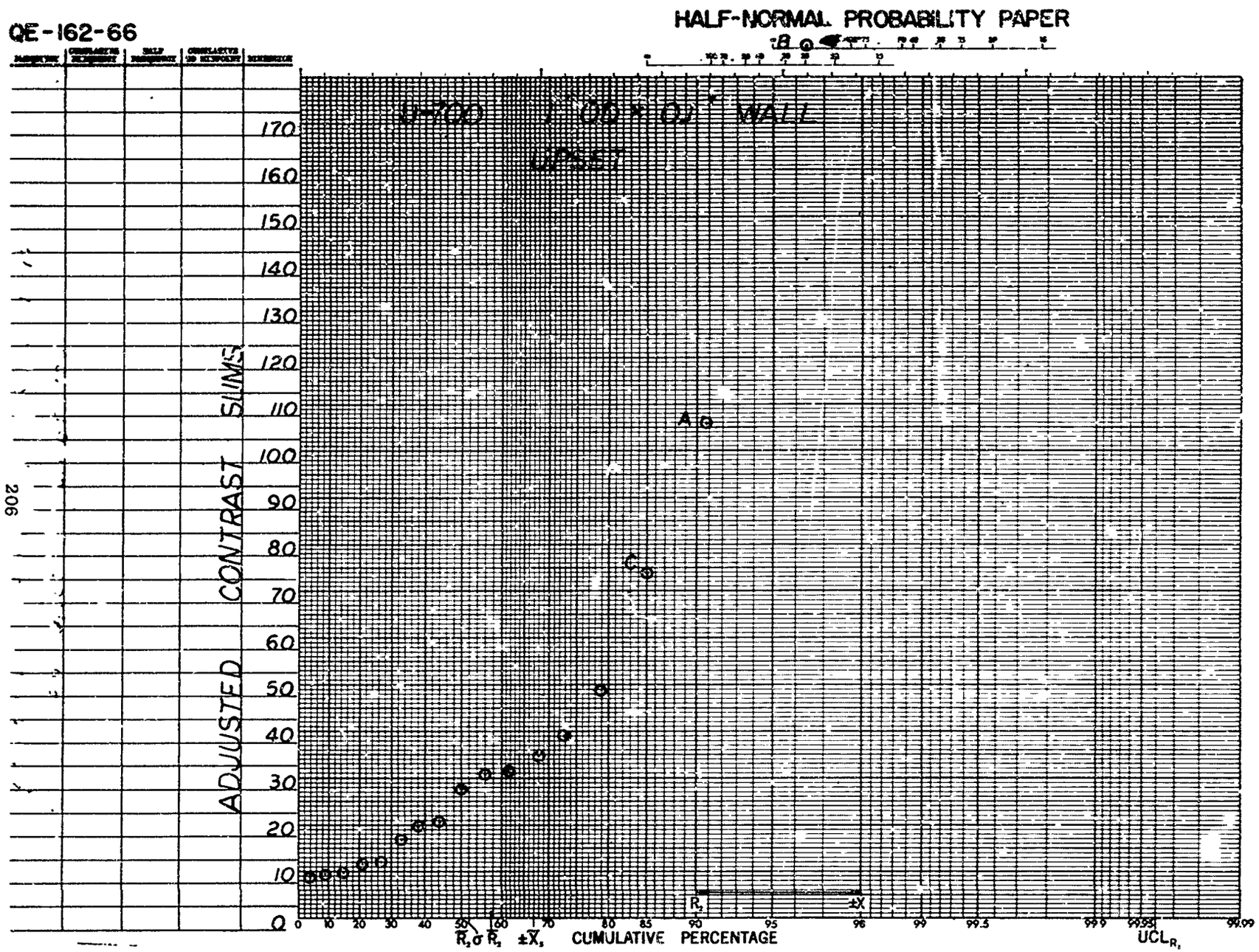

Figure 106 Half Normal Probability Plot for Upset of Udimet 700

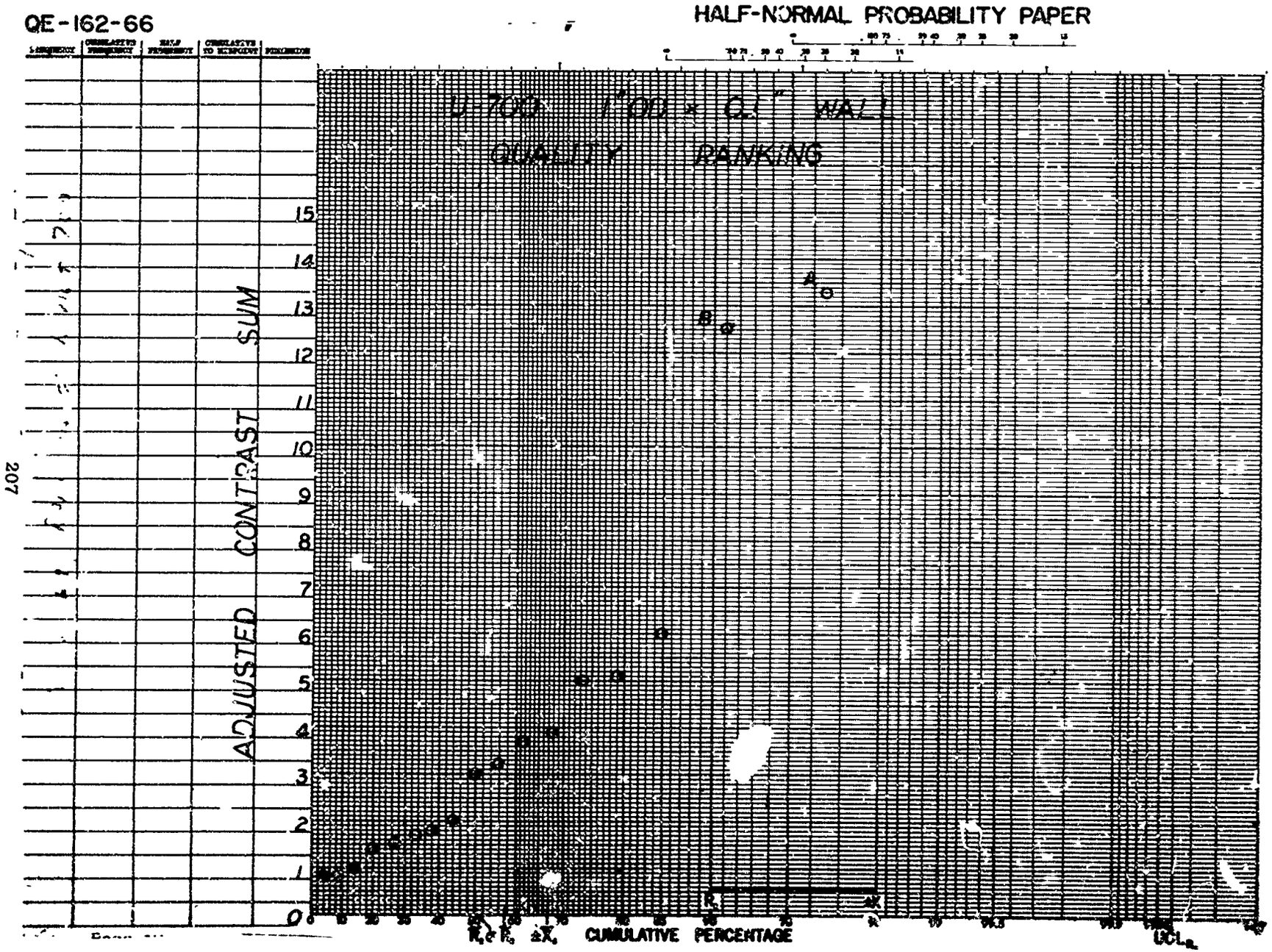

Figure 107 Half Normal Probability Plot for Quality Ranking of Udimet 700

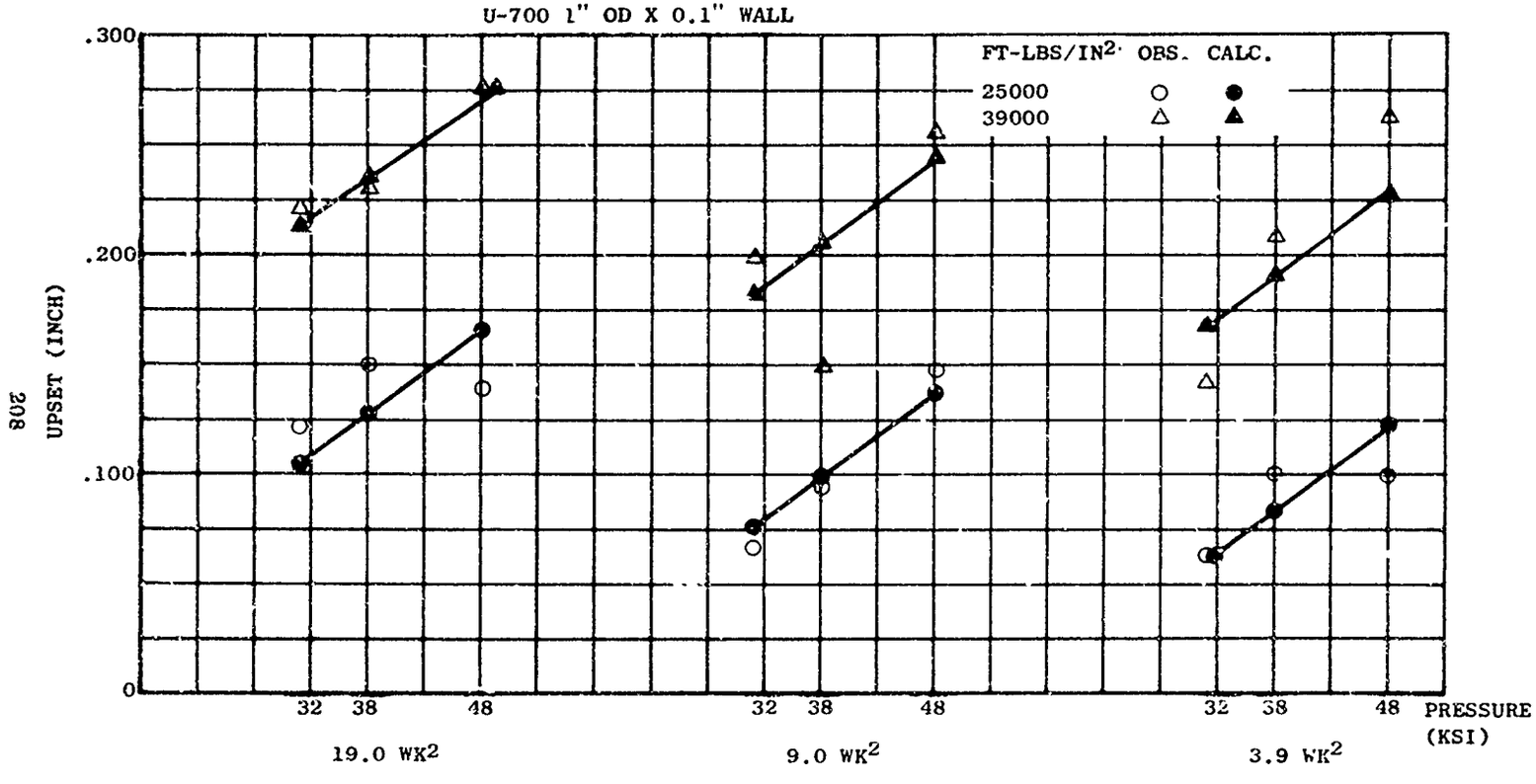

Figure 108 Observed and Caluclated Upset for Udimet 700

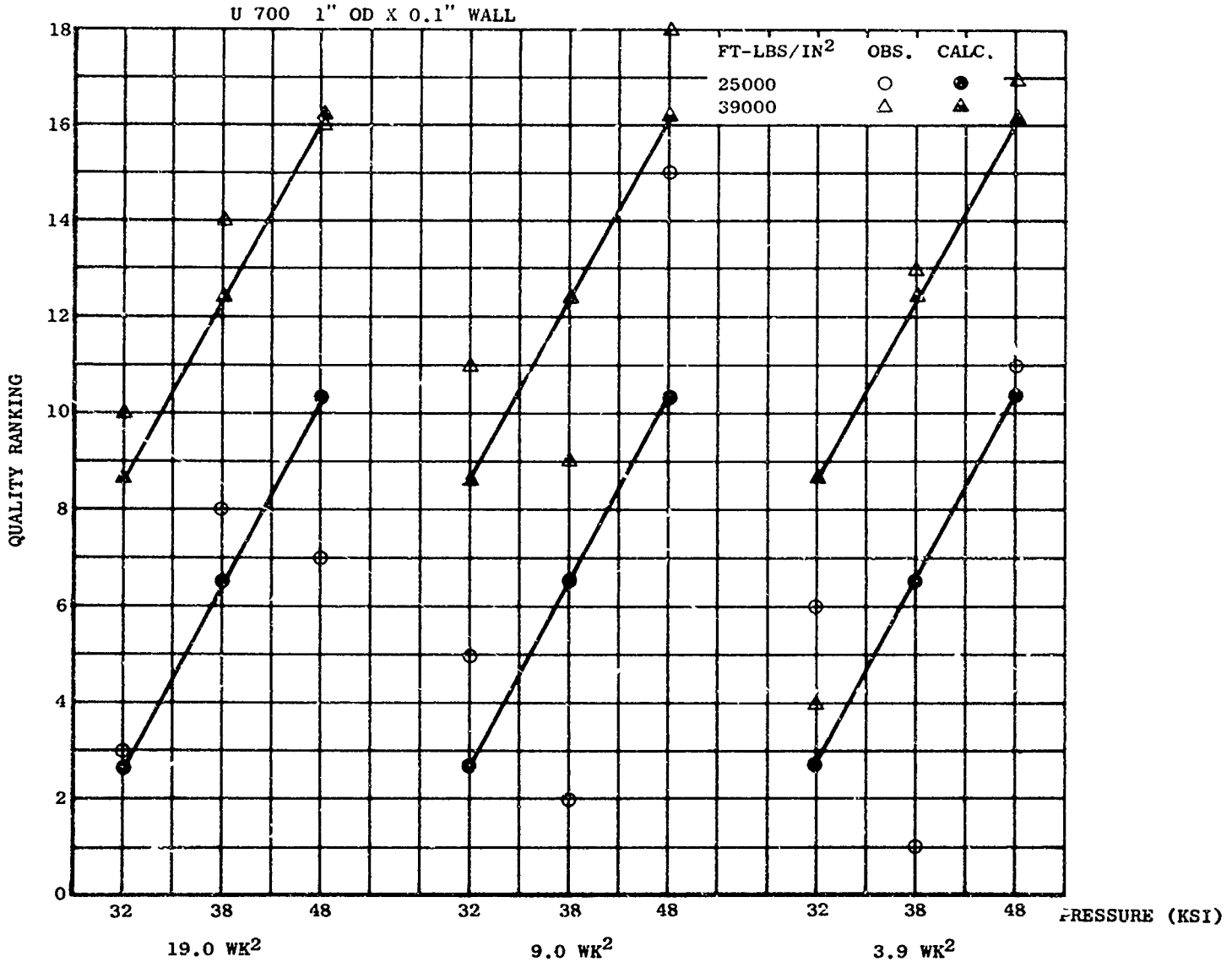

Figure 109 Observed and Calculated Quality Rankings for Udimet 700

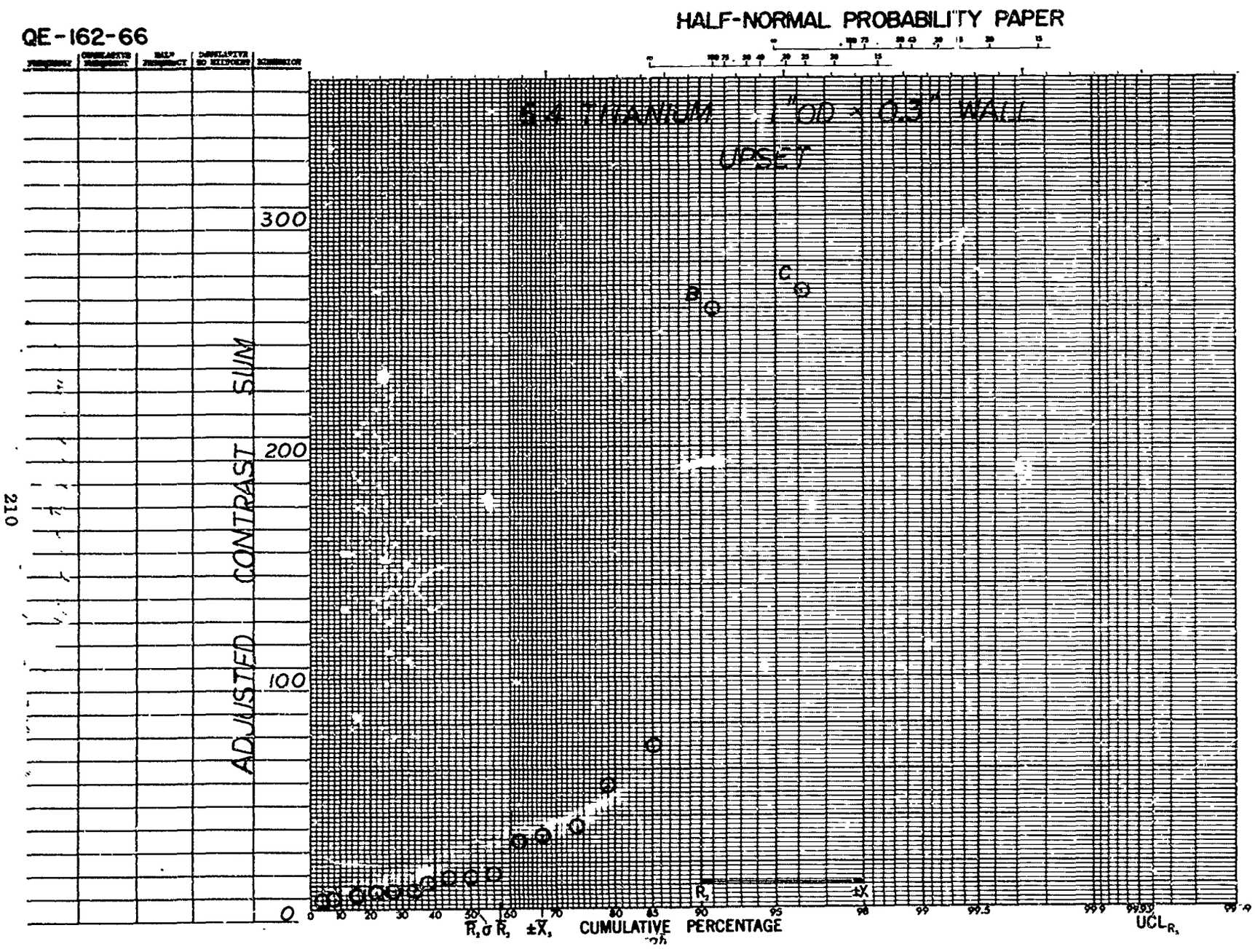

Figure 110 Half Normal Probability Plot for Upset of Titanium 6Al-4V

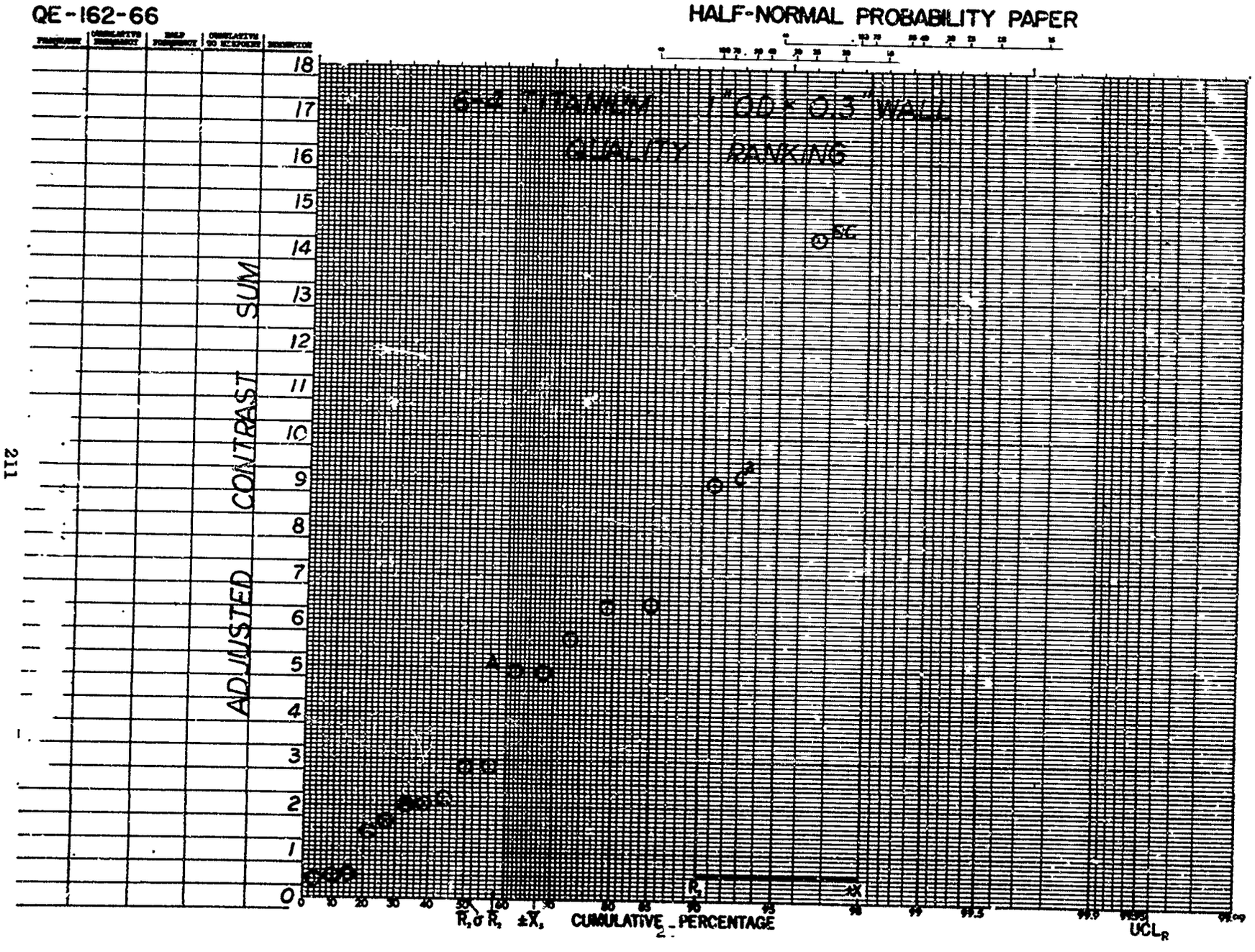

Figure 111 Half Normal Probability Plot for Quality Ranking of Titanium 6Al-4V

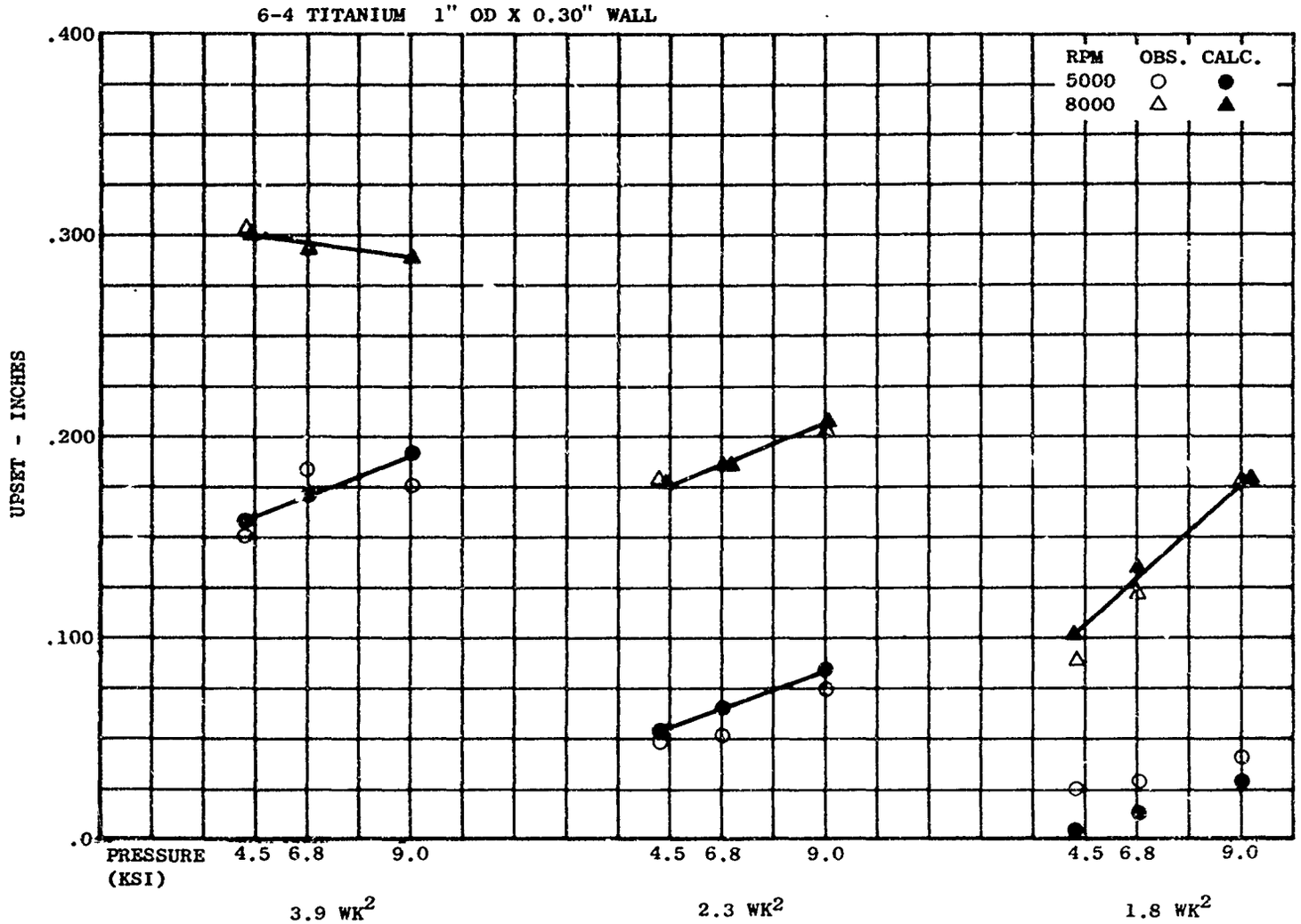

Figure 112 Observed and Calculated Upset for Titanium 6Al-4V

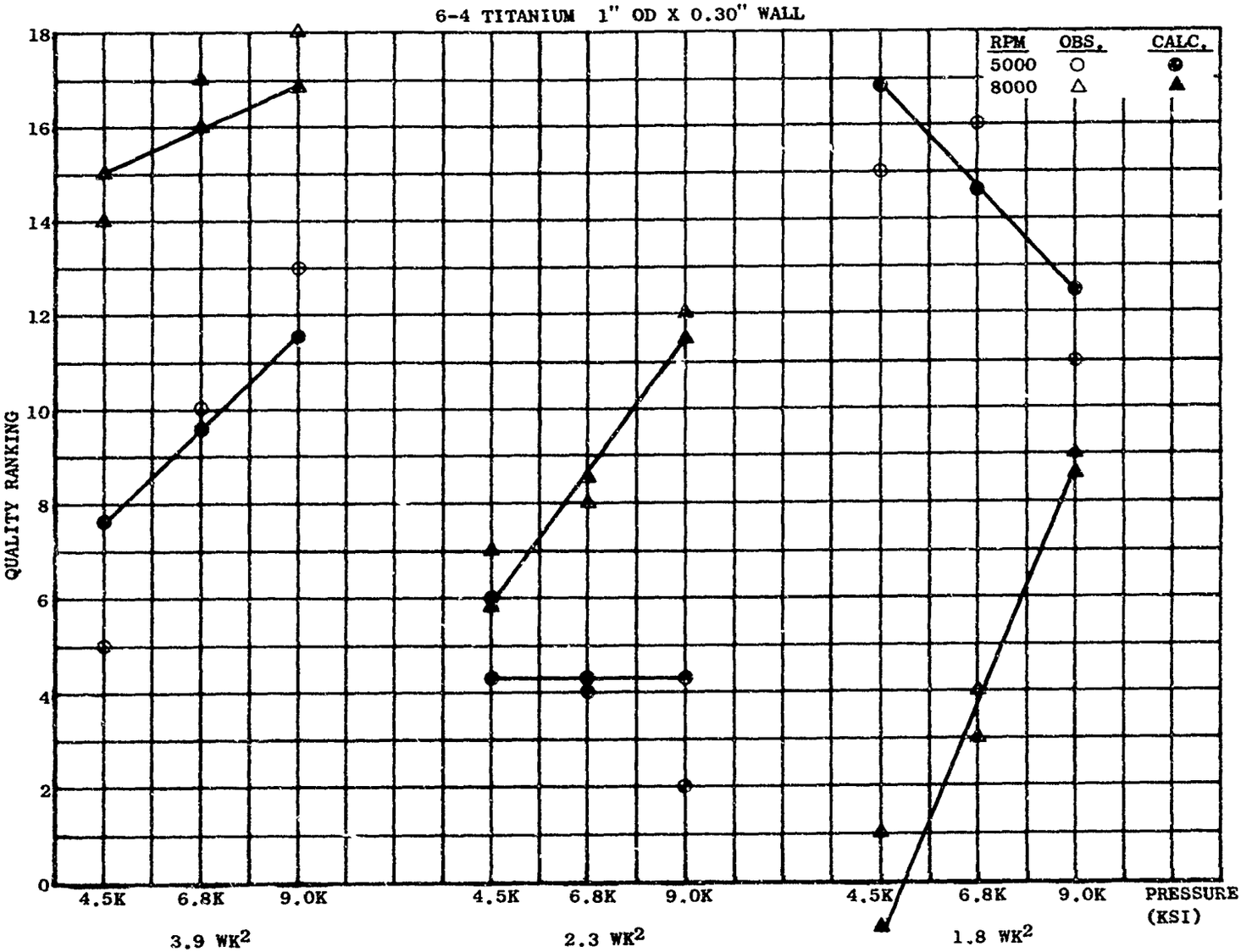

Figure 113 Observed and Calculated Quality Ranking of Titanium 6Al-4V

APPENDIX III

T58 TYPE ROTOR TEST

A. INTRODUCTION

The T58 rotor was fabricated from Inconel 718. This fabricated rotor consisted of 8 stages of compressor wheels, Figure 114. The proof test was a hydraulic pressure test. The test was a non-destructive proof test to ensure that the fabricated rotor had the capability to withstand the environment of an overspeed test and an actual engine test.

B. HYDRAULIC PROOF TEST

The T58 inertia welded rotor spool consisted of eight discs, each approximately one inch apart. The rotor was a smooth spool type with the welds positioned approximately halfway between the dovetail slots. There was a closely connected flange on the front of the rotor and a bolt circle on the aft stage for bolting to the aft compressor shaft. In the design of the hydraulic test, it was desirable to have a bi-axial state of stress which would approximate the state of stress in the engine. Therefore, in addition to the circumferential stresses due to pressure, an axial stress was needed. For this rotor geometry, the best combination of axial and circumferential stresses could be obtained by the use of end plates on the foreward flange and the aft wheel shaft bolt circle. The end plates were bolted to the end flanges and the unit was pressurized. The pressure loadings in the spool were approximately 65% higher than those during engine operating conditions. An axial expansion of 0.00626 inches was attained at 115 PSIG. The maximum stress level attained at the welds was calculated conservatively to be 4260 PSI. The limiting stresses in the pressure test were the high dovetail, spool and end plate bolt stresses.

The test setup was disassembled, and the rotor was zyglo-inspected. No crack indications were observed.

C. HIGH SPEED TEST

The T58 inertia welded rotor spool was bladed and assembled with fore and aft shafting. The rotor was then subjected to five high speed testing cycles. Each cycle held the speed at the desired level for 60 seconds. Following are the speeds and the calculated maximum stress in the welds:

Cycle 1 - 29,600 RPM with a maximum stress of 76,000 PSI
Cycle 2 - 27,000 RPM with a maximum stress of 63,000 PSI
Cycle 3 - 26,900 RPM with a maximum stress of 62,750 PSI
Cycle 4 - 26,800 RPM with a maximum stress of 62,500 PSI
Cycle 5 - 26,000 RPM with a maximum stress of 58,570 PSI

Vibration in the spin pit never exceeded 0.50 mils which was reached at approximately 23,000 RPM.

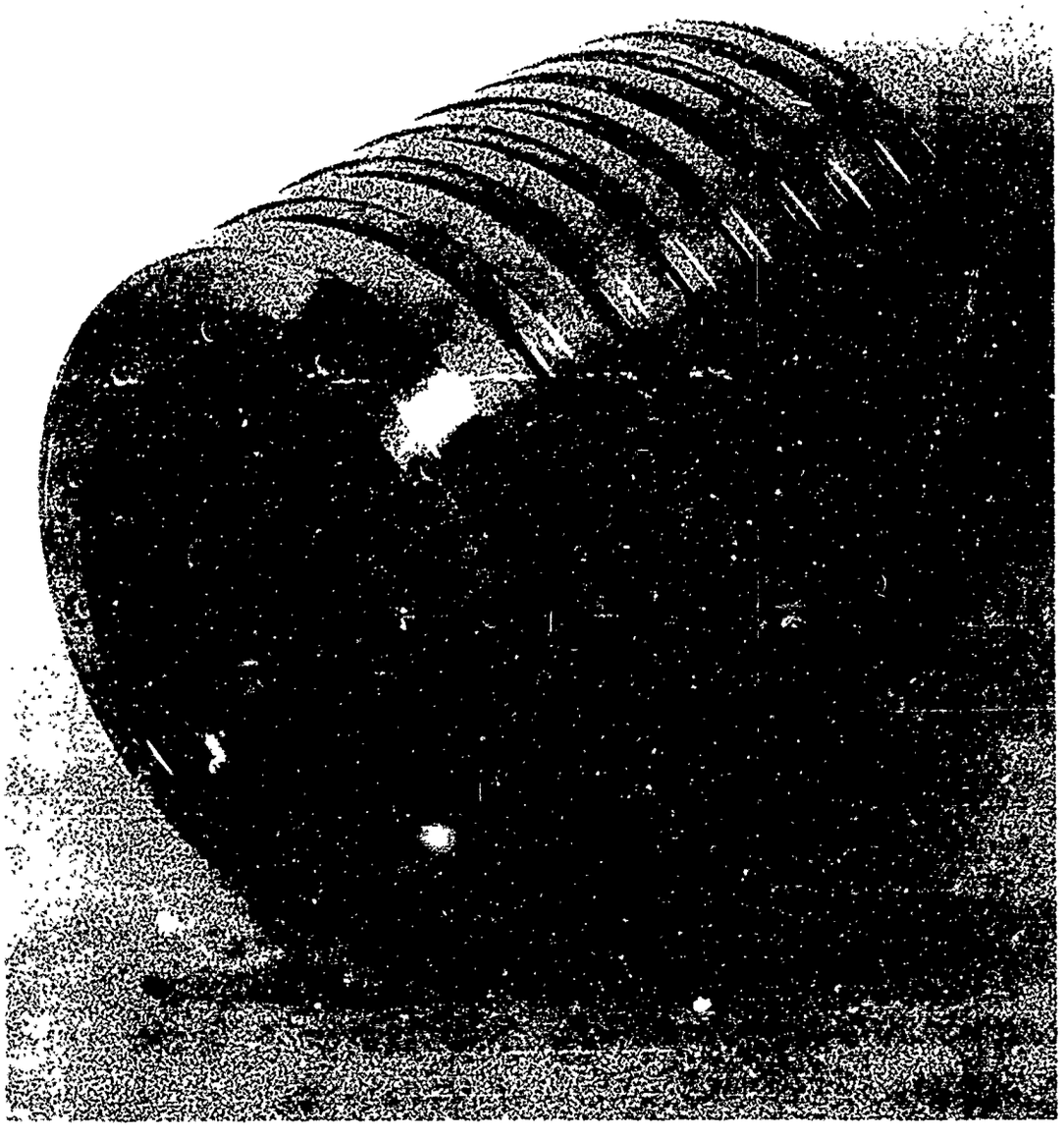

Figure 114 Inertia Welded T58 Compressor Rotor - Inco 718

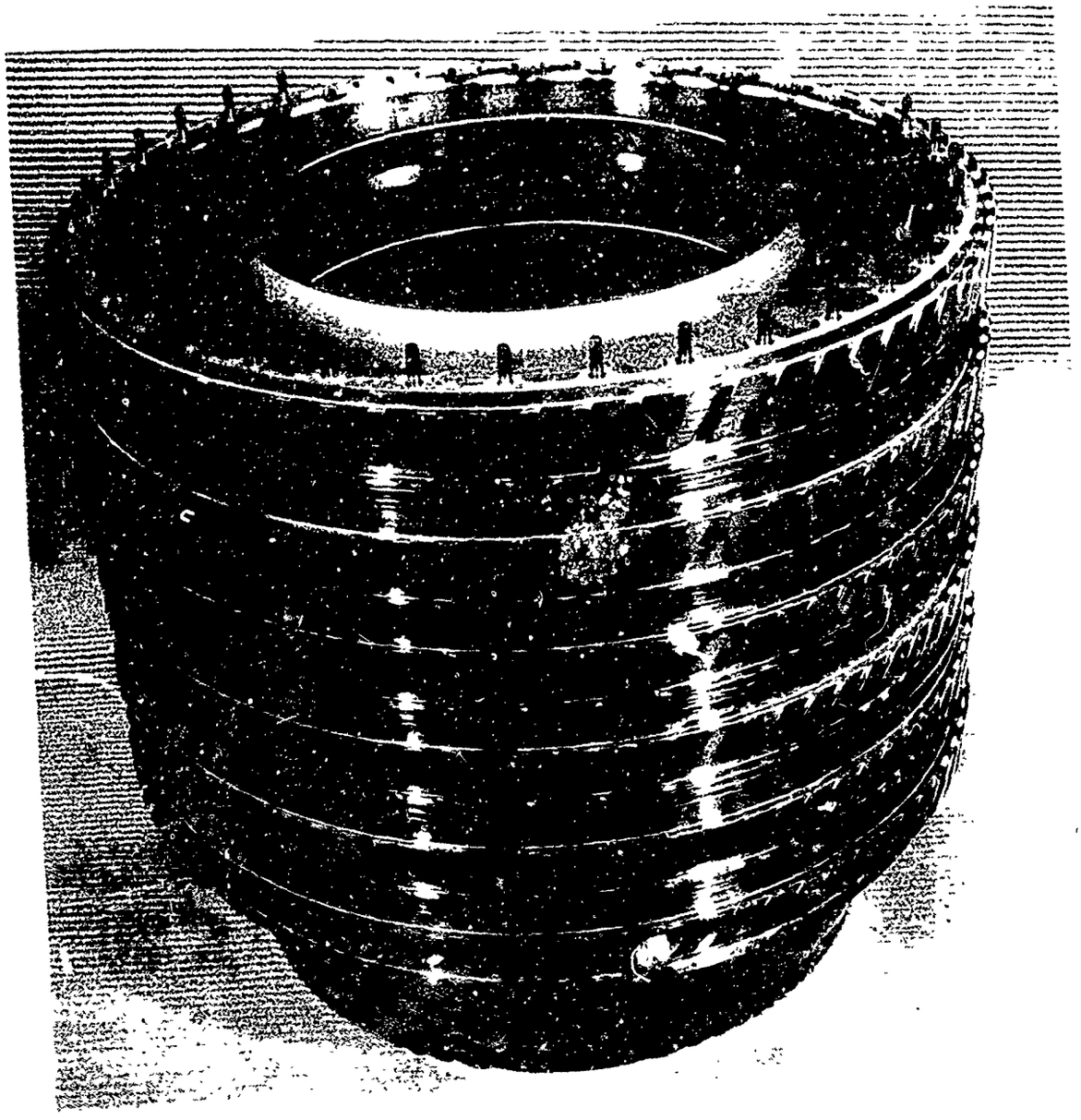

Figure 115 Inertia Welded F100 Rotor - Rene' 95

APPENDIX IV

F100/F400 TYPE ROTOR TEST

A. INTRODUCTION

The advance rotor was fabricated from Rene' 95 Alloy. This fabricated rotor consisted of six stages of compressor wheels and an integral conical aft shaft, Figure 115. The proof test was a hydraulic pressure test. The test was a nondestructive proof test to ensure that the fabricated rotor had the capability to withstand the environment of an actual engine test.

B. HYDRAULIC PROOF TEST

The inertia welded rotor spool consisted of six discs, each approximately two inches apart and connected near the outer diameter by cylindrical spacers. There was a closely coupled flange on the front end and a four and one-half inch long conical shaft connected to a flange on the aft end.

For design purposes, it was desirable to have a biaxial state of stress which would approximate the state of stress in the engine test. Therefore, in addition to the circumferential (Pr/t) stresses due to pressure, an axial stress was needed. The axial stress was provided internally by using the spool itself as a hydraulic cylinder, permitting the front flange loading to be free to move axially upon pressurization. Calculations showed that the front flange load ring should have an inner diameter of 15.396 inches to provide an optimum ratio of circumferential to axial stresses, and to duplicate the maximum axial separating loads at the welds. Further calculations showed that the six discs provided comparatively stiff supports to the cylindrical spacers and that the rather long aft cone would tend to stress higher than the inertia welds between rotor stages. Due to this, it was decided to limit the test by the stresses in the aft cone which had one inertia weld.

The maximum test pressure was thus selected at 1000 PSI.

C. TEST RESULTS

Table LX lists the calculated stress for each weld. Both the weld stresses calculated for engine test (DESIGN) and the weld stresses due to 1000 PSI pressure (PROOF TEST) are shown. In addition, the percentage ratio of the weld stresses to weld design stresses is given. As shown, the maximum weld design effective stress is 88.2 KSI, and the maximum weld proof test effective stress is 55.5 KSI. Hence, the pressure test demonstrated a maximum weld stress capability of 63% of maximum weld operating stresses.

After the over speed testing, the rotor was disassembled and dimensionally and non-destructively inspected. No dimensional changes or crack indications were observed.

D. ENGINE TEST

The inertia welded rotor spool was rebladed and assembled to make up a complete compressor rotor for engine testing in the T58 engine. The T58 engine is a turbo-shaft type gas turbine. The engine weighs approximately 300 pounds. The pressure ratio is 8.2/1 with an airflow of approximately 13 pounds per second. The military shaft horsepower is approximately 1,300 SHP at approximately 26,000 RPM. The inertia welded rotor was used in five different engine build ups with three complete military 150 hour model test cycles plus other short runs.

The engine test program for the inertia welded rotor is summarized in the following tabulation of the test time recorded:

Engine Build	Total Hours	Total Endurance Hours	Total Accels.*
042-13A	4	0	6
042-13B	440	332	630
042-14A	38	0	24
042-14A	29		18
042-C	192	150	290
	703	482	968

*Any acceleration from flight idle or below to normal rated power or above.

At full engine power the calculated maximum stress in the inertia welds is 60,000 PSI and the maximum temperature is 550°F.

After the completion of engine test No. 042-13B, the compressor rotor was disassembled and dimensionally and non-destructively inspected. No dimensional changes or crack indications were observed. The compressor rotor was considered to have completed all of the requirements for engine operation.

TABLE LX

STRESS IN RENE' 95 SPOOL INERTIA WELDS UNDER DESIGN AND TEST LOADINGS

Weld No.	Location	Loading	σ_e (In) KSI	σ_e (Out) KSI	σ_x KSI	σ_θ KSI	σ_{xz} KSI	$\sigma_{\theta z}$ KSI
1	Spacer 3 Forward	Design	76.2	77.8	5.4	79.4	6.0	1.9
		Test	37.2	46.5	14.1	34.0	-33.9	-10.8
		Percent	49	60				
2	Spacer 3 Aft	Design	69.9	77.1	4.9	71.1	29.7	9.4
		Test	43.3	31.9	12.3	24.1	35.9	11.4
		Percent	62	41				
3	Spacer 4 Forward	Design	69.5	68.6	5.9	71.8	3.8	-1.2
		Test	33.0	41.1	12.2	29.4	-30.6	-9.9
		Percent	47	60				
4	Spacer 4 Aft	Design	70.7	67.2	5.9	70.3	-15.8	-5.1
		Test	23.7	28.4	12.4	27.8	-11.3	-3.6
		Percent	34	42				
5	Spacer 5 Forward	Design	79.3	77.3	6.5	81.0	-8.7	-2.8
		Test	18.9	27.1	11.4	21.2	-16.3	-5.2
		Percent	24	35				
6	Spacer 6 Forward	Design	78.2	74.9	7.0	78.6	-15.7	-5.1
		Test	31.7	36.6	11.0	31.5	-22.8	-7.3
		Percent	41	49				
7	Spacer 7 Forward	Design	88.2	81.0	7.6	80.8	-39.4	-12.8
		Test	36.4	47.9	12.0	23.9	-42.1	-13.5
		Percent	41	59				
8	Rear Stub Shaft	Design	40.2	37.9	8.2	31.6	30.4	10.0
		Test	55.5	52.8	8.4	27.5	54.2	15.7
		Percent	138	139				

The stress equations used were as follows:

(1) $\epsilon_X = \frac{1}{E} \quad \sigma_X - \mu \sigma_\theta$

(2) $\epsilon_\theta = \frac{1}{E} \quad \sigma_\theta - \mu \sigma_X$

(3) $\sigma_X = \frac{E}{(1-\mu^2)} \quad \epsilon_X + \mu \epsilon_\theta$

(4) $\sigma_\theta = \frac{E}{(1-\mu^2)} \quad \epsilon_\theta + \mu \epsilon_X$

where:

ϵ_X = Axial Strain

ϵ_θ = Circumferential Strain

σ_X = Axial Stress

σ_θ = Circumferential Stress

E = Elastic Modulus

μ = Poisson's Ratio

After proof testing, all welds were inspected to fluorescent penetrant and drawing specifications. No detectable changes from pretest conditions were observed. The rotor was then assembled to the forward shaft, and the turbine shaft and rotor. The compressor and turbine rotor assembly was balanced and assembled in the engine.

D. ENGINE TEST

The engine test time as of March 1, 1970 was an accumulation of a series of different operating conditions.

The maximum operating stress and temperature at the welds was reached at an engine speed of 13,690 RPM. The should produce an effective stress on the inertia weld between stage 7 and stage 8 of 73,500 PSI and a temperature of 960°F. Forty-four minutes of engine test time was at 13,500 RPM, which whould produce an effective stress between stage 7 and stage 8 of 71,100 PSI and a temperature of 950°F. Nineteen hours and eight minutes of running time was accumulated at 12,400 RPM which should produce an effective stress between stage 7 and stage 8 of [illegible]00 PSI and a temperature of [illegible]00°F. All of these tests were run at static sea level conditions.

Twenty-eight hours and eight minutes of running time was at simulated altitude conditions of M.9 and 36,000 feet. In the altitude tests the effective stress in the inertia weld between stage 7 and stage 8 should be 58,400 PSI and the temperature should be 660°F.

A total of 24 starts have been made and a total of fifty-seven hours and seven minutes of engine running time accumulated. During the engine test program the inertia welded rotor was removed once for inspection. No defects of any type were disclosed and the rotor was reassembled in the engine and testing continued.

Unclassified
Security Classification

DOCUMENT CONTROL DATA - R & D

Security classification of title, body of abstract and indexing annotation must be entered when the overall report is classified)

1 ORIGINATING ACTIVITY (Corporate author) Material and Process Technology Laboratories Aircraft Engine Group General Electric Company Evendale, Ohio 45215	2a. REPORT SECURITY CLASSIFICATION Unclassified 2b GROUP N/A

3 REPORT TITLE

Improved Fabrication Methods of Jet Engine Rotors

4 DESCRIPTIVE NOTES (Type of report and inclusive dates)

Final Report (1 July 1967 - 31 March 1970)

5 AUTHOR(S) (First name, middle initial, last name)

Korton, George
Stalker, Kenneth W.

6 REPORT DATE May, 1970	7a. TOTAL NO OF PAGES 210	7b. NO OF REFS
8a CONTRACT OR GRANT NO F33615-67-C-1884 b. PROJECT NO PR: TF-7-MMP-1829/874-7 c. d.	9a. ORIGINATOR'S REPORT NUMBER(S) R70AEG279 9b. OTHER REPORT NO(S) (Any other numbers that may be assigned this report) AFME-TR-70-101	

10 DISTRIBUTION STATEMENT This document is subject to special export controls and each transmittal to foreign governments or foreign nationals may be made only with prior approval of the Manufacturing Technology Division, MAT, Air Force Materials Laboratory, Wright-Patterson Air Force Base, Ohio 45433.

11 SUPPLEMENTARY NOTES	12 SPONSORING MILITARY ACTIVITY Manufacturing Technology Division Air Force Materials Laboratory Wright-Patterson Air Force Base, Ohio 45433

13 ABSTRACT

This report summarizes the program to establish and demonstrate manufacturing methods for fabricating jet engine rotors as performed by the Contractor within the period of 1 July 1967 through 31 March 1970. The report contains: (1) mechanical property data on inertia welded Inco 718, U-700 and Ti 6Al-4V; (2) inertia welding parameters for Inco 718 and U-700; (3) metallographic and nondestructive inspection results of inertia welded Inco 718; (4) an analysis of transient temperature gradients in inertia welding; (5) mechanical property data on cold rim formed Inco 718 cross rolled plate; (6) shear forming data for cross rolled plate; (7) results of weld acceptance testing of the Caterpillar Model 400 inertia welder; (8) results of inertia welding TF39 Stages 14-16 Compressor rotor; (9) engine test results of various fabricated rotors; and (10) an overall evaluation of the program to develop and demonstrate manufacturing methods to fabricate compressor rotors from cross rolled plate and joined by inertia welding.

DD FORM 1 NOV 65 1473

UNCLASSIFIED
Security Classification

14 KEY WORDS	LINK A		LINK B		LINK C	
	ROLE	WT	ROLE	WT	ROLE	WT
Inertia Welding						
Friction Welding						
Cold Forming Inconel 718						
Welded Inco 713						
Welded U-700						
Welded Ti 6Al-4V						
Inconel 718 Plate						
Inertia Welded Inconel 718						
Fabricated Compressor Rotors						